AD NUMBER

AD345945

CLASSIFICATION CHANGES

TO: unclassified

FROM: confidential

LIMITATION CHANGES

TO:

Approved for public release, distribution unlimited

FROM:

Distribution authorized to U.S. Gov't. agencies and their contractors; Specific authority. Other requests shall be referred to U.S. Naval Research Laboratory, Washington, DC 20375-5320.

AUTHORITY

Nov 1971, Group-4, DoDD 5200.10.; NRL ltr, 26 Feb 2001

CONFIDENTIAL

NRL Memorandum Report 754

SUMMARY OF NAVY STUDY PROGRAM FOR F4H-1 WEAPON SYSTEM

(Unclassified Title)

VOLUME IX

J. C. Ryon, C. M. Loughmiller,
I. N. Bellavin, and R. L. Lister

RADAR DIVISION

November 1959

U. S. NAVAL RESEARCH LABORATORY
Washington, D.C.

CONFIDENTIAL

SECURITY

This document contains information affecting the national defense of the United States within the meaning of the Espionage Laws, Title 18, U.S.C., Sections 793 and 794. The transmission or the revelation of its contents in any manner to an unauthorized person is prohibited by law.

SUMMARY OF NAVY STUDY PROGRAM FOR F4H-1 WEAPON SYSTEM

(Unclassified Title)

VOLUME IX

J. C. Ryon C. M. Loughmiller
I. N. Bellavin R. L. Lister

NOVEMBER 1959

NAVY DEPARTMENT
NAVAL RESEARCH LABORATORY
RADAR DIVISION

ABSTRACT

(Confidential)

The Naval Research Laboratory is serving as technical directors of the Navy's Air to Air Missile Study. The results are presented in a series of volumes under NRL Memorandum Report 754. This volume is the ninth in the series. The study to date has been primarily concerned with the system employing the F4H-1 aircraft, the AN/APQ-72 radar and the Sparrow III6a missile. This volume represents a continuation of the study results presented in preceding volumes.

PROBLEM STATUS

This is an interim report; work on the problem is continuing.

AUTHORIZATION

NRL Problem 53R05-04
BuAer No. EL-42001

CONTENTS

TABLE OF CONTENTS (Cont)

LIST OF FIGURES

LIST OF FIGURES (Cont)

LIST OF FIGURES (Cont)

LIST OF FIGURES (Cont)

SUMMARY OF NAVY STUDY PROGRAM FOR F4H-1 WEAPON SYSTEM

INTRODUCTION

The Bureau of Aeronautics has contracted with the Naval Research Laboratory to conduct system studies directed toward establishing the tactical use capability of Navy Air to Air Missile Systems. These studies are conducted under the technical direction of the Naval Research Laboratory with all inputs derived from Navy sources. To date, study effort has been primarily directed toward revealing the tactical use capability of the F4H-1 Weapon System. In support of this effort, NRL has contracted with Westinghouse Air Arm Division for analytical services. Recommendations and conclusions to be drawn from analytical results are assumed to be a Navy responsibility, and in particular, the responsibility of the technical directors (NRL). This report is the ninth in a series directed toward revealing the tactical effectiveness of the F4H-1 Weapon System.

The Navy study has been and will continue to be a cooperative effort. Wherever possible, duplication has been avoided. Input data for the study has been obtained from the government facilities, which most logically would cover the particular field. For example, radar test data was obtained from NATC, Patuxent; Sidewinder performance data has been obtained from NOTS, Inyokern; and Sparrow III seeker performance data has been obtained from NMC, Pt. Mugu. In addition, the facilities of the various activities have been, in effect, pooled so that special talents and equipments can be employed. The results of NMC simulator studies to ascertain the allowable launch error for Sparrow III, and the effects of hydraulic oil limits have been incorporated in the overall study. In addition, NMC has conducted tests to verify the vectoring accuracies used in this study. They have conducted tests to determine if the field degradation applied to AI radar detection range in this study is valid. It is very important that everyone concerned recognize that a study such as this must be a team effort. It is every bit as important to continue this team effort on future studies under this program (Sparrow III6b and Eagle).

The study results to date have been presented in Vols. I, II, III, IV, VII and VIII of this series (references 1 thru 6). The study effort covered by these volumes carries the system through to Sparrow III6a

missile launch. At this point it is assumed that if the initial aircraft heading errors can be reduced to an acceptable launch error, the missile will fly perfectly to impact with the target. This volume presents a continuation of the effort. It is intended to present material not covered by the preceding volumes in such a fashion that the entire picture of system operation, up to the point of missile launch, will have been covered. The primary phases of investigation covered by this volume are:

1. System performance under perfect vectoring conditions in co-altitude attacks.

2. System performance under perfect vectoring conditions in pull-up attacks.

3. System performance under expected tactical conditions in co-altitude attacks.

   a. Nonmaneuvering targets
   b. Maneuvering targets
   c. Penetration effects considered

4. System performance under expected tactical conditions in pull-up attacks.

All future study of the F4H-1 Weapon System (Sparrow III6a) will be devoted to simulation and study of the entire system loop, including simulation of the missile.

The material contained in this memorandum report is intended primarily for Bureau information. During the contract negotiation phase, it was agreed that all distribution, except for government activities, will be handled through the Bureau channels.

STUDY PROCEDURE

The basic outline for the Navy's study was given in Volume I. It will be repeated here in modified form for quick reference and for clarification of changes which have occurred during the program. Table I gives this modified outline of the Navy's Air to Air Missile Study Program. As originally planned, the outline was intended to be a general guide having

flexible elements in order that additionally needed study areas which developed as the study progressed could be included if desired. A second investigation, considered separately for contractual reasons, was planned to be essentially a repeat, for the Sparrow II missile, of Phases I thru V of the basic study. The Sparrow II study of Table I was postponed so that more pressing problems could be investigated. Initial study effort considered the Sparrow III on the F8U-3 aircraft. Since there is no longer any competition between the two aircraft, the considerations of the F8U-3 have been dropped from the study program. In addition, Sparrow X will not be studied as originally intended, because of contract cancellation.

As listed in Volumes I and III, a working framework for the study, which consists of six parts, has been constructed against which the performance of each system combination is analyzed. This framework is repeated here:

Part 1: Development of effective theoretical co-altitude attack zones under ideal conditions.

Part 2: Development of effective theoretical non co-altitude attack zones under ideal conditions.

Part 3: Development of effective thoretical attack zones in the presence of the degradation of expected tactical conditions.

Part 4: Repeat Part 3 for possible improvements to the systems which are being considered by the Navy.

Part 5: Study to determine and assess realizable improvements.

Part 6: Study of infrared (IR) tie-in for AI fire control systems.

The material presented in Volumes I and III of this series was grouped to fit this framework. Most of this material will not be presented here. However, new results will be fitted into the appropriate phase in the framework.

TABLE I

OUTLINE OF NAVY AIR TO AIR MISSILE SYSTEM STUDY PROGRAM

PHASE I System Performance Under Ideal Conditions

A. Aircraft Characteristics

F4H-1

B. Altitudes (co-altitude case)

1. 1000 ft or less
2. 30,000 ft
3. 50,000 ft

C. Interceptor Velocity

F4H-1 at altitude (V_{max} and V_{cruise})

D. Target to Interceptor Speed Ratio for Interceptor at V_{max}

1. 0.45
2. 0.8
3. 1.0

} Some cases may be trivial and will not be used

Target speed resulting from above will be used for interceptor at V_{cruise}.

E. Conditions

1. Perfect vectoring
2. Straight line flight path
3. Current AI detection capability
4. B-47 size target
5. Preparation time - two cases determined by study
6. Sparrow III - capability of current seeker is to be used
7. Sparrow III - aerodynamic capability of current missile is to be used
8. Gimbal angle limits in F4H-1 aircraft
   a. APQ-72
   b. Seeker
9. Illumination consideration - geometry of keeping both target and missile illuminated. Illumination requirements to be determined by study.

PHASE II — System Snap-up Performance Under Ideal Conditions

A. A, C, D, and E - same as Phase I

B. Altitudes (snap-up case)

1. Target

a. 30,000 ft
b. 50,000 ft
c. 65,000 ft

2. Interceptor altitude - to be determined by study of system capability

PHASE III — System Performance Under Expected Tactical Conditions

A. Target maneuver

B. Vectoring accuracy

C. Weather

D. Limits imposed by interceptor tactics

1. Climb capability
2. Endurance
3. Dead time

E. Countermeasures

1. Airborne weapons system

PHASE IV — System Performance Under Expected Tactical Conditions with Addition of Currently Proposed Improvements

A. Improvements proposed:

1. Search volume optimization
2. Triangle system vectoring
3. Automatic alarm
4. Improved receiver noise figure
5. Back-biased range and display IF amplifier with broad-band switching
6. Gated narrowband angle track IF amplifier (home on jam)

7. Bright display
8. Provision for switching polarization (circular and vertical)
9. Broadbanding of the plumbing
10. Jittered PRF
11. Antenna with high altitude feed
12. Improved two-speed AFC
13. Relocation of CW injection plumbing to increase gimbal angle in elevation
14. Nonsaturating AGC

PHASE V Study to Determine and Assess Realizable System Improvements

A. AI Radar

B. Missile

C. Vectoring

D. Tactics

PHASE VI Study of IR Tie-in with the Fire Control System

PHASE VII Performance Capability of Sparrow III with an IR Seeker

PHASE VIII Repeat Study Phase I Through Phase VI for the Sidewinder

F4H-1 WEAPON SYSTEM PERFORMANCE UNDER IDEAL CONDITIONS - INPUT DATA

The system analysis under "ideal" conditions, which was started in Volume I, is continued here. As stated in Volume I and III, the resulting performance will indicate a capability representative of the best that can be achieved with high probability. The target is nonmaneuvering and the vectoring is perfect. However, "ideal" should be interpreted in a limited sense, since the performance of the weapon system subelements is defined by realizable rather than infinite quantities.

Radar Analyses

In Volumes I and III, the characteristics of the radar defined at that time as the 62 lot AN/APQ-72 were given. This radar is now known as the XN-2. Attack zones resulting from the use of this radar were presented for high, medium and low altitude targets. Detailed parameter plots for attacks made under these ideal conditions have been presented in Volumes VII and VIII.

In preceding volumes of this study, the investigation of radar performance influence on system capability under ideal conditions has been divided into two phases; performance of the XN-2 radar and performance of an improved AN/APQ-72. It is now believed that the performance of the improved APQ-72 will be available in the F4H-1 Weapon System in the XN-3 radar. For this reason, the results presented in this volume for the ideal attack conditions are restricted to those resulting from the XN-3 radar. The 85% probability of detection range for this radar against a B-47 size target flying at M 1.6 at 50,000 ft where $V_T / V_F = 0.8$ is shown by Fig. 1. Head-on, this radar has an 85% probability of detection at approximately 19 naut mi.

Aircraft Analyses

The performance of the F4H-1 aircraft has been detailed in Volumes I thru IV of this series. No changes in this performance has occurred during the study period covered by this report.

Missile Analyses

Data describing the performance of the Sparrow III missile used in the Navy's Air to Air Missile Study has been presented in preceding volumes.

Changes in input data related to this missile that have been entered into the study program are increased seeker lock-on range and increased minimum aerodynamic range (R_{min}). Figure 2 shows the 90% probability of seeker lock-on against a B-47 size target for the missile studied. This is the result of NMC tests (reference 7) scaled to the B-47 size target. It is seen that the seeker has a 90% lock-on capability against the B-47 size target, head-on, of 6.82 naut mi.

It is recognized that changes in aerodynamic performance of the Sparrow III 6a missile are occurring. The only change that has been incorporated into the study effort covered by this volume is R_{min} which is represented by the equation $R_{min} = R_2(h) + T_2V_c$. T_2 has been changed from 3.3 seconds to 4.3 seconds. $R_{2(h)}$ remains as shown on Fig. 15 in Volume I of this series of reports. Current simulation programming is taking into consideration the effects of all changes in the aerodynamic performance.

PHASE I - SYSTEM PERFORMANCE UNDER IDEAL CONDITIONS-HORIZONTAL ATTACKS

In Volumes I and III the effective attack zone overlays for the F4H-1 Weapon System (when employing the XN-2 radar) have been given. These results will not be repeated here. Figures 3 and 4 give the effective attack zone overlays when the XN-3 radar (19 naut mi detection range against head-on aspect of B-47 size target) and the improved seeker range (6.82 naut mi lock-on range head-on against B-47 size target) are employed.

Attack Zones

Figure 3 gives the resulting effective attack zone for a horizontal attack which occurs at 50,000 ft altitude. The interceptor is flying under V_{max} conditions (1940 ft/sec) and the speed ratio $V_T/V_F = 1.0$. Referring to this figure it is seen that the effective attack zone for high probability of success has an outer limit set by the Sparrow III seeker range (curve F), the 6.5 naut mi missile range interlock (curve G), and R_{max} (curve C). The inner boundary is set by the minimum aerodynamic range of the missile (R_{min}), and $N_z = 3$ (curve E). The approach courses are restricted for successful attacks to those between head-on and 68° off the target's nose. All others fail because of a lack of speed advantage.

Figure 4 shows the results for horizontal attacks made under the same conditions as those of Fig. 3, except the target speed has been reduced so that the speed ratio (V_T/V_F) is 0.8. The effective attack zone is essentially the same as that on Fig. 3. The inner boundary is now determined by R_{min}; around-the-clock attacks can be made. However, penetration distances are great due to low speed advantage.

As has been stressed in preceding volumes, the above two figures present the results for horizontal attacks made under "ideal conditions. When additional system settling time, beyond that required for AI radar

lock-on is considered, much of the effective attack zone in the forward hemisphere is eliminated. The Navy study has used 27 seconds as a mean settling time. This is arrived at from many simulator runs. Referring to Fig. 3, it is seen that if a line is drawn through the 27 second points on each run, much of the effective attack zone is eliminated.

Remaining Study

The results presented in this and preceding volumes for the horizontal attacks made under "ideal" conditions essentially concludes the study effort to be applied to this phase as related to the Sparrow III 6a. Any additional reporting on this phase will be restricted to introducing changes in aerodynamic performance of the missile.

PHASE II - SYSTEM CAPABILITIES FOR PULL-UP ATTACK UNDER IDEAL CONDITIONS

In Volumes I and III the pull-up capabilities of the F4H-1 Weapon System when employing either the XN-2 or the APQ-72 (XN-3) radar were presented. No additional results for the system employing the XN-2 radar will be presented in this volume. In addition, all results are for the system using the improved missile seeker lock-on range of Fig. 2. The intent of presenting additional results for this phase of the study is to give a complete picture of the resulting system capability under ideal conditions when attacks are started from any target aspect.

Conditions

The conditions of the pull-up attack investigation for this phase of the study are as follows:

a. Aircraft characteristics - F4H-1

b. Target altitudes - 50,000 and 65,000 ft

c. Interceptor altitudes - as capable from below

d. Reflective area - B-47 size target, assumed the same as for co-altitude case

e. Velocities - interceptor velocity at altitude, V_{max} and V_{cruise}

f. Target to interceptor speed ratios for interceptor at V_{max} - 0.8, 1.0. Resulting target speeds from above also used for interceptor at V_{cruise}

g. Perfect vectoring

h. Straight line flight path (target)

i. Current AI detection capability - 85% probability at 19 naut mi (head-on aspect B-47)

j. Time from detection to lock-on - 10 seconds

k. Seeker capability - current Sparrow III

l. Missile aerodynamics - current Sparrow III

m. Gimbal angle limitations of improved APQ-72 (XN-3) radar - ± 57° azimuth and elevation

n. Interceptor restricted to 3g pull-up or $C_{L_{max}}$ during tracking portion of the run

o. Allowable heading error for launching Sparrow III - 10°

For these around the clock attacks, it is assumed that the interceptor continues on the vectored pure collision course until pull-up occurs. While different doctrines have been proposed for pull-up attacks, one advantage of continuing on the pure collision course is reduction of penetration distance. Examples of other attack doctrines will be given later in the report as illustrations. Detections are assumed to occur on the 85% detection probability curve given by Fig. 1. Lock-on is assumed to occur 10 seconds later, but is further limited by the 50 naut mi maximum lock-on range of the improved radar.

A lead pursuit course is maintained by the interceptor after launch to provide illumination of the target. If the acceleration requirements of the course exceed the capability of the interceptor a $C_{L_{max}}$ course is flown. At impact it is assumed that the interceptor is maneuvered so that the lift vector and the gravity vector are working together (rapidly redirecting the interceptor downward). To date the recovery problem has received only superficial coverage. The investigation of recovery was done separately from the actual computer runs and detailed in Appendix II of Volume IV. On the computer runs the interceptor was allowed to follow a lead pursuit run as restricted by $C_{L_{max}}$ after impact. During this portion of the run the 3g limitation is removed because it is possible for the pilot to pull more g's when he is not trying to solve a fire control problem. If during the breakaway portion of the run a minimum L/W of 0.5 is maintained the run is considered successful. During this portion of the run the accelera-

tion conditions also must be such that C_{Lmax} is not exceeded. Two major simplifying assumptions are made. The first is that the pilot can fly a perfect C_{Lmax} course. This will yield optimistic results as far as recovery problems are concerned. The second simplification is that during the critical part of the recovery maneuver, thrust is assumed equal to drag. The inaccuracies resulting from these simplifications can be resolved only by more exact investigation. The method used represents a simplified approach to the problem.

Attack Zones

Figures 5 thru 34 show the resulting effective pull-up zones for these "ideal" pull-up attacks. The conditions of Fig. 5 are that of a target flying at 65,000 ft at M 2.0. The interceptor makes head-on pull-up attacks under V_{max} conditions from the range, and altitude conditions shown by the labeled points.

Referring to Fig. 5, zero time delay corresponds to AI radar detection range (19 naut mi). Throughout the Navy's study, a 10 second AI radar lock-on time has been used. As stated in previous volumes, it is believed that the pilot will not know how to initiate a pull-up attack prior to AI lock-on (10 second delay). Therefore, one boundary on the effective pull-up zone is that shown by the solid line at 10 seconds. If the interceptor must be able to reduce the initial heading error to 10° within the launch boundaries described previously, the effective pull-up zone is enclosed by the solid lines on Fig. 5. Pull-ups made from 58,000 ft at 10 and 15 second time delay are successes (error reduced to 0°). A pull-up attack from 58,000 ft and 20 second time delay is a failure (minimum error of 13°). The run initiated from 15 second time delay at 55,000 ft is marginally successful (ϵ = 9°).

Figure 6 gives the results when the interceptor approach course is from 15° off the target's nose (target aspect angle τ_o = 15°). The left-hand graph of Fig. 6 gives the results for pull-up attacks initiated with the interceptor operating at V_{max} conditions. The right-hand graph gives the results when the attacks are initiated with the interceptor operating under V_{cruise} conditions. All other conditions are the same as those of Fig. 5. Referring to the left-hand graph, it is seen that when the fighter initiates the pull-up attacks under V_{max} conditions, there is a very restricted pull-up zone against this M 2.0 target. The pull-up runs initiated at 58,000 ft and 15 second time delay, and at 55,000 ft

and 10 second time delay were failures. The primary reason that the effective pull-up zone is reduced compared to that of Fig. 5 is that at $\tau_o = 15°$, the AI detection range is smaller than for head-on (see Fig. 1). Thus, there is less time available for reducing errors. When the fighter speed is reduced to V_{cruise} at pull-up, all runs were failures because $\epsilon > 10°$ (see right-hand graph).

When the approach aspect angle is changed to $\tau_o = 30°$, the results are as shown on Fig. 7. Referring to the graph at the left of this figure, it is seen that when the interceptor initiates the pull-up attack while flying under V_{max} conditions, the pull-up zone is increased in size over that presented for the case of $\tau_o = 15°$. The reason for this is that there is more time available to make the pull-up attack (longer AI detection range as shown on Fig. 1 and slower closure rate). The runs which were failures (shown by ◈) failed because of $\epsilon > 10°$, $\lambda > 57°$, or the interceptor was unable to close on the target to R_{max}. It is interesting to note the trend at lower altitude. The reason for the zone at the lower altitudes is that the interceptor is flying slower and can maneuver faster to reduce the initial heading error, and to avoid gimbal angle problems.

Referring to the graph on the right side of Fig. 7, it is seen that when the interceptor initiates the attacks while flying at V_{cruise} no pull-up capability exists. The primary reasons for failures were $\lambda > 57°$, and lack of a speed advantage.

When the approach course is changed to that corresponding to $\tau_o = 45°$, the results are as shown on Fig. 8. It is seen that reduction of closure rate is now playing a significant part in the resulting effective pull-up zone. This zone, shown by the solid line, is increased markedly both in differential altitude and pull-up delay time. For example, at 58,000 ft the interceptor can initiate successful pull-up attacks from delay times of 10 seconds out to delay times of approximately 30 seconds. It is also seen that successful pull-up attacks can be initiated from 58,000 ft down to approximately 16,000 ft altitude.

It is to be noted that some of the runs, particularly for long pull-up delays, were failures because of excessive gimbal angle requirements in azimuth. For example, the pull-up run made from 20,000 ft altitude and 25 second delay failed because of R_{max} and $\lambda_a > 57°$. To investigate the

effect of steering in azimuth-only between lock-on and pull-up, this particular pull-up attack was rerun. The results will be discussed later (Table III).

Graphs are not presented for the case of $\tau_o = 45°$ while the interceptor is operating at V_{cruise}, since it is obvious that all runs would be failures because of lack of speed advantage.

Figure 9 gives the results for the case of $\tau_o = 60°$. For this situation all runs were failures because of $\lambda > 57°$ and lack of a speed advantage. It is obvious that against this high speed target it would be useless to examine additional situations for larger τ_o (aspect angles).

Figures 10 thru 19 give the results of pull-up attacks made under the same conditions as described for the preceding figures, except for the target velocity which is arbitrarily reduced to M 1.6. When the approach aspect is head-on ($\tau_o = 0°$) the results are as shown on Fig. 10. Comparing these results to those given previously for the M 2.0 target (Fig. 5), it is seen that the effective pull-up zone (bound by the solid line) is appreciably increased. Successful pull-ups can be made from differential altitudes of approximately 25,000 ft. For the case of the interceptor initiating attacks from 58,000 ft altitude, successful pull-ups can be made with time delays up to approximately 23 seconds. It is important to note that even though the zone has been increased, the situation is still extremely marginal when settling times associated with other than the "ideal" situation are considered. This will be discussed in more detail under the section on Pull-up Attacks Under Expected Tactical Conditions.

When τ_o is increased to 15° the results are as shown on Fig. 11. For the case of $V_F = V_{Fmax}$ shown at the left on Fig. 11, the resulting effective pull-up zone is reduced appreciably from that available for the head-on situation (see Fig. 10). This is due to reduced time available because of lower AI radar detection ranges (see Fig. 1). The primary reason for failure is due to the inability of the interceptor to reduce the error to an acceptable value for missile launch ($\epsilon > 10°$). When the interceptor initiates pull-ups under V_{cruise} conditions, the results are as shown on the right-hand graph of Fig. 11. The system has no pull-up capability ($\epsilon > 10°$).

Figure 12 shows the results when τ_o is increased to 30° with all other conditions the same as for the preceding figure. Comparing these results to those obtained against the M 2.0 target (see Fig. 7), it is seen that the same trend occurs. Looking at the graph to the left of Fig. 12, it is seen that there is an effective pull-up zone for attacks initiated at high altitude. At altitudes around 30,000 ft the interceptor cannot make a successful pull-up. Then, at low altitudes there is another effective pull-up zone. Each of the zones are slightly larger than those of Fig. 7 due to the fact that the closure rate is reduced (slower target). The reasons for failures were excessive error and inability to reach the maximum aerodynamic range of the missile. When the interceptor speed at pull-up corresponds to V_{cruise} the results are as shown to the right of Fig. 12. There is no pull-up capability. The primary reasons for failure were excessive gimbal angle ($\lambda > 57°$), and lack of a speed advantage.

When the approach aspect corresponds to $\tau_o = 45°$ the resulting effective pull-up attack zone is as shown on Fig. 13 by the solid line. Comparing these results to those given previously for the M 2.0 target (see Fig. 8), it is seen that the widths of the effective pull-up zones are approximately the same. However, reducing the target velocity allows effective pull-up attacks to be made from slightly greater differential altitudes.

The zone bound by the solid line on Fig. 14 gives the resulting effective pull-up attack zones against this M 2.0 target when $\tau_o = 60°$. This zone is approximately 35 sec wide and covers the altitude range from approximately 15,000 ft to 58,000 ft. The primary reasons for failure are excessive error and excessive gimbal angle. Comparing these results to those given previously for the M 2.0 target on Fig. 9, it is seen that having a speed advantage changes the situation from one of no pull-up capability to one of having a significant pull-up zone available. Referring to the pull-up runs on Fig. 14, which were initiated from long pull-up delays (45 sec), and altitudes in the region between 15,000 ft and 30,000 ft, it is seen that one of the reasons for failure was the requirement for excessive azimuth gimbal angle ($\lambda_a > 57°$). Two of these pull-up runs (the one originating from 30,000 ft altitude and 45 sec delay, and the one originating from 20,000 ft altitude and 45 sec delay) were re-examined to determine the effect on pull-up capability of changing the doctrine from flying a pure collision course between lock-on and pull-up to steering in azimuth-only between lock-on and pull-up. The results are detailed in Table III.

When the approach aspect is increased toward $\tau_o = 180°$, the results are as shown on Figs. 15 thru 19. For each of these cases there are large effective pull-up zones. However, as we approach the tail aspect the penetration distances get large because of the low closure rates involved. An indication of extent of these penetration distances can be obtained by referring to Fig. 4. Figure 15 shows the results for the case of $\tau_o = 75°$. The extent of the effective pull-up zone is shown by the area enclosed by the solid line. Referring to this figure, one interesting new trend is observed. The inner bound on the effective pull-up zone is no longer the AI radar lock-on range (10 sec pull-up delay). If the pilot attempts a pull-up too soon after lock-on, the runs fail because the intereceptor is unable to maintain the climb attitude required to close the range to R_{max}. It is also interesting to note that 58,000 ft altitude is no longer the upper limit on effective pull-ups. Runs which are initiated from this altitude fail because of excessive azimuth gimbal angle ($\lambda_a > 57°$). When the pull-up runs are started from an initial approach aspect of $\tau_o = 90°$, the resulting effective pull-up zone is as shown on Fig. 16. The same trend as described above for the $\tau_o = 75°$ case prevails for this case. Comparing these results with those of Fig. 15, it is seen that the inner bound is pushed even further out in time. The pilot, would have to wait approximately 230 sec or longer after AI radar lock-on before starting pull-up or the interceptor will not be able to maintain the climb attitude required to close to R_{max}. The reason for the greater difference in delay times from which pull-ups can be made is that the detection range at 90° is much larger than at 75°. Thus, the interceptor has to close over a greater range.

When the initial aspect angle is changed to $\tau_o = 120°$, the results are as shown on Fig. 17. The delay time before successful pull-ups can be made is not as great as for the case of $\tau_o = 90°$ (see Fig. 16) because the detection range is not as large. However, inability of the interceptor to close to R_{max} is playing a more prominent part in causing run failures particularly at the lower altitudes. The upper limit on effective pull-up zone, as in the cases of $\tau_o = 75°$ and 90°, is no longer a straight line drawn at 58,000 ft. However, the reason for the limit is slightly different. On the preceding figures, the primary reasons for failures at the higher altitudes is that the gimbal angles were excessive. In the results shown on Fig. 17, the upper limit is due to inability of the interceptor to close to R_{max}. The upper limit in the zone, shown by the solid line, is slanted and would eventually intersect the 58,000 ft altitude line. If the delay times are long enough the interceptor will

close to R_{max} and can complete a successful pull-up. Two sample runs from this figure will be re-examined to see the effect of changing the doctrine to permit the pilot to steer in azimuth-only between lock-on and pull-up. The results will be shown on Table III.

Figure 18 shows the results when τ_o is increased to 150°. The resulting effective pull-up zone has the same general shape as that of the preceding figure. The reasons for failures are the same. However, it is important to note the large delay times required before the interceptor can make a successful pull-up. Penetration distances will be large. Figure 19 shows the results of increasing τ_o to 180°. Again the penetration distances (large delay times required) will be large.

Figures 20 thru 34 show the results of pull-up attacks made under "ideal" conditions when the target altitude is reduced to 50,000 ft. Figure 20 shows the results of pull-up attacks against a M 2.0 target flying at 50,000 ft. The approach aspect is head-on ($\tau_o = 0°$). The effective pull-up zone is again enclosed by the solid line. Successful pull-ups can be made from differential altitudes of 17,000 ft. A new reason for failure is shown on this figure. The co-altitude run made with a 25 sec delay failed because the interceptor was inside of the minimum aerodynamic range of the missile (R_{min}). The last launch point (missile launch prior to R_{min}) is shown on the figure at 22.5 seconds delay. When τ_o is increased to 15° the results are as shown on Fig. 21. When the interceptor initiates the attack under V_{max} conditions, the pull-up zone shown on the left-hand graph of Fig. 21 is obtained. It is seen that the primary limitation is one due to the inability to reduce the error to an acceptable limit ($\epsilon > 10°$). For the co-altitude situation (both target and interceptor at 50,000 ft) the limit is due to R_{min}. Ten seconds after lock-on, the interceptor would be inside of R_{min}. When the interceptor begins the pull-up attacks under V_{cruise} conditions the results are as shown at the right of Fig. 21. Comparing this to the corresponding case for the 65,000 ft altitude target (see Fig. 6), it is seen that there is a major change in effective attack zone. Against this 50,000 ft altitude target, successful pull-ups can be made from differential altitudes of 25,000 ft. The primary reason for failure is excessive error. It is of interest to examine the co-altitude situation. It is seen that errors of 5° and 19° are obtained at 20 and 25 secs pull-up delay respectively. These errors result from the criteria that is used throughout the pull-up investigation reported. It is assumed that the interceptor continues on the vectored course (pure collision) until

pull-up. In the co-altitude situation, the pilot would certainly zero the "dot" as soon as possible. If this is the case, the limiting factor would be R_{min}.

When the approach aspect is increased to $\tau_o = 30°$, the results are as shown on Fig. 22. The case where $V_F = V_{Fmax}$ is shown at the left of Fig. 22. The limiting factors on successful pull-ups are $\epsilon > 10°$, R_{min} and $\lambda > 57°$. The graph at the right of Fig. 22 shows the results when $V_F = V_{cruise}$ at the beginning of pull-up. Under these conditions all runs were failures because of excessive gimbal angles and lack of a speed advantage. The remaining cases for the M 2.0 target flying at 50,000 ft are shown on Figs. 23 and 24. The last case examined is that shown by Fig. 24 ($\tau_o = 60°$). It is seen that the system has no pull-up capability because of excessive gimbal angles. For any approach aspect beyond this point, this system will be either limited by gimbals or lack of a speed advantage.

When the target speed is reduced to M 1.6 at 50,000 ft altitude, the results are as shown on Figs. 25 thru 34. For the head-on situation, shown on Fig. 25, it is seen that successful pull-up attacks can be made from differential altitudes of 50,000 ft. The primary reasons for failures were $\epsilon > 10°$, R_{min}, R_{max}, and $L/W < 0.5$. The trend in the pull-up attacks for the various τ_o situations examined for this M 1.6 target at 50,000 ft (see Figs. 26 thru 34) is, in general, the same as that described previously for the M 1.6 target flying at 65,000 ft. However, there is one detail that should be explained. For example, on Fig. 31, a new limitation (R_{LO}) enters the picture. This represents the limitation due to the radar's inability to lock on targets at ranges greater than 50 naut mi.

The results of the pull-up attacks made under the ideal conditions are summarized on Table II.

TABLE II

PULL-UP ATTACKS UNDER "IDEAL" CONDITIONS

Interceptor Velocity at Pull-up	Initial Target Aspect Angle (τ_o)	Primary Reasons for Failure	Comments
		Target Velocity - M 2.0 Target Altitude - 65,000 ft	
V_{max}	Head-on	$\epsilon > 10°$	Successful pull-ups from differential altitudes of 15,000 ft.
V_{max}	15°	$\epsilon > 10°$	Marginal zone available
V_{cruise}	15°	$\epsilon > 10°$	No pull-up capability
V_{max}	30°	$\epsilon > 10°$, $\lambda > 57°$, R_{max}	Successful pull-up zone available
V_{cruise}	30°	$\lambda > 57°$, lack of speed advantage	No pull-up capability
V_{max}	45°	$\epsilon > 10°$, $\lambda_a > 57°$, R_{max}	Successful pull-ups from differential altitudes of 48,000 ft
V_{max}	60°	$\lambda > 57°$, lack of speed advantage	No pull-up capability
		Target Velocity - M 1.6 Target Altitude - 65,000 ft	
V_{max}	Head-on	$\epsilon > 10°$	Successful pull-up zone available
V_{max}	15°	$\epsilon > 10°$	Marginal zone available
V_{cruise}	15°	$\epsilon > 10°$	No pull-up capability
V_{max}	30°	$\epsilon > 10°$, R_{max}	Successful pull-up zone available
V_{cruise}	30°	$\lambda > 57°$, lack of speed advantage	No pull-up capability

TABLE II (cont)

Interceptor Velocity at Pull-up	Initial Target Aspect Angle (τ_o)	Primary Reasons for Failure	Comments
V_{max}	45°	$\epsilon > 10°, \lambda_a > 57°, R_{max}$	Successful pull-ups from differential altitudes of 52,000 ft
V_{max}	60°	$\epsilon > 10°, \lambda > 57°$	Successful pull-ups from differential altitudes of 50,000 ft
V_{max}	75°	$\epsilon > 10°, \lambda > 57°, R_{max}$	Successful pull-up zone available; penetration distance enters picture
V_{max}	90°	$\epsilon > 10°, \lambda > 57°, R_{max}$	Pull-up zone available; penetration distances critical; early pull-ups cause failures
V_{max}	120°	$\epsilon > 10°, \lambda_e > 57°, R_{max}$	Pull-up zone available; penetration distances critical; early pull-ups cause failures
V_{max}	150°	$\epsilon > 10°, \lambda_e > 57°, R_{max}$	Pull-up zone available; penetration distances unacceptable; early pull-ups cause failures
V_{max}	180°	$\epsilon > 10°, \lambda_e > 57°, R_{max}$	Pull-up zone available; penetration distances unacceptable; early pull-ups cause failures
		Target Velocity - M 2.0 Target Altitude - 50,000 ft	
V_{max}	Head-on	$\epsilon > 10°$	Successful pull-ups from differential altitudes of 17,000 ft
V_{max}	15°	$\epsilon > 10°, R_{min}$	Marginal zone available
V_{cruise}	15°	$\epsilon > 10°, \lambda > 57°$	Successful pull-ups from differential altitudes of 25,000 ft

TABLE II (Cont)

Interceptor Velocity at Pull-up	Initial Target Aspect Angle (τ_o)	Primary Reasons for Failures	Comments
V_{max}	30°	$\epsilon > 10°$, $\lambda > 57°$, R_{min}	Successful pull-ups from differential altitudes of 34,000 ft
V_{cruise}	30°	$\lambda > 57°$, lack of speed advantage	No pull-up capability
V_{max}	45°	$\epsilon > 10°$, $\lambda_a > 57°$, R_{max}	Successful pull-ups from differential altitudes of 34,000 ft
V_{max}	60°	$\lambda > 57°$, lack of speed advantage	No pull-up capability
		Target Velocity - M 1.6 Target Altitude - 50,000 ft	
V_{max}	Head-on	$\epsilon > 10°$, L/W < 0.5, R_{max}, R_{min}	Successful pull-ups from differential altitudes of 50,000 ft
V_{max}	15°	$\epsilon > 10°$, R_{min}	Marginal zone available
V_{cruise}	15°	$\epsilon > 10°$, $\lambda_e > 57°$, R_{max}	Pull-up zone available
V_{max}	30°	$\epsilon > 10°$, R_{max}, R_{min}	Successful pull-ups from differential altitudes of 50,000 ft
V_{cruise}	30°	$\lambda > 57°$, lack of speed advantage	No pull-up capability
V_{max}	45°	$\epsilon > 10°$, R_{min}, R_{max}	Large pull-up zone available
V_{max}	60°	$\epsilon > 10°$, $\lambda_a > 57°$	Large pull-up zone available
V_{max}	75°	$\epsilon > 10°$, $\lambda_a > 57°$	Large pull-up zone available
V_{max}	90°	$\epsilon > 10°$, $\lambda_a > 57°$, R_{LO}	Large pull-up zone available

TABLE II (cont)

Interceptor Velocity at Pull-up	Initial Target Aspect Angle (τ_o)	Primary Reasons for Failure	Comments
V_{max}	120°	$\epsilon > 10°, \lambda > 57°$	Large pull-up zone available; penetration distances excessive
V_{max}	150°	$\epsilon > 10°, \lambda_e > 57°$ R_{max}, R_{min}	Large pull-up zone available; penetration distances excessive
V_{max}	180°	$\epsilon > 10°, \lambda_e > 57°$ R_{min}	Large pull-up zone available; penetration distances excessive

Effect of Steering in Azimuth-Only Between Lock-on Range and Pull-up Range

The preceding section presented the results of pull-up attacks made under "ideal" conditions. The attack doctrine used was that the interceptor flies a collision course between lock-on range and pull-up range. It is now of interest to investigate the effect on pull-up capability resulting from changing this doctrine to one where the pilot steers in azimuth-only between lock-on and pull-up. Sample pull-up runs, which have been presented previously on Figs. 8, 14 and 17 were rerun using the steering in azimuth-only doctrine. These results are shown on Table III. The first run given on Table III corresponds to one given previously on Fig. 8, the second two runs correspond to runs given previously on Fig. 14, and the last two runs correspond to runs given previously on Fig. 17. Referring to the results, it is seen that steering in azimuth-only does not solve the problem. In those cases where λ_a was the limitation, this restriction was removed but new ones, such as λ_e and excessive error (ϵ), were introduced. In general, steering in azimuth-only also causes the interceptor to be drawn around toward the tail of the target. This results in the interceptor being unable to close to R_{max}. Based on this limited look at the problem, one would question whether steering in azimuth-only is of any value as a tactical doctrine. Additional investigation of this problem will be discussed later in this report.

Remaining Study

The preceding sections described additional study effort beyond that presented in previous volumes on pull-up attacks under ideal conditions. The results presented along with those presented in Volumes I and III of this series should give the reader a good overall picture of system pull-up capability under these "ideal" conditions. No further study effort is intended for this phase.

PHASE III - F4H-1 WEAPON SYSTEM PERFORMANCE UNDER EXPECTED TACTICAL CONDITIONS - XN-2 RADAR

Probability of successful arrival to missile launch results when the system is employing the XN-2 radar have been presented previously in Volumes I and III of this report. These results have covered the co-altitude and pull-up attack cases. No further study of the system employing this unimproved radar is anticipated. Thus, this phase of the study is considered completed.

TABLE III

EFFECT OF STEERING IN AZIMUTH-ONLY BETWEEN LOCK-ON RANGE AND PULL-UP RANGE

Interceptor Alt. at Pull-up ($Ftx10^3$)	Interceptor Velocity	Pull-Up Delay (Secs)	Target Altitude ($Ftx10^3$)	Initial Target Aspect Angle τ_o	Target Velocity	Results - Pure Collision Course Until Pull-up	Results - Azimuth-Only Steering
20	V_{Fmax}	25	65	45°	M 2.0	Run failed; excessive azimuth gimbal requirements ($\lambda_a > 57°$); could not close range to R_{max}	Run failed; excessive elevation gimbal requirements ($\lambda_e > 57°$); could not close range to R_{max}
30	V_{Fmax}	45	65	60°	M 1.6	Run failed; excessive azimuth gimbal requirements ($\lambda_a > 57°$)	Run failed; excessive elevation gimbal requirements ($\lambda_e > 57°$); excessive error ($\epsilon = 70.7°$) could not close range to R_{max}
20	V_{Fmax}	45	65	60°	M 1.6	Run failed; excessive azimuth gimbal requirements ($\lambda_a > 57°$)	Run failed; excessive elevation gimbal requirements ($\lambda_e > 57°$); could not close range to R_{max}
30	V_{Fmax}	175	65	120°	M 1.6	Run failed; excessive elevation gimbal requirements ($\lambda_e > 57°$)	Run failed; could not close range to R_{max}
30	V_{Fmax}	180	65	120°	M 1.6	Run failed; excessive elevation gimbal requirements ($\lambda_e > 57°$)	Run failed; could not close range to R_{max}

PHASE IV - SYSTEM PERFORMANCE UNDER EXPECTED TACTICAL CONDITIONS - AN/APQ-72 (XN-3) RADAR

The preceding sections have extended the description of results for the "ideal" situation given previously in Volumes I and III of this series. The results given represent the best that one would hope to achieve with a high probability of success when certain sources of error are neglected. It is now of interest to look at the degradation resulting from a more realistic tactical situation. The degrading factors which have been considered in the study program are:

1. Vectoring accuracy
2. Target maneuver
3. Weather
4. Countermeasures agains the airborne weapon system
5. Limits imposed by interceptor tactics
   - (a) climb capability
   - (b) endurance
   - (c) dead time

Primary emphasis will be placed on items 1, 2, and 5 in the remainder of this report.

The input conditions, as related to vectoring accuracy, are the same as those used in preceding volumes of this study. The vectoring accuracies which have been used throughout the Navy's Air to Air Missile Study are:

$1\ \sigma = \pm 3$ naut mi - azimuth

$1\ \sigma = \pm 3$ naut mi - range

$1\ \sigma = \pm 1$ naut mi - altitude

Probability of Successful Arrival to Missile Launch - AN/APQ-72(XN-3) Radar

In Volume III of this series, the resulting proability of successful arrival to missile launch for co-altitude attacks occurring at 50,000, 30,000, and 1000 ft altitude were given. The study at that time was restricted to head-on, $\tau_0 = 30°$ and $60°$ interceptor approach courses. The AI radar 85% probability of detection was 19 naut mi head-on. The gimbal limits used were $\pm 57°$ in azimuth and elevation. The vectoring accuracy was $1\ \sigma = \pm 3$ naut mi in azimuth and range, and ± 1 naut mi in elevation.

The criteria for success was that the interceptor must be able to reduce the initial heading errors to $\epsilon \leq 10°$ between R_{max} and R_{min} of the missile. Once the missile is launched it is assumed to behave perfectly. The actual aerodynamics of the missile will be considered in a later phase of the study. The interceptor is vectored on a pure collision course and continues to fly this pure collision course until lock-on range. Maneuvers are restricted to 3g's or C_{Lmax}.

The results presented here are a continuation of the results presented in preceding volumes. The 30,000 ft altitude attack is examined in detail around-the-clock. Figure 35 shows the resulting probability curves for two speed conditions -- $V_T/V_F = 1.0$ and $V_T/V_F = 0.8$ where V_F = M 1.91. Examining the curve for $V_T/V_F = 1.0$ it is seen that the probability of successful arrival to missile launch is 75% head-on. The probability rises slowly to 87% at 30°. Beyond 45° the probability drops sharply. The reason this occurs is that gimbal angle problems are encountered and the interceptor lacks a speed advantage.

When target speed is reduced so that the speed ratio (V_T/V_F) equals 0.8, the probability of successful arrival to missile launch is uniformly high around the clock. However, penetration problems are ignored in the results presented on Fig. 35. This will be discussed in later sections of this volume. Referring to the curve for $V_T/V_F = 0.8$, it is seen that the probability of success is 85% for the head-on case (primary limit is lack of time). At 45° initial aspect angle, the probability of success is 97%. At 75°, the probability is reduced to 82% because of gimbal angle problems. Beyond 120° initial aspect angle, the probability is 100% if penetration is ignored.

Probability of Successful Arrival to Missile Launch - AN/APQ-72(XN-3) Radar - Maneuvering Target

The results of a preliminary investigation of the effects of target maneuvers on probability of successful arrival to missile launch was presented in Volume III of this series. The study at that time was limited to initial aspect angle approaches of $\tau_o = 0°$ to $\tau_o = 60°$. This volume extends these results to include around the clock attacks. The attack altitude is 30,000 ft. At lock-on, the target starts maneuvering. This maneuver consists of a 1 g lateral turn (L/W = 1.414), which crisscrosses the desired flight path, with a maximum deviation of target heading from this path of 30°. The resulting effects of target maneuvers on probability

of successful arrival to missile launch in co-altitude attacks is compared with the results presented previously for the nonmaneuvering target by the three curves on Fig. 36. These results are for the cases of $V_T/V_F = 1.0$. When the speed ratio is reduced to $V_T/V_F = 0.8$, the results are as shown on Fig. 37. Referring to these figures, it is seen that the degrading effect of the target maneuver studied is negligible. Table IV summarizes the probability of successful arrival to missile launch studies for co-altitude attacks against maneuvering and nonmaneuvering targets.

Probability of Successful Arrival to Missile Launch - AN/APQ-72(XN-3) Radar - Penetration Effects Considered

On Figs. 35 thru 37, the resulting probability of successful arrival to missile launch versus initial target aspect angle (τ_o) for co-altitude attacks against both maneuvering and nonmaneuvering targets were presented. However, target penetration effects were ignored. It is now of interest to determine what reduction in probability of successful arrival to missile launch occurs when penetration effects are considered. In Volume III the target penetration problem was examined. Variables considered were initial search radar range, system dead time, and speed ratio. The following is intended as a continuation of this study as applied to the probability of successful arrival to missile launch. The assumptions made are:

1. Initial target detection by AEW of surface search radar occurs at 300 naut mi from fleet center. In terms of capability available to date this range appears optimistic.

2. System dead time between initial target detection and the initial vectoring command to the interceptor is 3 minutes. Again, in terms of current capability this number appears to be optimistic.

3. The interceptor is on CAP at 100 naut mi from fleet center under cruise conditions. Acceleration toward V_{max} commences with vectoring.

4. The target carries 100 naut mi air to surface missiles. Thus, the minimum range at which the target must be shot down is 100 naut mi from fleet center.

5. During the vectoring phase the interceptor is restricted to 2g turns to reduce slowdown effects.

TABLE IV

PROBABILITY OF SUCCESSFUL ARRIVAL TO MISSILE LAUNCH - CO-ALTITUDE ATTACKS (30,000 FT) - MANEUVERING AND NONMANEUVERING TARGETS

Interceptor Velocity (Mach)	Speed Ratio V_T/V_F	Aspect Angle τ_o (Deg)	Probability of Successful Arrival to Missile Launch (%)		
			Nonmaneuvering Target	Initial Maneuver to the Right	Initial Maneuver to the Left
1.91	1.0	0	75	72	72
		15	84	81	87
		30	87	79	90
		45	86	88	88
		60	8	8	8
		75	0	0	0
		90	0	0	0
		120	0	0	0
		150	0	0	0
		180	0	0	0
	0.8	0	85	82	82
		15	93	91	95
		30	92	87	94
		45	97	95	97
		60	89	89	89
		75	82	82	82
		90	91	91	91
		120	100	100	100
		150	100	100	100
		180	100	100	100

Figure 38 shows the resulting probability of successful arrival to missile launch versus initial target aspect angle (τ_o) when target penetration is considered for two speed ratios (V_T/V_F = 1.0 and 0.8). Referring to the curve for V_T/V_F = 1.0 and comparing these to the corresponding results on Fig. 35 it is seen that penetration effects are negligible. The reason for this is that other parameters are the limiting factors (gimbal angle and lack of a speed advantage). In effect, for attacks occurring at $\tau_o = 60^\circ$ and larger, the target would reach the minimum range (its own weapon release range) whether penetration problems are considered or not since the interceptor does not have a speed advantage.

When the speed ratio is reduced to V_T/V_F = 0.8, the results, if penetration effects are considered, are as shown by the second curve on Fig. 38. Comparing this curve to the one given previously on Fig. 35 it is seen that around to aspect angles of 60° the results are essentially the same. However, from 60° aft the probability of success drops rapidly to zero. This is because the interceptor is pulled around onto a tail attack, thus large distances are involved in overtaking the target.

The resulting probability of successful arrival to missile launch for co-altitude attacks against maneuvering targets when penetration distances are considered as shown on Figs. 39 and 40. Tables V and VI show a comparison of the co-altitude attack probability of successful arrival to missile launch results.

Probability of Successful Arrival to Missile Launch - AN/APQ-72(XN-3) Radar - Pull-up Attacks

The next phase of the study is that of probability of successful arrival to missile launch for pull-up attacks. In preceding volumes of this report this phase of the study was restricted to head-on pull-up attacks. The results detailed in this volume extend the results presented previously to include around the clock attacks. The 85% probability of detection of the AI radar corresponds to that of the AN/APQ-72(XN-3) radar, and is 19 naut mi against a B-47 size, high-speed, head-on target aspect. The gimbal limits are ± 57° in azimuth and elevation. The vectoring distribution is the same as that used previously, 1 σ = ± 3 naut mi in azimuth. It is assumed that CIC is attempting to vector the interceptor on a pure collision course in azimuth and the vectoring inaccuracies are normally distributed about this pure collision

TABLE V

COMPARISON OF PROBABILITY OF SUCCESSFUL ARRIVAL TO MISSILE LAUNCH - NONMANEUVERING TARGET - CO-ALTITUDE ATTACKS (30,000 FT) - WITH AND WITHOUT TARGET PENETRATION CONSIDERATIONS

Interceptor Velocity (Mach)	Speed Ratio V_T/V_F	Aspect Angle τ_o (Deg)	Probability of Successful Arrival to Missile Launch (%)	
			Penetration Not Considered	Penetration Considered
1.91	1.0	0	75	75
		15	84	84
		30	87	87
		45	86	86
		60	8	0
		75	0	0
		90	0	0
		120	0	0
		150	0	0
		180	0	0
	0.8	0	85	85
		15	93	93
		30	92	92
		45	97	97
		60	89	89
		75	82	7
		90	91	0
		120	100	0
		150	100	0
		180	100	0

TABLE VI

COMPARISON OF PROBABILITY OF SUCCESSFUL ARRIVAL TO MISSILE LAUNCH - MANEUVERING TARGET - Co-ALTITUDE (30,000 ft) ATTACKS WITH AND WITHOUT TARGET PENETRATION CONSIDERATIONS

Interceptor Veloc. (Mach)	Speed Ratio V_T/V_F	Aspect Angle (deg) τ_o	Probability of Successful Arrival to Missile Launch (%)			
			Penetration Not Considered		Penetration Considered	
			Initial Maneuver to Right	Initial Maneuver to Left	Initial Maneuver to Right	Initial Maneuver to Left
1.91	1.0	0	72	72	72	72
1.91	1.0	15	81	87	81	87
1.91	1.0	30	79	90	79	90
1.91	1.0	45	88	88	88	79
1.91	1.0	60	8	8	8	0
1.91	1.0	75	0	0	0	0
1.91	1.0	90	0	0	0	0
1.91	1.0	120	0	0	0	0
1.91	1.0	150	0	0	0	0
1.91	1.0	180	0	0	0	0
1.91	0.8	0	82	82	82	82
1.91	0.8	15	91	95	91	95
1.91	0.8	30	87	94	87	94
1.91	0.8	45	95	97	95	97
1.91	0.8	60	89	89	89	89
1.91	0.8	75	82	82	32	7
1.91	0.8	90	91	91	0	0
1.91	0.8	120	100	100	0	0
1.91	0.8	150	100	100	0	0
1.91	0.8	180	100	100	0	0

course. No corrections are made in altitude or azimuth until AI radar lock-on (10 secs after detection). Upon lock-on the interceptor starts an immediate 3g pull-up until it is on a lead pursuit course. The criteria for success is that the error can be reduced to 10° or less between the R_{max} or R_{min} boundary without a requirement of load factor exceeding 3 or C_{Lmax}, the gimbal angles of the AI radar are not exceeded and a minimum recovery of L/W = 0.5 is encountered. The resulting probabilities of successful arrival to missile launch versus fighter altitude at which the pull-up was initiated are shown on Figs. 41 thru 74. A summary of these results are given on Table VII. Referring to this table, it is seen that the results are presented in families (separated by heavy lines). Within these families the fighter speed, target altitude, and target velocity are the same for all cases examined. The families are further subdivided into groups (separated by dashed line). Within these groups, the initial target aspect angles are the same for all runs examined. These groups are numbered IA, IB, IC....IIA...etc.

It is now of interest to examine several of these groups. Referring to group IA, it is seen that in head-on pull-up attacks the probability of successful arrival to missile launch against this high speed target flying at 65,000 ft is unacceptable for the cases when the interceptor initiates pull-up from altitudes below 50,000 ft. If, for the moment, we assume that the missile will have a resulting probability of 72%, that it will successfully guide and fuze (85% for guidance; 85% for fuzing) and that the overall desired or acceptable system probability of kill is 50%, then the probability of successful arrival to missile launch must be

$$0.50 \div 0.72 = 0.695 \text{ or } 69.5\%$$

For this condition even pull-ups from 50,000 ft are unacceptable.

Referring to group IC, when the target is flying at 65,000 ft under M 2.0 conditions, and the initial approach aspect is 30° off the nose of the target the probability of successful arrival to missile launch is unacceptable for all cases where pull-up is initiated from altitudes below approximately 45,000 ft if the criteria as above is used.

As has been stressed in the past volumes, the model selected is subject to "breakdown" under particular and in most cases unusual situations. Examples of such a situation are shown on Figs. 71 and 72.

TABLE VII

PROBABILITY OF SUCCESSFUL ARRIVAL TO MISSILE LAUNCH - PULL-UP ATTACKS

Groups	Interceptor Veloc.	Initial Interceptor Altitude ($Ftx10^3$)	Target Altitude ($Ftx10^3$)	Target Veloc. (Mach)	Initial Target Aspect Angle τ_o (deg)	Probability of Successful Arrival to Missile Launch (%)	Primary Reasons For Failures
IA	V_{Fmax}	20	65	2	Head-on	10	$\epsilon > 10^o$
	V_{Fmax}	30	65	2	Head-on	22.5	$\epsilon > 10^o$
	V_{Fmax}	40	65	2	Head-on	40	$\epsilon > 10^o$
	V_{Fmax}	50	65	2	Head-on	61.5	$\epsilon > 10^o$
	V_{Fmax}	58	65	2	Head-on	75	$\epsilon > 10^o$
IB	V_{Fmax}	10	65	2	15	0	
	V_{Fmax}	20	65	2	15	3	$\epsilon > 10^o$, $\lambda > 57^o$ L/W < 0.5
	V_{Fmax}	30	65	2	15	12.5	$\epsilon > 10^o$, $\lambda > 57^o$
	V_{Fmax}	40	65	2	15	28	$\epsilon > 10^o$
	V_{Fmax}	50	65	2	15	46.5	$\epsilon > 10^o$
	V_{Fmax}	58	65	2	15	80	$\epsilon > 10^o$
IC	V_{Fmax}	10	65	2	30	0	$\lambda > 57^o$, R_{max}
	V_{Fmax}	20	65	2	30	51	$\epsilon > 10^o$, $\lambda > 57^o$ R_{max}
	V_{Fmax}	30	65	2	30	53	$\epsilon > 10^o$, $\lambda > 57^o$
	V_{Fmax}	40	65	2	30	63.5	$\epsilon > 10^o$, $\lambda > 57^o$

TABLE VII (cont.)

Groups	Interceptor Veloc.	Initial Interceptor Altitude ($Ft \times 10^3$)	Target Altitude ($Ft \times 10^3$)	Target Veloc. (Mach)	Initial Target Aspect Angle τ_o (Deg)	Probability of Successful Arrival to Missile Launch (%)	Primary Reasons For Failures
	V_{Fmax}	50	65	2	30	78.5	$\epsilon > 10^o, \lambda > 57^o$
	V_{Fmax}	58	65	2	30	88	$\epsilon > 10^o, \lambda > 57^o$
ID	V_{Fmax}	10	65	2	45	0	$\lambda > 57^o$, R_{max}
	V_{Fmax}	20	65	2	45	46	$\lambda > 57^o$, R_{max}
	V_{Fmax}	30	65	2	45	75.5	$\lambda > 57^o$, R_{max}
	V_{Fmax}	40	65	2	45	86	$\lambda > 57^o$
	V_{Fmax}	50	65	2	45	86.5	$\lambda > 57^o$
	V_{Fmax}	58	65	2	45	59	$\lambda > 57^o$
IE	V_{Fmax}	10	65	2	60	0	$\lambda > 57^o$, R_{max}
	V_{Fmax}	20	65	2	60	0	$\lambda > 57^o$, R_{max}
	V_{Fmax}	30	65	2	60	25	$\lambda > 57^o$, R_{max}
	V_{Fmax}	40	65	2	60	25	$\lambda > 57^o$, R_{max}
	V_{Fmax}	50	65	2	60	25	$\lambda > 57^o$, R_{max}
	V_{Fmax}	58	65	2	60	0	$\lambda > 57^o$, R_{max}
IF	V_{Fmax}	10	65	2	70	0	$\lambda > 57^o$, R_{max}
	V_{Fmax}	20	65	2	70	0	$\lambda > 57^o$, R_{max}
	V_{Fmax}	30	65	2	70	8.5	$\lambda > 57^o$, R_{max}
	V_{Fmax}	40	65	2	70	8.5	$\lambda > 57^o$, R_{max}
	V_{Fmax}	50	65	2	70	8.5	$\lambda > 57^o$, R_{max}

TABLE VII (cont.)

Groups	Interceptor Veloc.	Initial Interceptor Altitude ($Ftx10^3$)	Target Altitude ($Ftx10^3$)	Target Veloc. (Mach)	Initial Target Aspect Angle τ_o (Deg)	Probability of Successful Arrival to Missile Launch (%)	Primary Reasons For Failures
	V_{Fmax}	58	65	2	70	0	$\lambda>57^\circ$, R_{max}
	M 0.9	25	65	2	0,15,30	0	
IIA	M 0.9	30	65	2	0,15,30	0	
	M 0.9	40	65	2	0,15,30	0	
	M 0.9	50	65	2	0,15,30	0	
	M 0.9	55	65	2	0,15,30	0	
	V_{Fmax}	0	65	1.6	Head-on	0	$\lambda>57^\circ$, R_{max}
	V_{Fmax}	10	65	1.6	Head-on	3.5	$\lambda>57^\circ$, R_{max} $L/W<0.5$
	V_{Fmax}	20	65	1.6	Head-on	45	$\epsilon>10^\circ$, R_{max}
	V_{Fmax}	30	65	1.6	Head-on	32	$\epsilon > 10^\circ$
IIIA	V_{Fmax}	40	65	1.6	Head-on	43.5	$\epsilon > 10^\circ$
	V_{Fmax}	50	65	1.6	Head-on	61	$\epsilon > 10^\circ$
	V_{Fmax}	58	65	1.6	Head-on	80	$\epsilon > 10^\circ$
	V_{Fmax}	0	65	1.6	15	0	$\lambda>57^\circ$, R_{max}, $L/W<0.5$
IIIB	V_{Fmax}	10	65	1.6	15	23	$\lambda>57^\circ$, R_{max}, $L/W<0.5$
	V_{Fmax}	20	65	1.6	15	56	$\epsilon>10^\circ$, $L/W<0.5$

TABLE VII (cont.)

Groups	Interceptor Veloc.	Initial Interceptor Altitude ($Ftx10^3$)	Target Altitude ($Ftx10^3$)	Target Veloc. (Mach)	Initial Target Aspect Angle τ_o (Deg)	Probability of Successful Arrival to Missile Launch (%)	Primary Reasons For Failures
	V_{Fmax}	30	65	1.6	15	38	$\epsilon > 10^o$
	V_{Fmax}	40	65	1.6	15	43.5	$\epsilon > 10^o$
	V_{Fmax}	50	65	1.6	15	67	$\epsilon > 10^o$
	V_{Fmax}	58	65	1.6	15	91	$\epsilon > 10^o$
IIIC	V_{Fmax}	0	65	1.6	30	0	$\lambda > 57^o$, R_{max}
	V_{Fmax}	10	65	1.6	30	30	$\lambda > 57^o$, R_{max}
	V_{Fmax}	20	65	1.6	30	80	$\epsilon > 10^o$, $L/_W < 0.5$
	V_{Fmax}	30	65	1.6	30	69	$\epsilon > 10^o$
	V_{Fmax}	40	65	1.6	30	73	$\epsilon > 10^o$
	V_{Fmax}	50	65	1.6	30	82	$\epsilon > 10^o$
	V_{Fmax}	58	65	1.6	30	91.5	$\epsilon > 10^o$
IIID	V_{Fmax}	0	65	1.6	45	0	
	V_{Fmax}	10	65	1.6	45	0	$\lambda > 57^o$, R_{max}
	V_{Fmax}	20	65	1.6	45	91	$\lambda > 57^o$, R_{max}
	V_{Fmax}	30	65	1.6	45	95.5	$\lambda > 57^o$, $\epsilon > 10^o$
	V_{Fmax}	40	65	1.6	45	95.5	$\lambda > 57^o$, $\epsilon > 10^o$
	V_{Fmax}	50	65	1.6	45	96.5	$\lambda > 57^o$
	V_{Fmax}	58	65	1.6	45	94	$\lambda > 57^o$

TABLE VII (cont.)

Groups	Interceptor Veloc.	Initial Interceptor Altitude ($Ftx10^3$)	Target Altitude ($Ftx10^3$)	Target Veloc. (Mach)	Initial Target Aspect Angle τ_o (Deg)	Probability of Successful Arrival to Missile Launch (%)	Primary Reasons For Failures
IIIE	V_{Fmax}	0	65	1.6	60	0	
	V_{Fmax}	10	65	1.6	60	0	$\lambda>57^o$, R_{max}
	V_{Fmax}	20	65	1.6	60	50	$\lambda>57^o$, R_{max}
	V_{Fmax}	30	65	1.6	60	87	$\lambda > 57^o$
	V_{Fmax}	40	65	1.6	60	91	$\lambda > 57^o$
	V_{Fmax}	50	65	1.6	60	92	$\lambda > 57^o$
	V_{Fmax}	58	65	1.6	60	66	$\lambda>57^o$, R_{max}
IIIF	V_{Fmax}	0	65	1.6	75	0	
	V_{Fmax}	10	65	1.6	75	0	
	V_{Fmax}	20	65	1.6	75	0	
	V_{Fmax}	30	65	1.6	75	0	$\lambda>57^o$, R_{max}
	V_{Fmax}	40	65	1.6	75	8	$\lambda>57^o$, R_{max}
	V_{Fmax}	50	65	1.6	75	8	$\lambda>57^o$, R_{max}
	V_{Fmax}	58	65	1.6	75	0	$\lambda>57^o$, R_{max}
IIIG	V_{Fmax}	0	65	1.6	82	0	
	V_{Fmax}	10	65	1.6	82	0	
	V_{Fmax}	20	65	1.6	82	0	
	V_{Fmax}	30	65	1.6	82	0	

TABLE VII (cont.)

Groups	Interceptor Veloc.	Initial Interceptor Altitude ($Ftx10^3$)	Target Altitude ($Ftx10^3$)	Target Veloc. (Mach)	Initial Target Aspect Angle τ_o (Deg)	Probability of Successful Arrival to Missile Launch (%)	Primary Reasons For Failures
	V_{Fmax}	40	65	1.6	82	4.5	$\lambda>57^o$, R_{max}
	V_{Fmax}	50	65	1.6	82	4.5	$\lambda>57^o$, R_{max}
	V_{Fmax}	58	65	1.6	82	0	$\lambda>57^o$, R_{max}
IIIH	V_{Fmax}	58	65	1.6	90	0	$\lambda>57^o$, R_{max}
	V_{Fmax}	50	65	1.6	90	0	$\lambda>57^o$, R_{max}
III-I	V_{Fmax}	58	65	1.6	120	0	$\lambda>57^o$, R_{max}
	V_{Fmax}	50	65	1.6	120	0	$\lambda>57^o$, R_{max}
IVA	M 0.9	30	65	1.6	0,15,30	0	
	M 0.9	40	65	1.6	0,15,30	0	
	M 0.9	55	65	1.6	0,15,30	0	
V A	V_{Fmax}	10	50	2.0	Head-on	16	$\epsilon>100$, $\lambda>57^o$
	V_{Fmax}	20	50	2.0	Head-on	46	$\epsilon>10^o$
	V_{Fmax}	30	50	2.0	Head-on	65	$\epsilon>10^o$
	V_{Fmax}	40	50	2.0	Head-on	75	$\epsilon>10^o$
	V_{Fmax}	50	50	2.0	Head-on	75	$\epsilon>10^o$
	V_{Fmax}	10	50	2	15	15	$\lambda>57^o$, R_{max}

TABLE VII (cont.)

Groups	Interceptor Veloc.	Initial Interceptor Altitude ($Ft \times 10^3$)	Target Altitude ($Ft \times 10^3$)	Target Veloc. (Mach)	Initial Target Aspect Angle τ_o (Deg)	Probability of Successful Arrival to Missile Launch (%)	Primary Reasons For Failures
V B	V_{Fmax}	20	50	2	15	34	$\epsilon > 10^o$
	V_{Fmax}	30	50	2	15	39	$\epsilon > 10^o$
	V_{Fmax}	40	50	2	15	62	$\epsilon > 10^o$
	V_{Fmax}	50	50	2	15	84	$\epsilon > 10^o$
V C	V_{Fmax}	10	50	2	30	1	$\lambda > 57^o$, R_{max}
	V_{Fmax}	20	50	2	30	68.5	$\epsilon > 10^o$, $\lambda > 57^o$, R_{max}
	V_{Fmax}	30	50	2	30	67	$\epsilon > 10^o$, $\lambda > 57^o$
	V_{Fmax}	40	50	2	30	78.5	$\epsilon > 10^o$, $\lambda > 57^o$
	V_{Fmax}	50	50	2	30	89	$\epsilon > 10^o$
V D	V_{Fmax}	10	50	2	45	0	$\lambda > 57^o$, R_{max}
	V_{Fmax}	20	50	2	45	59.5	$\lambda > 57^o$, R_{max}
	V_{Fmax}	30	50	2	45	84	$\lambda > 57^o$
	V_{Fmax}	40	50	2	45	87	$\lambda > 57^o$
	V_{Fmax}	50	50	2	45	87.5	$\lambda > 57^o$
V F	V_{Fmax}	10	50	2	60	0	
	V_{Fmax}	20	50	2	60	0	$\lambda > 57^o$, R_{max}
	V_{Fmax}	30	50	2	60	25	$\lambda > 57^o$, R_{max}

TABLE VII (cont.)

Groups	Interceptor Veloc.	Initial Interceptor Altitude ($Ftx10^3$)	Target Altitude ($Ftx10^3$)	Target Veloc. (Mach)	Initial Target Aspect Angle τ_o (Deg)	Probability of Successful Arrival to Missile Launch (%)	Primary Reasons For Failures
	V_{Fmax}	40	50	2	60	25	$\lambda>57^o$, R_{max}
	V_{Fmax}	50	50	2	60	25	$\lambda>57^o$, R_{max}
V G	V_{Fmax}	10	50	2	70	0	
	V_{Fmax}	20	50	2	70	0	$\lambda>57^o$, R_{max}
	V_{Fmax}	30	50	2	70	8	$\lambda>57^o$, R_{max}
	V_{Fmax}	40	50	2	70	8	$\lambda>57^o$, R_{max}
	V_{Fmax}	50	50	2	70	8	$\lambda>57^o$, R_{max}
VI A	M 0.9	20	50	2	15	10	$\lambda>57^o$, R_{max}, $L/W < 0.5$
	M 0.9	30	50	2	15	52	$\lambda>57^o$, $L/W<0.5$
	M 0.9	40	50	2	15	81	$\epsilon > 10^o$
	M 0.9	50	50	2	15	77	$\epsilon > 10^o$
VIB	M 0.9	30	50	2	30	0	
	M 0.9	40	50	2	30	0	
	M 0.9	50	50	2	30	0	
	V_{Fmax}	0	50	1.6	Head-on	0	$\lambda>57^o$, R_{max} $L/W< 0.5$
	V_{Fmax}	10	50	1.6	Head-on	80	$\epsilon >10^o$, R_{max}

TABLE VII (cont.)

Groups	Interceptor Veloc.	Initial Interceptor Altitude ($Ftx10^3$)	Target Altitude ($Ftx10^3$)	Target Veloc. (Mach)	Initial Target Aspect Angle τ_o (Deg)	Probability of Successful Arrival to Missile Launch (%)	Primary Reasons For Failures
VIIA	V_{Fmax}	20	50	1.6	Head-on	56	$\epsilon > 10^o$
	V_{Fmax}	30	50	1.6	Head-on	61	$\epsilon > 10^o$
	V_{Fmax}	40	50	1.6	Head-on	76	$\epsilon > 10^o$
	V_{Fmax}	50	50	1.6	Head-on	84	$\epsilon > 10^o$
VIIB	V_{Fmax}	0	50	1.6	15^o	49	$\lambda > 57^o$, R_{max} L/W< 0.5
	V_{Fmax}	10	50	1.6	15^o	82	$\epsilon > 10^o$, $\lambda > 57^o$ R_{max}
	V_{Fmax}	20	50	1.6	15^o	60	$\epsilon > 10^o$
	V_{Fmax}	30	50	1.6	15^o	66	$\epsilon > 10^o$
	V_{Fmax}	40	50	1.6	15^o	81	$\epsilon > 10^o$
	V_{Fmax}	50	50	1.6	15^o	90	$\epsilon > 10^o$
VIIC	V_{Fmax}	0	50	1.6	30^o	41	$\lambda > 57^o$, R_{max}
	V_{Fmax}	10	50	1.6	30^o	89	$\lambda > 57^o$, R_{max}
	V_{Fmax}	20	50	1.6	30^o	82	$\epsilon > 10^o$
	V_{Fmax}	30	50	1.6	30^o	84	$\epsilon > 10^o$
	V_{Fmax}	40	50	1.6	30^o	89	$\epsilon > 10^o$
	V_{Fmax}	50	50	1.6	30^o	91	$\epsilon > 10^o$

TABLE VII (cont.)

Groups	Interceptor Veloc.	Initial Interceptor Altitude ($Ftx10^3$)	Target Altitude ($Ftx10^3$)	Target Veloc. (Mach)	Initial Target Aspect Angle τ (Deg)	Probability of Successful Arrival to Missile Launch (%)	Primary Reasons For Failures
VIID	V_{Fmax}	0	50	1.6	45	0	$\lambda>57^\circ$, R_{max}
	V_{Fmax}	10	50	1.6	45	37	$\lambda>57^\circ$, R_{max}
	V_{Fmax}	20	50	1.6	45	94	$\lambda > 57^\circ$
	V_{Fmax}	30	50	1.6	45	86.5	$\varepsilon>10^\circ$, $\lambda>57^\circ$
	V_{Fmax}	40	50	1.6	45	88	$\lambda > 57^\circ$
	V_{Fmax}	50	50	1.6	45	97	$\lambda > 57^\circ$
VIIE	V_{Fmax}	0	50	1.6	60	0	
	V_{Fmax}	10	50	1.6	60	9	$\lambda>57^\circ$, R_{max}
	V_{Fmax}	20	50	1.6	60	75	$\lambda > 57^\circ$
	V_{Fmax}	30	50	1.6	60	88	$\lambda > 57^\circ$
	V_{Fmax}	40	50	1.6	60	92	$\lambda > 57^\circ$
	V_{Fmax}	50	50	1.6	60	89	$\lambda > 57^\circ$
VIIF	V_{Fmax}	0	50	1.6	75	0	
	V_{Fmax}	10	50	1.6	75	0	$\lambda>57^\circ$, R_{max}
	V_{Fmax}	20	50	1.6	75	50	$\lambda > 57^\circ$
	V_{Fmax}	30	50	1.6	75	76	$\lambda > 57^\circ$
	V_{Fmax}	40	50	1.6	75	82	$\lambda > 57^\circ$
	V_{Fmax}	50	50	1.6	75	82	$\lambda > 57^\circ$

TABLE VII (cont.)

Groups	Interceptor Veloc.	Initial Interceptor Altitude ($Ft \times 10^3$)	Target Altitude ($Ft \times 10^3$)	Target Veloc. (Mach)	Initial Target Aspect Angle τ_o (Deg)	Probability of Successful Arrival to Missile Launch (%)	Primary Reasons For Failures
VIIG	V_{Fmax}	0	50	1.6	90	0	
	V_{Fmax}	10	50	1.6	90	0	$\lambda > 57^o$, R_{max}
	V_{Fmax}	20	50	1.6	90	25	$\lambda > 57^o$, R_{max}
	V_{Fmax}	30	50	1.6	90	75	$\lambda > 57^o$
	V_{Fmax}	40	50	1.6	90	91	$\lambda > 57^o$
	V_{Fmax}	50	50	1.6	90	91	$\lambda > 57^o$
VIIH	V_{Fmax}	0	50	1.6	120	0	
	V_{Fmax}	10	50	1.6	120	0	R_{max}
	V_{Fmax}	20	50	1.6	120	79	$\lambda > 57^o$
	V_{Fmax}	30	50	1.6	120	99	$\lambda > 57^o$
	V_{Fmax}	40	50	1.6	120	100	
	V_{Fmax}	50	50	1.6	120	100	
VII-I	V_{Fmax}	0	50	1.6	150	0	
	V_{Fmax}	10	50	1.6	150	0	R_{max}
	V_{Fmax}	20	50	1.6	150	100	
	V_{Fmax}	30	50	1.6	150	100	
	V_{Fmax}	40	50	1.6	150	100	
	V_{Fmax}	50	50	1.6	150	100	

TABLE VII (cont.)

Groups	Interceptor Veloc.	Initial Interceptor Altitude ($Ftx10^3$)	Target Altitude ($Ftx10^3$)	Target Veloc. (Mach)	Initial Target Aspect Angle τ_o	Probability of Successful Arrival to Missile Launch (%)	Primary Reasons For Failures
VIIIA	M 0.9	10	50	1.6	15	45	$\lambda > 57^\circ$, R_{max} $L/W < 0.5$
	M 0.9	20	50	1.6	15	68	$L/W < 0.5$
	M 0.9	30	50	1.6	15	88	$L/W < 0.5$
	M 0.9	40	50	1.6	15	96	$\epsilon > 10^\circ$
	M 0.9	50	50	1.6	15	92	$\epsilon > 10^\circ$
VIIIB	M 0.9	10	50	1.6	30	1.5	$\lambda > 57^\circ$, R_{max}
	M 0.9	20	50	1.6	30	41	$\lambda > 57^\circ$, R_{max}
	M 0.9	30	50	1.6	30	41	$\lambda > 57^\circ$, R_{max}
	M 0.9	40	50	1.6	30	41	$\lambda > 57^\circ$, R_{max}
	M 0.9	50	50	1.6	30	48	$\lambda > 57^\circ$

Referring to the pull-up runs initiating from 10,000 ft altitude it is seen that the interceptor was unable to close to R_{max}. The reason for this is that pull-up was initiated from radar lock-on and the interceptor continued to pull up as long as possible, regardless of slowdown effects. If penetration effects are ignored, the interceptor could climb, for instance, to 40,000 ft, level off, and close to R_{max}. However, if penetration effects are considered, the resulting probability of success still would be very low.

Effect on Pull-Up Capability of Steering in Azimuth-Only and Delaying Pull-Up

The criteria that has been used throughout the study of probability of successful arrival to missile launch in pull-up attacks are:

1. The interceptor is vectored on a pure collision course and continues to fly a pure collision course until lock-on.

2. All pull-ups are initiated at lock-on.

Previously, under the section on pull-up attacks under "ideal" conditions, a preliminary study of the effect of steering in azimuth-only after lock-on was made, which showed no improvement in pull-up capability. Referring to the results of probability of success in pull-up attacks given on Table VII, it is observed that on many runs a failure resulted because the interceptor failed to close range to R_{max}. The question immediately arises as to what would happen if the pilot steered in azimuth-only after lock-on and delayed pull-up until a range consistent with the snap-up range equation proposed by Raytheon is reached. The snap-up equation is given by

$$R_{su} = R_{max} + 10\ V_c - 6000$$

R_{su} = Snap-up range in feet

R_{max} = Maximum aerodynamic range of the missile in feet

V_c = Closing velocity in feet/sec

This steering in azimuth-only until R_{su} criteria will be used on a selected number of runs from three aspect angles to determine its effect on proba-

bility of successful arrival to missile launch in pull-up attacks. To aid the reader, a picture of the probability grid used to get the resulting probabilities of Table VII, is given on Fig. 75. The center line corresponds to the initial aspect angle to which the fighter direction center attempts to vector the interceptor. About this center line there is a distribution in azimuth associated with the vectoring inaccuracy and a distribution in range associated with the probability of lock-on. The weight of the individual boxes is the product of the corresponding weight of the appropriate row and column. Pull-up runs from boxes in this grid at three different aspect angles (τ_o) were examined using the criteria of steering in azimuth-only until R_{su}. The results are given on Table VIII. The initial conditions are given by the first six columns of this table. The first four runs on the table are from the probability grid associated with the point on Fig. 53, and with Group III-F of Table VII where the fighter pulls up from 50,000 ft altitude. Examination of the runs in the probability grid when the interceptor pulls up at lock-on gives the results shown in Column 7 of Table VIII. When the interceptor employs steering in azimuth-only and delaying pull-up, the results of Column 8 of Table VIII are obtained. Comparing the first four values in each of these columns, it is seen that the doctrine of steering in azimuth-only until R_{su} does not improve the situation. In fact, those runs which failed using the criteria of pulling up at AI lock-on range were more of a failure when the criteria of steering in azimuth-only until R_{su} was employed. Detailed examination of these runs reveals that steering in azimuth-only lengthens the flight path of the interceptor by drawing him further toward the tail of the target. Interceptor slowdown effects are greater and the interceptor is unable to close range to R_{su} (snap-up range). Comparable results are shown for the case of τ_o = 90 and 120°.

The results of preliminary investigations of the effect on pull-up attacks made under ideal conditions of steering in azimuth-only were given previously. This section shows the results on pull-up attack probability of success of steering in azimuth-only and delayed pull-up. Based upon the results obtained under these two different pull-up conditions, it is concluded that steering in azimuth-only results in a degradation of pull-up capability. It is better for the interceptor to continue on the vectored course until pull-up.

TABLE VIII

EFFECT ON PULL-UP CAPABILITY OF STEERING IN AZIMUTH-ONLY AND DELAYING PULL-UP

Initial Target Aspect τ_o (deg)	Target Altitude H_T ($Ft \times 10^3$)	Target Velocity V_T (M)	Initial Interceptor Velocity V_F (M)	Origin of Run from Probability Grid	Interceptor Altitude at Pull-up H_F ($Ft \times 10^3$)	Results of Pull-up at Lock-on	Results of Azimuth-only Steering and Delaying Pull-up until Range Corresponds to $R_{su} = R_{max} + 10\ V_c - 6000$
75	65	1.6	2.0	F-4	50	Run successful. ϵ reduced to zero	Run successful. ϵ reduced to zero
75	65	1.6	2.0	E-1	50	Run failed. Could not reduce range to R_{max}	Run failed. R_{su} not reached
75	65	1.6	2.0	D-1	50	Same as above	Same as above
75	65	1.6	2.0	B-1	50	Same as above	Same as above
90	65	1.6	2.0	F-2	50	Same as above	Same as above
90	65	1.6	2.0	D-2	50	Same as above	Same as above
90	65	1.6	2.0	A-3	50	Same as above	Same as above
120	65	1.6	2.0	G-1	50	Same as above	Same as above

Effect on Pull-up Capability of Delaying Pull-ups

In the above section it was shown that steering in azimuth-only and delaying pull-up until the range defined as R_{su} is reached does not improve pull-up capability. In fact, the situation is degraded. However, the primary cause of degradation was steering in azimuth-only. It is now of interest to try another criteria and investigate the resulting effect on pull-up capability. The interceptor will continue to fly the vectored pure collision course, but pull-ups will be delayed until the range corresponds to

$$R_{su} = R_{max} + 10\ V_c - 6000$$

Two situations were investigated and the resulting probability of successful arrival to missile launch was compared with the results obtained previously when the interceptor pulls up at lock-on. This comparison is shown on Figs. 76 and 77. The conditions of Fig. 76 are that the target is flying at 65,000 ft at M 1.6, and the interceptor is flying at V_{max} and initiates pull-up from 50,000 ft altitude. Curve A shows the resulting probability of successful arrival to missile launch as a function of relative angle off target's nose (initial target aspect angle τ_o) for the case where the interceptor pulls up at lock-on. This curve is a cross-plot of information presented previously. When the interceptor does not pull up until R_{su} is reached, the results are as shown by Curve B. It is seen that for initial target aspect angles greater than 60° there is an improvement in probability of successful arrival to missile launch. In fact, the improvement is largely in the region of 90° (from 0% to 41%). This improvement results from the fact that by delaying the pull-up the effect of interceptor slowdown is not as great and the range can be closed to R_{max}. Beyond 100°, the probability is still zero because of a lack of speed advantage. The line drawn between 90° and 100° is shown dashed because the exact point where the probability returns to zero is not known (runs not made).

Comparable results for the case when the interceptor initiates attacks from 30,000 ft are shown on Fig. 77. For this case there is no change in probability of success when pull-up is delayed.

The improvement shown on Fig. 76 resulting from delayed pull-ups, indicates that there is an advantage to be gained. Further study is needed to determine the full extent of the improvement and if the currently defined R_{su} is optimum.

Remaining Study

There are areas where additional analyses are needed to allow more complete definition of the performance of the improved system. Among these are:

1. Inclusion of actual missile performance during ejection launch and after launch. This includes transient effects during launch and radome and target noise during the flight of the missile.

2. Inclusion of the effects of noise and missile orientation both with and without "English Bias."

3. More extensive study of the effect of waiting until snap-up range (R_{SU}) is needed.

The three areas above are now under study and will be reported on in another volume of this series.

PHASE V - STUDY TO DETERMINE AND ASSESS REALIZABLE IMPROVEMENTS

This phase is of necessity a continuing one. In those areas where it appeared that important gains could be made by incorporation of improvements which could be realized within a useful time scale, action recommendations have been made to the Bureau. Among the areas where recommendations have been made are:

1. Incorporation of optimized search areas in the AI radar.
2. Bandwidth switching in the AI radar.
3. Incorporation of bright display.
4. Optimization of AI radar antenna size and required gimbal coverage.
5. Incorporation of Triangle System.
6. Doctrine and procedures for employing the aircraft, radar, missile combination under tactical conditions.
7. Relationship of NTDS, ATDS to tactical requirements.

Appraisal of the impact of possible improvements in subsystem on overall tactical effectiveness is continuing. During the next study phase primary emphasis will be placed on investigation of sensitivity of system effectiveness to changes in missile performance.

PHASE VI - STUDY OF IR TIE-IN FOR AI FIRE CONTROL SYSTEMS

No additional study effort beyond that reported in previous volumes has been devoted to this phase. In addition, it is not anticipated that any additional study of this phase will be conducted during the remainder of the program.

PHASE VII - REPEAT STUDY PHASES I THRU VI FOR SPARROW III WITH IR SEEKER

No additional study effort beyond that reported in previous volumes has been devoted to this phase. It is anticipated that during the next study phase, the tactical effectiveness of a multimode seeker (Sparrow III CW and IR) will be investigated.

PHASE VIII - REPEAT STUDY PHASES I THRU VI FOR SIDEWINDER

To date, only limited data on the performance of the proposed Sidewinder IC has been received. This data is primarily restricted to aerodynamics performance of the missile. In Volume III of this series, one preliminary attack zone overlay was given for Sidewinder IC. This study phase is extended in this volume to cover other speed and altitude conditions and to modify this preliminary overlay given previously. Figs. 78 thru 81 give co-altitude attack zone overlays for Sidewinder IC when the attacks are conducted under ideal conditions. The interceptor arrives at AI radar detection, shown by Curve A, on a perfect lead pursuit course. Lock-on occurs 10 secs later as shown by Curve B. The pilot must be able to fly the pure pursuit course until the aerodynamic zone (shown by heavy curve) of Sidewinder IC is entered without exceeding 3 g's. The aerodynamic zone was obtained from Ref. 8. The 3 g contour is shown by Curve C.

Figure 78 shows the results of co-altitude attacks made at 50,000 ft when the interceptor velocity (V_F) is 1940 ft/sec and V_T/V_F = 1.0. Referring to this figure, it is seen that there is essentially one course (that originating from approximately 58° off the target's nose) that can be flown to an acceptable missile launch point. All other courses either require more than 3 g's (see course originating from 50°) or miss the aerodynamic zone

(see course originating from 60°). All runs aft of the beam fail because of lack of speed advantage.

When the velocity of the target (V_T) is reduced such that $V_T/V_F = 0.8$ the results are as shown on Fig. 79. It is seen that successful runs are restricted to those originating from approximately 60° off the target's nose to tail-on. As we go toward the tail, penetration effects become more pronounced because of increased time required to close to an acceptable release range.

When the co-altitude attack occurs at 30,000 ft altitude the results are as shown on Figs. 80 and 81. Figure 80 gives the results for the case of $V_T/V_F = 1.0$. As shown, the interceptor cannot enter the acceptable aerodynamic zone for Sidewinder IC. This is due to excessive "g" requirements and lack of speed advantage coupled with the very small aerodynamic zone available. When the speed ratio V_T/V_F is reduced to 0.8, the results are as shown on Fig. 81. Successful attacks can be made under these conditions from 60° off the target's nose around to tail-on. However, as we go toward the tail the times required to close to the aerodynamic zone for Sidewinder IC are large.

The attack zone overlays presented on the above four figures represent an extension of results presented previously. However, these overlays are still very preliminary in nature. Additional study is needed to include the actual seeker performance of Sidewinder IC and to develop actual probability of success curves. In addition, analysis effort is needed in an attempt to develop optimum tactics for employment of Sparrow III and Sidewinder IC as a mixed load.

CONCLUSIONS AND RECOMMENDATIONS

Introduction

The conclusions and recommendations presented here in no way void those given previously in Volumes I and III. Data in this volume represents an extension of that given previously and includes subsystem changes that have occurred and additional areas of investigation. The areas of investigation detailed in this volume are restricted to the system using the AN/APQ-72 (XN-3) radar. Many distinctly different tactical situations are examined. For this reason the reader is encouraged to refer to the text for the full meaning of the conclusions and recommendations which follow.

A. Co-altitude Attack Investigation

1. The results of the study using the barrier method of analysis (wherein each barrier represents 85%-90% probability) of the ideal situation for high altitude (co-altitude) attacks given in this document are in agreement with those given previously in Volumes I and III. Additional results for the system employing the AN/APQ-72 (XN-3) radar are presented in this volume. The following conclusions are indicated:

(a) When $V_T/V_F = 1.0$ where $V_F = V_{max}$ and the attack altitude is 50,000 ft, the interceptor must start his approach from forward of 68° off the target's nose if entry into the effective attack zone is to be made (see Fig. 3).

(b) When the speed ratio (V_T/V_F) is reduced to 0.8 where $V_F = V_{max}$ and the attack altitude is 50,000 ft, around the clock attacks are possible. However, penetration distances are great because of having only a 20% speed advantage.

2. The probability of successful arrival to missile launch in co-altitude attacks, when limited by some of the degrading factors to be encountered in the tactical situation, such as vectoring inaccuracies, gimbal angle limits, allowable missile launch error, etc., are given in Volumes I and III for many tactical situations. The analyses detailed in this volume represent an extension of this investigation and result in the following conclusions:

(a) When the attack altitude is 30,000 ft, $V_T/V_F = 1.0$ and V_F = M 1.91, the probability of successful arrival to missile launch is 75% head-on, rises slowly to 87% at 30° off the target's nose and drops sharply beyond 45° off the target's nose.

(b) When the conditions are the same as those of item (a), except $V_T/V_F = 0.8$, the probability of successful arrival to missile launch is 85% head-on, 97% at 45° off the target's nose, 89% at 60° off the target's nose. Beyond 60° the probability drops sharply to zero because of target penetration effects.

(c) When the target performs a simple 1 g crisscross maneuver, the resulting effect on probability of successful arrival to missile launch is negligible.

B. Pull-up Attack Investigation

1. The pull-up attack investigation of the "ideal" situation detailed in Volumes I and III was restricted to head-on attacks. This investigation is extended in this volume to include around the clock pull-up attacks made under the "ideal" or perfect vectoring situation. The following conclusions are indicated:

(a) When the target is flying at M 2.0 at 65,000 ft altitude and the interceptor starts the pull-up run under V_{max} conditions, the pull-up zone available for the head-on aspect is small both in terms of differential altitude and time available. When the aspect angle is increased to 15° off the target's nose there is essentially no pull-up zone available. When the aspect angle is increased to 45°, the zone is also increased in size to one where attack from differential altitudes of 48,000 ft can be made. At 60° off the target's nose there is no zone available. (See Figs. 5 thru 9).

(b) When the target is flying at M 2.0 at 65,000 ft altitude and the interceptor starts the pull-up run under V_{cruise} conditions, there is no pull-up zone available (see Figs. 6 and 7).

(c) When the target is flying at M 1.6 at 65,000 ft altitude and the interceptor starts the pull-up run under V_{max} conditions, the pull-up zones available for aspect angles of head-on and 15° are still small in terms of differential altitude and time available. At 45° the zone available is large and pull-up attacks can be made from differential altitudes of 52,000 ft. For aspect angles of 60° and greater, the zone available is large. However, for aspect angles of 90° or larger, the target penetration distances will be large (see Figs. 10 thru 19).

(d) When the target is flying at M 1.6 at 65,000 ft altitude and the interceptor starts the pull-up runs under V_{cruise} conditions, there is no pull-up zone available (see Figs. 11 and 12).

(e) When the M 2.0 targets altitude is reduced to 50,000 ft, the pull-up zone available is increased in size. However, the zones available at aspect angles of head-on, 15° and 30° are very limited timewise. When

the aspect angle is increased to 45°, the zone is increased in size to the point where differential altitude attacks of 34,000 ft can be made (from 16,000 up to co-altitude). For aspect angles of 60° or greater of the target's nose there is no zone available (see Figs. 20 thru 24).

(f) When the interceptor starts the pull-up run under V_{cruise} conditions against this M 2.0 target flying at 50,000 ft there is a marginal zone available at 15° off the target's nose (see Figs. 21 and 22).

(g) When the 50,000 ft altitude target's speed is reduced to M 1.6, the trend is the same as that described under items (c) and (d) above.

(h) From the above results on pull-up attacks it is concluded that the optimum approach aspect for successfully attacking high speed targets is 45° off the target's nose. It is recommended that tactical doctrines be developed which will result in placement of the interceptor at this initial approach aspect.

(i) From the above results on pull-up attacks, it is concluded that it is tactically wrong to start a pull-up attack with the interceptor operating under V_{cruise} conditions.

(j) Extreme differential pull-up attacks should be avoided because of the small time available in the pull-up zone.

2. The probability of successful arrival to missile launch in pull-up attacks when limited by some of the degrading factors to be encountered in the tactical situation, such as vectoring inaccuracies, gimbal angle limits, allowable launch errors, etc., are given in Volume III for the head-on attack case. A study, reported herein, extends this investigation to include around the clock attacks. In the text it is assumed that

(a) the resulting overall system probability of success must be 50% or greater to be acceptable,

(b) the probability that the missile will successfully guide and fuze after being launched is $\approx$ 70%, and

(c) the resulting probability of successful arrival to missile launch must be $\approx$ 70%.

If these assumptions are valid, the following conclusions are indicated:

(a) When the target is flying at M 2.0 at 65,000 ft and the fighter starts pull-up runs under V_{max} conditions, the fighter must be vectored to a position in the region of 30° to 45° off the target's nose if the resulting pull-up probability of success and associated differential altitude band available is to be acceptable. The optimum position for vectoring is 45° off the target's nose (see Figs. 41 thru 46).

(b) If the fighter starts pull-up runs under V_{cruise} conditions against a M 2.0 target at 65,000 ft, the results are unacceptable (see Fig. 47).

(c) When the target velocity is reduced to M 1.6 at 65,000 ft and the fighter starts pull-up runs under V_{max} conditions, the fighter must be vectored to a position in the region of 30° to 60° off the target's nose if the resulting pull-up probability of success and associated differential altitude band available is to be acceptable. Again the optimum approach aspect is 45° (see Figs. 48 thru 55).

(d) If the target is flying at M 1.6 at 65,000 ft altitude and the fighter starts pull-up runs under V_{cruise} conditions, the results are unacceptable.

(e) When the target is flying at M 2.0 but the altitude is reduced to 50,000 ft and the fighter starts pull-up runs under V_{max} conditions, the same general trend as described under item (a) is observed. The fighter has the largest pull-up probability of success along with the largest differential altitude band in the region of 30° to 45° off the target's nose. Again the optimum approach aspect is in the region of 45° off the target's nose (see Figs. 57 thru 62).

(f) When the target is flying at 50,000 ft altitude and the speed is reduced to M 1.6, the V_{max} fighter can make successful around the clock pull-up attacks. However, when target penetration is considered, attacks initiated aft of the beam will, in effect, result in failures (see Figs. 64 thru 72).

3. In the pull-up attack investigation it was found that some of the failures which occurred could be attributed to the pull-up doctrine employed. The doctrine employed was that the interceptor is vectored on a pure collision course and continues to fly this course until pull-up. Variation of

this doctrine was investigated with the following results:

(a) The situation is not improved if the pilot steers in azimuth-only between AI radar lock-on and pull-up. In general, steering in azimuth-only causes the interceptor to be drawn around toward the tail of the target (see Table III).

(b) The situation is not improved if the pilot steers in azimuth-only and delays pull-up until snap-up range (R_{su}). In fact, those runs which failed (using the initial doctrine) were more of a failure when the criteria of steering in azimuth-only until R_{su} is employed (see Table VIII).

(c) The preliminary investigation conducted to date indicates that when the interceptor continues on the vectored course (pure collision) but pull-up is delayed until R_{su} , there is an improvement in probability of success. The improvement is most evident at aspect angles in the vicinity of 90° off the target's nose.

FUTURE STUDY EFFORT

There are several areas where investigation is needed before the performance of the F4H-1 (Sparrow III 6a) System, under tactical conditions, can be clearly defined. These are as follows:

1. Further study effort is needed on the low altitude and lookdown investigation when results of planned tests become available.

2. Determine by study and analysis the acceleration launching transients occurring during the Sparrow III missile launch and the effects of these transients upon dynamic performance of the missile internal functions and missile trajectory to the target.

3. Determine by study and analysis the effects of noise and missile orientation on system accuracy, both with and without "English Bias."

4. Determine by study and analysis the illumination requirements after Sparrow III launch in conjunction with breakaway requirements and aircraft normal flight recovery requirements.

5. Determine by study and analysis the feasibility and possible advantages of using multimode guidance systems.

6. Investigation of system performance using the Sidewinder IC is needed. However, this cannot proceed because of a lack of data describing the performance of this missile.

The study effort required in those areas covered by items 2, 3 and 4 above has been completed. Data are being reduced and the results will be published in the near future. A preliminary study of the problem of item 5 has been made and a report is in preparation. It is anticipated that with the reporting of this additional study effort, the Navy's Air to Air Missile Study as related to the F4H-1 (Sparrow III 6a) Weapon System will be complete. Additional study of the problems of items 1, 5 and 6 will be conducted under the Navy's Air to Air Missile Study as related to the F4H- (Sparrow III 6b) Weapon System, which is currently in progress.

ACKNOWLEDGEMENTS

The data presented in this report represents the results, to date, of the Navy's Air to Air Missile Study Program. The analytical results including those from which the figures were derived are the results of the computational work underway at Westinghouse Air Arm Division. In addition, results of analyses underway at NMC, Pt. Mugu are included. The data from which the definition of the Sparrow III missile and the AN/APA-128 computer resulted, were obtained from the Raytheon Company. Definition of the aircraft performance resulted from the cooperative effort of the McDonnell Aircraft Company. Performance data on the Sidewinder IC was supplied by NOTS, Inyokern. Test data on AI radar performance were obtained from NATC, Patuxent. The authors would like to thank members of these activities for their cooperation.

In addition, the authors would like to thank Laurence Gilchrist of the Equipment Research Branch, Radar Division for his contribution to this report.

REFERENCES

1. NRL Report 754, Volume I, November 1957, Confidential, "Summary of Navy Study Program for F4H-1 and F8U-3 Weapons Systems."

2. NRL Report 754, Volume II, Confidential, "Summary of Navy Study Program for F4H-1 and F8U-3 Weapons Systems."

3. NRL Report 754, Volume III, May 1958, Confidential, "Summary of Navy Study Program for F4H-1 and F8U-3 Weapons System."

4. NRL Report 754, Volume IV, Confidential, "Summary of Navy Study Program for F4H-1 and F8U-3 Weapons System."

5. NRL Report 754, Volume VIII, Confidential, "Summary of Navy Study Program for F4H-1 and F8U-3 Weapon Systems, Parameter Plots for Co-Altitude Attacks."

6. NRL Report 754, Volume VIII, December 1958, Confidential, "Summary of Navy Study Program for F4H-1 and F8U-3 Weapons System, Parameter Plots for Pull-up Attacks."

7. Secret, "Comparison of Project V and Sparrow III Seekers," (Preliminary) Project TED MTC GM-3410, NAMTC.

8. Conference held at NOTS, Inyokern, on 7 November 1958.

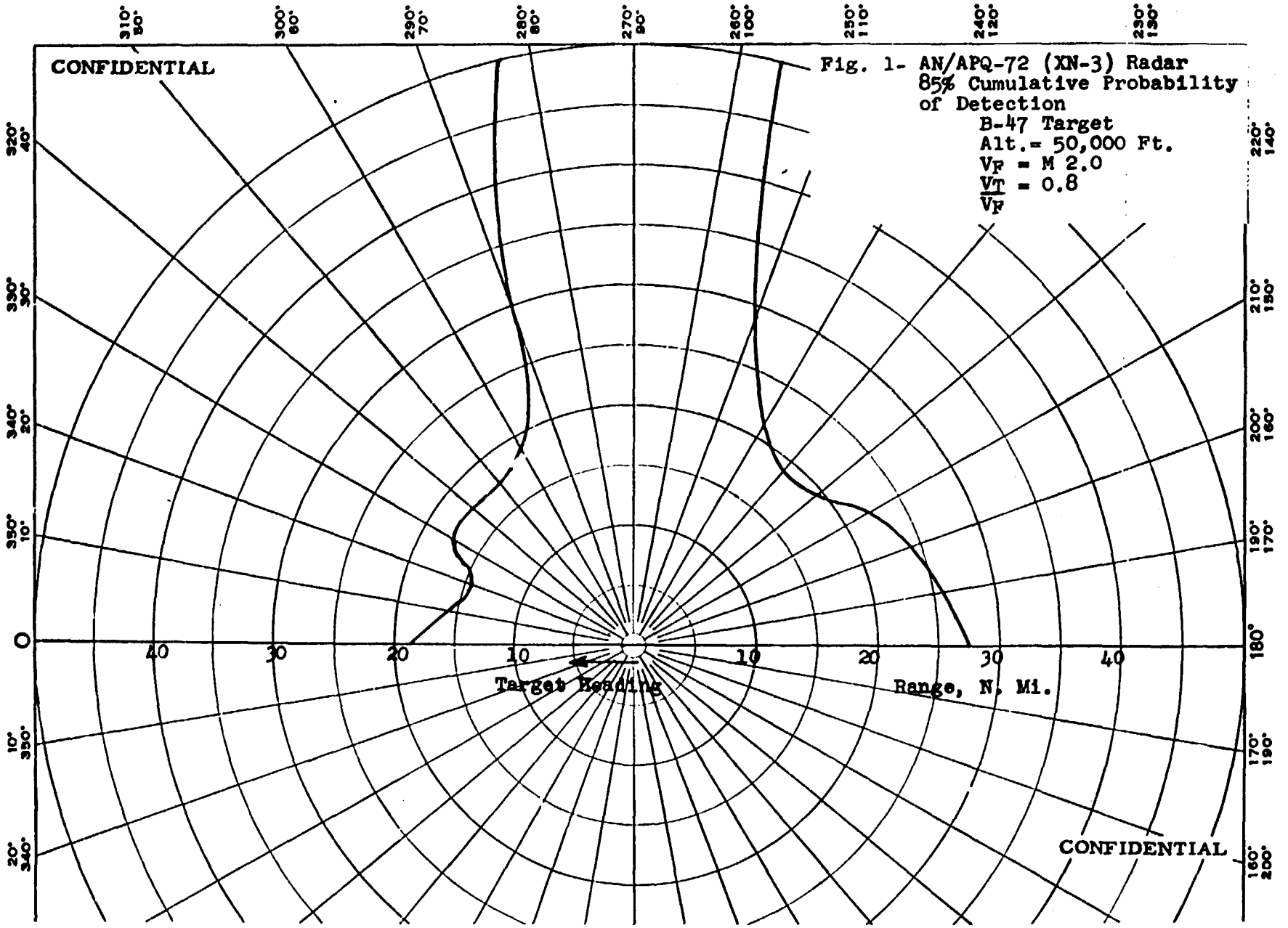
CONFIDENTIAL
Fig. 1- AN/APQ-72 (XN-3) Radar
85% Cumulative Probability
of Detection
B-47 Target
Alt.= 50,000 Ft.
V_F = M 2.0
$\frac{V_T}{V_F}$ = 0.8
310° 50°
300° 60°
290° 70°
280° 80°
270° 90°
260° 100°
250° 110°
240° 120°
230° 130°
320° 40°
330° 30°
340° 20°
350° 10°
0
10° 350°
20° 340°
220° 140°
210° 150°
200° 160°
190° 170°
180°
170° 190°
160° 200°
40
30
20
10
10
20
30
40
Target Heading
Range, N. Mi.
CONFIDENTIAL

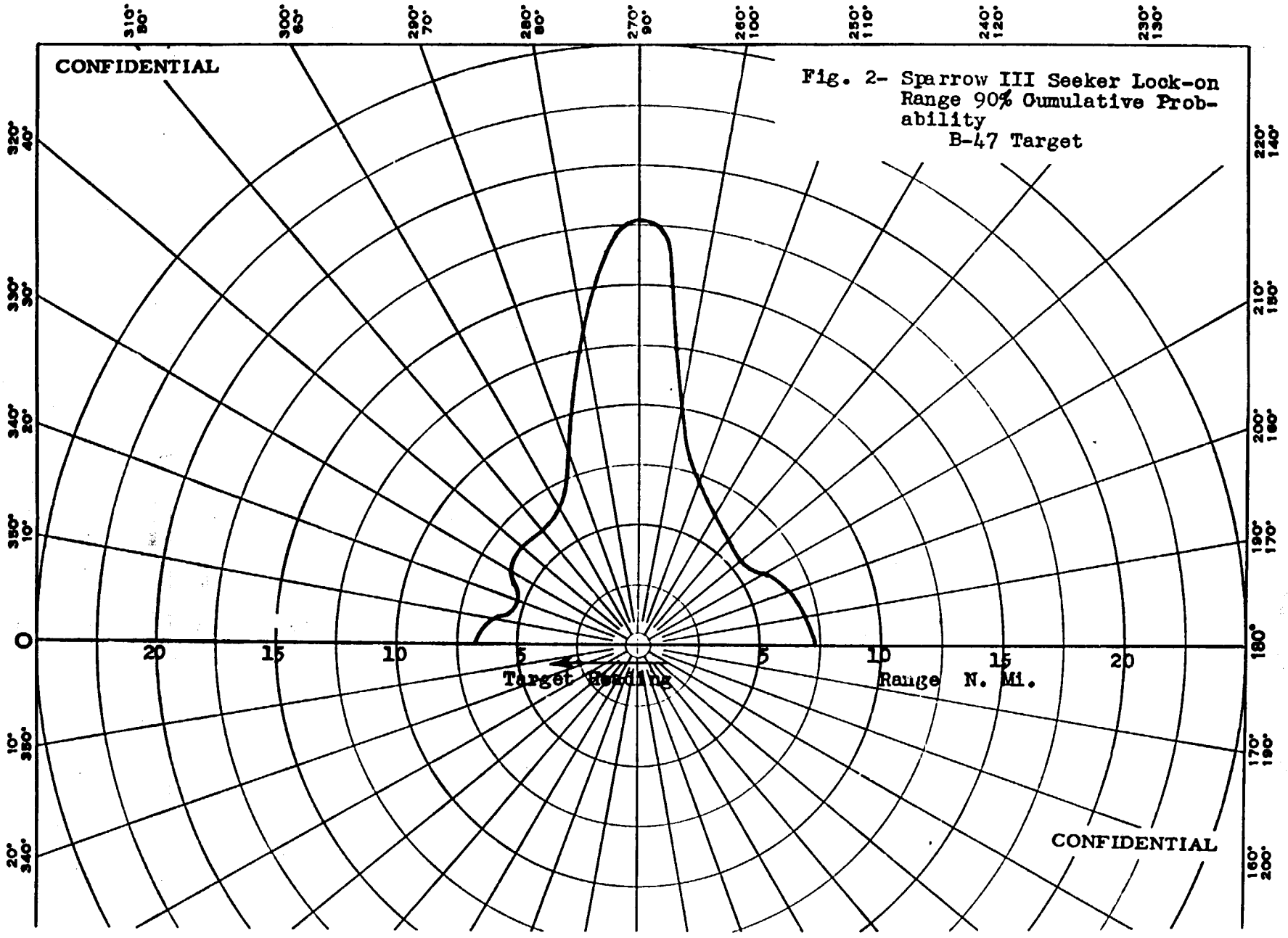

Fig. 2- Sparrow III Seeker Lock-on Range 90% Cumulative Probability
B-47 Target

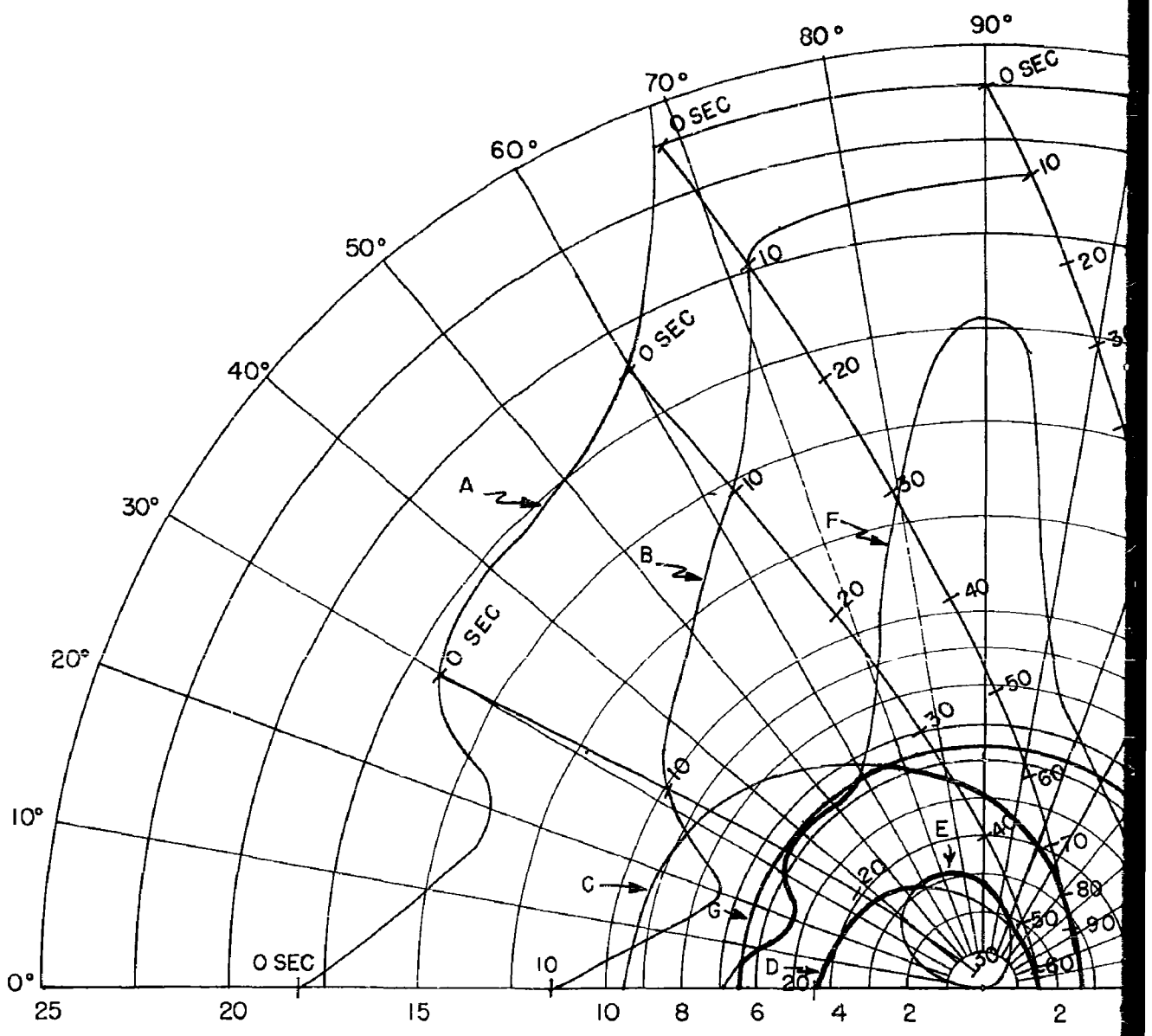

← TARGET HEADING

V_F = 1940 FT/SEC (F4H-1)(F8U-3)
V_T = 1940 FT/SEC
ALTITUDE = 50,000 FT.

A - 85% DETECTION RANGE
B - LOCK-ON RANGE (10 SEC. LOCK-ON
C - SPARROW III MAX. AERODYNAMIC
D - SPARROW III MIN. AERODYNAMIC
E - CONSTANT LOAD FACTOR LOCUS
F - 90% SPARROW III SEEKER LOCK
G - 6.5 N.M. INTERLOCK

1

FIG. 3 - CO-ALTITUDE LEAD PURSUIT ATTACK ZONE OVERLAYS.

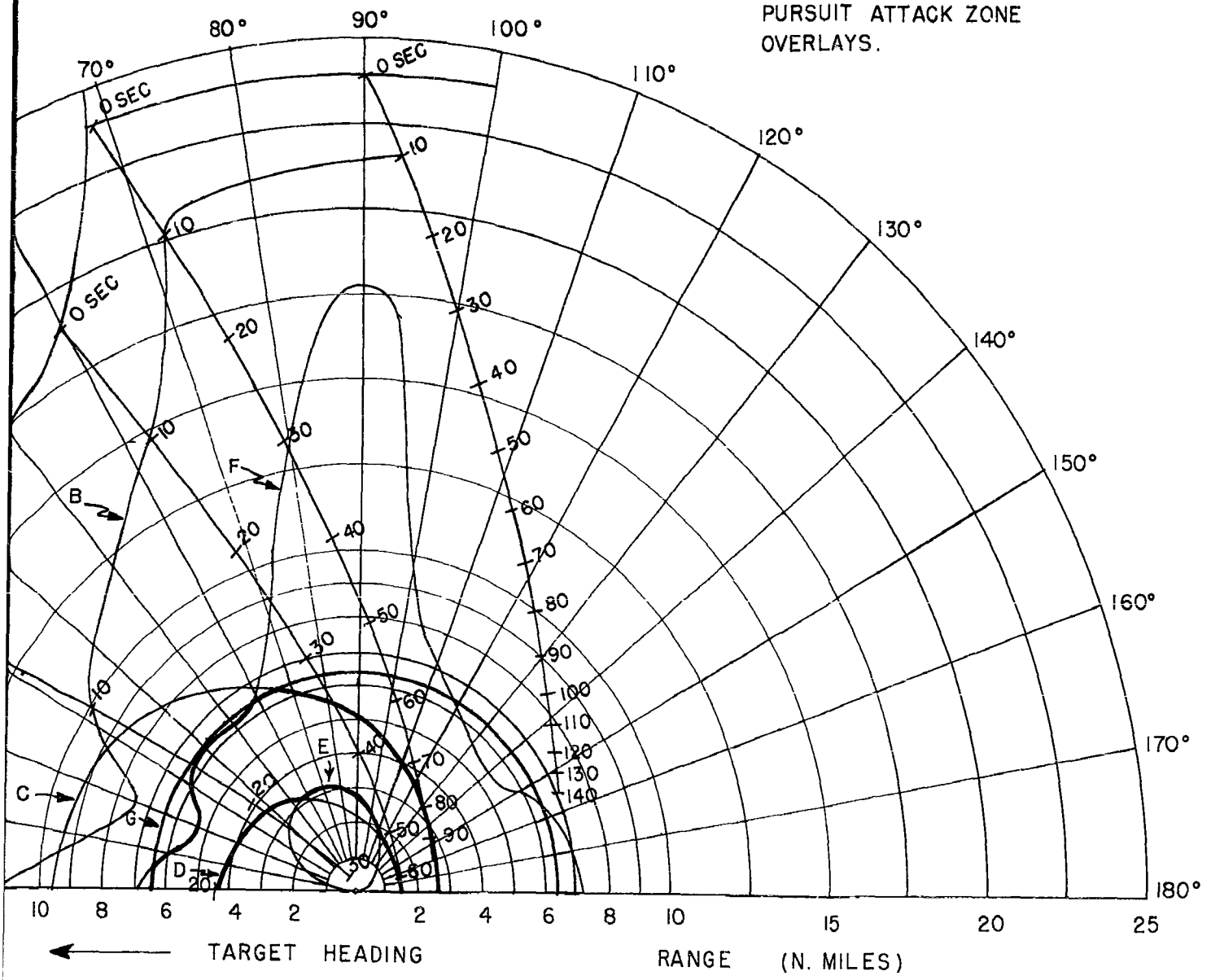

A - 85% DETECTION RANGE
B - LOCK-ON RANGE (10 SEC. LOCK-ON TIME)
C - SPARROW III MAX. AERODYNAMIC RANGE
D - SPARROW III MIN. AERODYNAMIC RANGE
E - CONSTANT LOAD FACTOR LOCUS ($N_Z = 3$)
F - 90% SPARROW III SEEKER LOCK-ON RANGE
G - 6.5 N.M. INTERLOCK

2

CONFIDENTIAL

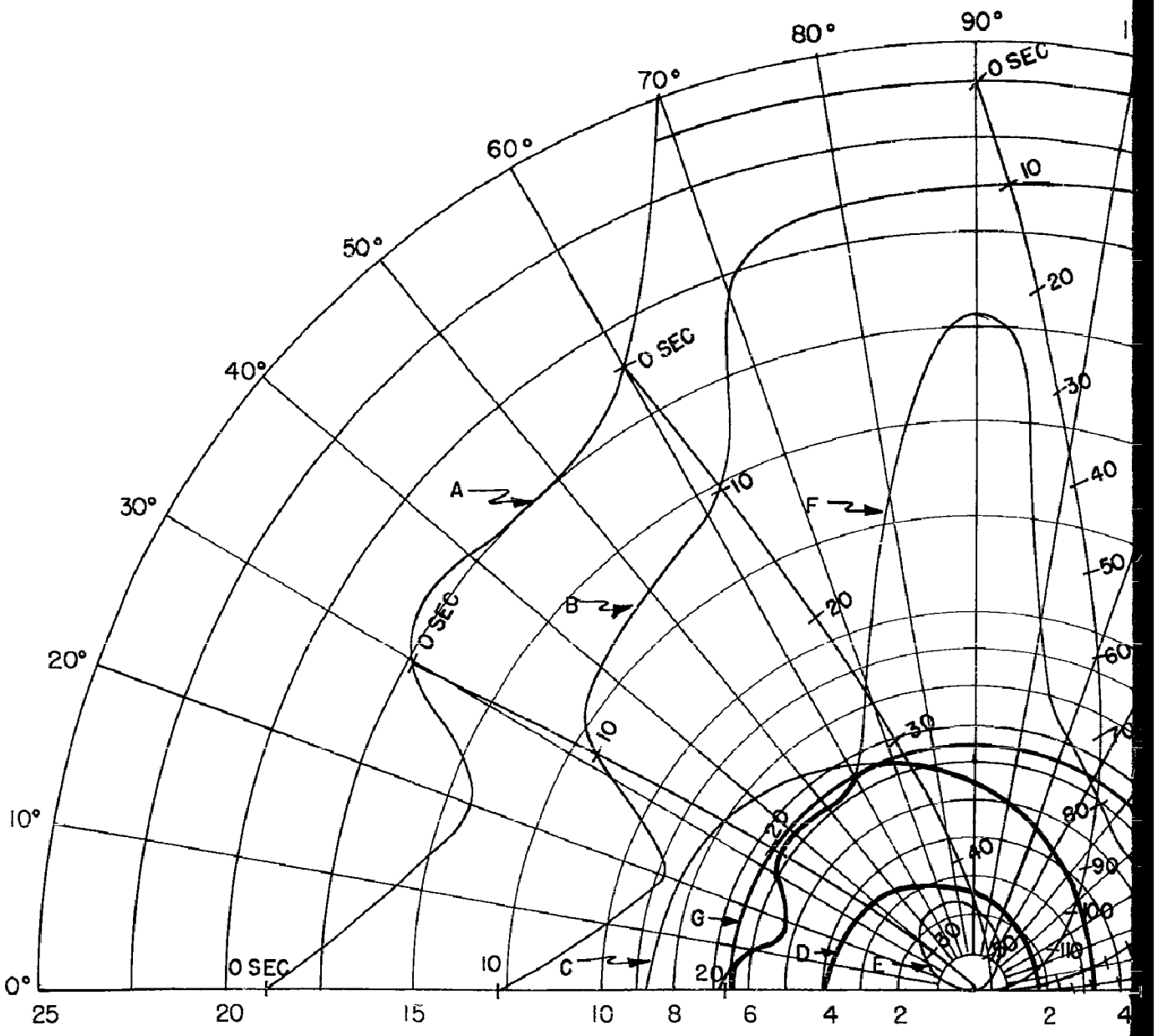

TARGET HEADING

V_F = 1940 FT/SEC (F4H-1)(F8U-3)

V_T = 1552 FT/SEC

ALTITUDE = 50,000 FT.

A - 85% DETECTION RANGE
B - LOCK-ON RANGE (10 SEC. LOCK-ON
C - SPARROW III MAX. AERODYNAMIC R
D - SPARROW III MIN. AERODYNAMIC
E - CONSTANT LOAD FACTOR LOCUS
F - 90% SPARROW III SEEKER LOCK-
G - 6.5 N.M. INTERLOCK

1

FIG. 4 - CO-ALTITUDE LEAD PURSUIT ATTACK ZONE OVERLAYS.

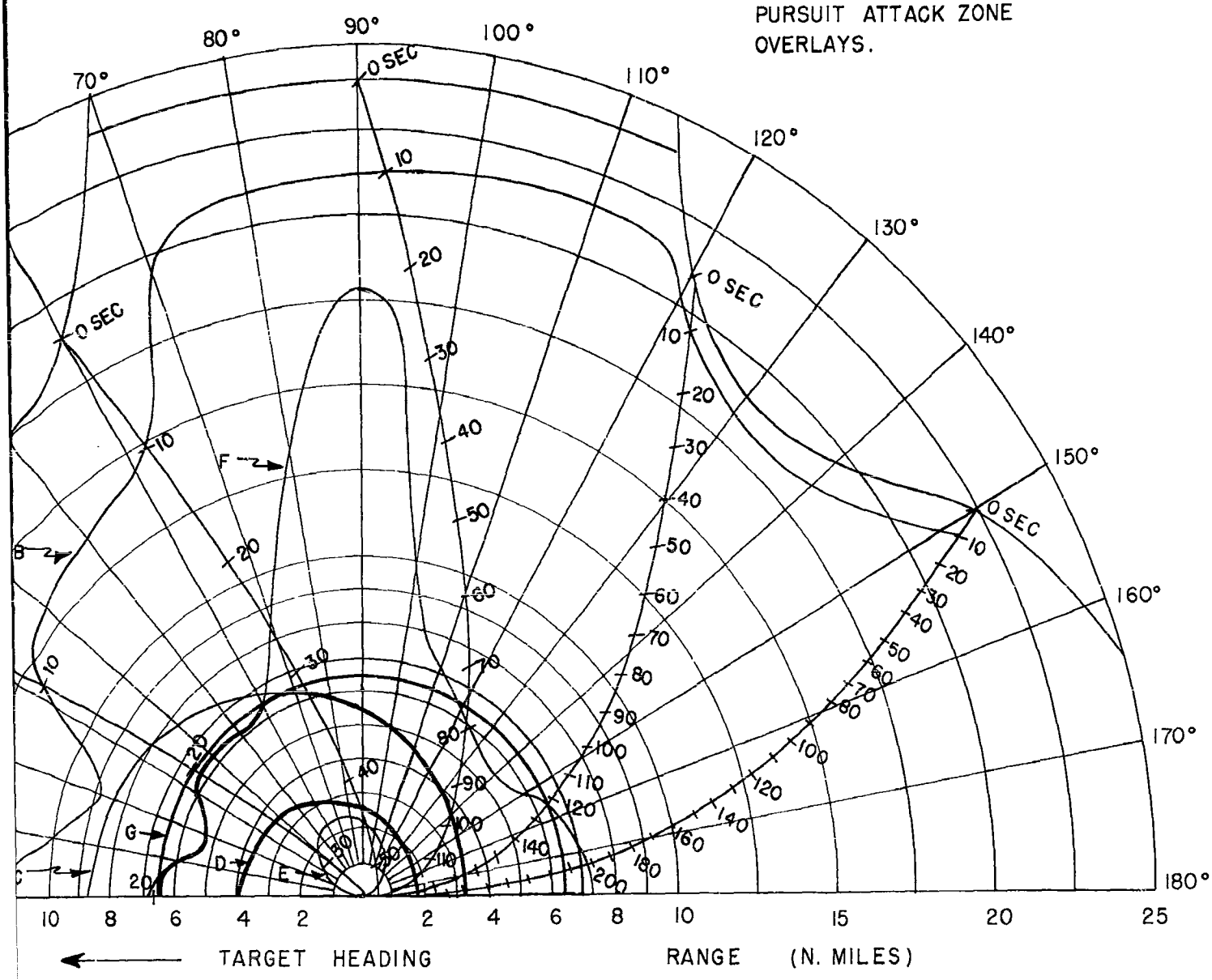

A - 85% DETECTION RANGE
B - LOCK-ON RANGE (10 SEC. LOCK-ON TIME)
C - SPARROW III MAX. AERODYNAMIC RANGE
D - SPARROW III MIN. AERODYNAMIC RANGE
E - CONSTANT LOAD FACTOR LOCUS ($N_Z = 3$)
F - 90% SPARROW III SEEKER LOCK-ON RANGE
G - 6.5 N.M. INTERLOCK

CONFIDENTIAL

Fig. 5 - Full-up Attacks - Head-on
Mach 2.0 Target, 65,000 Ft.
75% Detection Probability - B-47
Full-up 3g or $C_{L_{Max}}$
AN/APQ-72 (XN-3) Radar

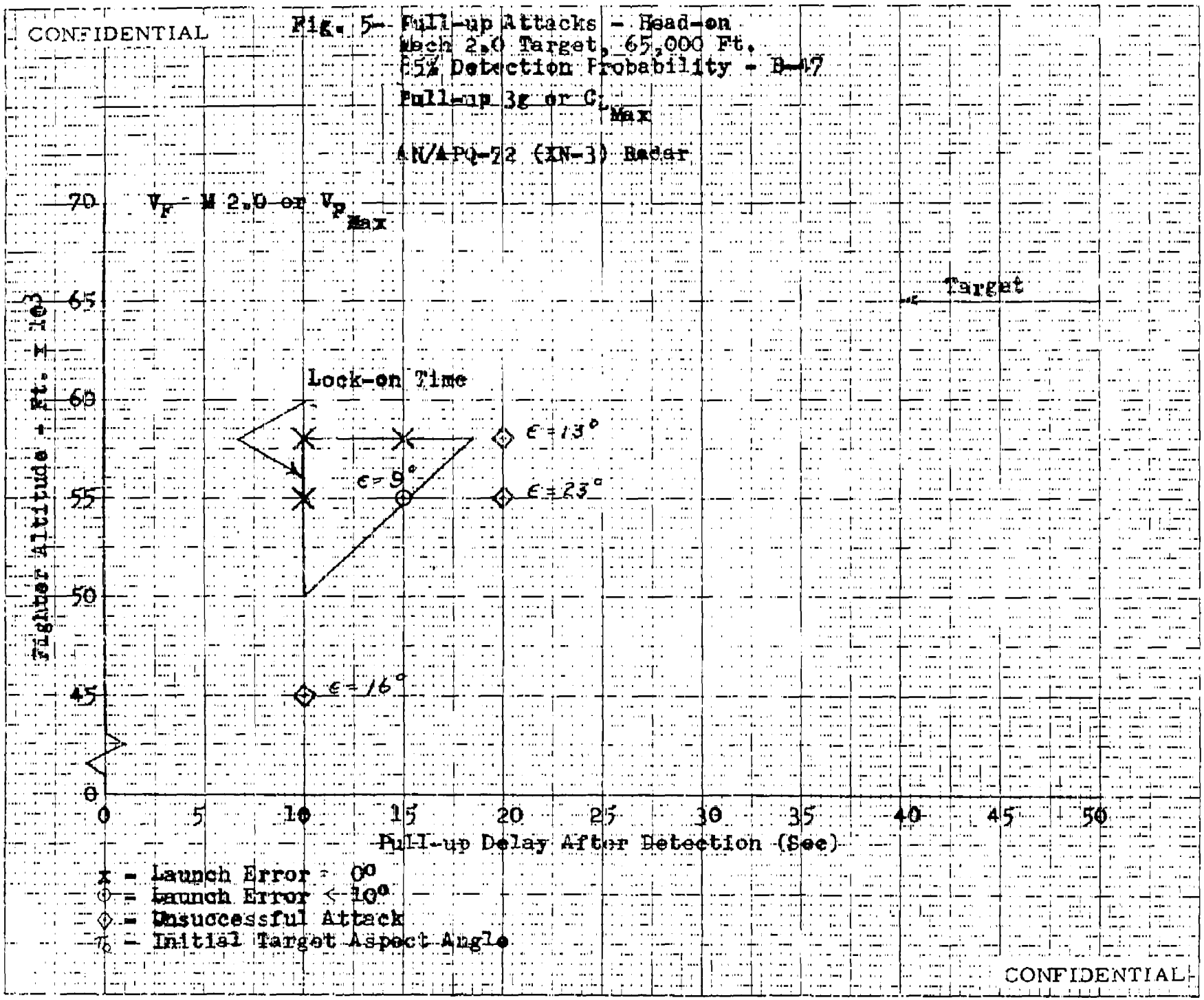

CONFIDENTIAL

CONFIDENTIAL

Fig. 6 - Pull-up Attacks - $\tau_o = 15^o$
Mach 2.0 Target, 65,000 Ft.
85% Detection Probability - B-47
Pull-up 3g or C-$_{Max}$
AN/APQ-72, (XN-3) Radar

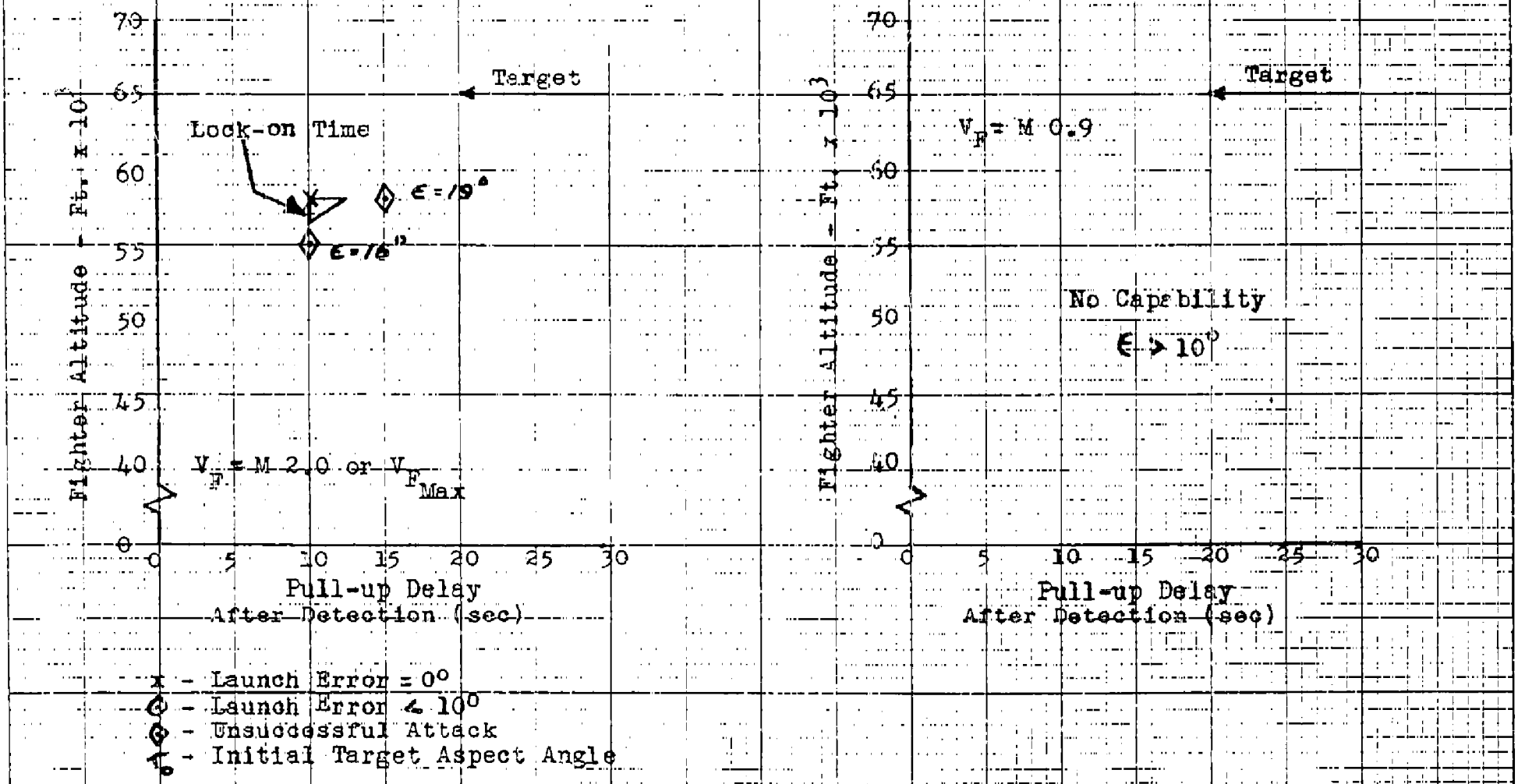

x - Launch Error = 0^o
⊙ - Launch Error < 10^o
⊗ - Unsuccessful Attack
τ_o - Initial Target Aspect Angle

CONFIDENTIAL

CONFIDENTIAL

Fig. 7 - Pull-up Attacks - $\tau_o = 30^o$
Mach 2.0 Target, 65,000 Ft.
85% Detection Probability - B-47
Pull-up 3g or $C_{L_{Max}}$
AN/APQ-72 (XN-3) Radar

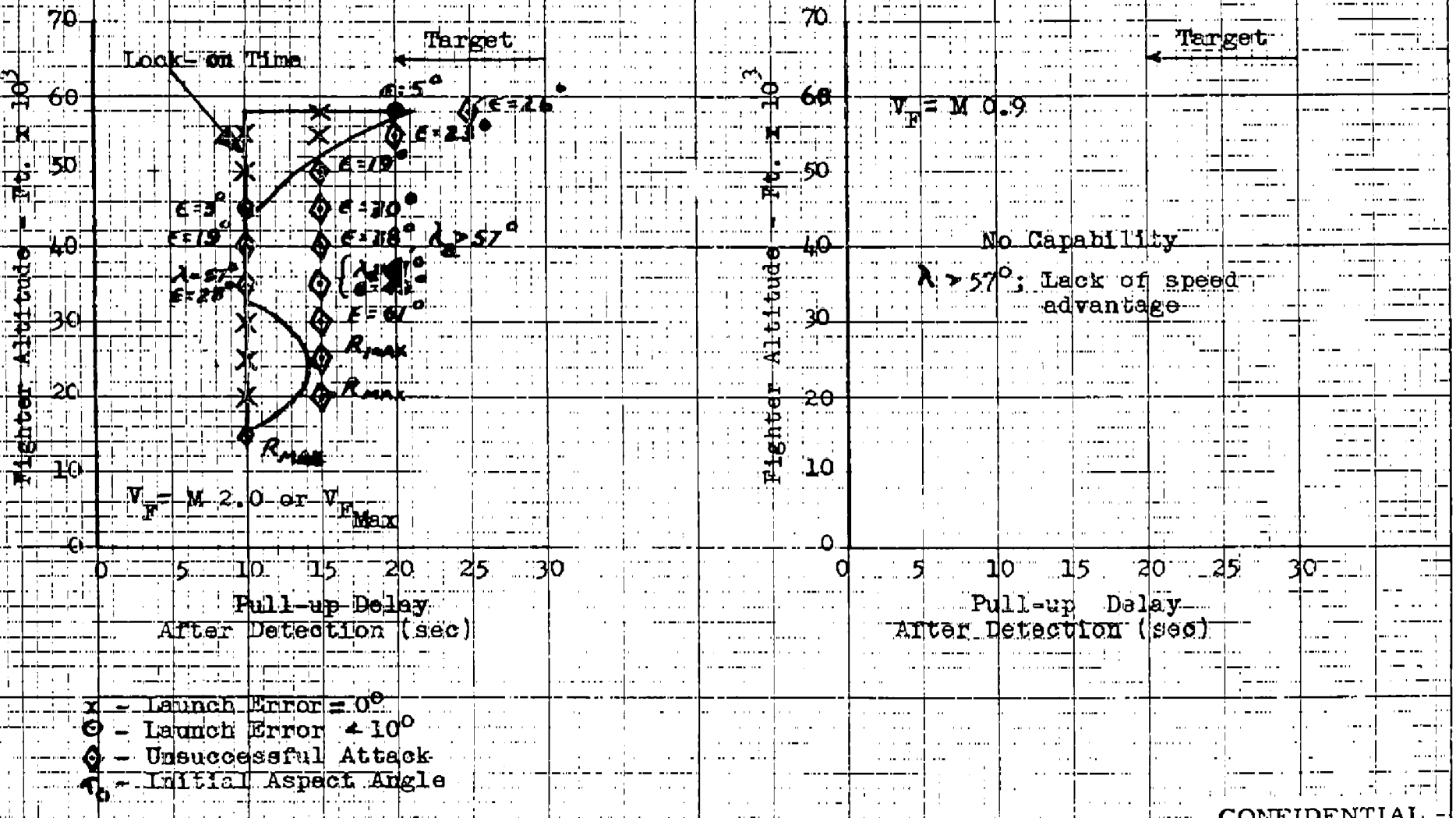

x - Launch Error = 0^o
⊙ - Launch Error < 10^o
◇ - Unsuccessful Attack
τ_o - Initial Aspect Angle

CONFIDENTIAL

CONFIDENTIAL

Fig. 8 - Pull-up Attacks - $\tau_0 = 45^\circ$
Mach 2.0 Target 65,000 Ft.
85% Detection Probability - B-47
Pull-up 3G or $C_{L_{Max}}$
AN/APQ-72 (XN-5) Radar

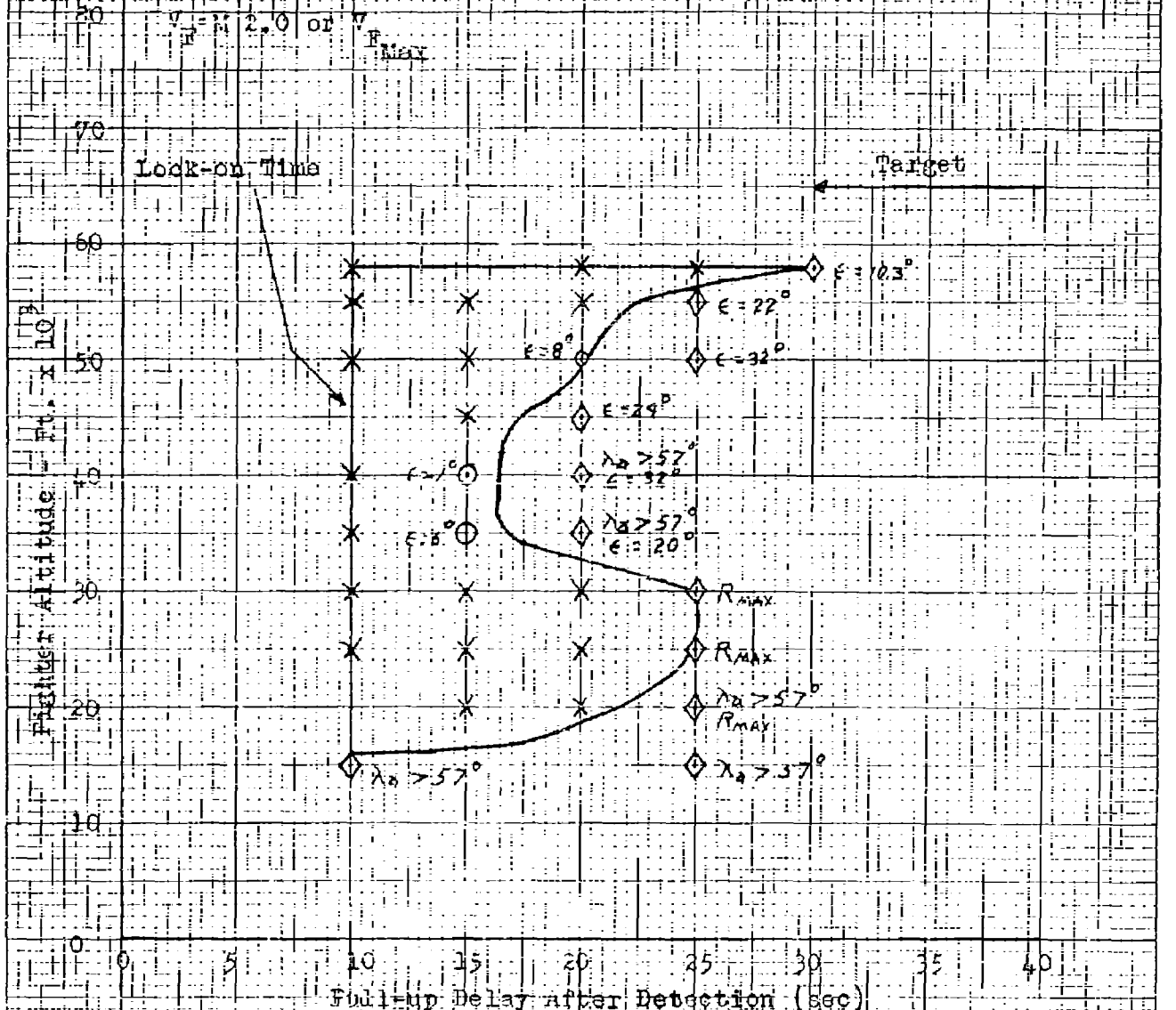

X - Launch Error = 0°
O - Launch Error $\leq 10^\circ$
◇ - Unsuccessful Attack
λ_a - Initial Target Aspect Angle

CONFIDENTIAL

CONFIDENTIAL

Fig. 9 - Pull-up Attack - $\gamma_o = 60^o$
Mach 2.0 Target, 65,000 Ft.
85% Detection Probability - B-47
Pull-up 3g or $C_{L_{Max}}$
AN/APQ-72 (XN-3) Radar

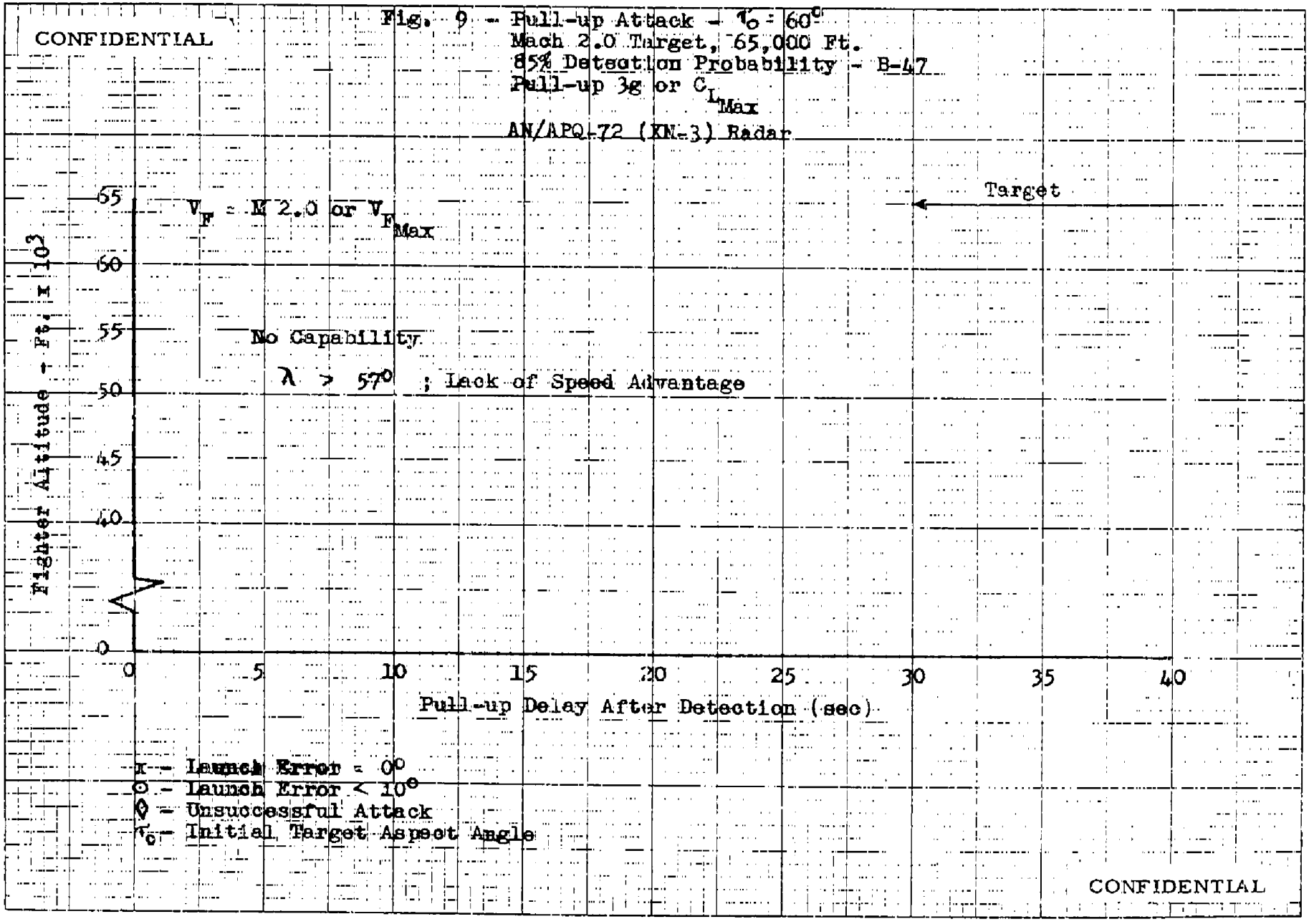

CONFIDENTIAL

CONFIDENTIAL

Fig. 10 - Pull-up Attack - Head-On
Mach 1.6 Target, 65,000 Ft.
85% Detection Probability - B-47
Pull-up 3g or $C_{L_{Max}}$
AN/APG-72 (XN-3) Radar

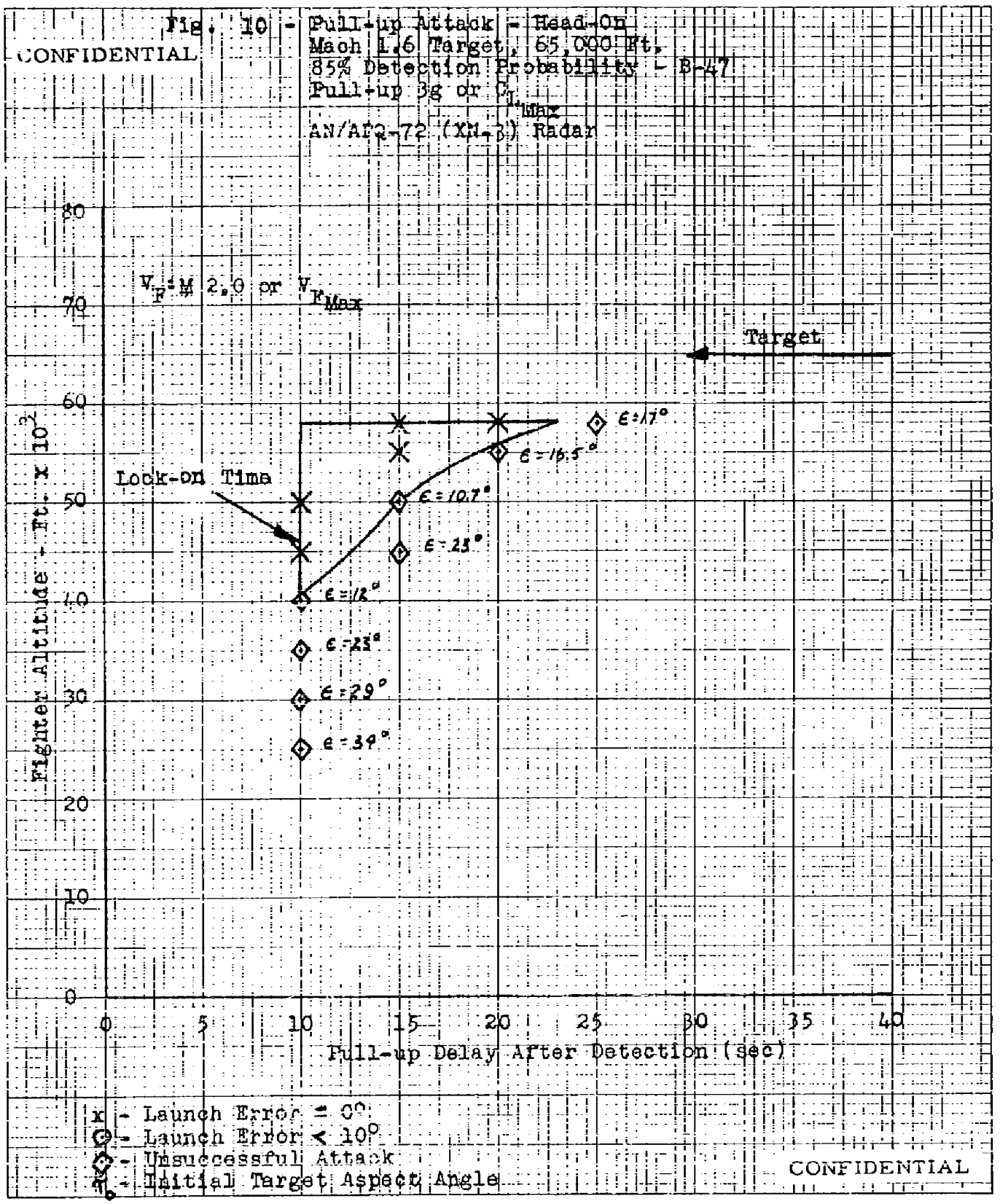

x - Launch Error = 0°
⊙ - Launch Error < 10°
◇ - Unsuccessful Attack
ε - Initial Target Aspect Angle

CONFIDENTIAL

CONFIDENTIAL

Fig. 11 - Pull-up Attacks - $\tau_o = 15^o$
Mach 1.6 Target, 65,000 Ft.
85% Detection Probability - B-47
Pull-up 3g or $C_{L_{Max}}$ - AN/APQ-72 (XN-3) Radar

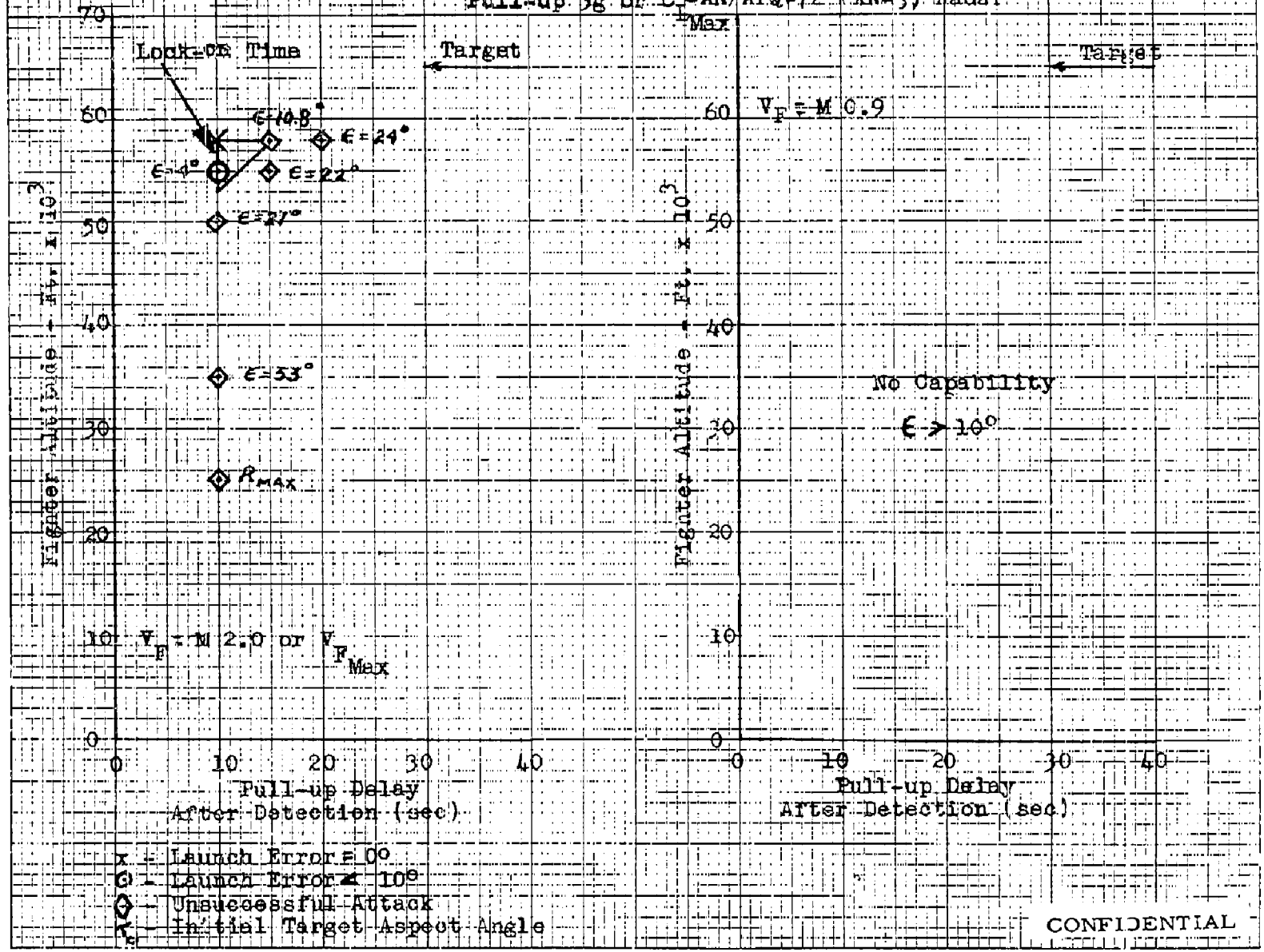

CONFIDENTIAL

CONFIDENTIAL

Fig. 12 - Pull-up Attacks - $\tau_0 = 30^0$
Mach 1.6 Target, 65,000 Ft.
85% Detection Probability - B-47
Pull-up 3g or $C_{L_{Max}}$
AN/APQ-72 (XN-3) Radar

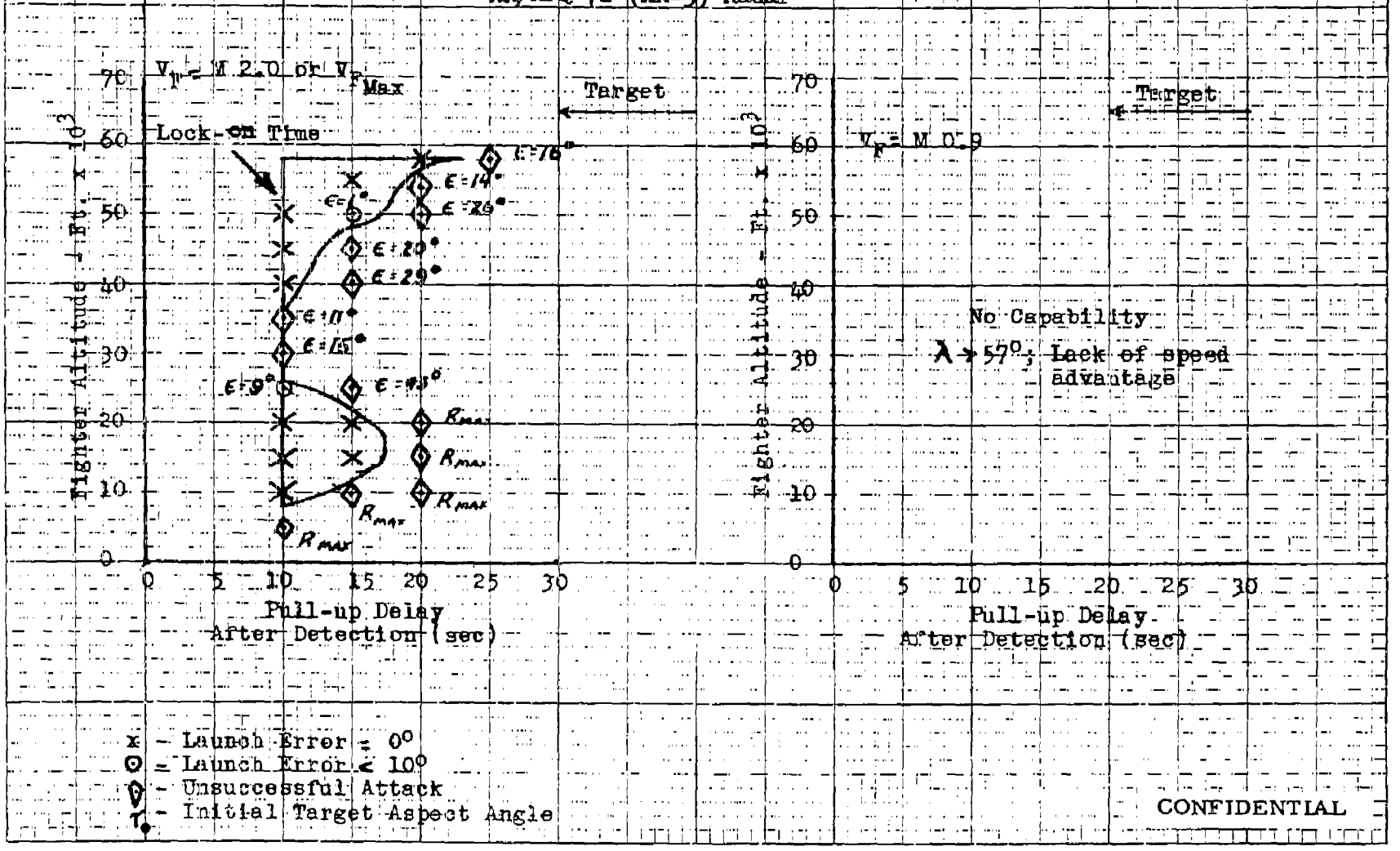

x - Launch Error = 0^0
⊙ - Launch Error < 10^0
◇ - Unsuccessful Attack
τ - Initial Target Aspect Angle

CONFIDENTIAL

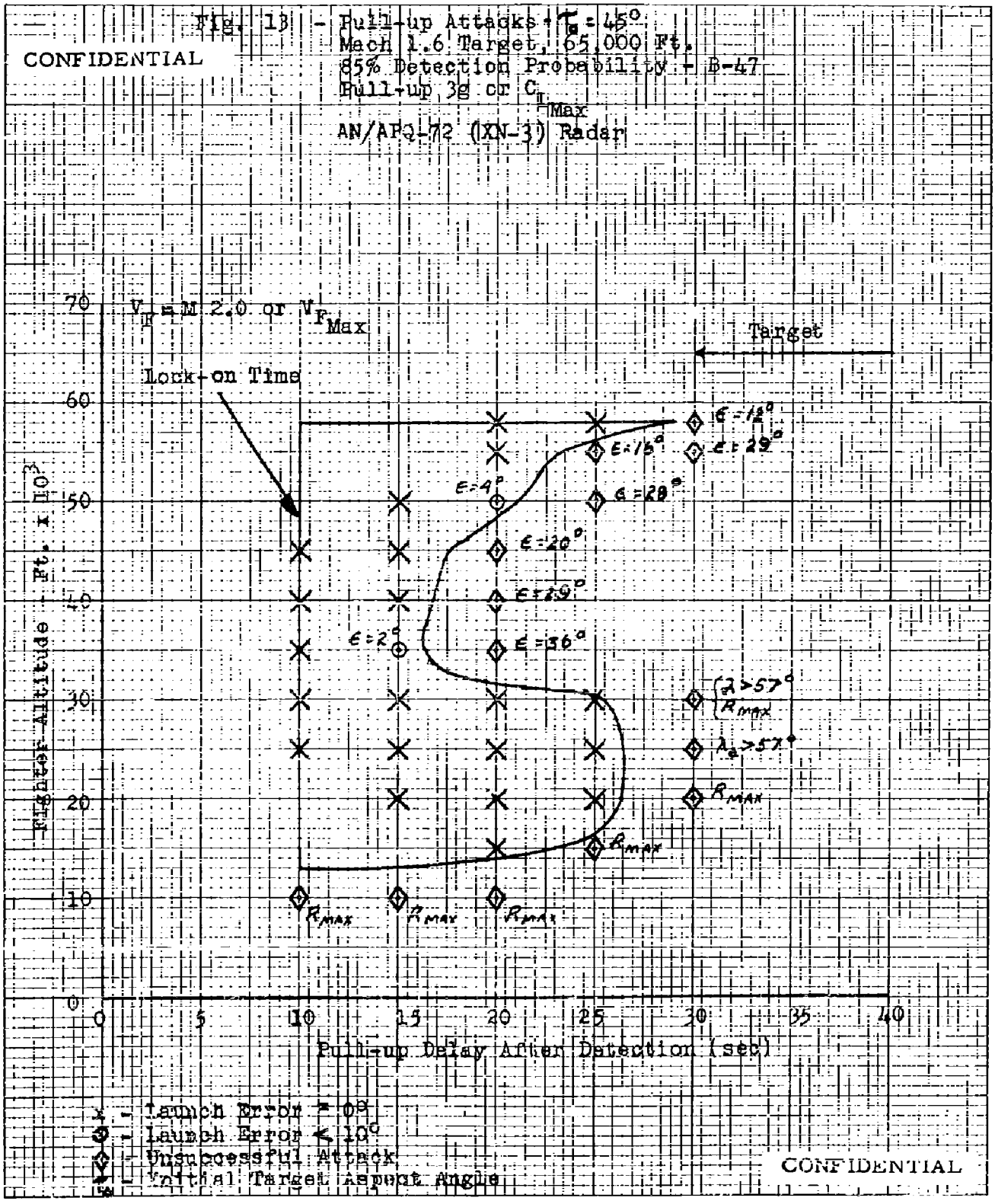
Fig. 13 - Pull-up Attacks - $T_a = 45°$
Mach 1.6 Target, 65,000 Ft.
85% Detection Probability - B-47
Pull-up 3g or $C_{n_{Max}}$
AN/APQ-72 (XN-3) Radar
CONFIDENTIAL
V_T = M 2.0 or $V_{T_{Max}}$
Target
Lock-on Time
ϵ=12°
ϵ=15°
ϵ=29°
ϵ=4°
ϵ=28°
ϵ=20°
ϵ=2.9°
ϵ=2°
ϵ=36°
$\lambda > 57°$ R_{max}
$\lambda_a > 57°$
R_{MAX}
R_{max}
R_{MAX} R_{MAX} R_{MAX}
Target Altitude - Ft. x 10^3
70
60
50
40
30
20
10
0
0 5 10 15 20 25 30 35 40
Pull-up Delay After Detection (sec)
x - Launch Error = 0°
- Launch Error ≤ 10°
- Unsuccessful Attack
- Initial Target Aspect Angle
CONFIDENTIAL

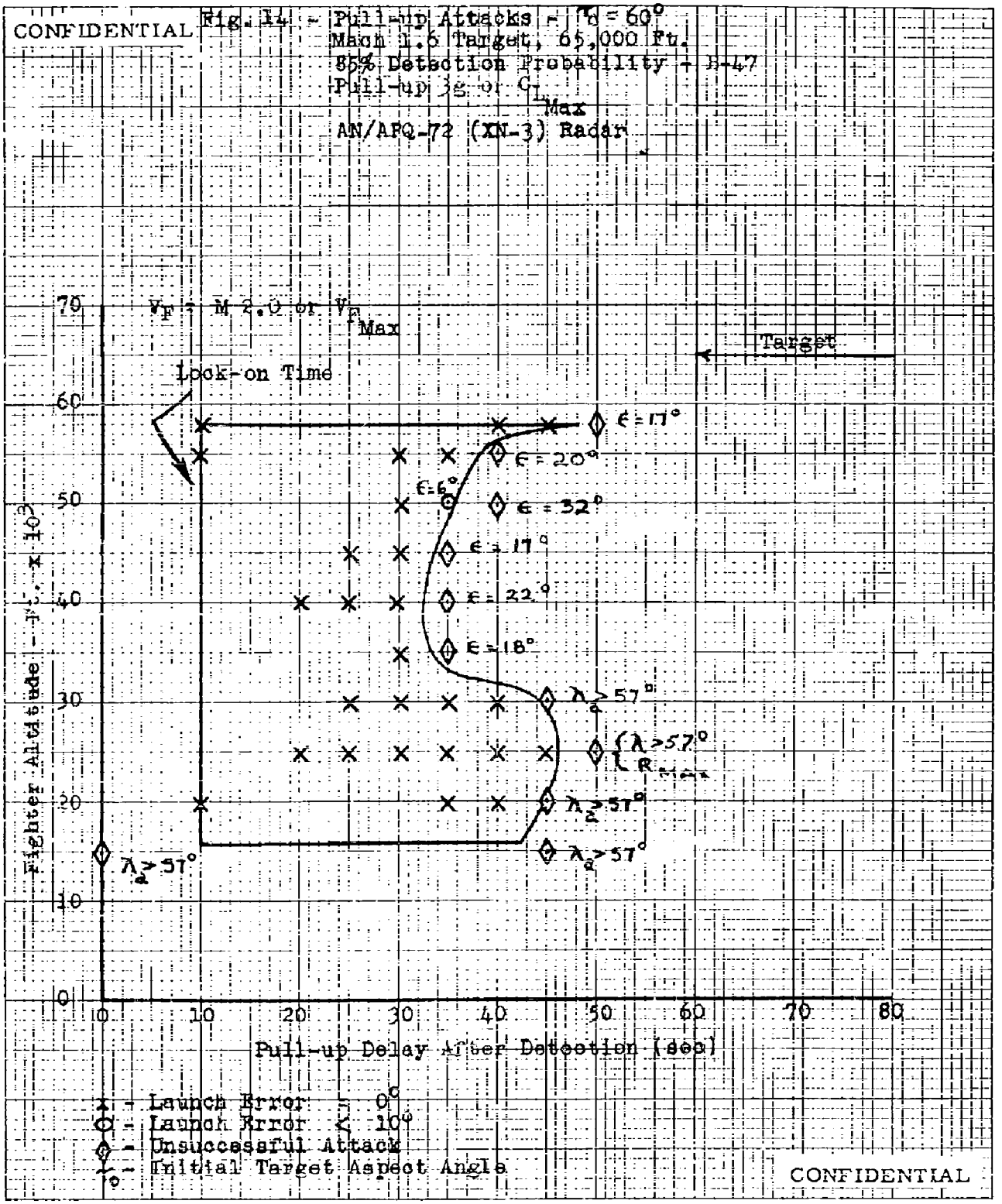
Fig. 14 - Pull-up Attacks - $\gamma_o = 60°$
Mach 1.6 Target, 65,000 Ft.
85% Detection Probability - B-47
Pull-up 3g or $C_{L_{Max}}$
AN/APQ-72 (XN-3) Radar
V_F = M 2.0 or $V_{D_{Max}}$
Target
Lock-on Time
$\epsilon = 17°$
$\epsilon = 20°$
$\epsilon = 6°$
$\epsilon = 32°$
$\epsilon = 17°$
$\epsilon = 22°$
$\epsilon = 18°$
$\lambda_a > 57°$
$\lambda_a > 57°$
$\lambda_a > 57°$
$\lambda_a > 57°$
$\lambda_a > 57°$
Fighter Altitude - $Y_F \times 10^3$
Pull-up Delay After Detection (sec)
0
10
20
30
40
50
60
70
80
- Launch Error = 0°
- Launch Error < 10°
- Unsuccessful Attack
- Initial Target Aspect Angle

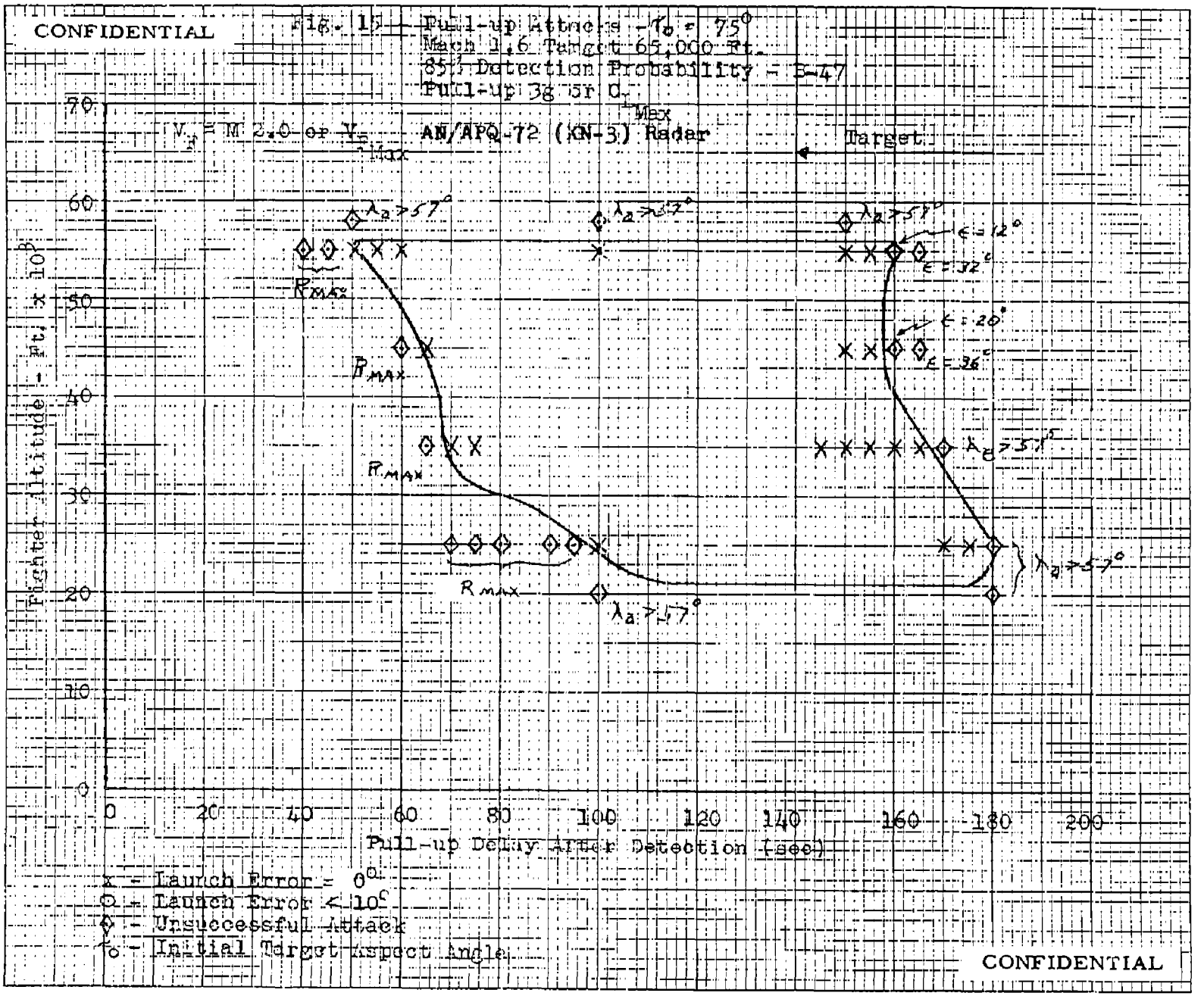
CONFIDENTIAL
Fig. 15
Pull-up Attack - γ_o = 75°
Mach 1.6 Target 65,000 Ft.
85% Detection Probability = 5.47
Pull-up 3g or n_{max}
V_i = M 2.0 or $V_{i\,max}$
AN/APQ-72 (XN-3) Radar
Target
$\lambda_a > 57°$
R_{max}
ϵ = 12°
ϵ = 32°
ϵ = 20°
ϵ = 36°
Fighter Altitude - Ft. x 10^3
70
60
50
40
30
20
10
0
0
20
40
60
80
100
120
140
160
180
200
Pull-up Delay After Detection (sec)
x - Launch Error = 0°
o - Launch Error < 10°
◇ - Unsuccessful Attack
ε - Initial Target Aspect Angle
CONFIDENTIAL

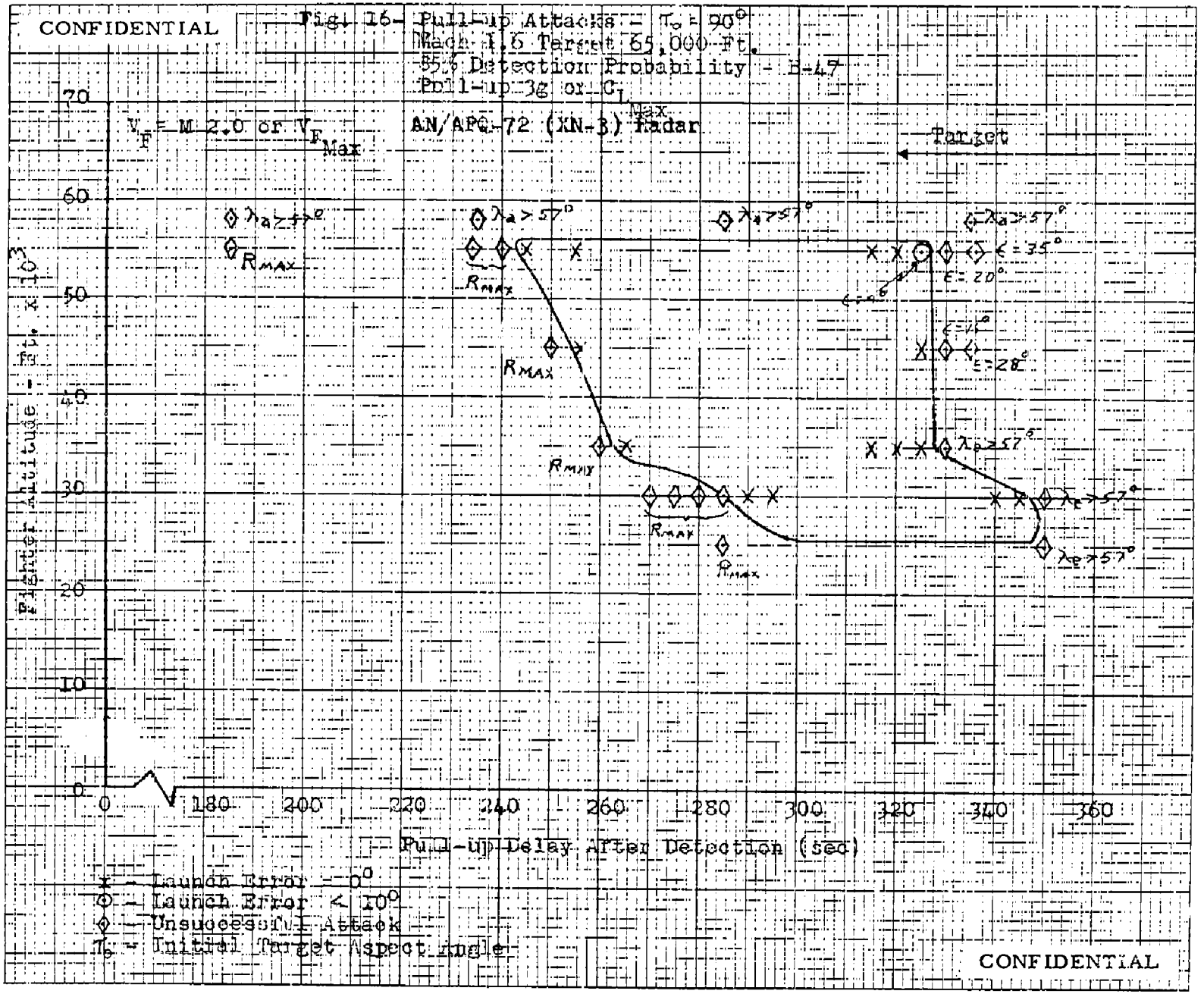
CONFIDENTIAL
Fig. 16- Pull-up Attacks - T_o = 90°
Mach 1.6 Target 65,000 Ft.
85% Detection Probability - B-47
Pull-up 3g or $C_{L_{Max}}$
V_F = M 2.0 or $V_{F_{Max}}$
AN/APG-72 (XN-3) Radar
Target
Pursuit Altitude - Thousands of Ft.
Pull-up Delay After Detection (sec)
x — Launch Error = 0°
⊙ — Launch Error < 10°
◊ — Unsuccessful Attack
T_o = Initial Target Aspect Angle
CONFIDENTIAL

CONFIDENTIAL

Fig. 17- Pull-up Attacks - $\tau_o = 120°$
Mach 1.6 Target - 65,000 Ft.
85% Detection Probability - B-47
Pull-up Delay after I_{Max}
AN/APQ-72 (XN-1) Radar

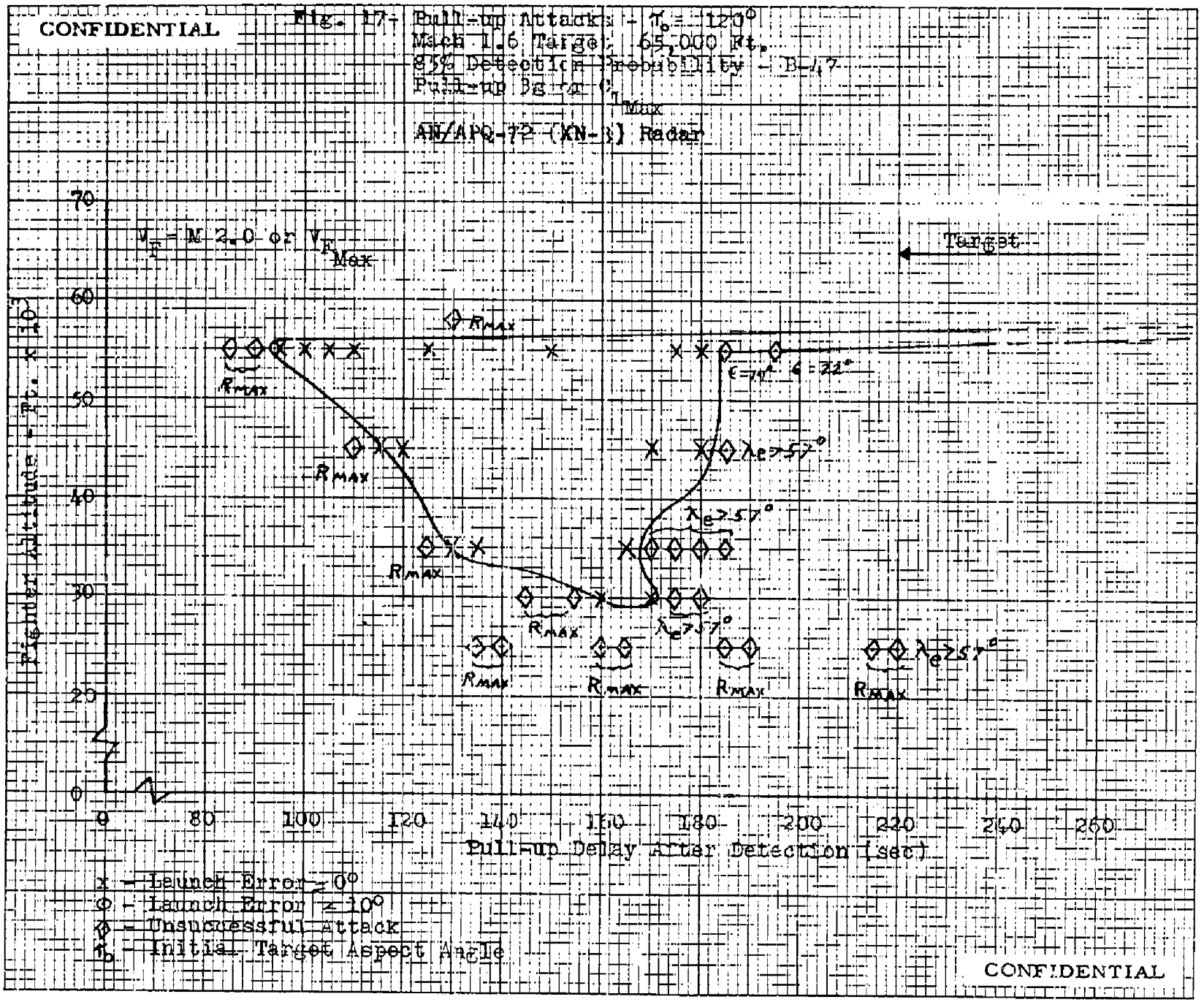

x - Launch Error = 0°
Φ - Launch Error = 10°
◊ - Unsuccessful Attack
τ_o - Initial Target Aspect Angle

CONFIDENTIAL

CONFIDENTIAL

Fig. 18 Pull-up Attacks $\tau_o = 150°$
Mach 1.6 Target 65,000 Ft.
85% Detection Probability - β=47
Pull-up 3g or G_{max}
AN/APQ-72 (XN-3) Radar

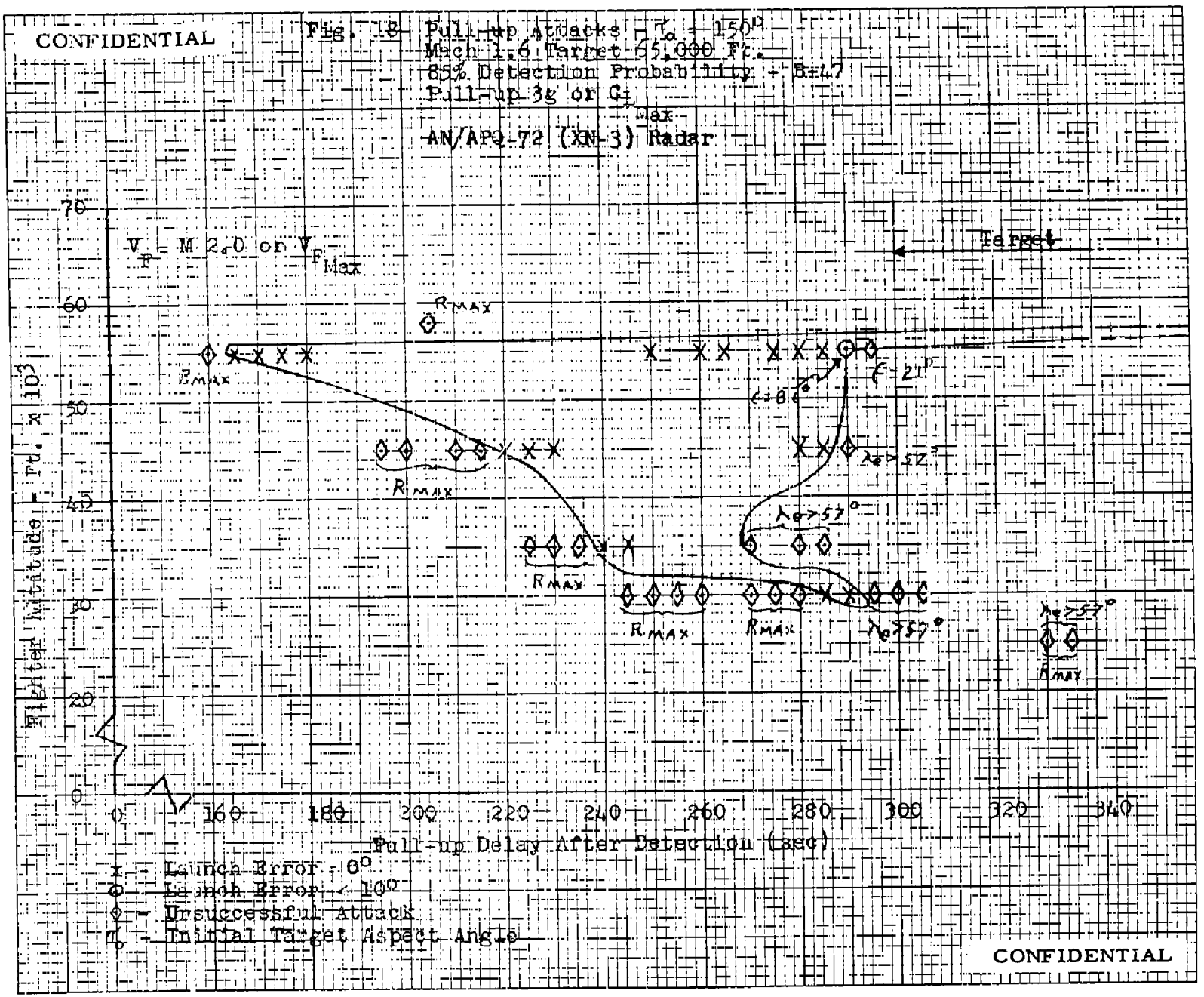

x - Launch Error - 6°
o - Launch Error - 10°
◇ - Unsuccessful Attack
τ_o - Initial Target Aspect Angle

CONFIDENTIAL

CONFIDENTIAL

Fig. 19 - Pull-up Attack - τ_o = 180°
Mach 1.6 Target 65,000 Ft.
85% Detection Probability - P-47
Pull-up 3g or $\theta_{1\,Max}$
AN/APQ-72 (XN-3) Radar

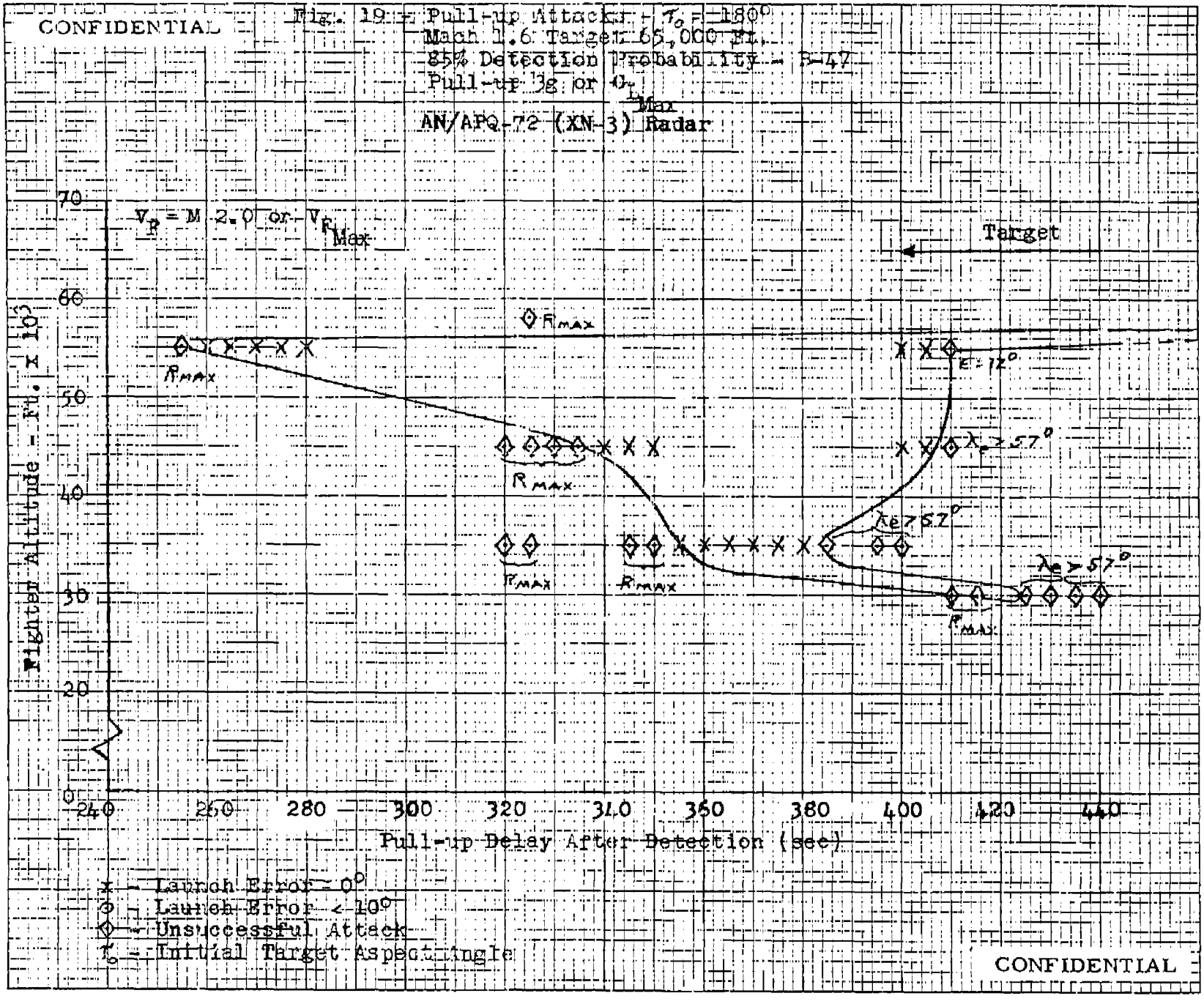

x - Launch Error = 0°
⊘ - Launch Error < 10°
◇ - Unsuccessful Attack
τ_o - Initial Target Aspect Angle

CONFIDENTIAL

CONFIDENTIAL

Fig. 20 - Pull-up Attacks - Head-on
Mach 2.0 Target, 50,000 Ft.
85% Detection Probability - E-47
Pull-up 3g or $C_{L_{Max}}$
AN/APQ-72 (XN-3) Radar

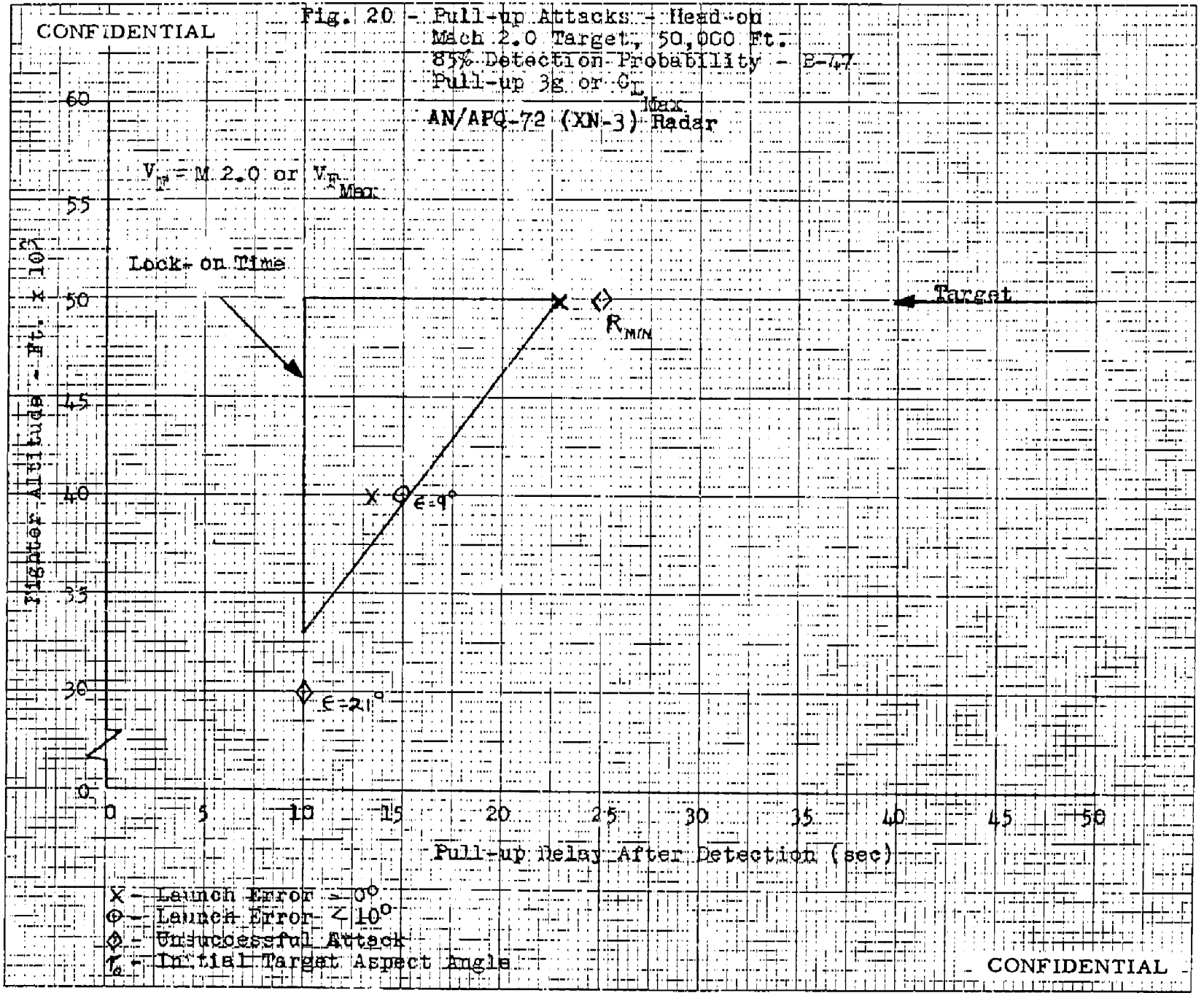

CONFIDENTIAL

CONFIDENTIAL

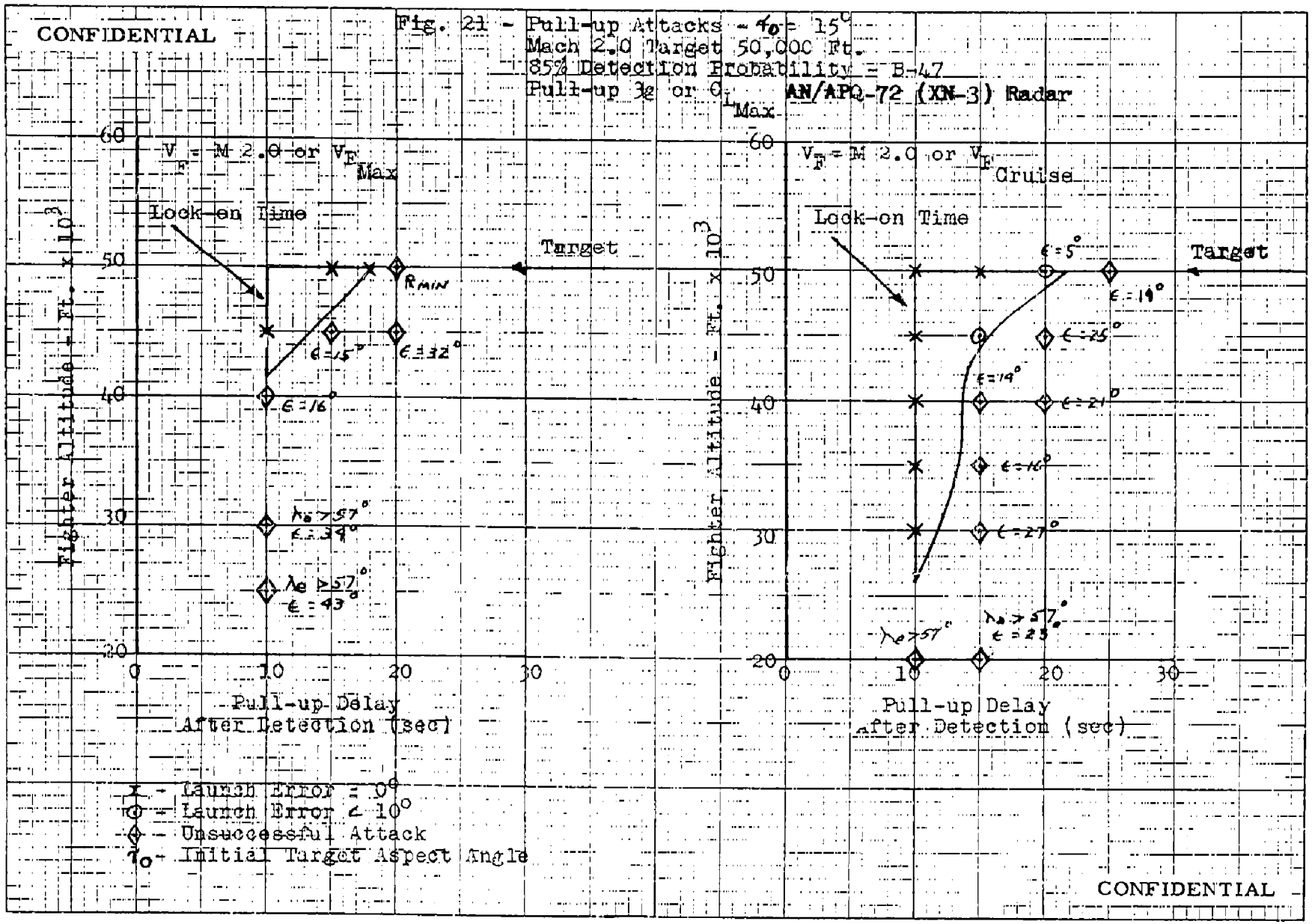

CONFIDENTIAL

CONFIDENTIAL

Fig. 22 - Pull-up Attacks - $\tau_o = 30^\circ$
Mach 2.0 Target, 50,000 Ft.
85% Detection Probability - B-47
AN/APQ-72 (XN-3) Radar

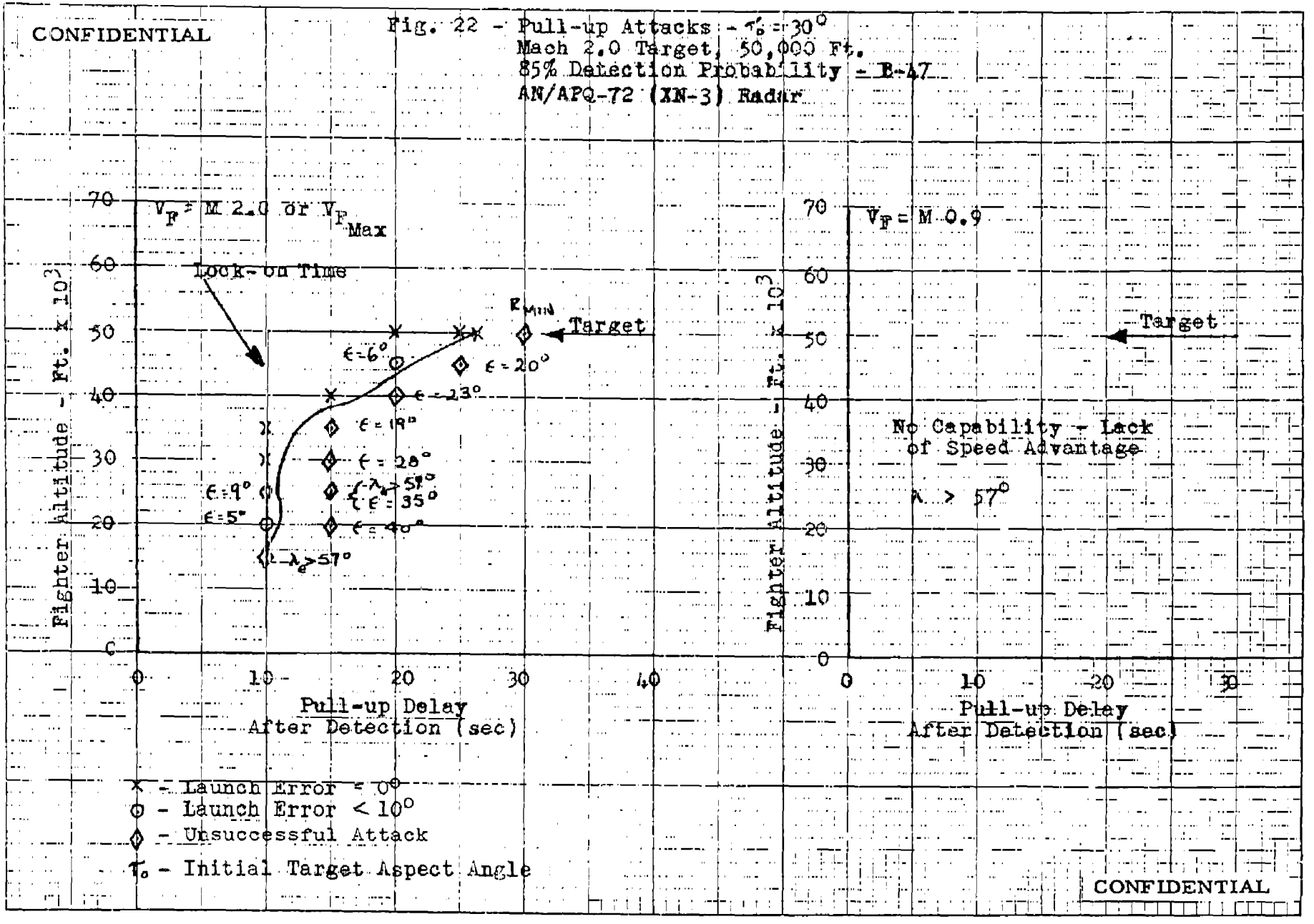

CONFIDENTIAL

CONFIDENTIAL

Fig. 23 - Pull-up Attacks, $\gamma_o = 45^\circ$
Mach 2.0 Target, 50,000 Ft.
85% Detection Probability - B-47
Pull-up 3g or $C_{L_{Max}}$
AN/APQ-72 (XN-3) Radar

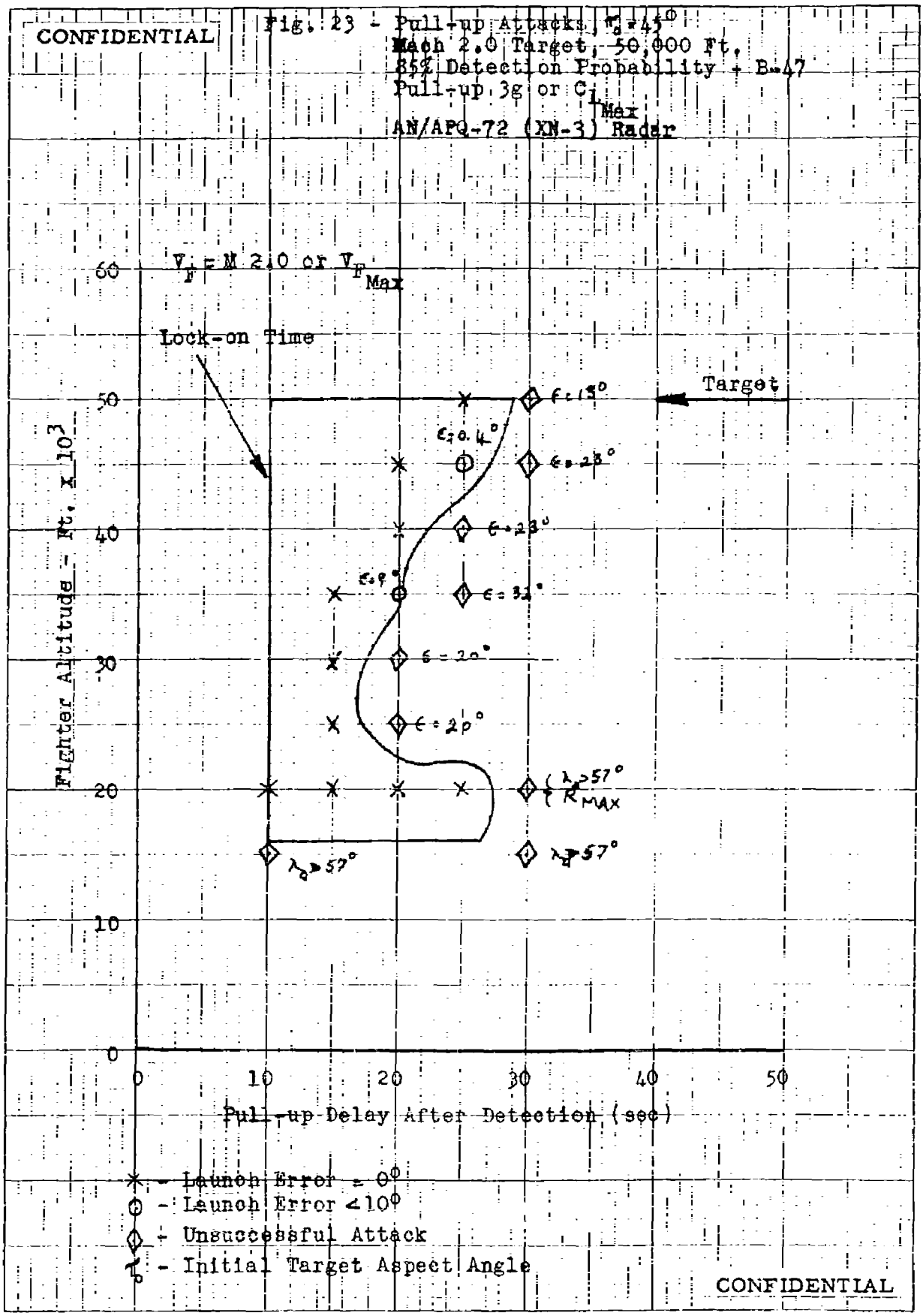

✳ - Launch Error = 0°
⊙ - Launch Error < 10°
◇ - Unsuccessful Attack
γ_o - Initial Target Aspect Angle

CONFIDENTIAL

CONFIDENTIAL

Fig. 24 - Pull-up Attacks - $\tau_o = 60^o$
Mach 2.0 Target, 50,000 Ft.
85% Detection Probability - B-47
Pull-up 3g or $C_{L_{Max}}$
AN/APQ-72 (XN-3) Radar

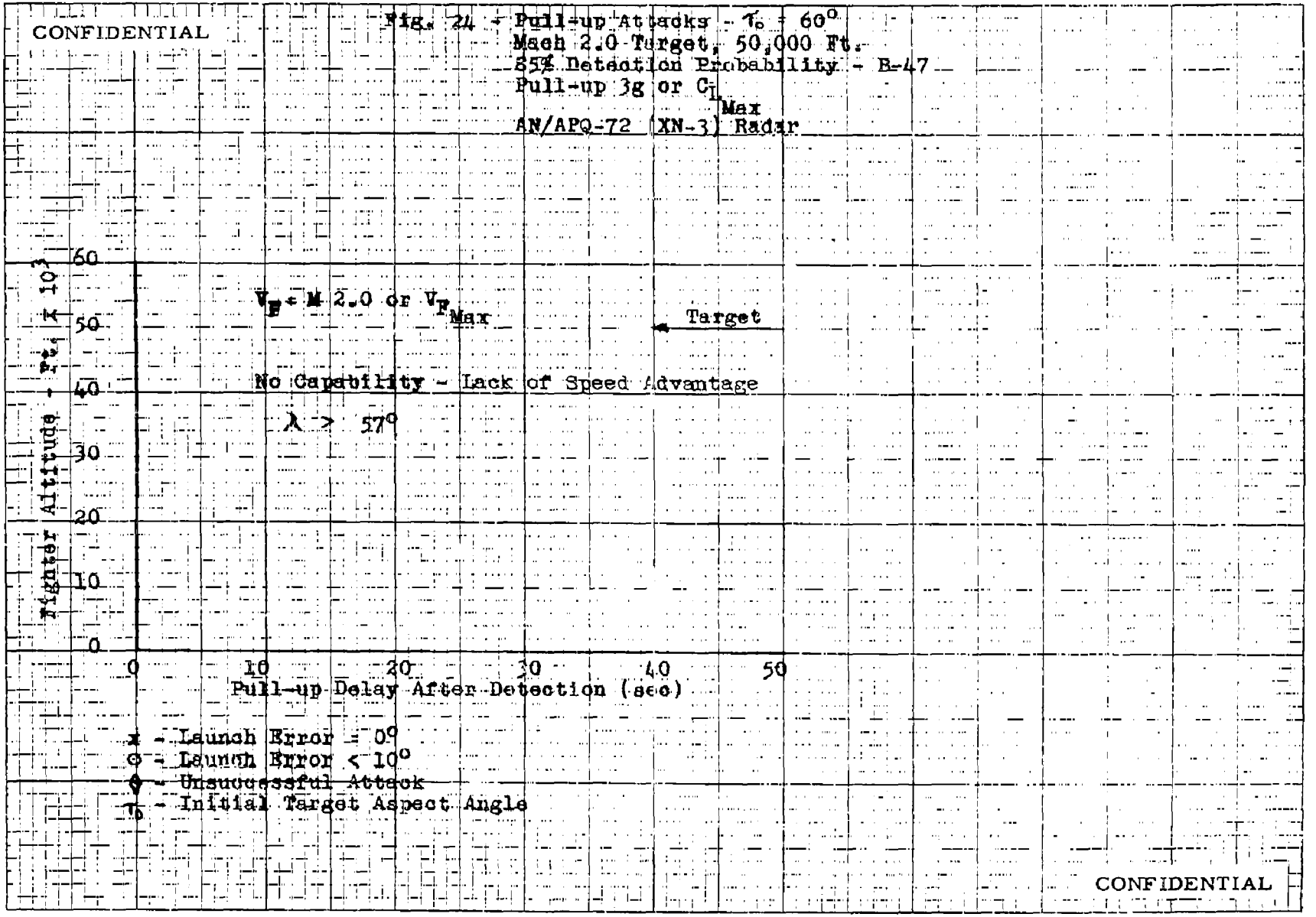

CONFIDENTIAL

CONFIDENTIAL

Fig. 25 - Pull-up Attack - Head On
Mach 1.6 Target, 50,000 Ft.
85% Detection Probability - B-47
Pull-up 3g or $C_{L_{Max}}$
AN/APQ-72 (XN-3) Radar

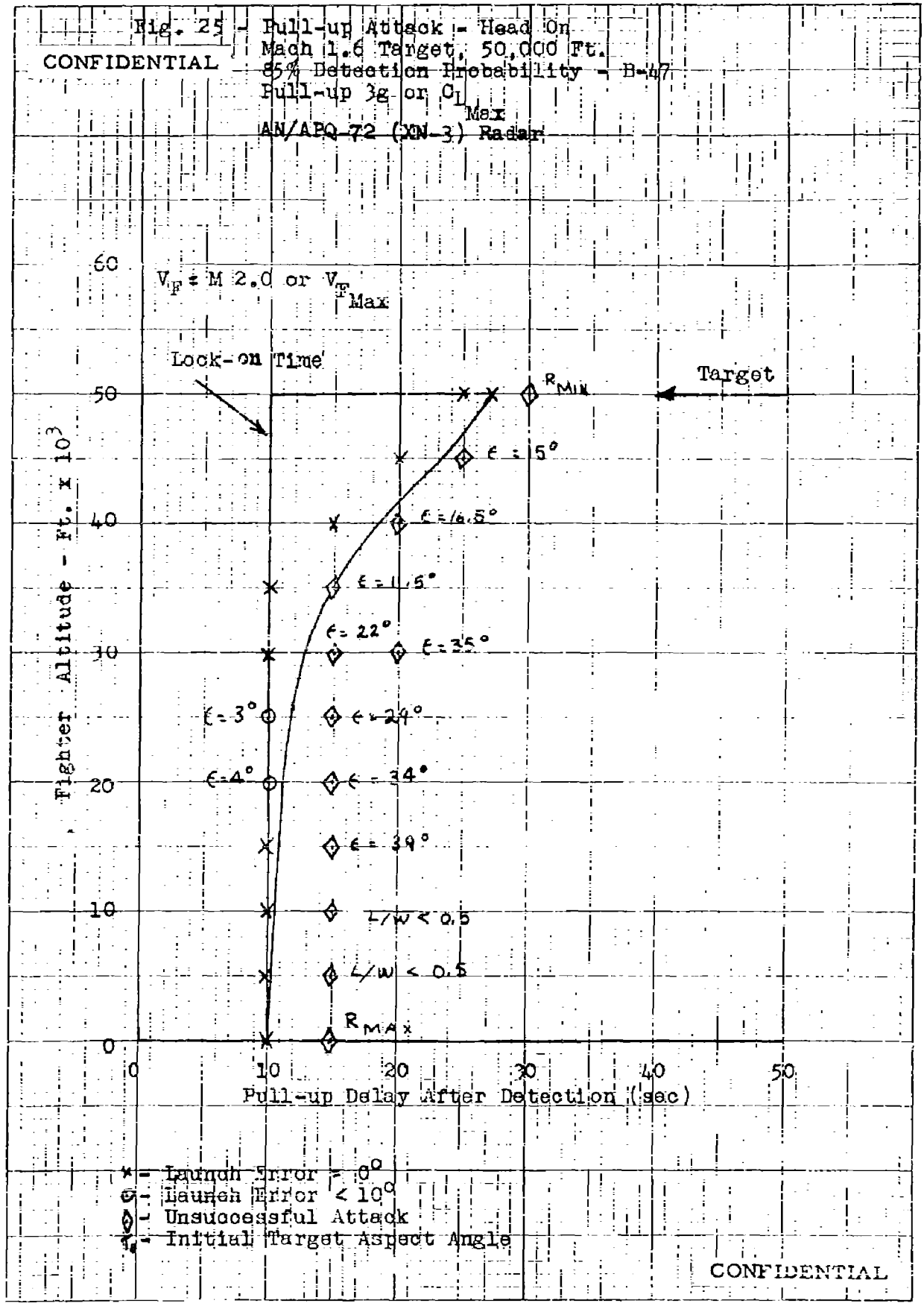

* - Launch Error = 0°
⊙ - Launch Error < 10°
◇ - Unsuccessful Attack
ϵ - Initial Target Aspect Angle

CONFIDENTIAL

CONFIDENTIAL

Fig. 26 - Pull-up Attacks - τ_o = 15°
Mach 1.6 Target 50,000 Ft.
85% Detection Probability - B-47
Pull-up 3 g or $C_{L_{Max}}$
AN/APQ-72 (XN-3) Radar

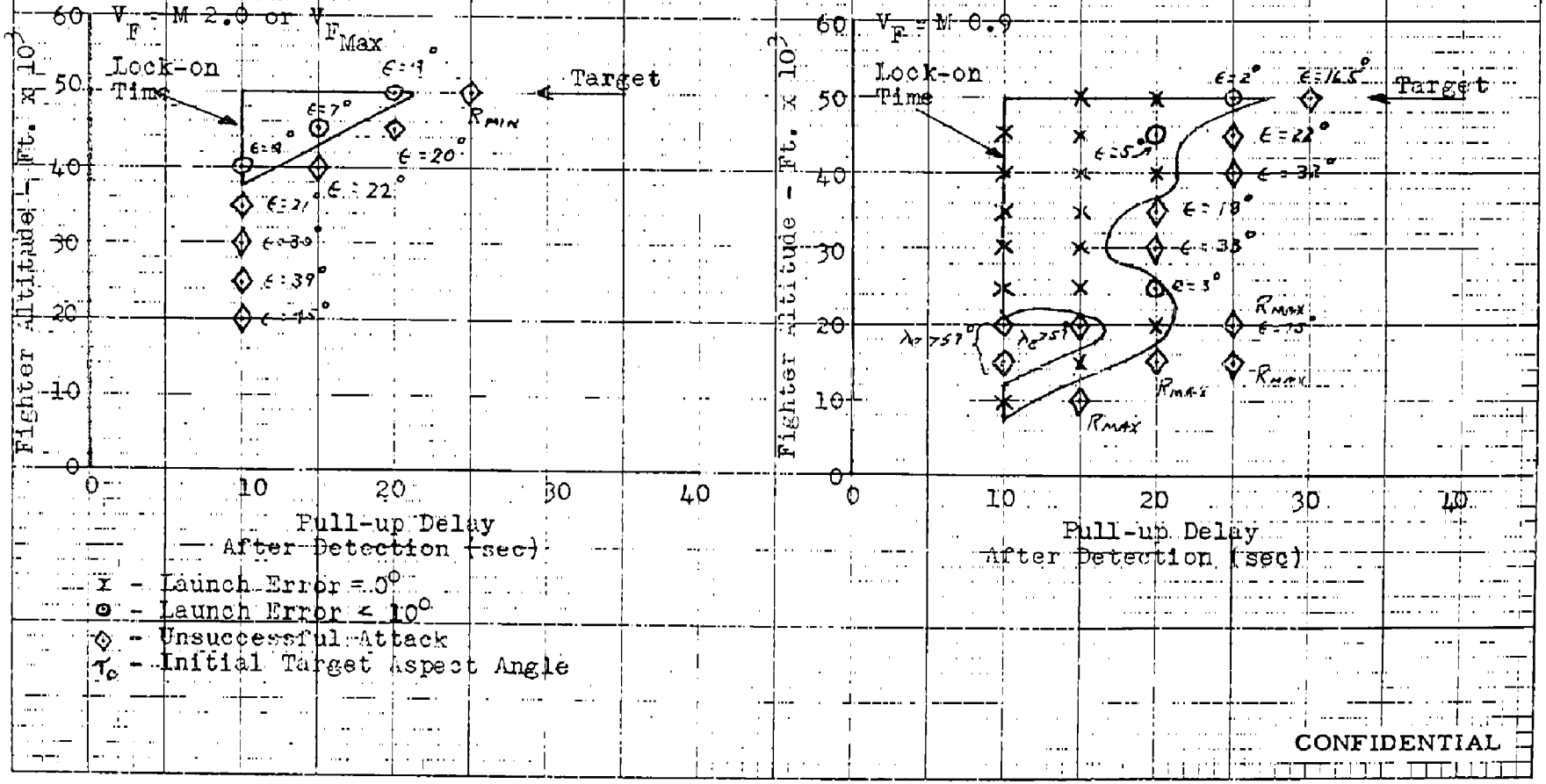

X - Launch Error = 0°
⊙ - Launch Error ≤ 10°
◇ - Unsuccessful Attack
τ_o - Initial Target Aspect Angle

CONFIDENTIAL

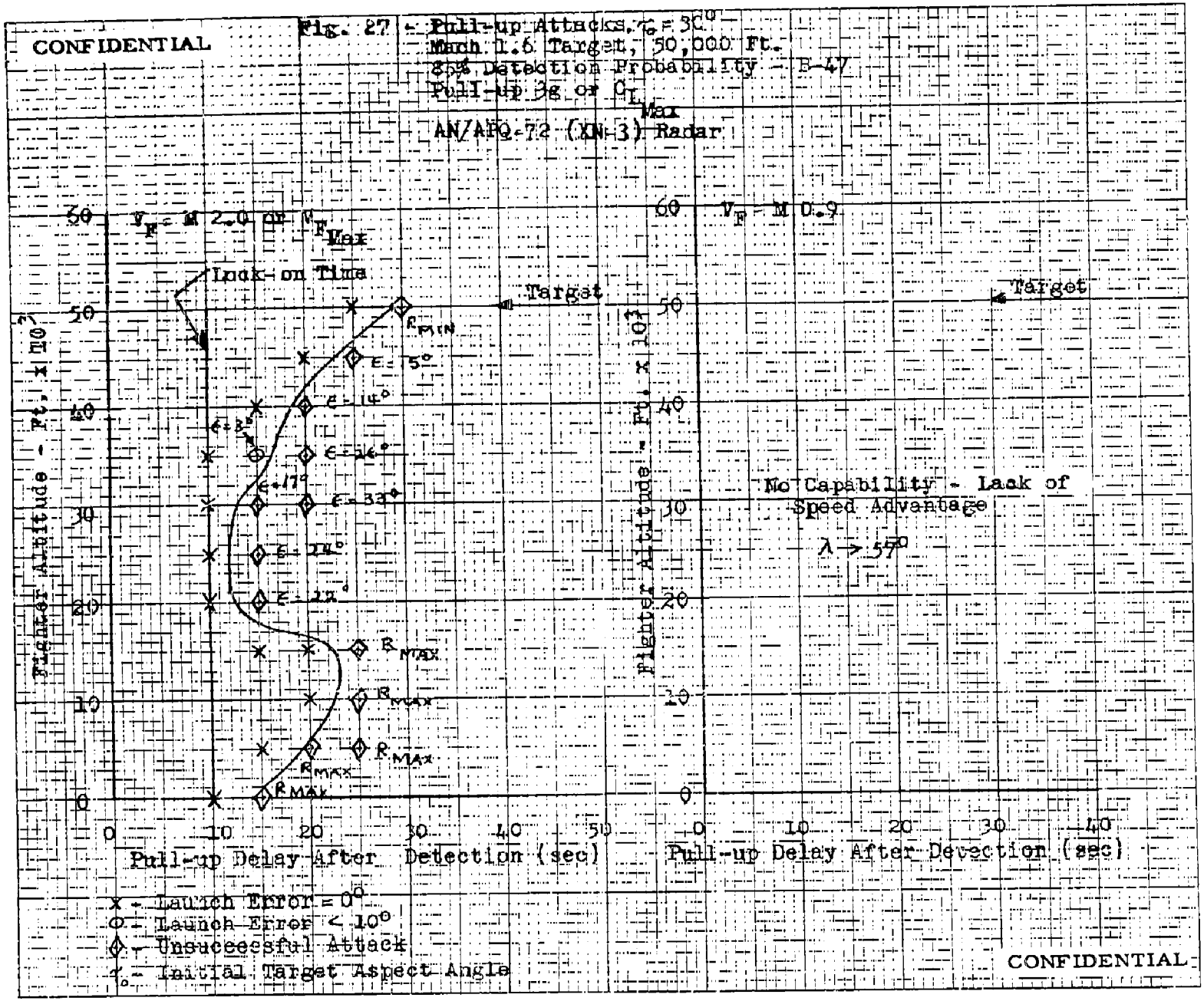
CONFIDENTIAL
Fig. 27 - Pull-up Attacks, $\alpha_o = 30^0$
Mach 1.6 Target, 50,000 Ft.
85% Detection Probability - F-4V
Pull-up 3g or $C_{L_{Max}}$
AN/AFQ-72 (XN-3) Radar
V_F = M 2.0 or $V_{F_{Max}}$
Lock-on Time
Target
R_{MIN}
$\epsilon = 5^0$
$\epsilon = 14^0$
$\epsilon = 24^0$
$\epsilon = 33^0$
$\epsilon = 17^0$
$\epsilon = 28^0$
$\epsilon = 22^0$
R_{MAX}
Fighter Altitude - P_o x 10³
Pull-up Delay After Detection (sec)
V_F = M 0.9
Target
No Capability - Lack of Speed Advantage
$\lambda > 57^0$
Fighter Altitude - P_o x 10³
Pull-up Delay After Detection (sec)
X - Launch Error = 0^0
O - Launch Error < 10^0
◇ - Unsuccessful Attack
α_o - Initial Target Aspect Angle
CONFIDENTIAL

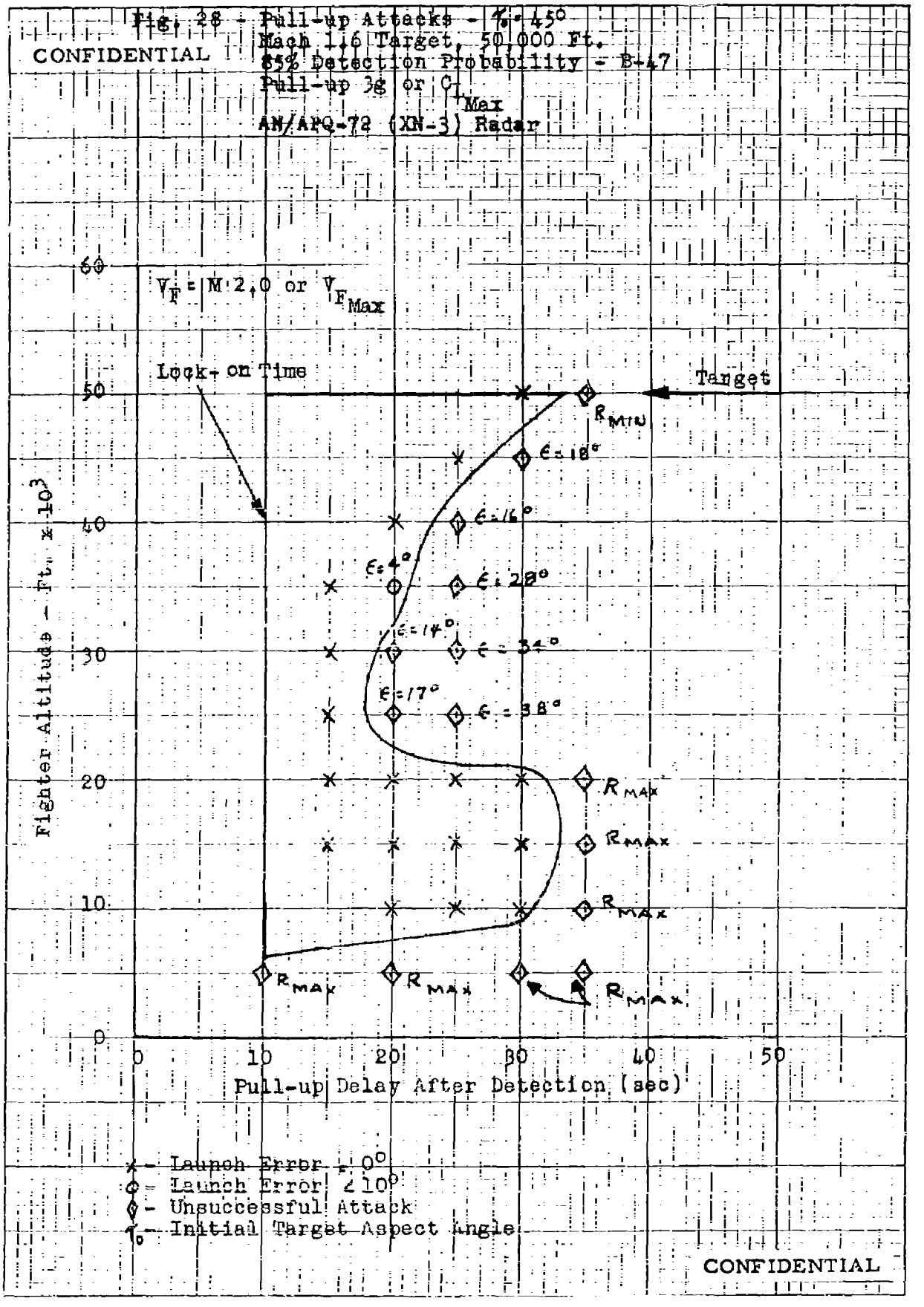
Fig. 28 - Pull-up Attacks - $\gamma_o = 45°$
Mach 1.6 Target, 50,000 Ft.
85% Detection Probability - B-47
Pull-up 3g or $C_{L_{Max}}$
AN/APQ-72 (XN-3) Radar
CONFIDENTIAL
V_F = M 2.0 or $V_{F_{Max}}$
Lock-on Time
Target
R_{MIN}
$\epsilon = 18°$
$\epsilon = 16°$
$\epsilon = 4°$
$\epsilon = 20°$
$\epsilon = 14°$
$\epsilon = 34°$
$\epsilon = 17°$
$\epsilon = 38°$
R_{MAX}
Fighter Altitude - Ft. x 10^3
Pull-up Delay After Detection (sec)
x - Launch Error ± 0°
o - Launch Error ± 10°
◊ - Unsuccessful Attack
γ_o - Initial Target Aspect Angle
CONFIDENTIAL

Fig. 29 - Pull-up Attacks, $\gamma_o = 60°$
Mach 1.6 Target, 50,000 Ft.
85% Detection Probability - B-47
Pull-up 3g or $C_{L_{Max}}$
AN/APQ-72 (XN-3) Radar

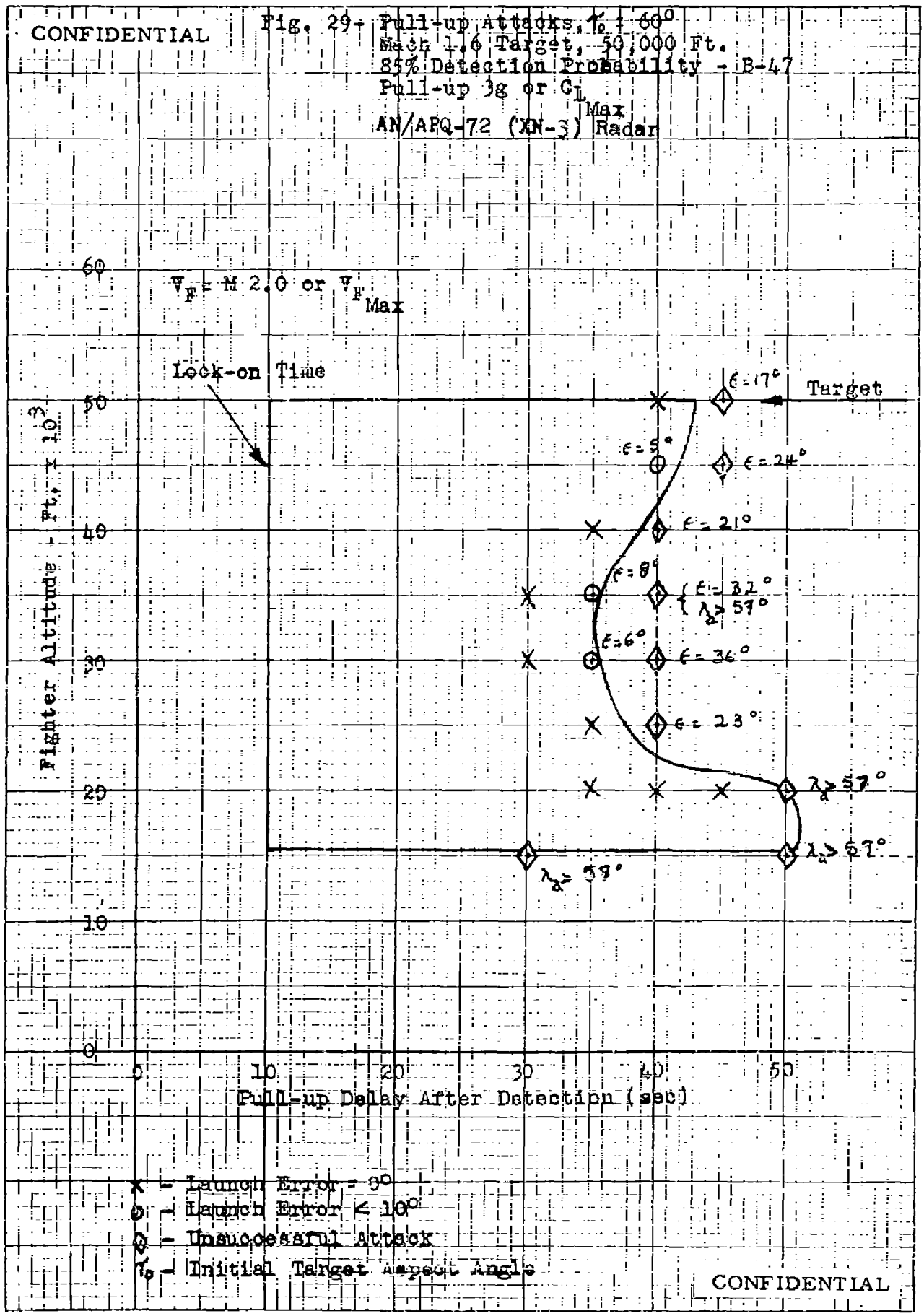

× - Launch Error = 0°
⊙ - Launch Error < 10°
◇ - Unsuccessful Attack
γ_o - Initial Target Aspect Angle

CONFIDENTIAL

Fig. 30 - Pull-up Attacks, $T_o = 75°$
Mach 1.6 Target, 50,000 Ft.
85% Detection Probability - B-47
Pull-up 3g or $C_{L_{Max}}$
AN/APQ-72 (XN-3) Radar

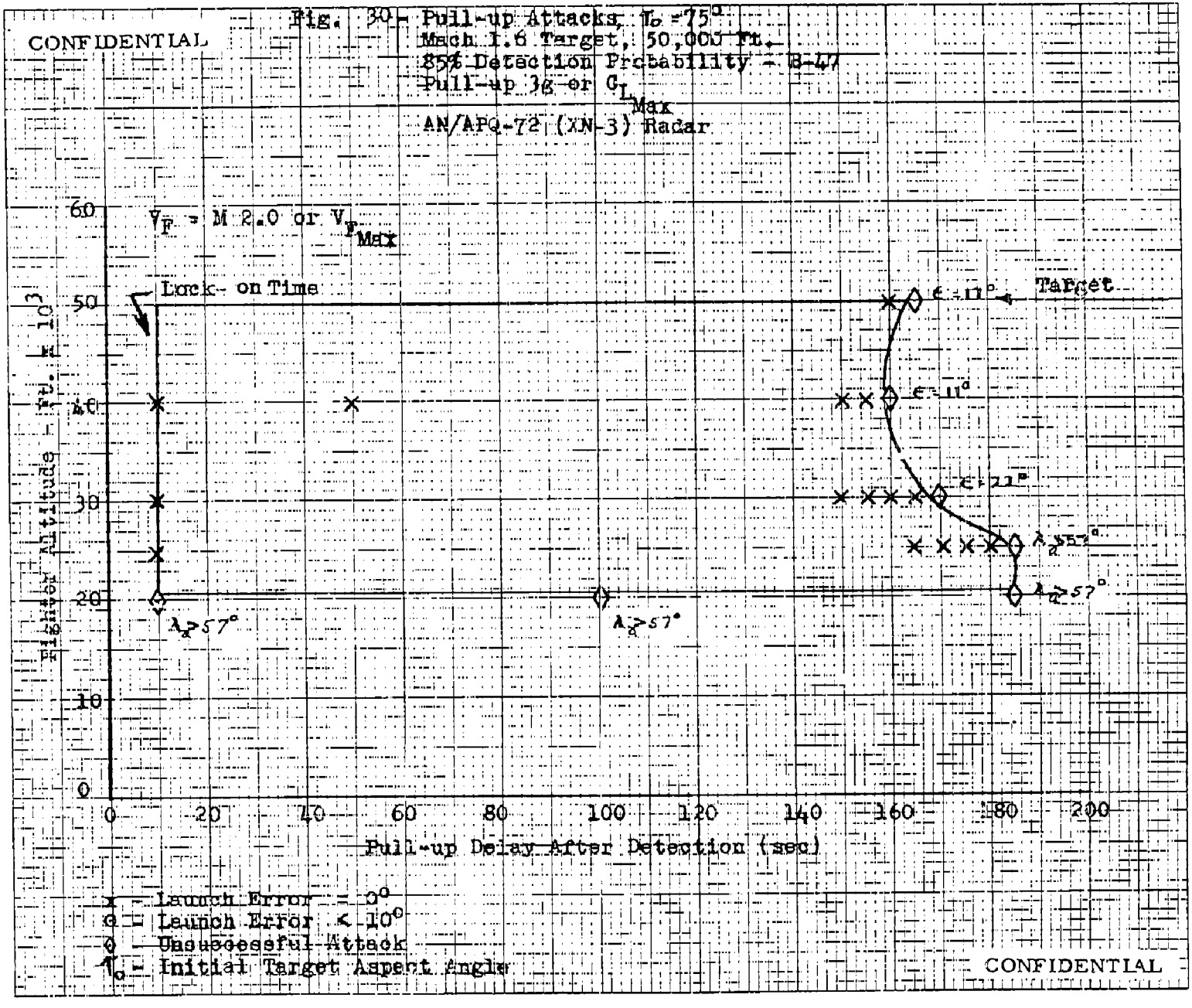

x - Launch Error = 0°
o - Launch Error < 10°
◊ - Unsuccessful Attack
T_o - Initial Target Aspect Angle

CONFIDENTIAL

CONFIDENTIAL

Fig. 31 - Pull-up Attacks $\tau_o = 90^o$
Mach 1.6 Target, 50,000 Ft.
85% Detection Probability - B-47
Pull-up 3g or $C_{L_{Max}}$
AN/APQ-72 (XN-3) Radar

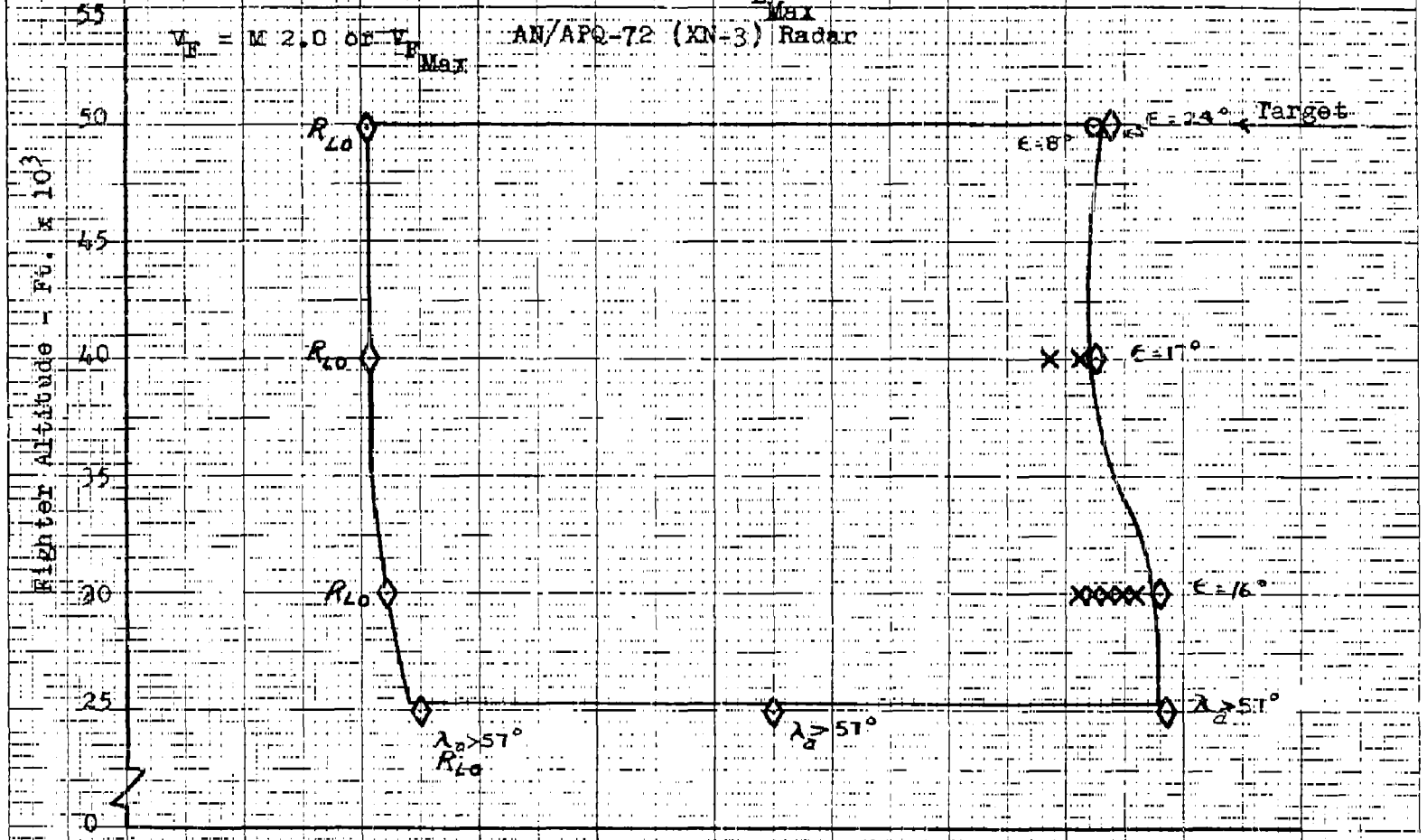

x - Launch Error $\pm 0^o$
o - Launch Error $< 10^o$
◊ = Unsuccessful Attack
τ_o - Initial Target Aspect Angle

CONFIDENTIAL

CONFIDENTIAL

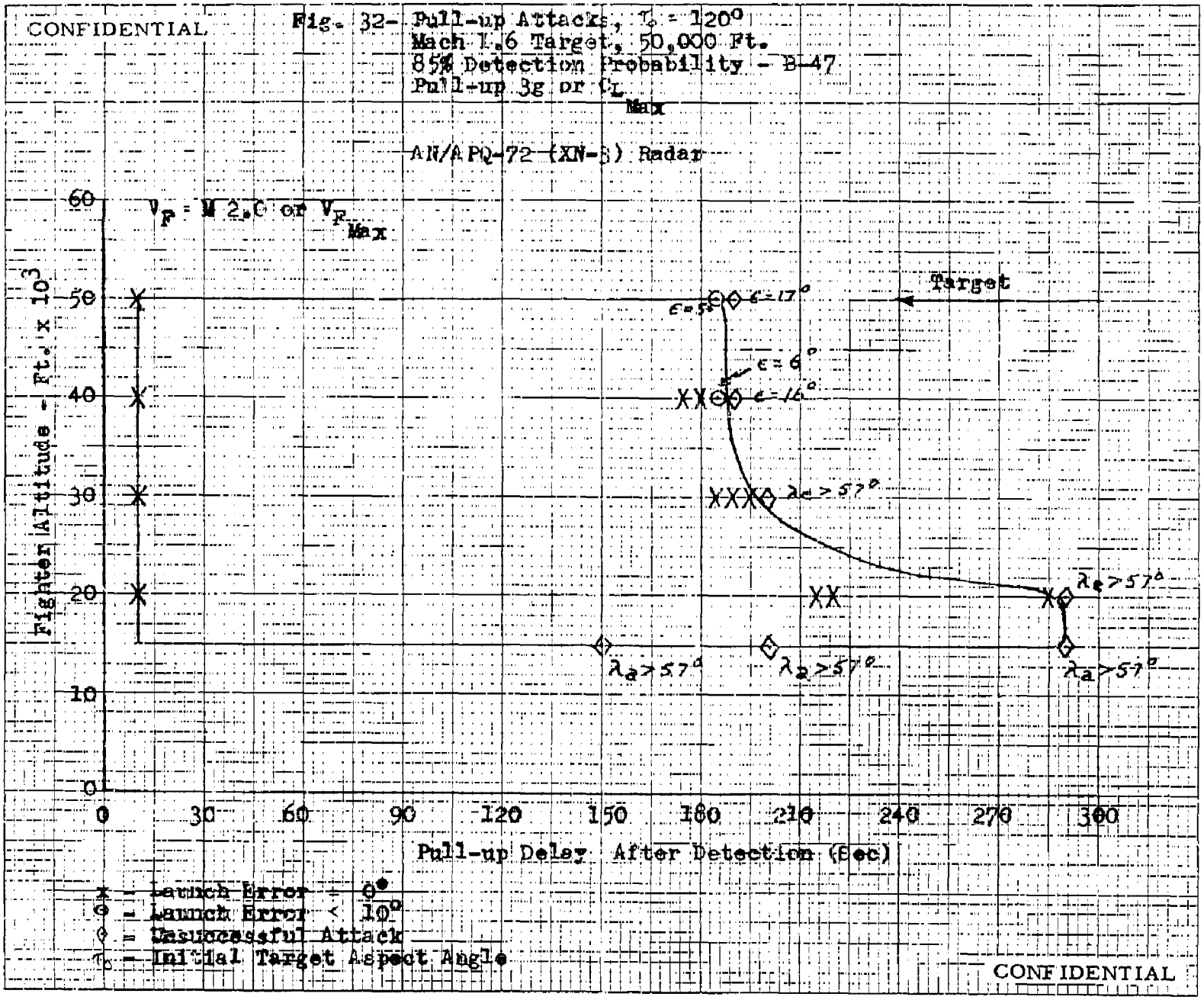

CONFIDENTIAL

CONFIDENTIAL

Fig. 33- Pull-up Attacks - $\tau_o = 150^o$
Mach 1.6 Target, 50,000 Ft.
85% Detection Probability - B-47
Pull-up 3g or $C_{L_{Max}}$
AN/APQ-72 (XN-3) Radar

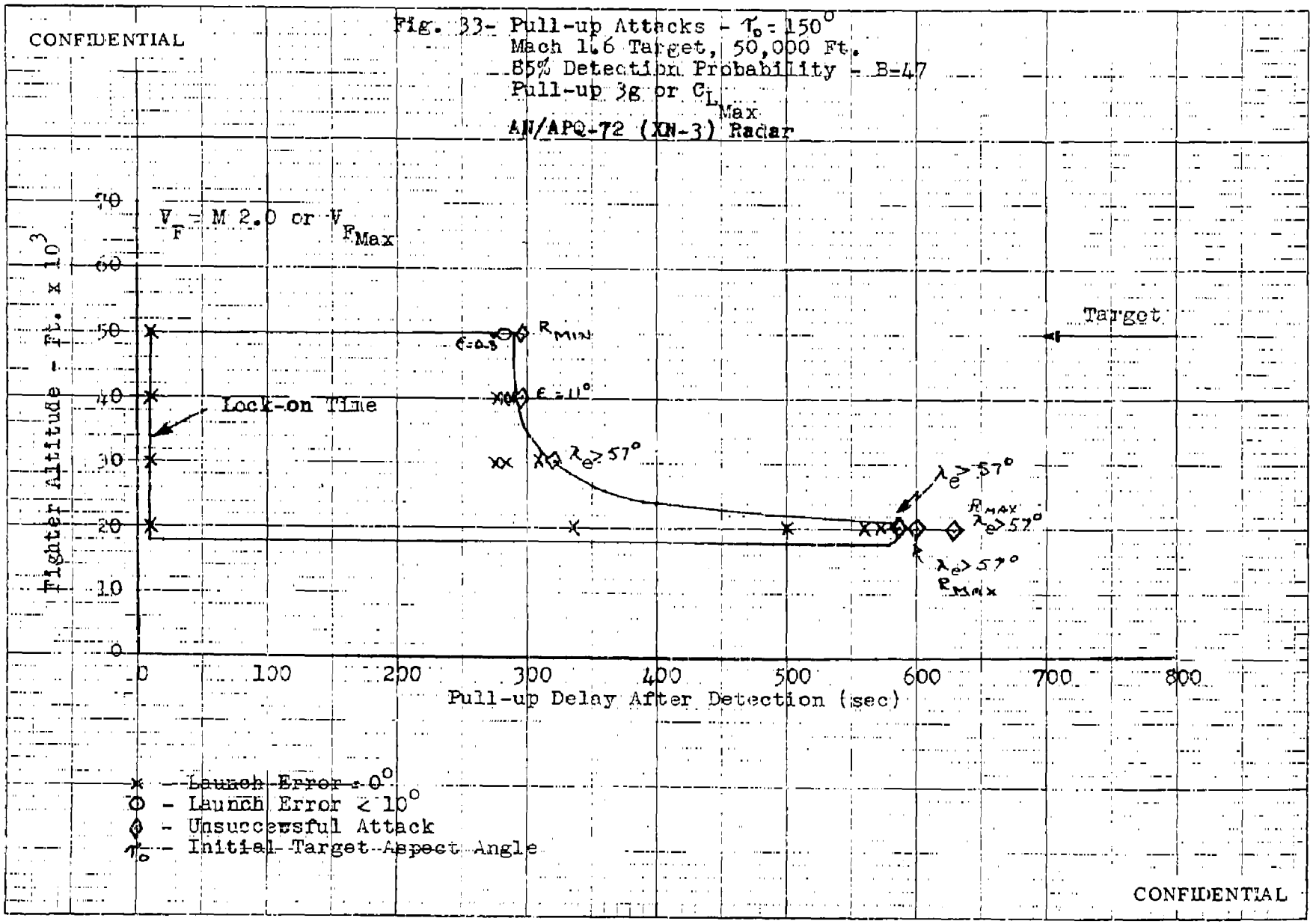

CONFIDENTIAL

CONFIDENTIAL

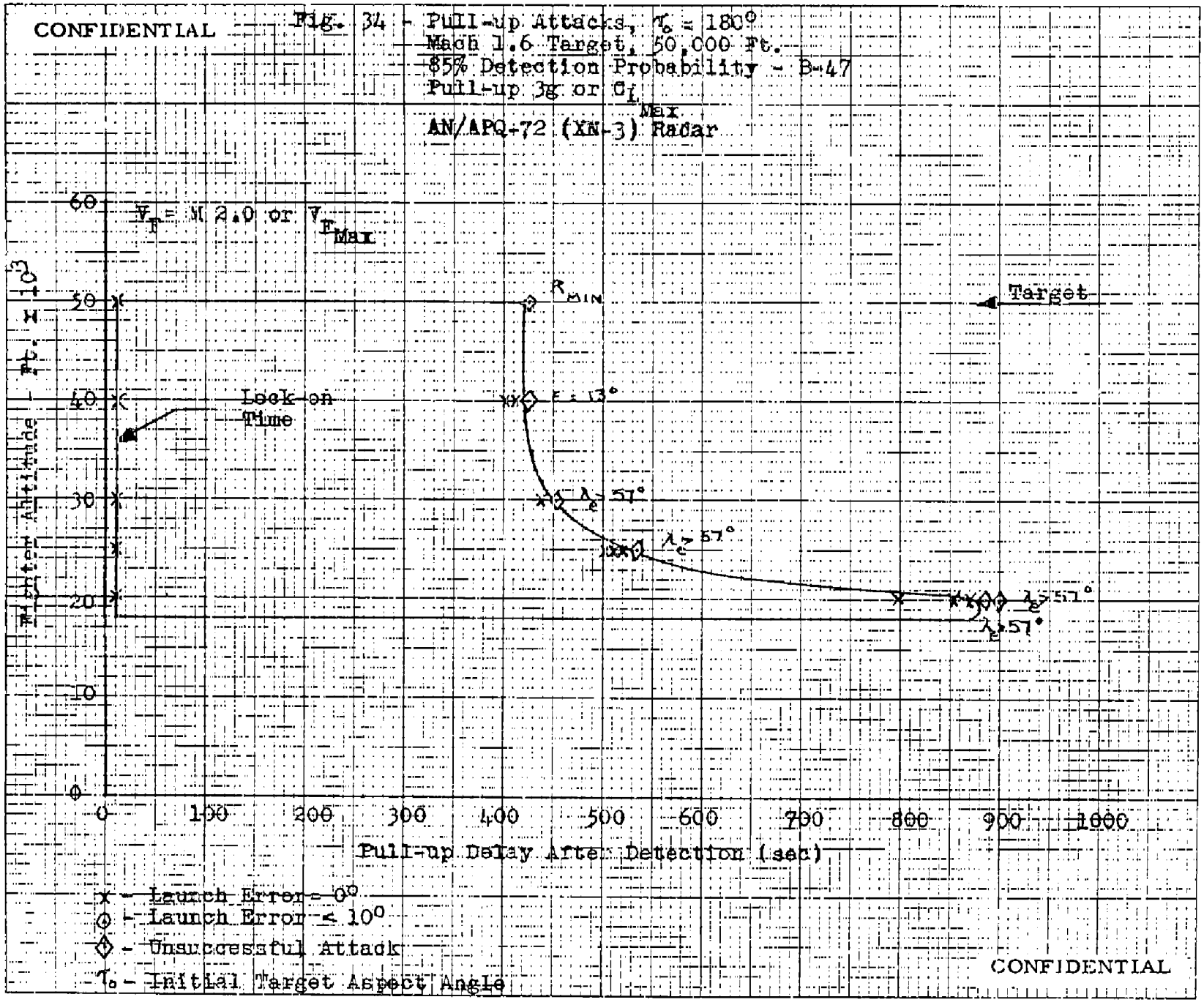

CONFIDENTIAL

CONFIDENTIAL

Fig. 35 - Probability of Successful Arrival to Missile Launch vs Relative Vectoring Angle - AN/APQ-72 (XN-3) Radar

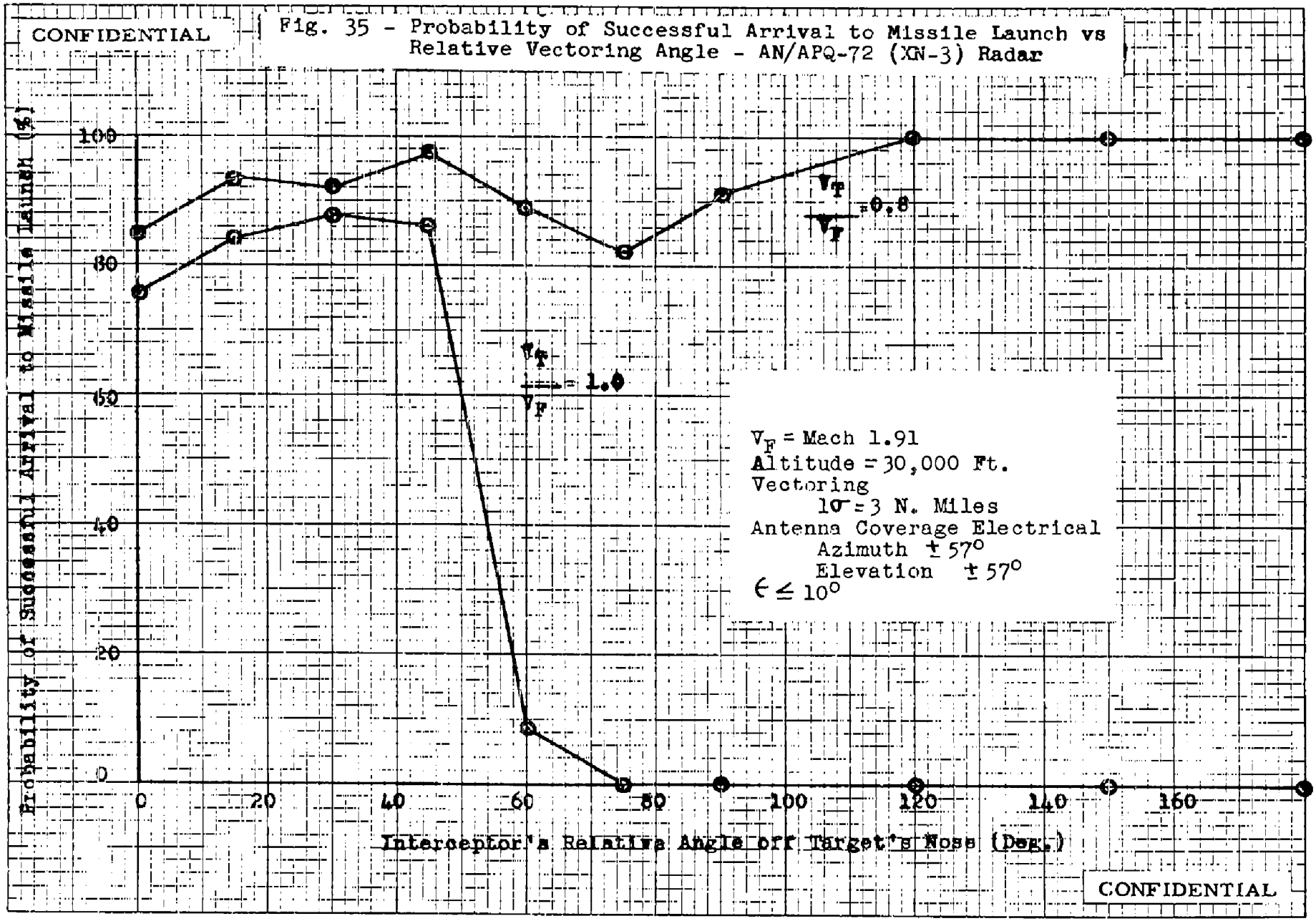

CONFIDENTIAL

CONFIDENTIAL

Fig. 36 - Probability of Successful Arrival to Missile Launch vs Relative Vectoring Angle - AN/APQ-72 (XN-3) Radar Comparision of Maneuvering and Non-maneuvering Target

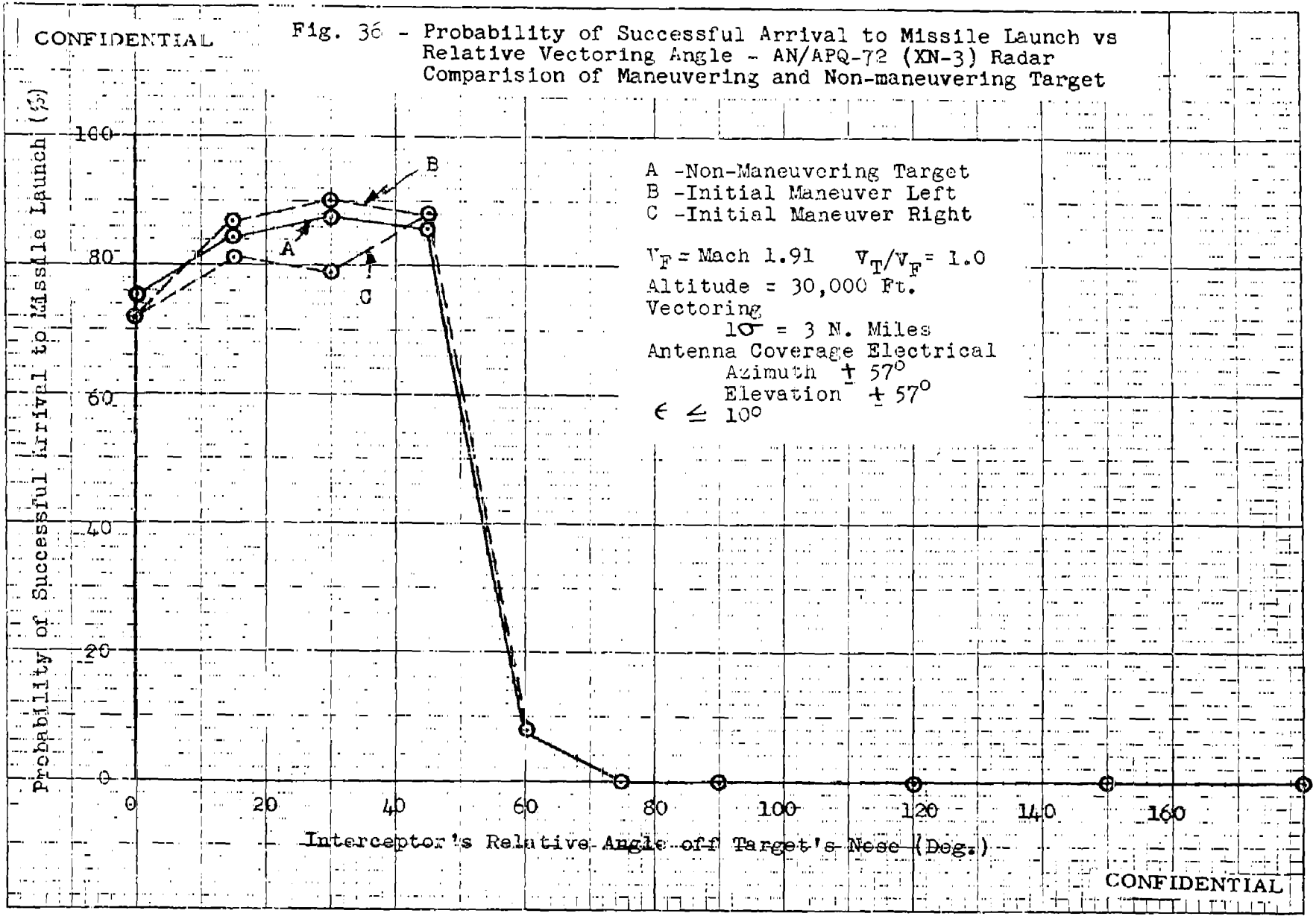

CONFIDENTIAL

CONFIDENTIAL

Fig. 37 - Probability of Successfull Arrival to Missile Launch vs Relative Vectoring Angle - AN/APQ-72 (XN-3) Radar Comparison of Maneuvering and Non-maneuvering Target

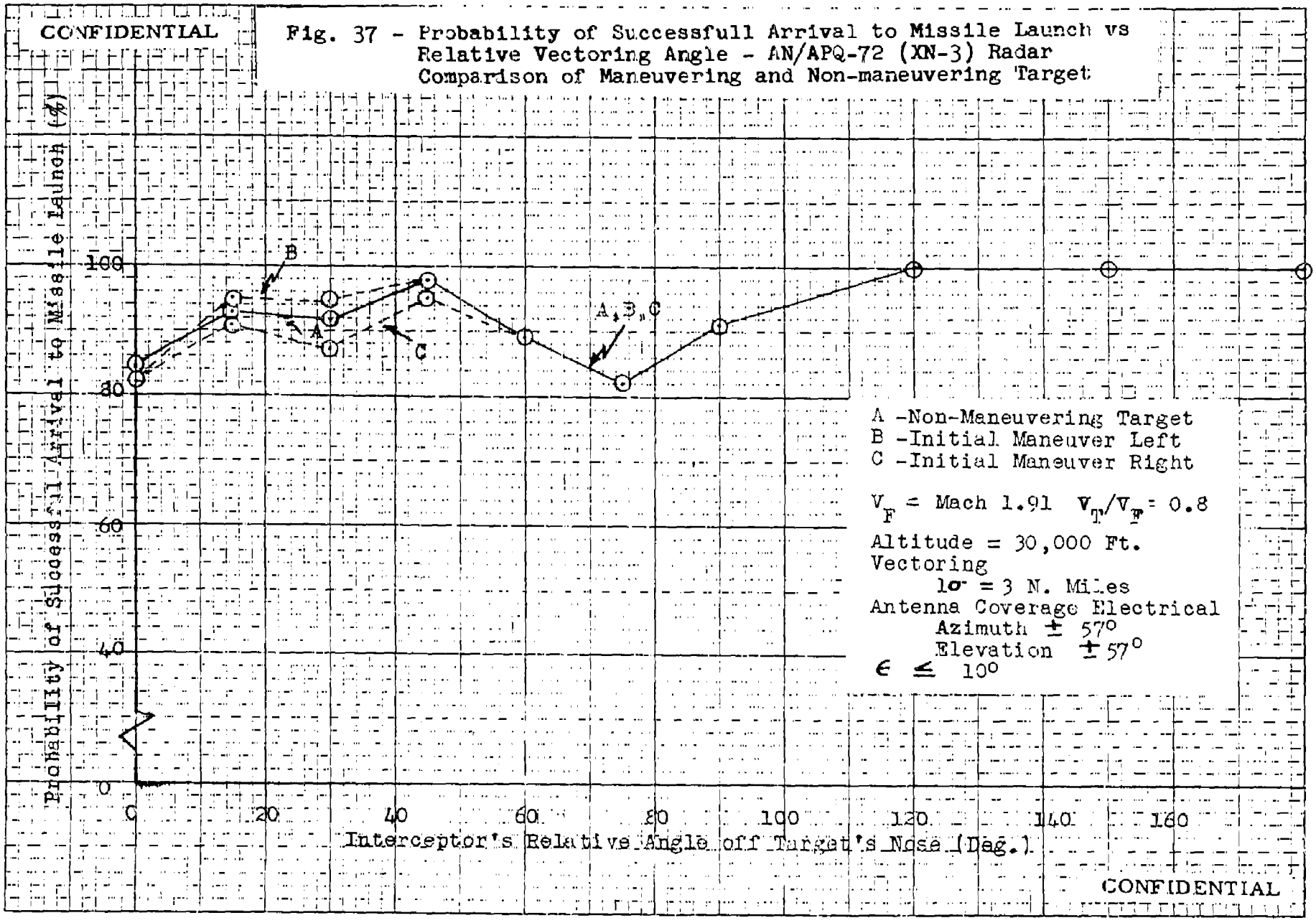

CONFIDENTIAL

CONFIDENTIAL

Fig. 38 - Probability of Successful Arrival to Missile Launch vs Relative Vectoring Angle - AN/APQ-72 (XN-3) Radar Penetration Effects Considered

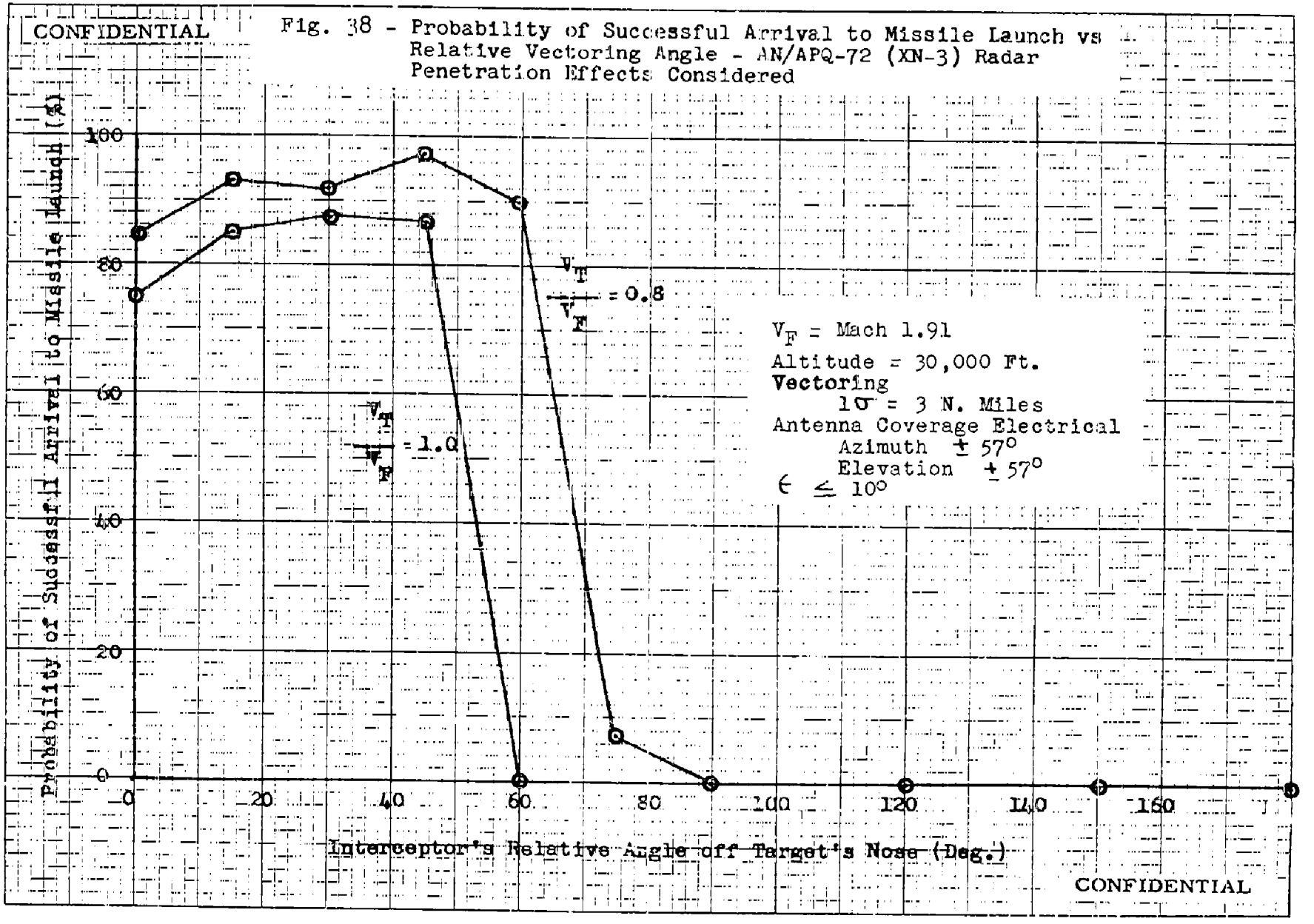

CONFIDENTIAL

CONFIDENTIAL

Fig. 39 - Probability of Successful Arrival to Missile Launch vs Relative Vectoring Angle - AN/APQ-72 (XN-3) Radar Comparison of Maneuvering and Non-maneuvering Target Penetration Effects Considered

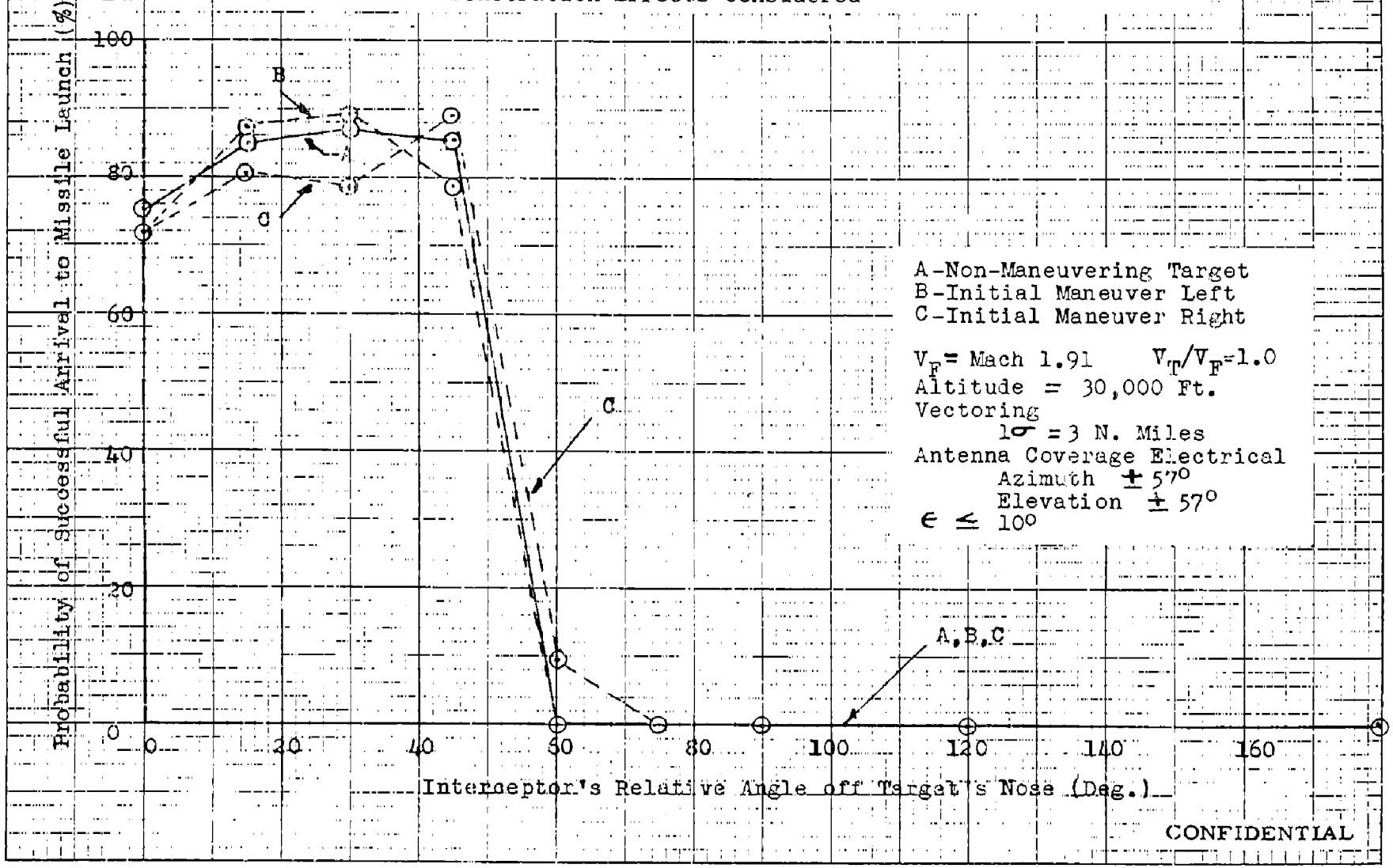

CONFIDENTIAL

CONFIDENTIAL

Fig. 40 - Probability of Successful Arrival to Missile Launch vs Relative Vectoring Angle - AN/APQ-72 (XN-3) Radar Comparison of Maneuvering and Non-maneuvering Target Penetration Effects Considered

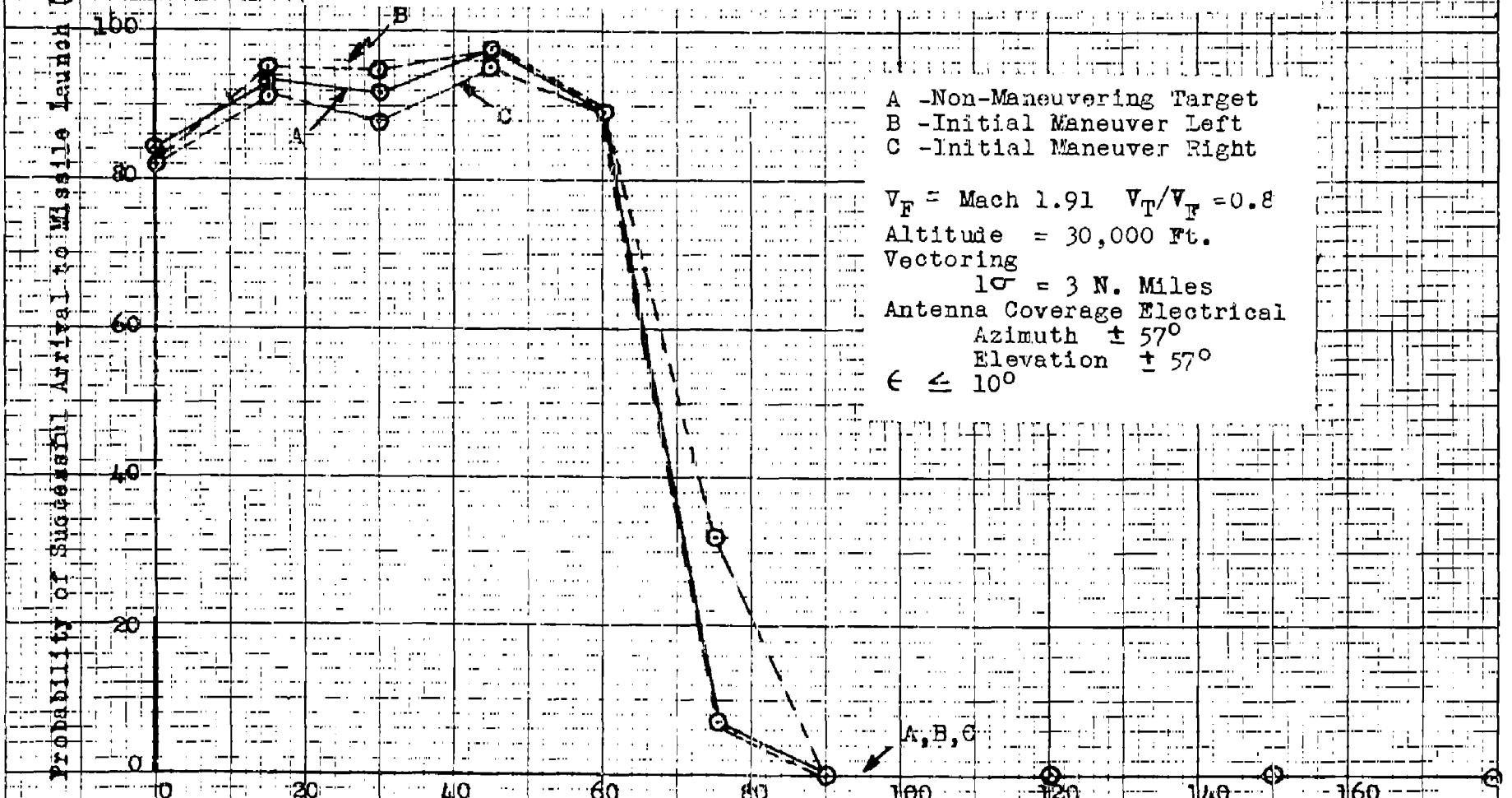

CONFIDENTIAL

CONFIDENTIAL

Fig. 41- Probability of Successful Arrival to Missile Launch for Pull-up Attacks, Head-on - AN/APQ-72 (XN-3) Radar
Mach 2.0 Target 65,000 Ft.
Pull-up 3g or $C_{L_{Max}}$

Vectoring Accuracy- $1\sigma = 3$ N. Miles in Azimuth
Antenna Coverage:
Azimuth $\pm 57^{\circ}$
Elevation $\pm 57^{\circ}$
τ_o = Initial Target Aspect Angle
ϵ = Restriction Due to Error $> 10^{\circ}$
λ = Restriction Due to Gimbal Angle $> 57^{\circ}$
L/W = Restriction Due to Recovery $L/W < 0.5$
R_{Max} = Restriction Due to Interceptor Slow Down

V_F = M 2.0 or $V_{F_{Max}}$

Probability of Successful Arrival to Missile Launch (%)

100
90
80
70
60
50
40
30
20
10
0

0 10 20 30 40 50 60 70 80

Fighter Altitude - Ft. x 10^3

CONFIDENTIAL

CONFIDENTIAL

Fig. 42- Probability of Successful Arrival to Missile Launch for Pull-up Attacks, τ_o: 15° - AN/APQ-72 (XN-3) Radar
Mach 2.0 Target 65,000 Ft.
Pull-up 3g or $C_{L_{Max}}$

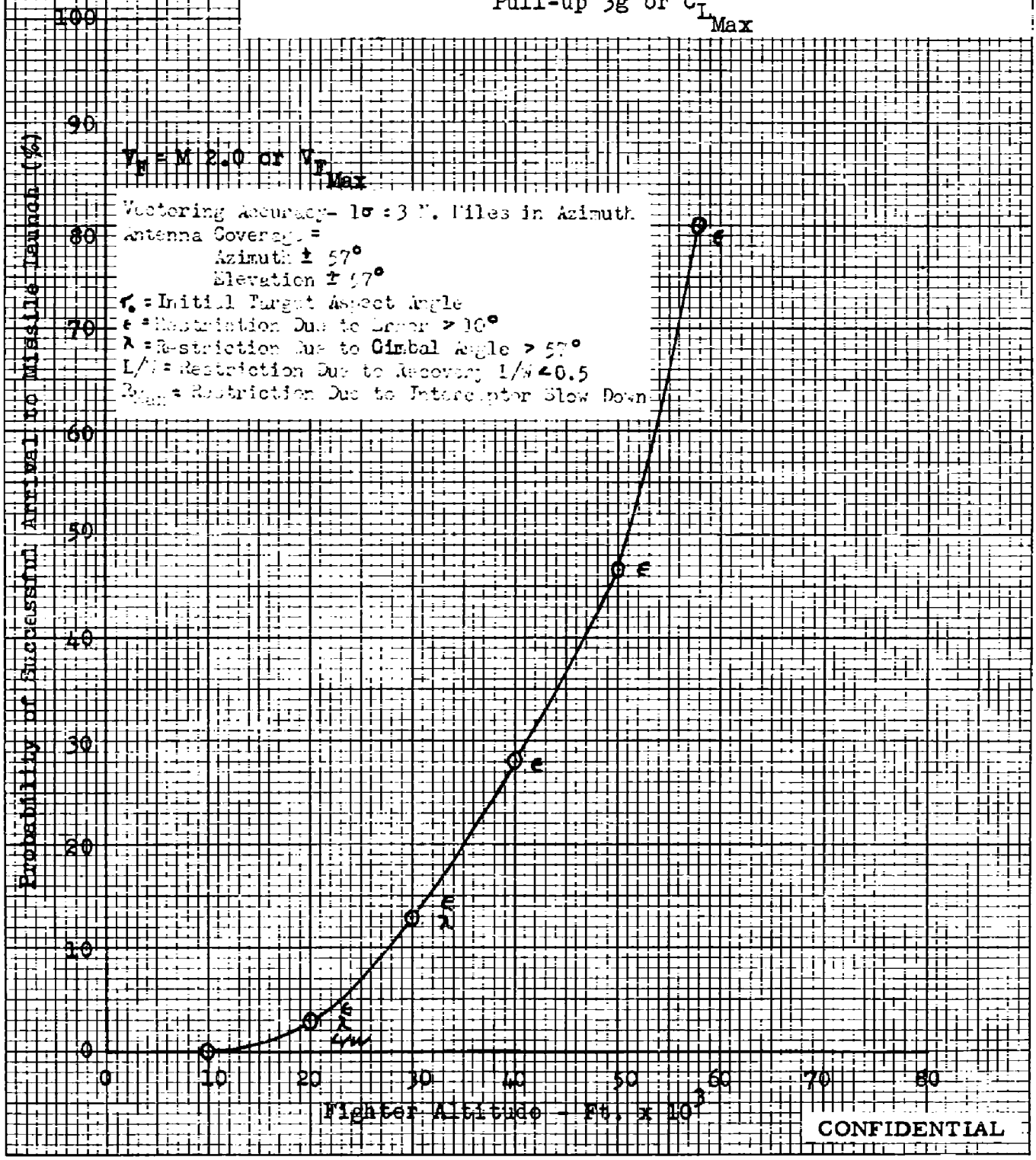

CONFIDENTIAL

Fig. 43- Probability of Successful Arrival to Missile Launch for Pull-up Attacks, $\tau_o = 30^o$ - AN/APQ-72 (XN-3) Radar
Mach 2.0 Target 65,000 Ft.
Pull-up 3g or $C_{L_{Max}}$

CONFIDENTIAL

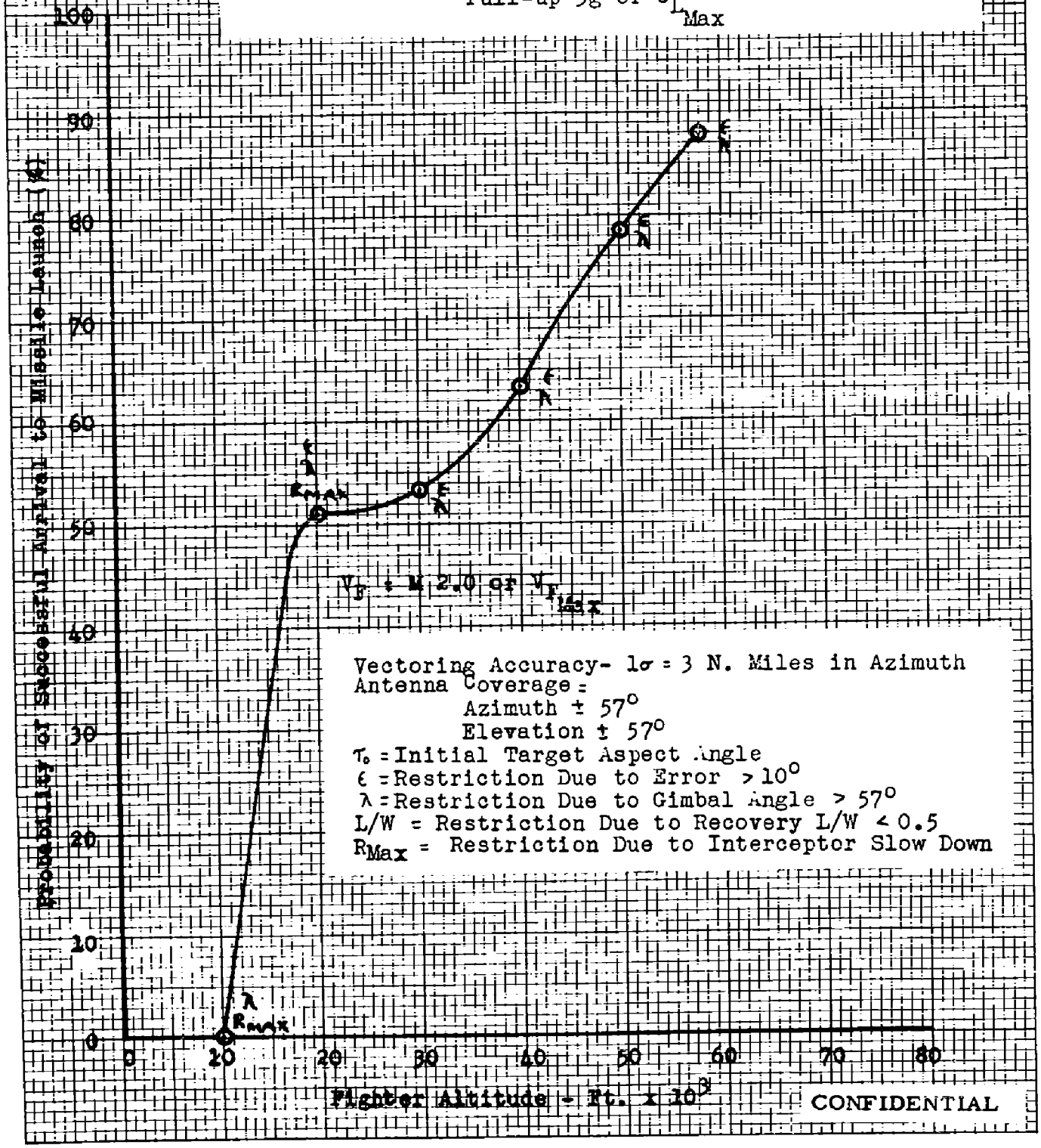

CONFIDENTIAL

CONFIDENTIAL

Fig. 44- Probability of Successful Arrival to Missile Launch for Pull-up Attacks, $\tau_o = 45^o$ - AN/APQ-72 (XN-3) Radar
Mach 2.0 Target 65,000 Ft.
Pull-up 3g or $C_{L_{Max}}$

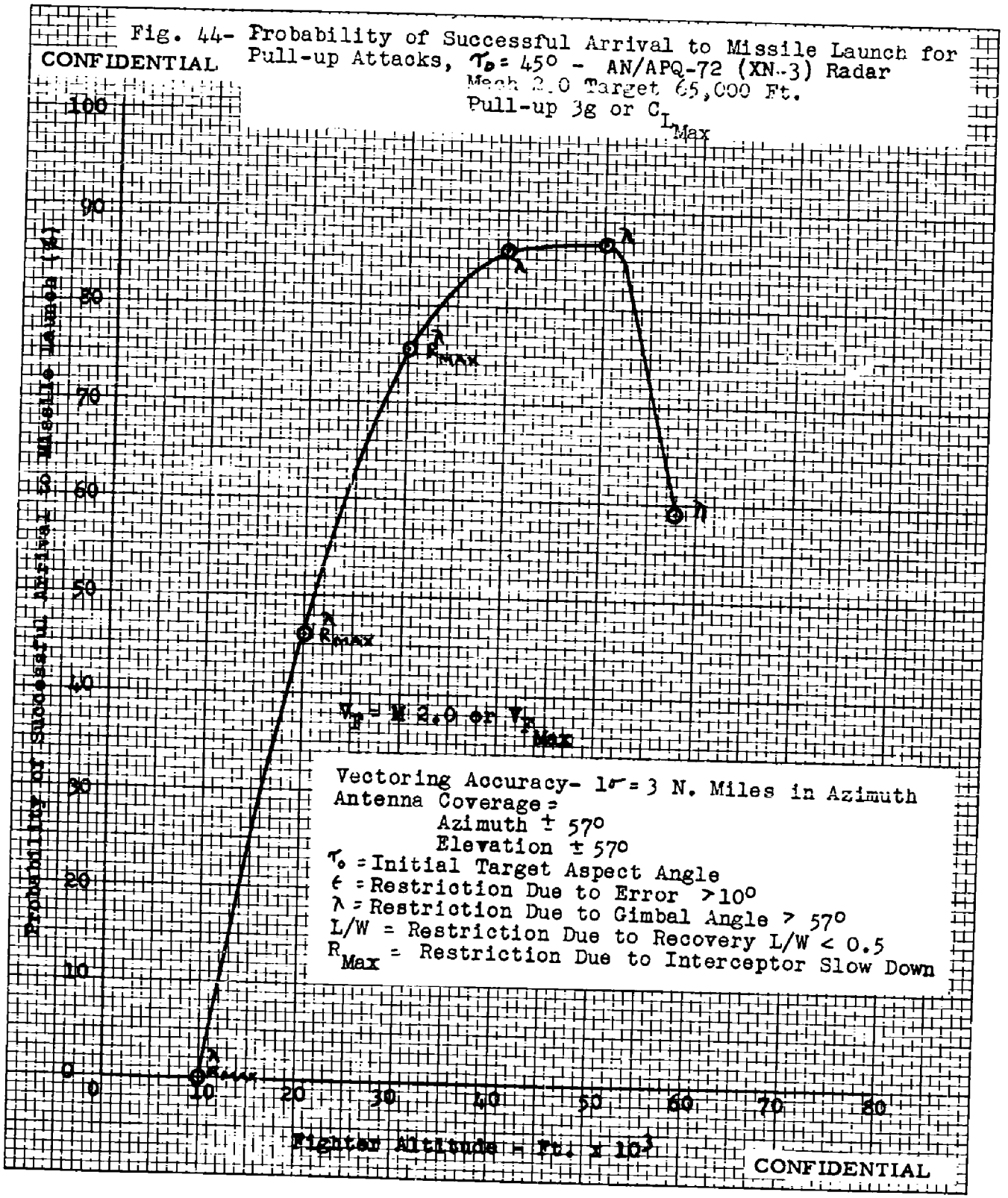

CONFIDENTIAL

CONFIDENTIAL

Fig. 45- Probability of Successful Arrival to Missile Launch for Pull-up Attacks, $\tau_o = 60^o$ - AN/APQ-72 (XN-3) Radar
Mach 2.0 Target 65,000 Ft.
Pull-up 3g or $C_{L_{Max}}$

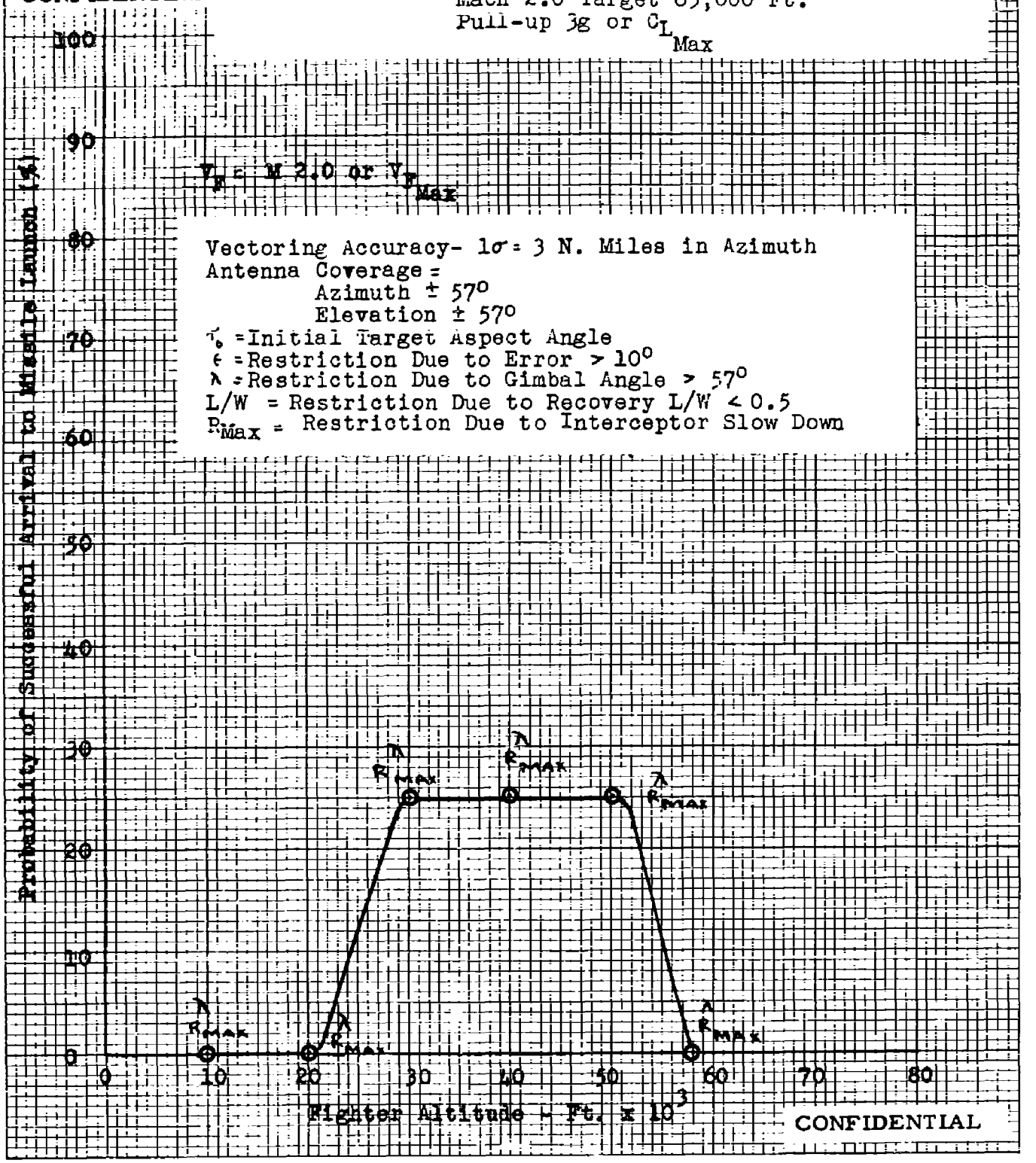

CONFIDENTIAL

CONFIDENTIAL

Fig. 46- Probability of Successful Arrival to Missile Launch for Pull-up Attacks, $\tau_o = 70^o$- AN/APQ-72 (XN-3) Radar
Mach 2.0 Target 65,000 Ft.
Pull-up 3g or $C_{L_{Max}}$

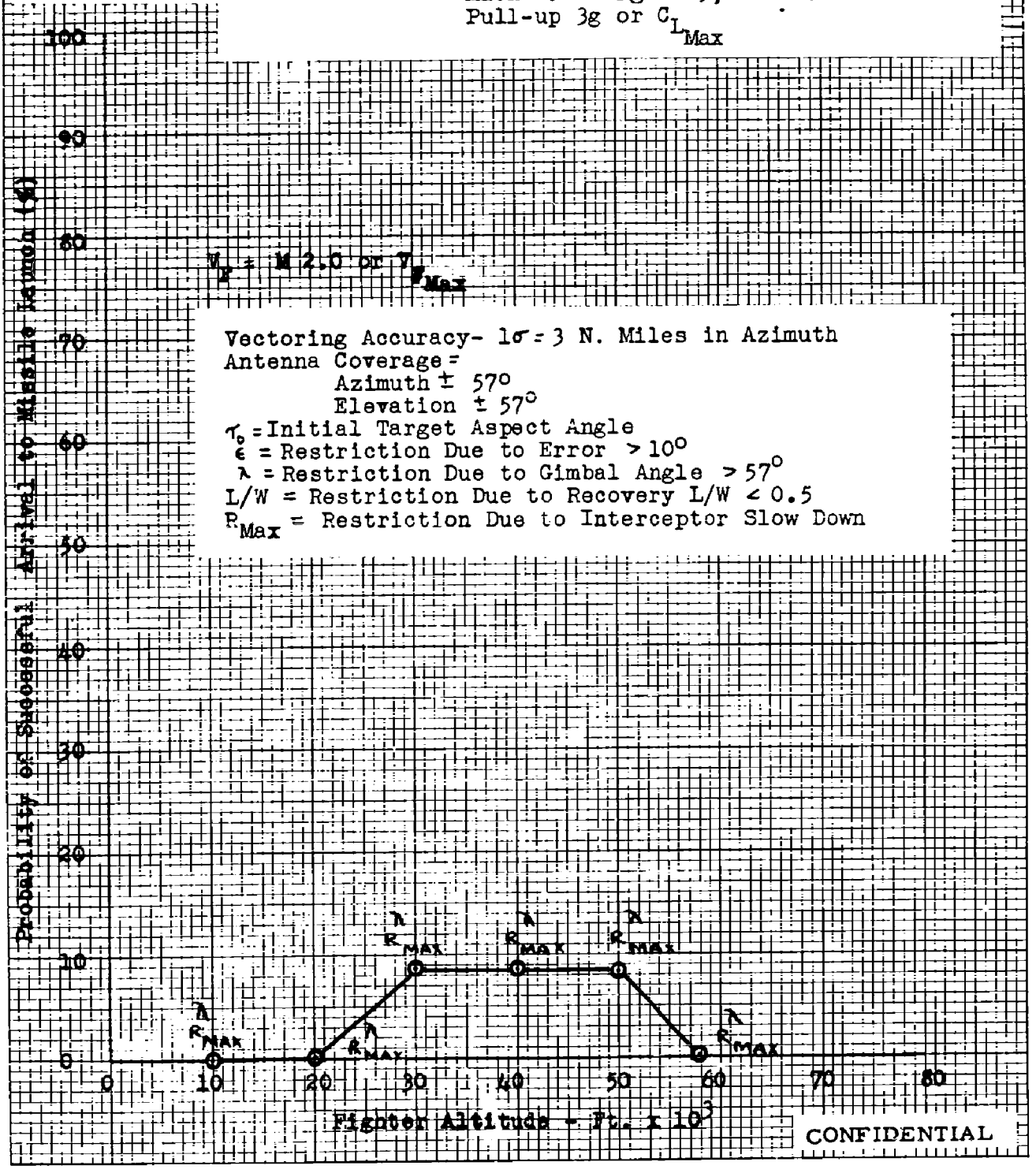

CONFIDENTIAL

CONFIDENTIAL

Fig. 47- Probability of Successful Arrival to Missile Launch for Pull-up Attacks, τ_o = 0°, 15°, 30°- AN/APQ-72 (XN-3) Radar
Mach 2.0 Target 65,000 Ft.
Pull-up 3g or $C_{L_{Max}}$

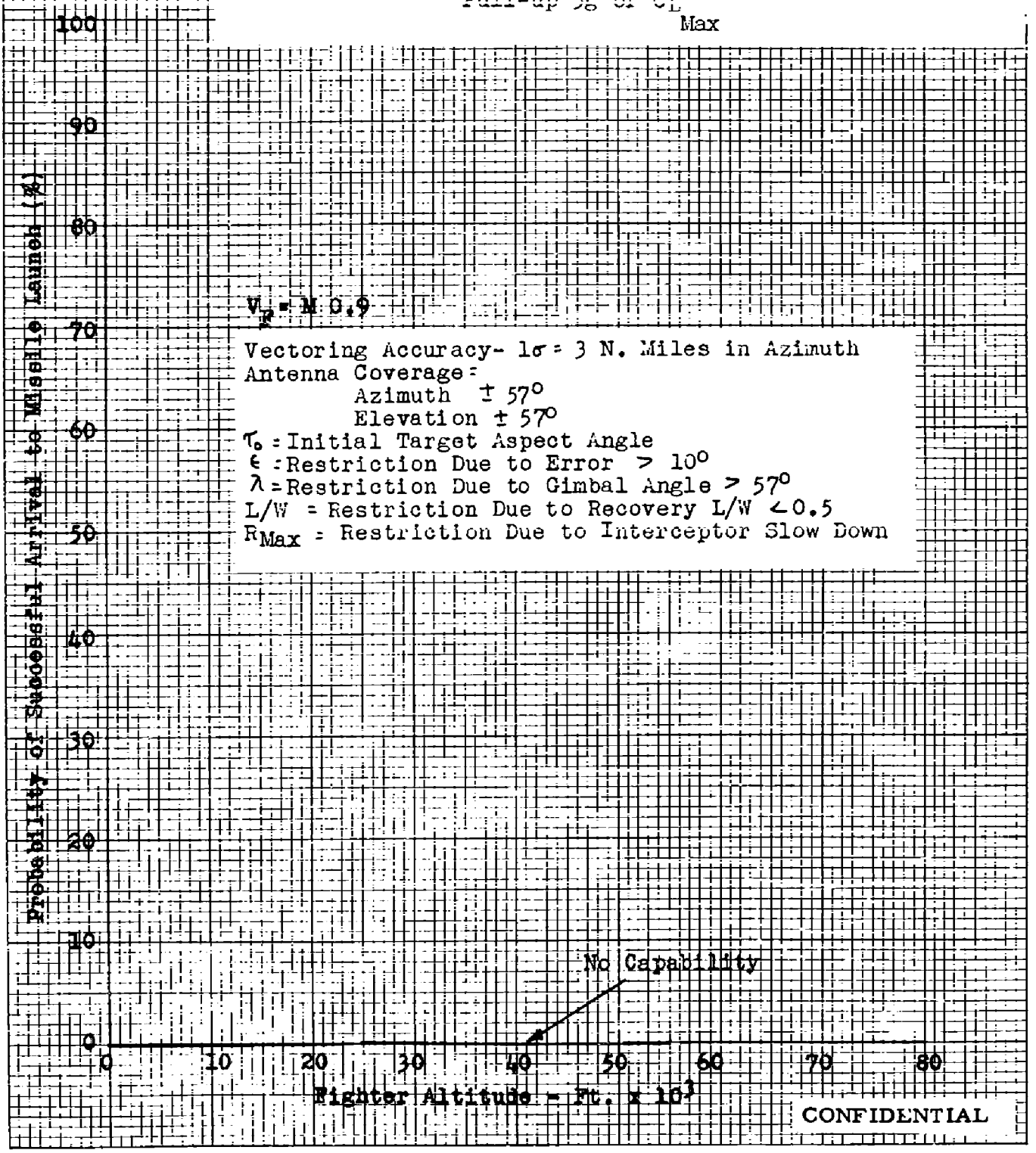

CONFIDENTIAL

CONFIDENTIAL

Fig. 48- Probability of Successful Arrival to Missile Launch for Pull-up Attacks, Head-on - AN/APQ-72 (XN-3) Radar
Mach 1.6 Target 65,000 Ft.
Pull-up 3g or $C_{L_{max}}$

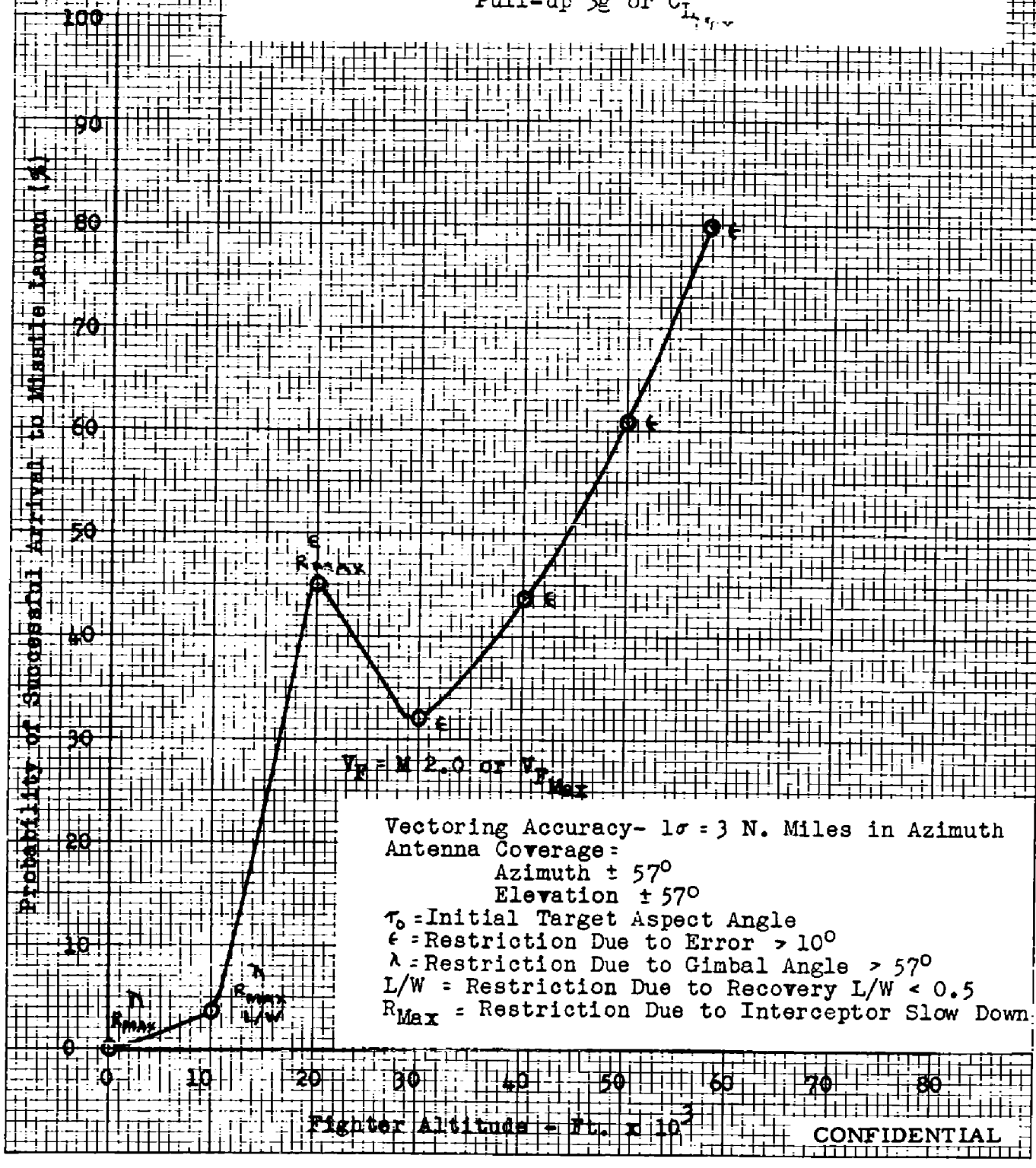

CONFIDENTIAL

CONFIDENTIAL

Fig. 49- Probability of Successful Arrival to Missile Launch for Pull-up Attacks, $\tau_o = 15^o$ - AN/APQ-72 (XN-3) Radar
Mach 1.6 Target 65,000 Ft.
Pull-up 3g or $C_{L_{Max}}$

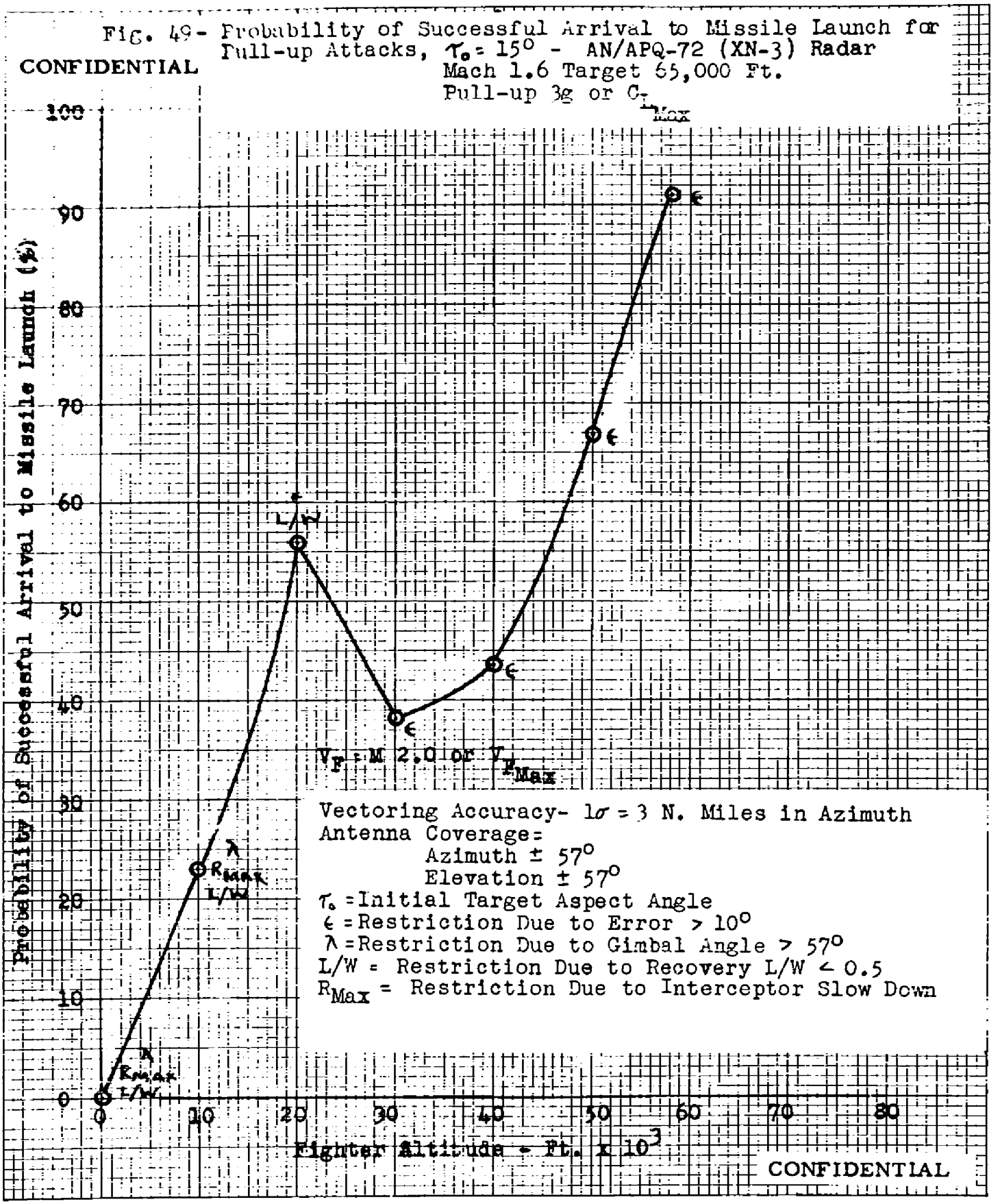

CONFIDENTIAL

CONFIDENTIAL

Fig. 50- Probability of Successful Arrival to Missile Launch for Pull-up Attacks, $\tau_o = 30^o$ - AN/APQ-72 (XN-3) Radar
Mach 1.6 Target 65,000 Ft.
Pull-up 3g or $C_{L_{Max}}$

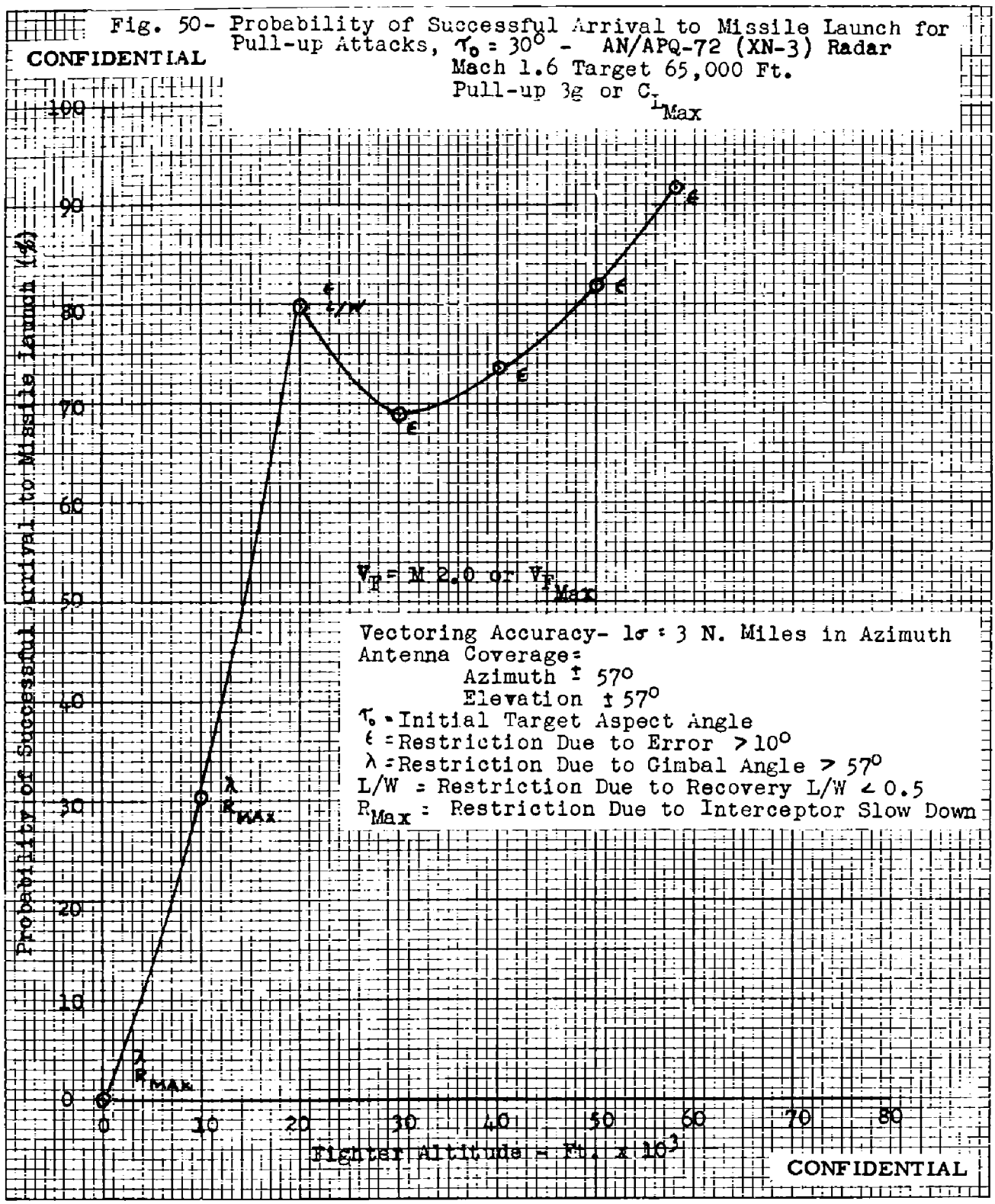

CONFIDENTIAL

CONFIDENTIAL

Fig. 51- Probability of Successful Arrival to Missile Launch for Pull-up Attacks, $\tau_o = 45^o$ - AN/APQ-72 (XN-3) Radar
Mach 1.6 Target 65,000 Ft.
Pull-up 3g or $C_{L_{Max}}$

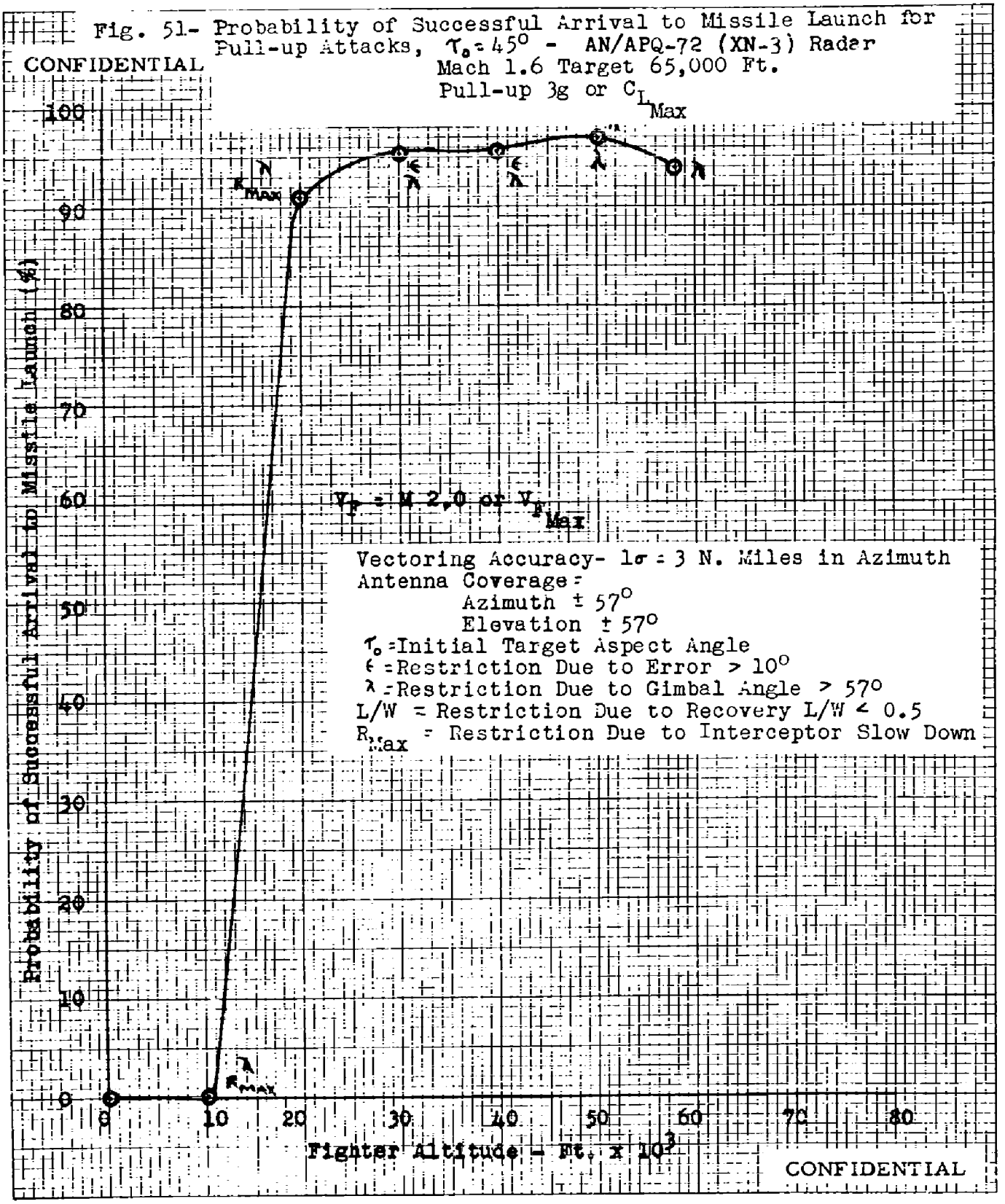

CONFIDENTIAL

CONFIDENTIAL

Fig. 52- Probability of Successful Arrival to Missile Launch for Pull-up Attacks, $\tau_o = 60^o$ - AN/APQ-72 (XN-3) Radar
Mach 1.6 Target 65,000 Ft.
Pull-up 3g or $C_{L_{Max}}$

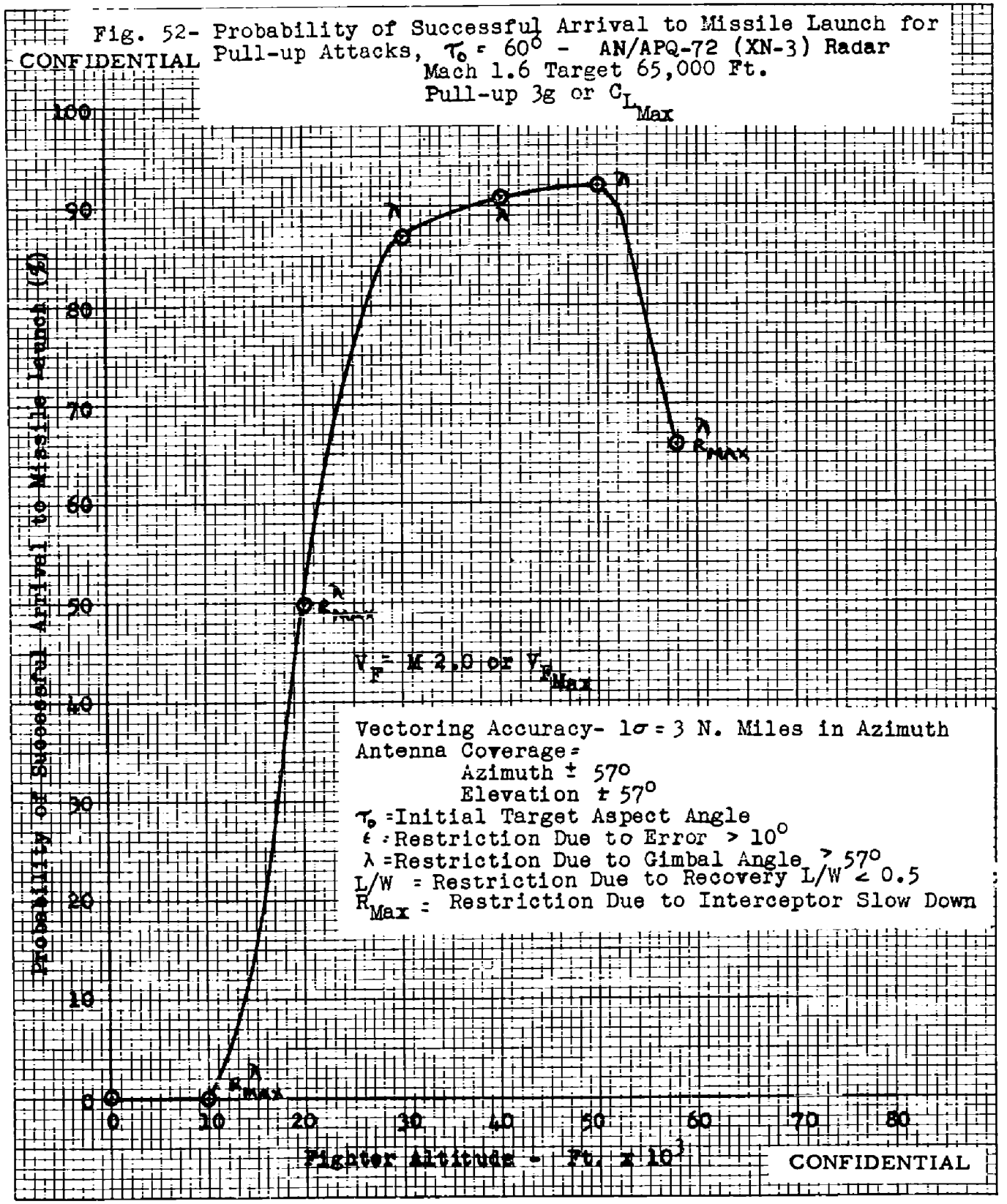

CONFIDENTIAL

CONFIDENTIAL

Fig. 53- Probability of Successful Arrival to Missile Launch for Pull-up Attacks, $\tau_0 = 75^\circ$ - AN/APQ-72 (XN-3) Radar
Mach 1.6 Target 65,000 Ft.
Pull-up 3g or $C_{L_{Max}}$

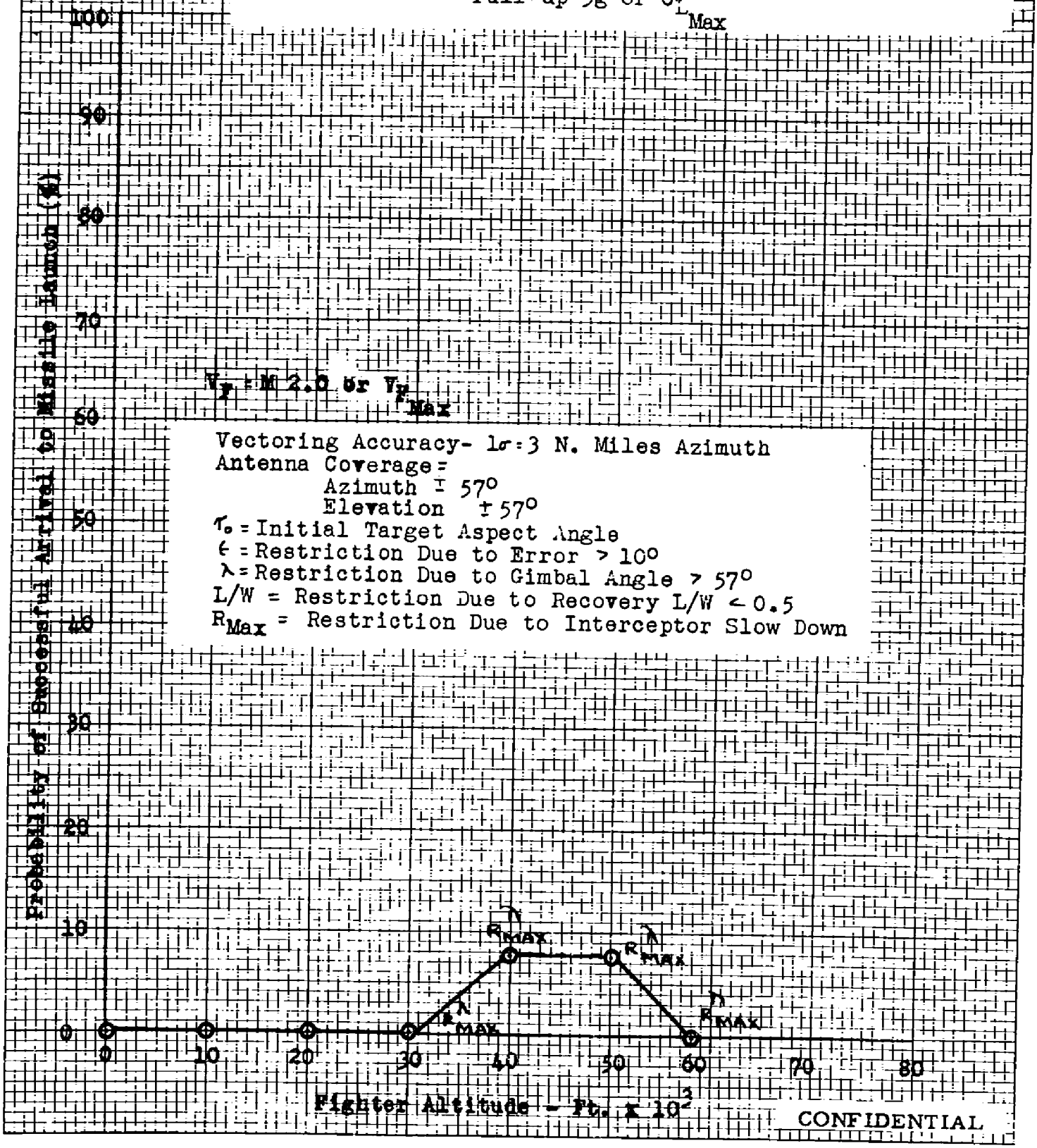

CONFIDENTIAL

Fig. 54- Probability of Successful Arrival to Missile Launch for Pull-up Attacks, $\tau_o < 82^o$ - AN/APQ-72 (XN-3) Radar
Mach 1.6 Target 65,000 Ft.
Pull-up 3g or $C_{L_{Max}}$

CONFIDENTIAL

V_M = M 2.0 or $V_{M_{Max}}$

Vectoring Accuracy- 1σ = 3 N. Miles in Azimuth
Antenna Coverage=
Azimuth ± 57°
Elevation ±57°
τ_o = Initial Target Aspect Angle
ϵ = Restriction Due to Error > 10°
λ = Restriction Due to Gimbal Angle > 57°
L/W = Restriction Due to Recovery L/W < 0.5
R_{max} = Restriction Due to Interceptor Slow Down

Probability of Successful Arrival to Missile Launch (%)

100
90
80
70
60
50
40
30
20
10
0

0 10 20 30 40 50 60 70 80

Fighter Altitude - Ft. x 10^3

R_{MAX} R_{MAX} R_{MAX}

CONFIDENTIAL

CONFIDENTIAL

Fig. 55- Probability of Successful Arrival to Missile Launch for Pull-up Attacks, $\tau_o = 90^o$, 120^o - AN/APQ-72 (XN-3) Radar
Mach 1.6 Target 65,000 Ft.
Pull-up 3g or $C_{L_{Max}}$

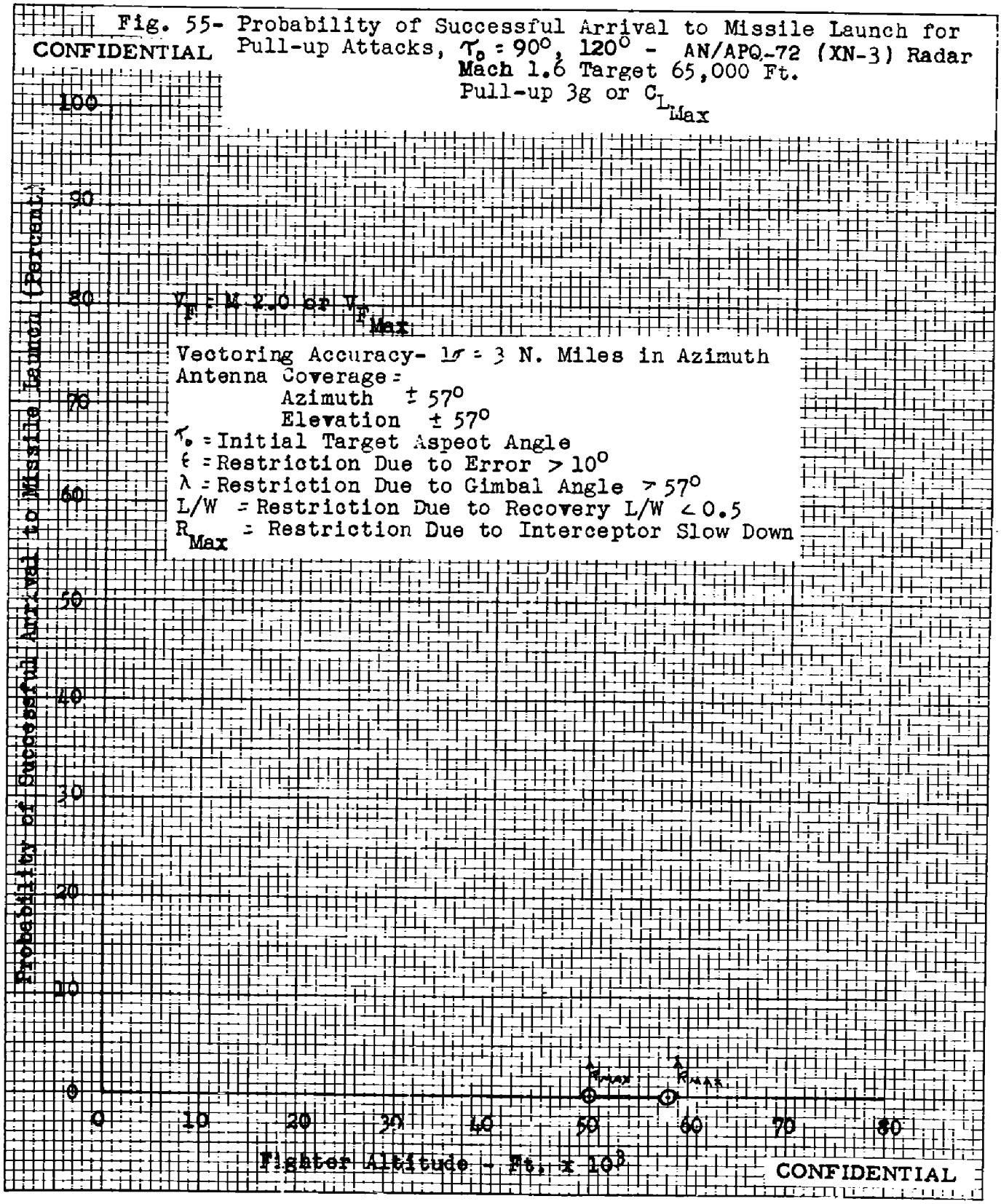

CONFIDENTIAL

CONFIDENTIAL

Fig. 56- Probability of Successful Arrival to Missile Launch for Pull-up Attacks, τ_o = 0°, 15°, 30° - AN/APQ-72 (XN-3) Radar
Mach 1.6 Target 65,000 Ft.
Pull-up 3g or $C_{L_{Max}}$

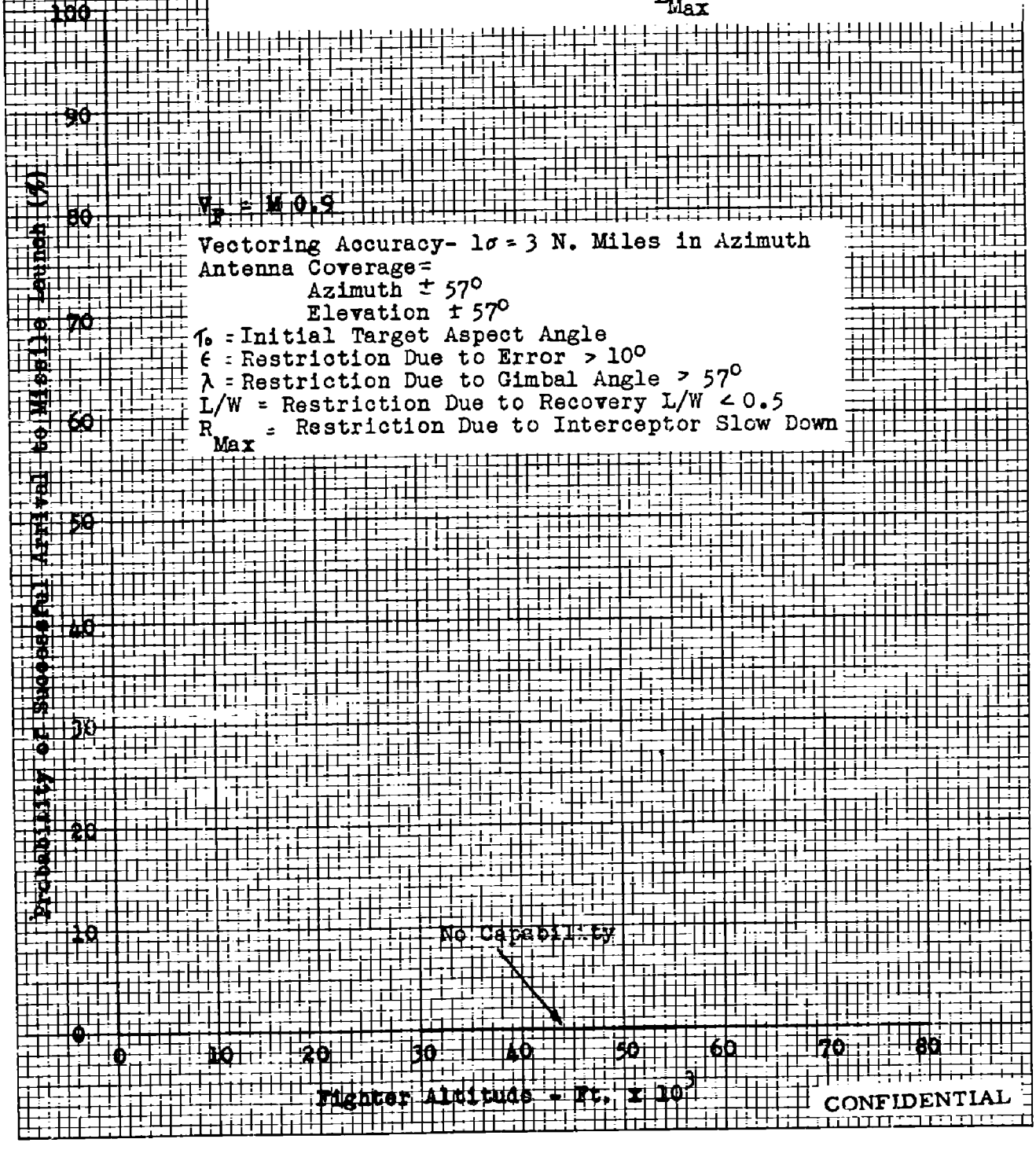

CONFIDENTIAL

CONFIDENTIAL

Fig. 57- Probability of Successful Arrival to Missile Launch for Pull-up Attacks, Head-on - AN/APQ-72 (XN-3) Radar
Mach 2.0 Target 50,000 Ft.
Pull-up 3g or $C_{L_{Max}}$

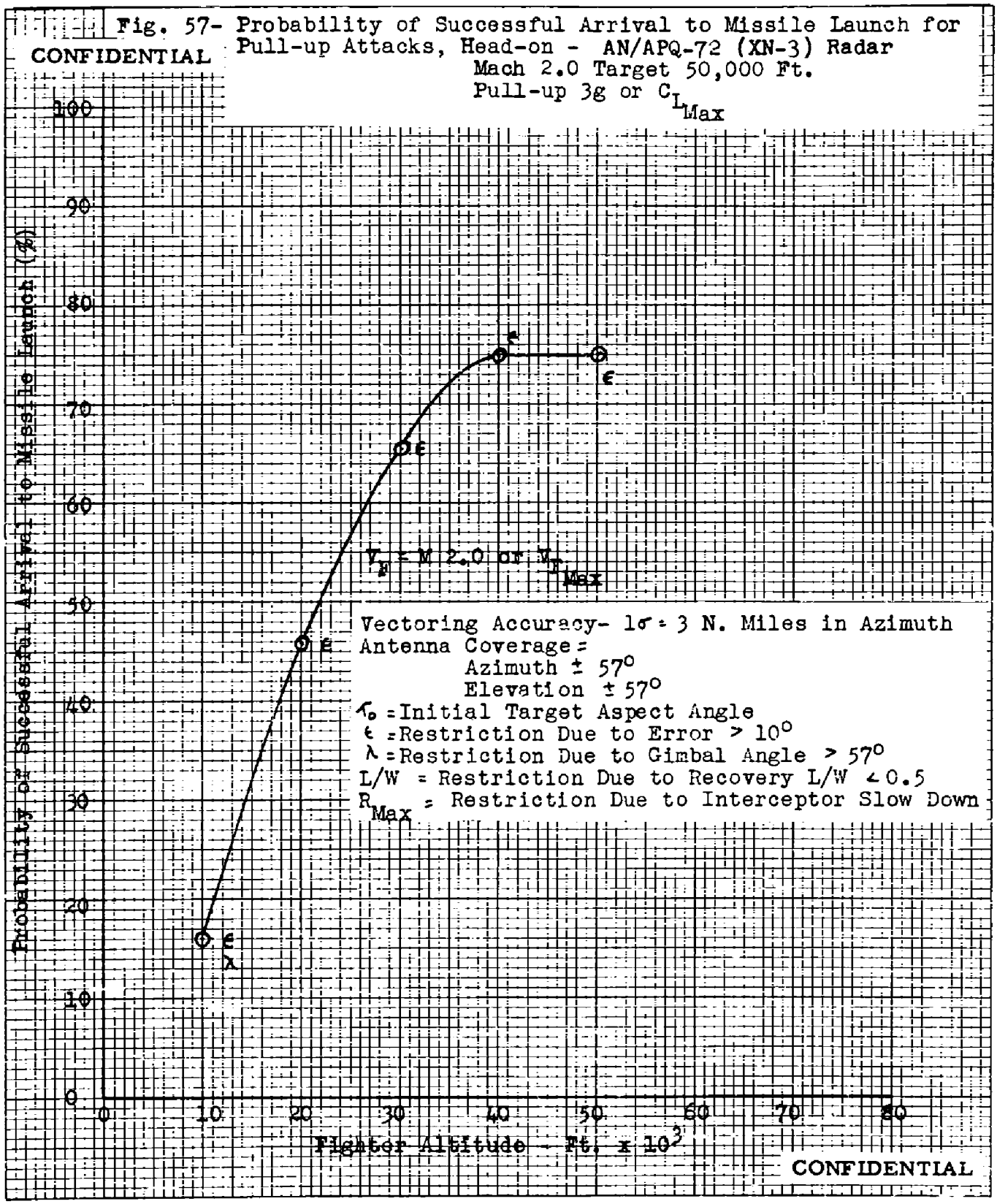

CONFIDENTIAL

CONFIDENTIAL

Fig. 58- Probability of Successful Arrival to Missile Launch for Pull-up Attacks, $\tau_o = 15^o$ - AN/APQ-72 (XN-3) RADAR
Mach 2.0 Target 50,000 Ft.
Pull-up 3g or $C_{L_{Max}}$

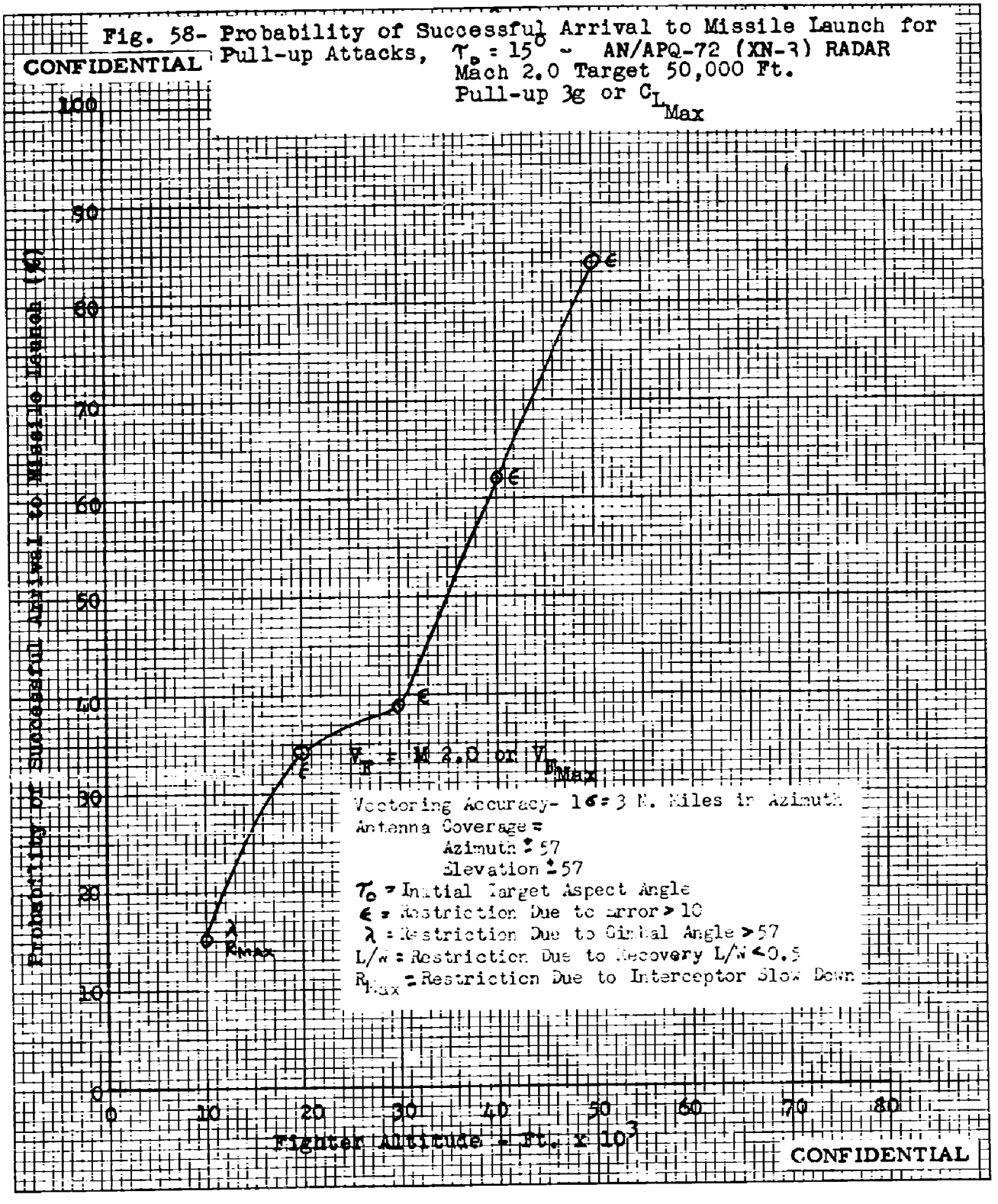

CONFIDENTIAL

CONFIDENTIAL

Fig. 59- Probability of Successful Arrival to Missile Launch for Pull-up Attacks, $\tau_o = 30^o$ - AN/APQ-72 (XN-3) Radar
Mach 2.0 Target 50,000 Ft.
Pull-up 3g or $C_{L_{Max}}$

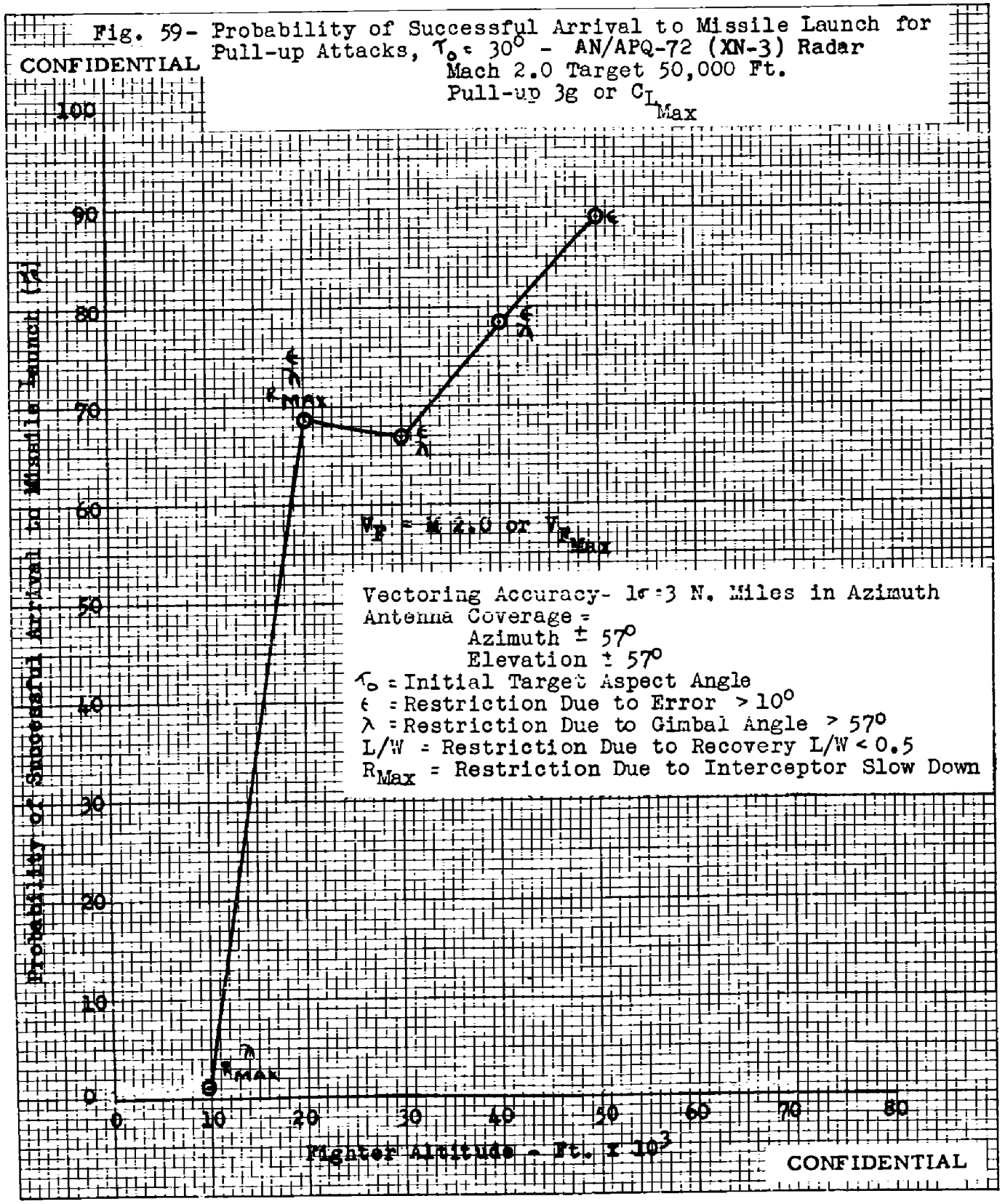

CONFIDENTIAL

CONFIDENTIAL

Fig. 60- Probability of Successful Arrival to Missile Launch for Pull-up Attacks, $\tau_o = 45^o$ - AN/APQ-72 (XN-3) Radar
Mach 2.0 Target 50,000 Ft.
Pull-up 3g or $C_{L_{Max}}$

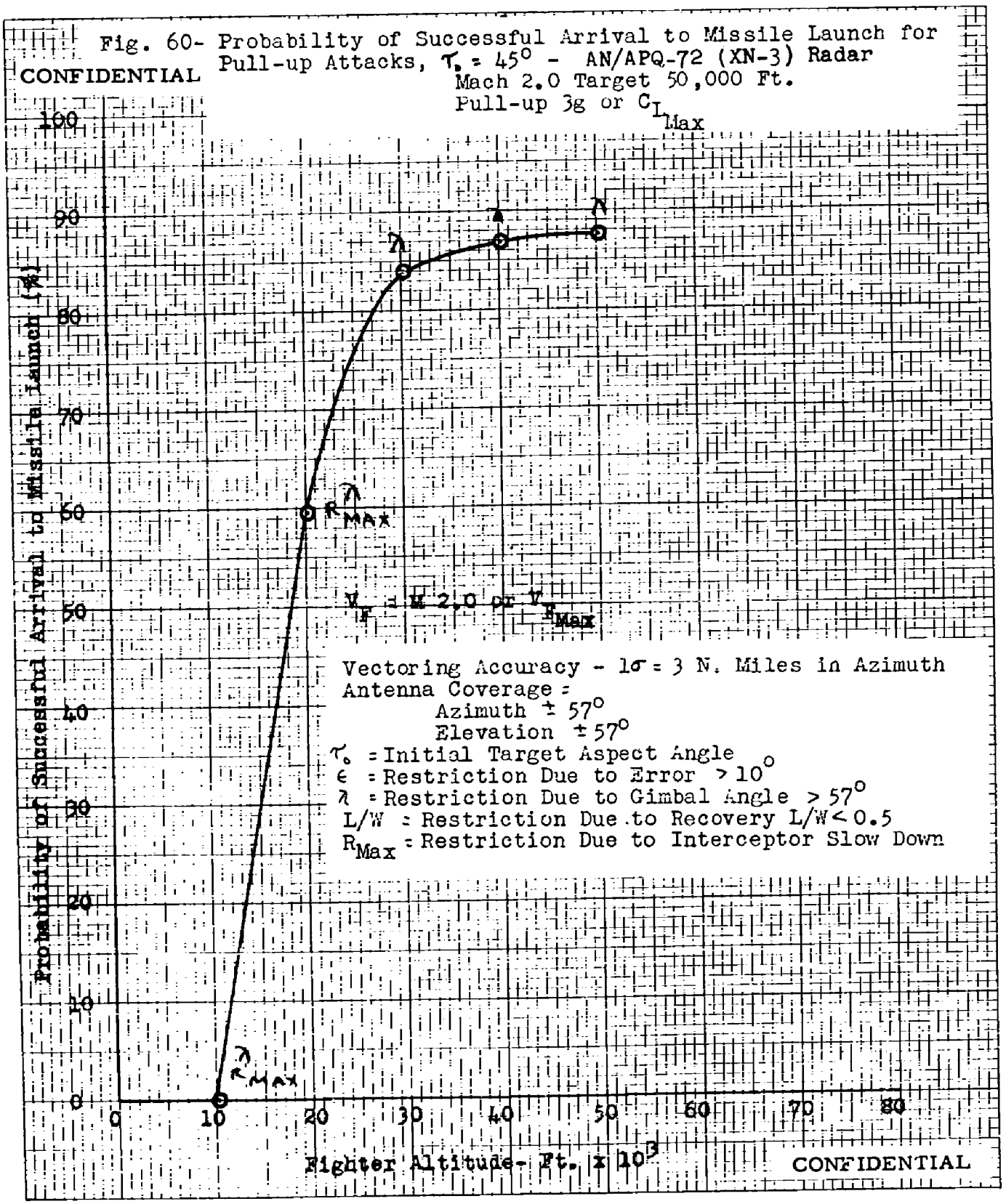

CONFIDENTIAL

CONFIDENTIAL

Fig. 61- Probability of Successful Arrival to Missile Launch for Pull-up Attacks, $\tau_o = 60^o$ - AN/APQ-72 (XN-3) Radar
Mach 2.0 Target 50,000 Ft.
Pull-up 3g or $C_{L_{Max}}$

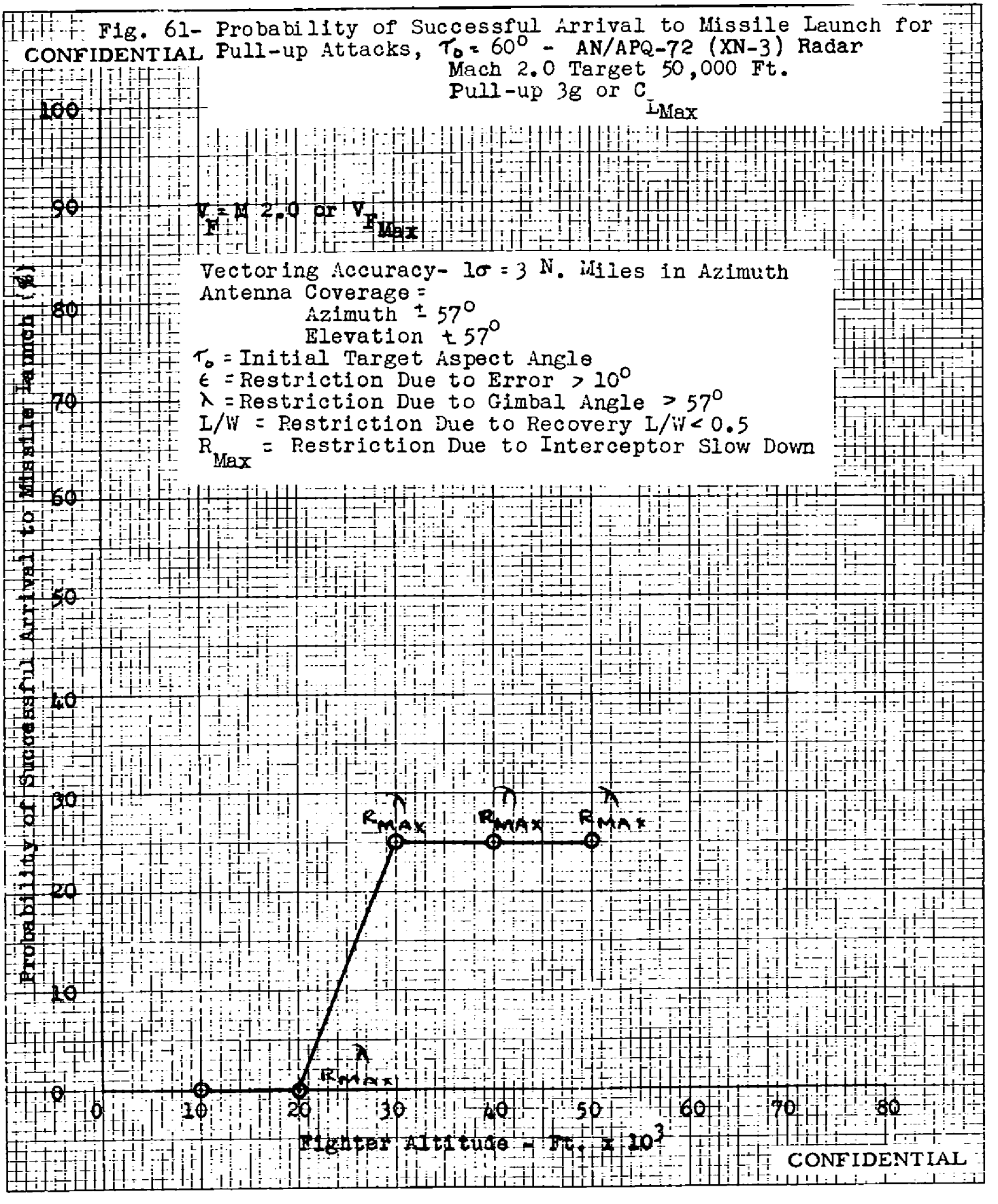

CONFIDENTIAL

CONFIDENTIAL

Fig. 62- Probability of Successful Arrival to Missile Launch for Pull-up Attacks, $\tau_o = 70^\circ$ - AN/APQ-72 (XN-3) Radar
Mach 2.0 Target 50,000 Ft.
Pull-up 3g or $C_{L_{Max}}$

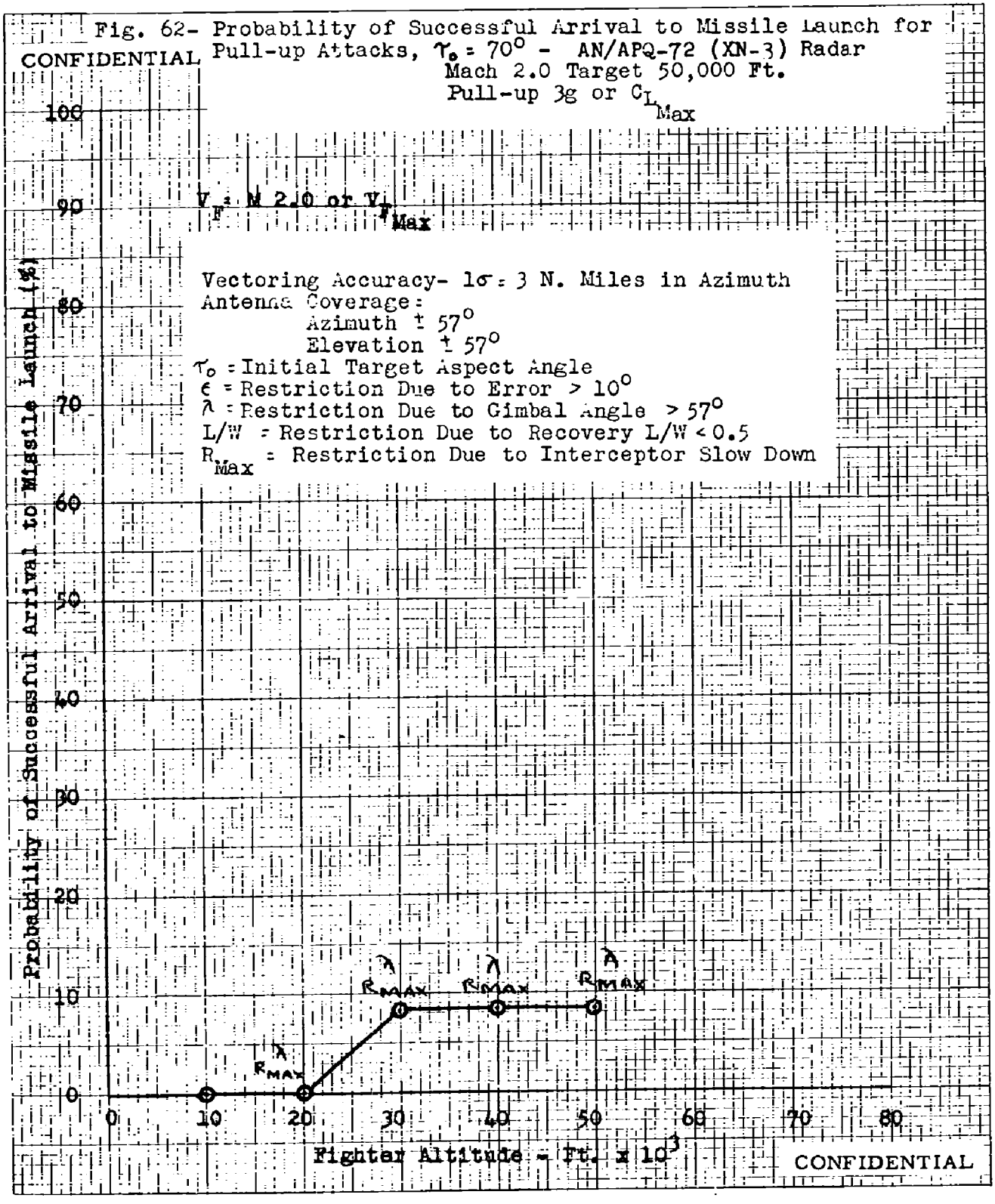

CONFIDENTIAL

CONFIDENTIAL

Fig. 63- Probability of Successful Arrival to Missile Launch for Pull-up Attacks, τ_o = 15°, 30° - AN/APQ-72 (XN-3) Radar
Mach 2.0 Target 50,000 Ft.
Pull-up 3g or $C_{L_{Max}}$

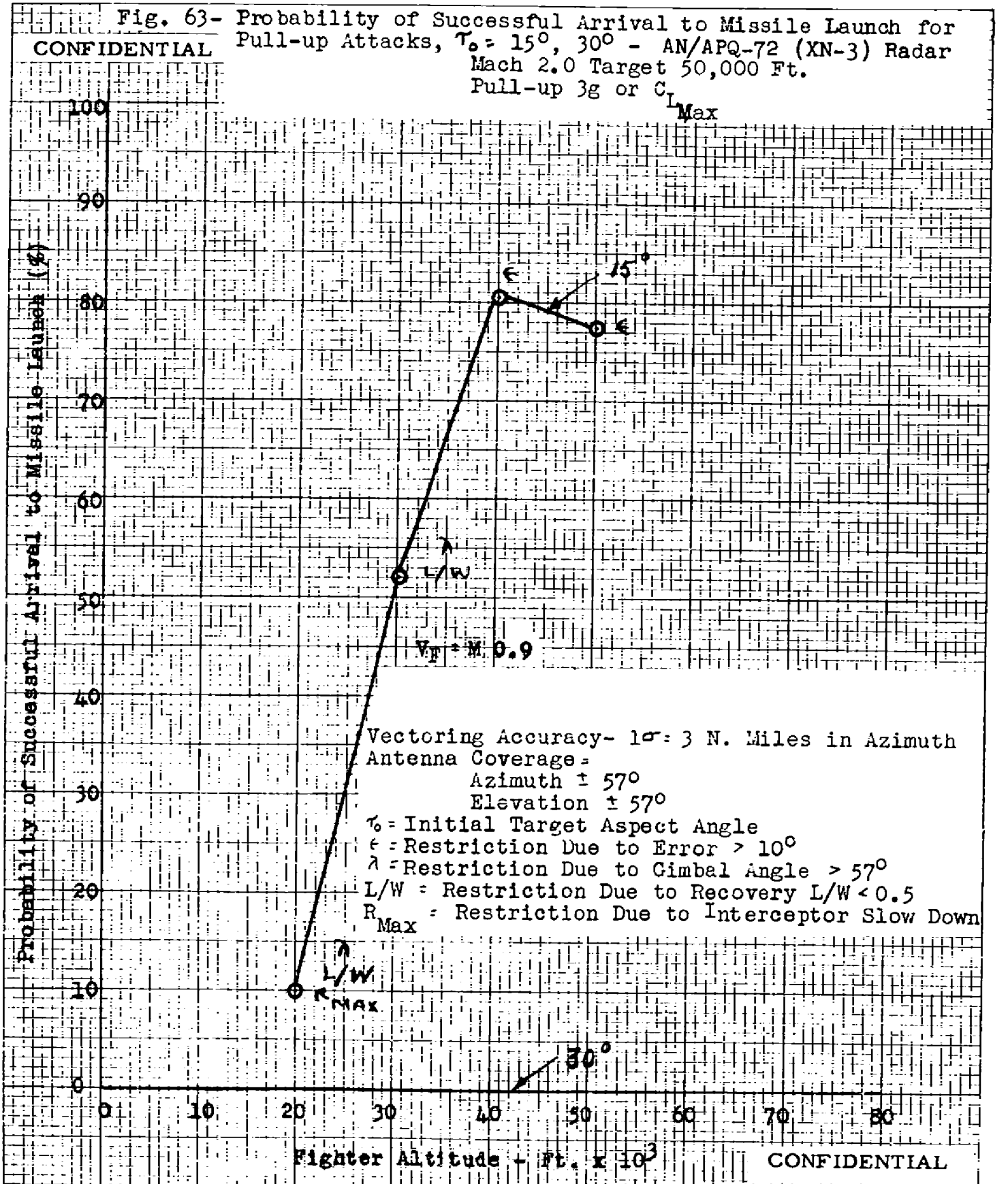

CONFIDENTIAL

CONFIDENTIAL

Fig. 64- Probability of Successful Arrival to Missile Launch for Pull-up Attacks, Head-on - AN/APQ-72 (XN-3) Radar
Mach 1.6 Target 50,000 Ft.
Pull-up 3g or $C_{L_{Max}}$

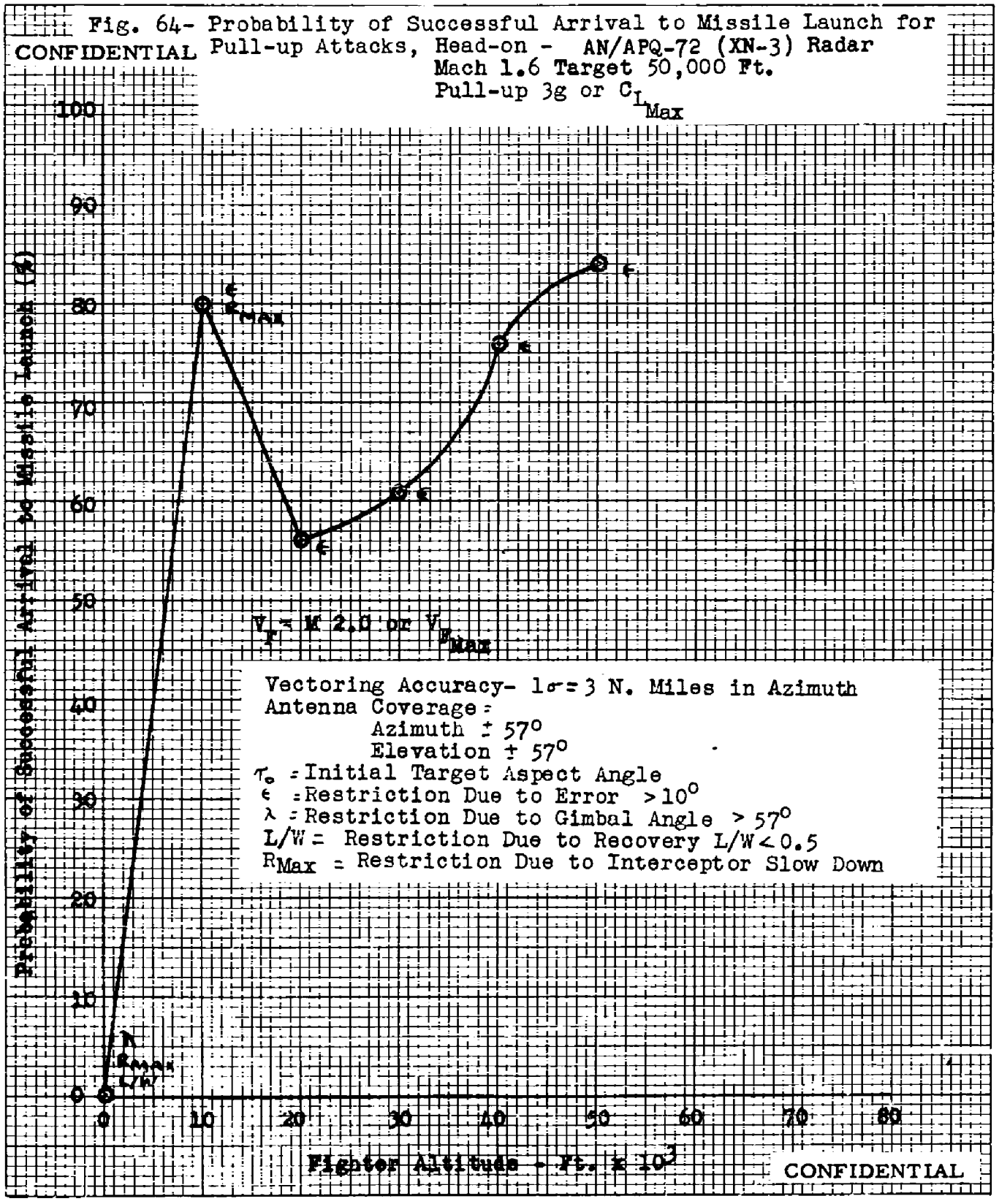

CONFIDENTIAL

CONFIDENTIAL

Fig. 65- Probability of Successful Arrival to Missile Launch for Pull-up Attacks, $\tau_o = 15^o$ - AN/APQ-72 (XN-3) Radar
Mach 1.6 Target 50,000 Ft.
Pull-up 3g or $C_{L_{Max}}$

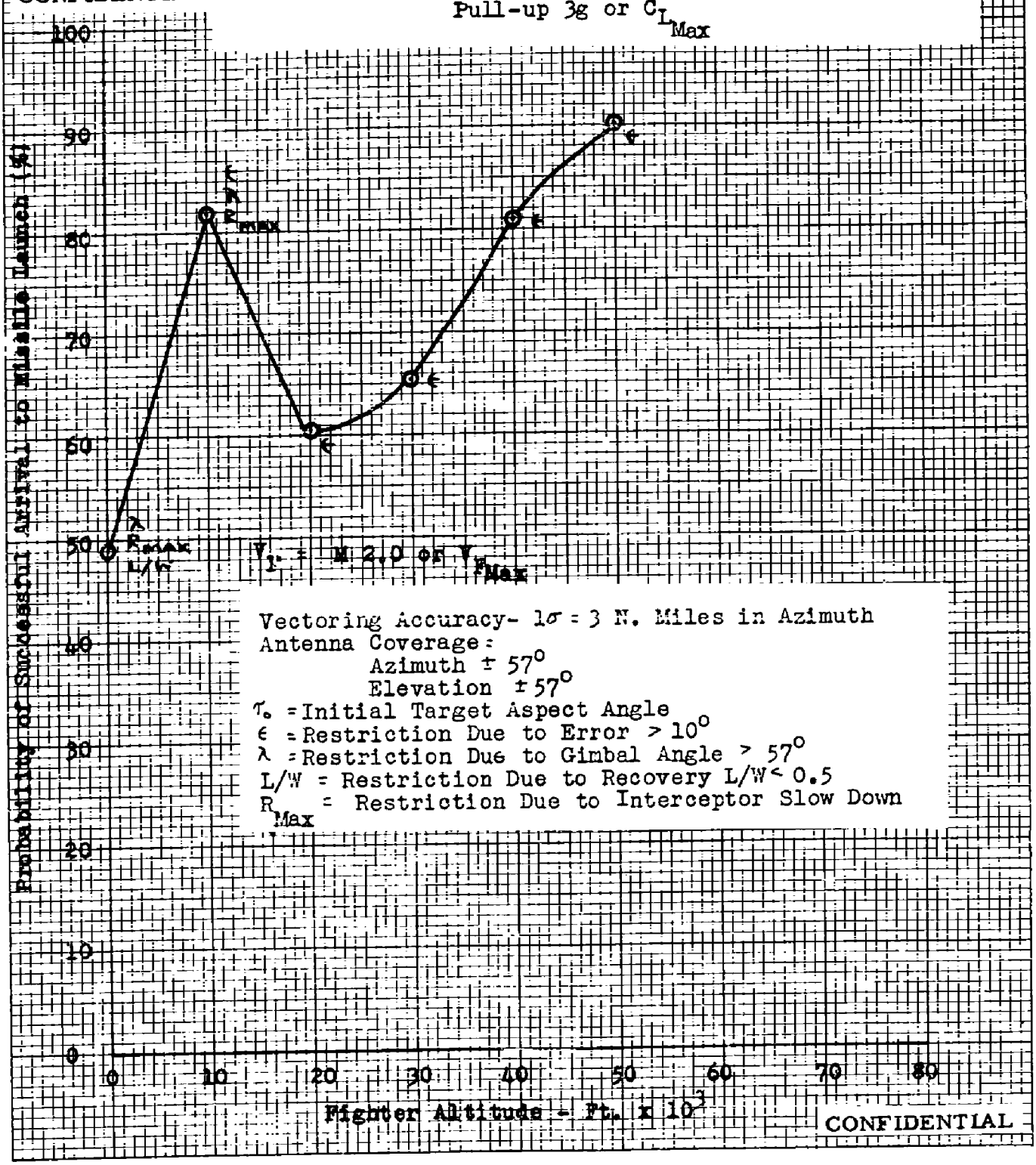

CONFIDENTIAL

Fig. 66- Probability of Successful Arrival to Missile Launch for Pull-up Attacks, $\tau_o = 30^\circ$ - AN/APQ-72 (XN-3) Radar
Mach 1.6 Target 50,000 Ft.
Pull-up 3g or $C_{L_{Max}}$

CONFIDENTIAL

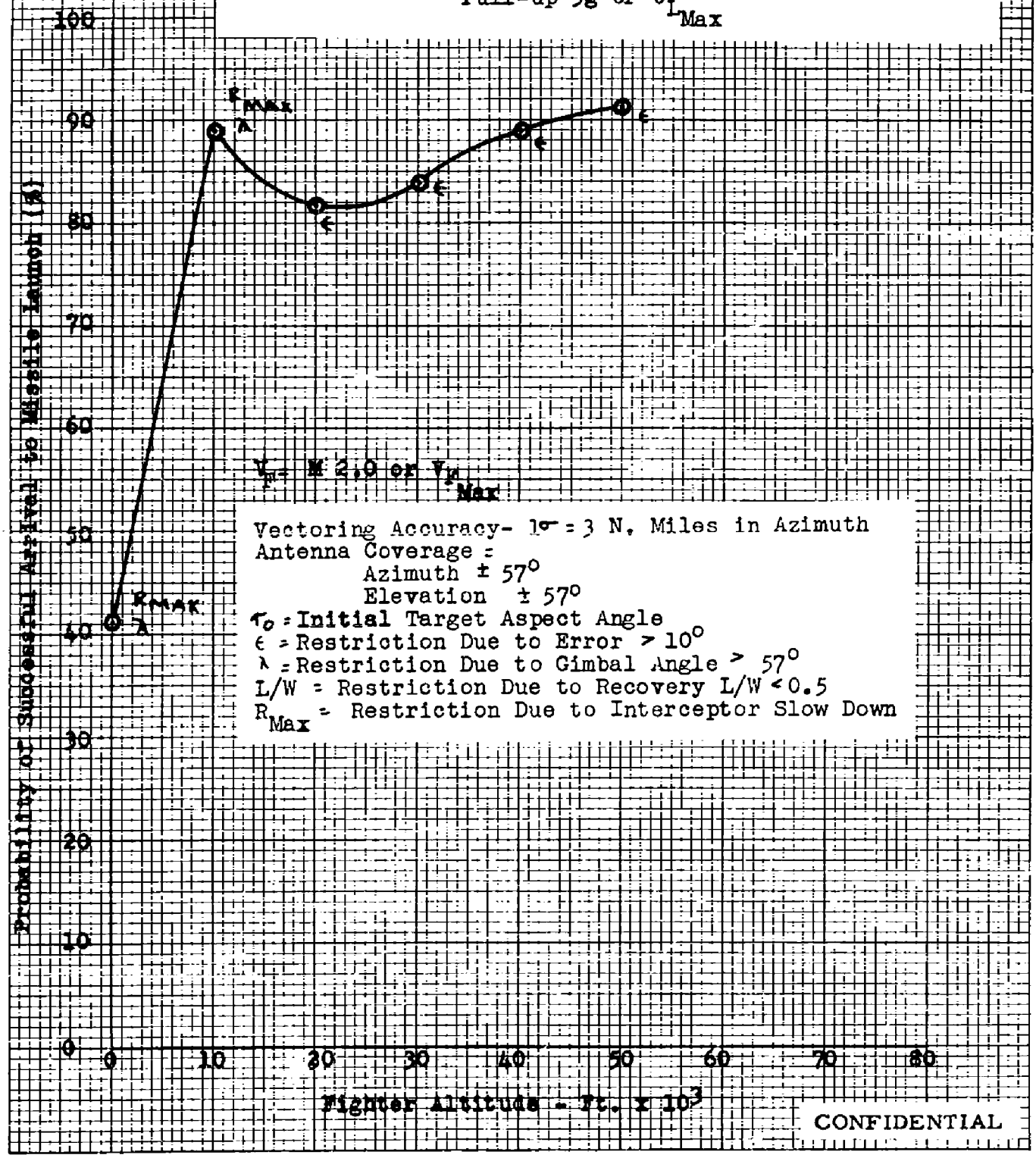

CONFIDENTIAL

Fig. 67- Probability of Successful Arrival to Missile Launch for Pull-up Attacks, τ_o = 45° - AN/APQ-72 (XN-3) Radar
Mach 1.6 Target 50,000 Ft.
Pull-up 3g or $C_{L_{Max}}$

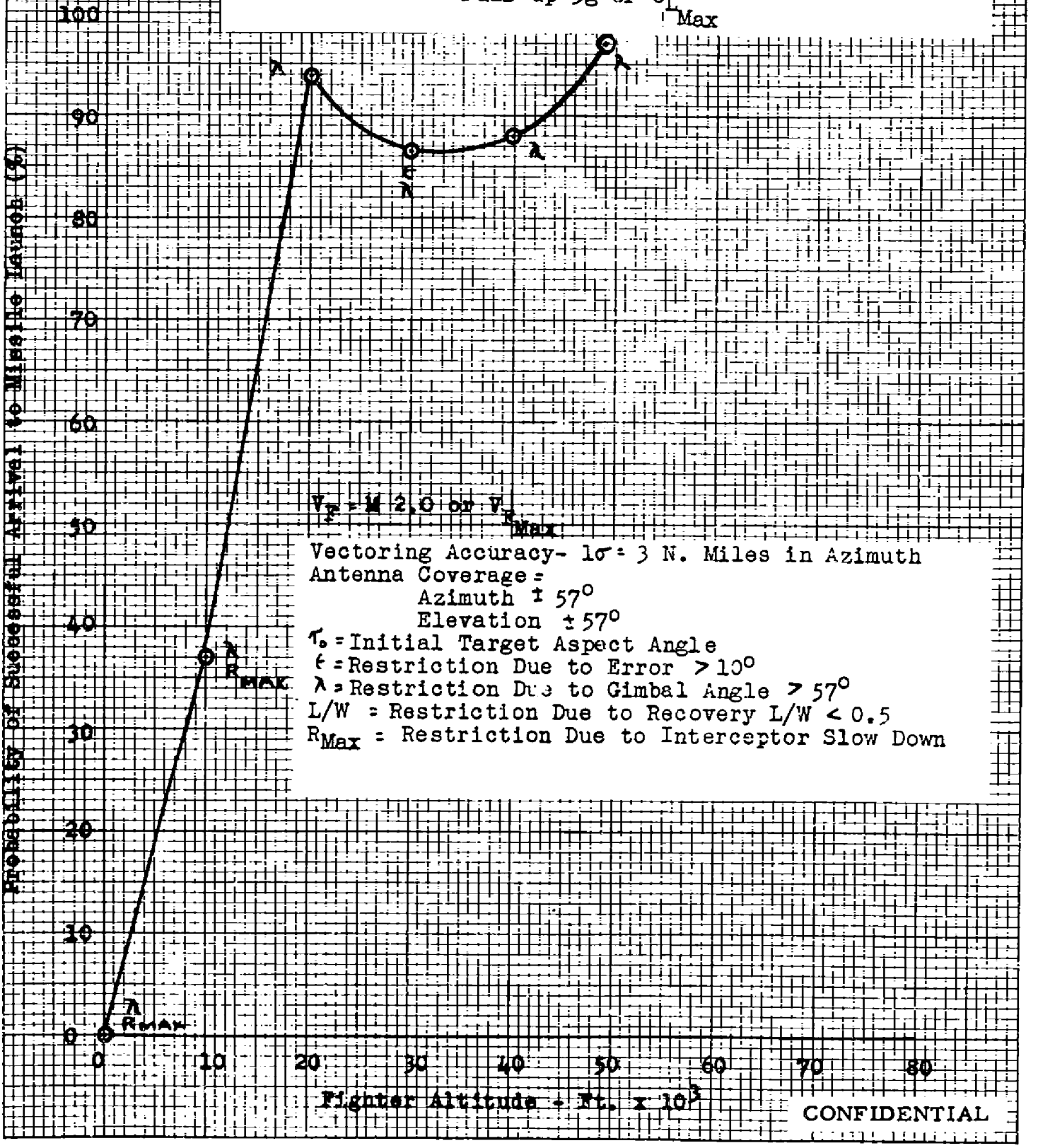

Fig. 68- Probability of Successful Arrival to Missile Launch for Pull-up Attacks, $\tau_o = 60^o$ - AN/APQ-72 (XN-3) Radar
Mach 1.6 Target 50,000 Ft.
Pull-up 3g or $C_{L_{Max}}$

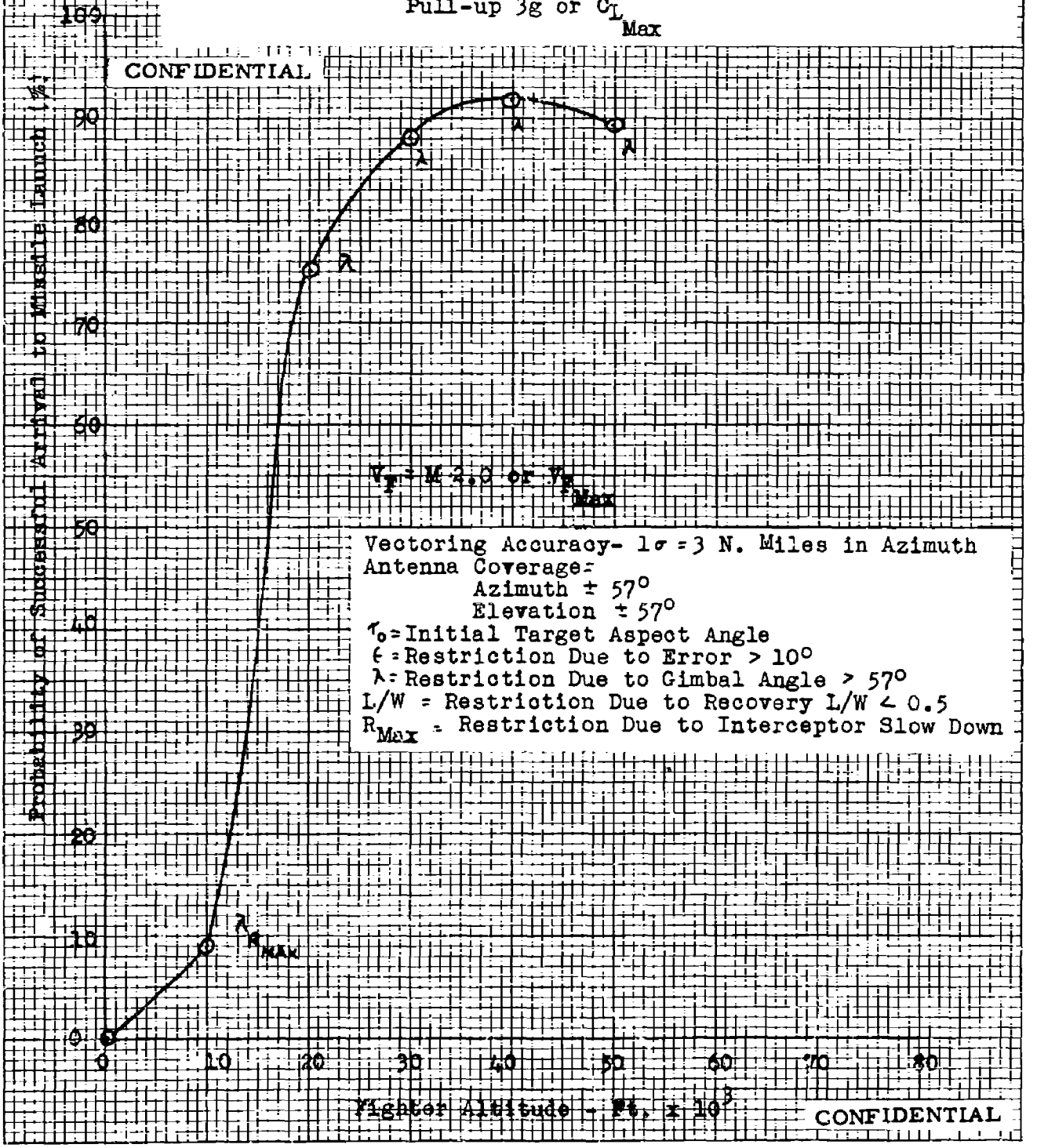

Fig. 69- Probability of Successful Arrival to Missile Launch for Pull-up Attacks, $\tau_o = 75^o$ - AN/APQ-72 (XN-3) Radar
Mach 1.6 Target 50,000 ft.
Pull-up 3g or $C_{L_{Max}}$

CONFIDENTIAL

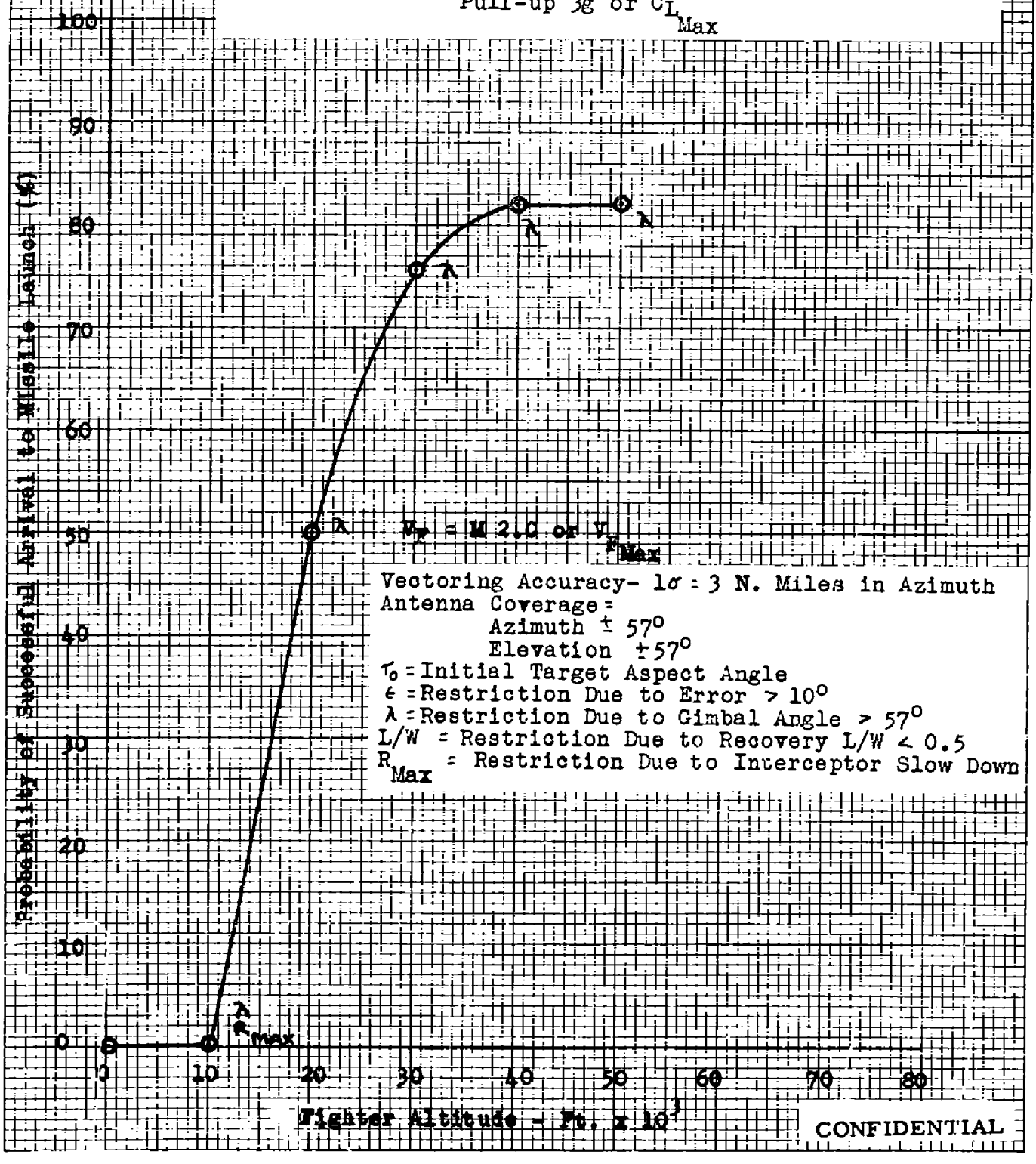

CONFIDENTIAL

CONFIDENTIAL

Fig. 70- Probability of Successful Arrival to Missile Launch for Pull-up Attacks, $\tau_o = 90^o$ - AN/APQ-72 (XN-3) Radar
Mach 1.6 Target 50,000 Ft.
Pull-up 3g or $C_{L_{Max}}$

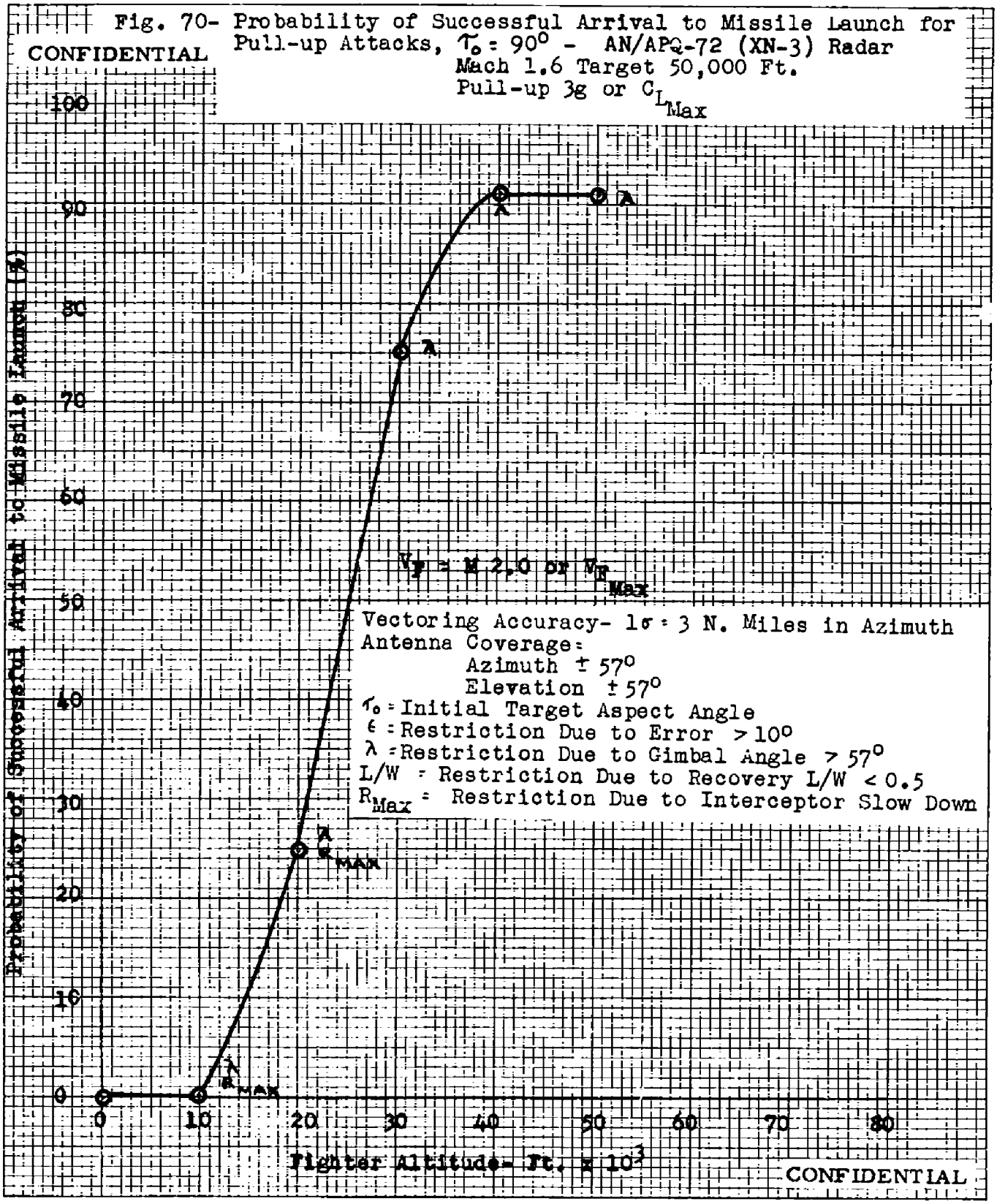

CONFIDENTIAL

Fig. 71- Probability of Successful Arrival to Missile Launch for Pull-up Attacks, $\tau_o = 120^o$, AN/APQ-72 (XN-3) Radar
Mach 1.6 Target 50,000 Ft.
Pull-up 3g or $C_{L_{Max}}$

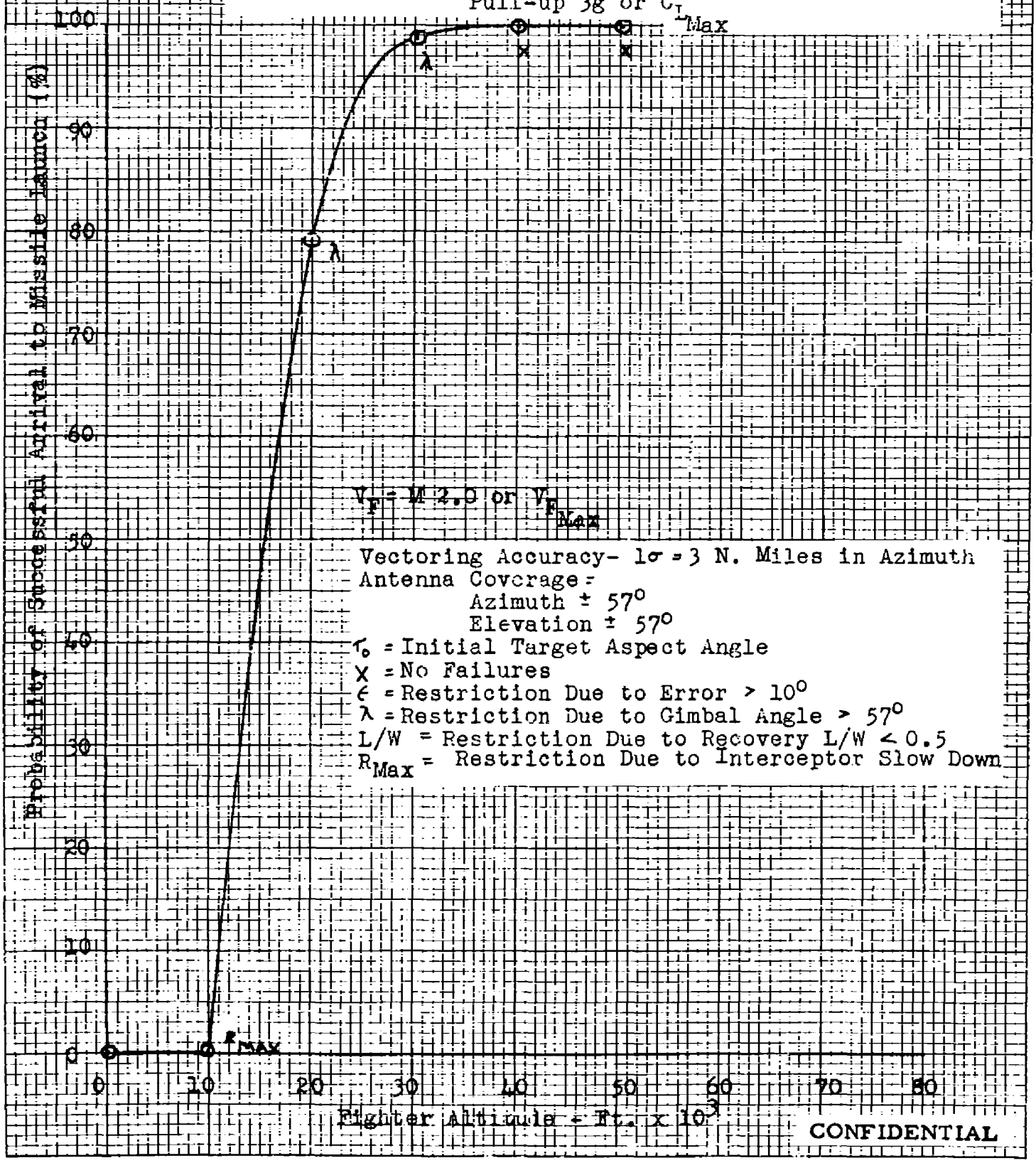

Vectoring Accuracy- $1\sigma = 3$ N. Miles in Azimuth
Antenna Coverage:
Azimuth ± 57°
Elevation ± 57°

τ_o = Initial Target Aspect Angle
X = No Failures
ϵ = Restriction Due to Error > 10°
λ = Restriction Due to Gimbal Angle > 57°
L/W = Restriction Due to Recovery L/W < 0.5
R_{Max} = Restriction Due to Interceptor Slow Down

Fig. 72- Probability of Successful Arrival to Missile Launch for Pull-up Attacks, $\tau_o = 150^o$ - AN/APG-72 (XN-3) Radar

CONFIDENTIAL

Mach 1.6 Target 50,000 Ft.
Pull-up 3g or $C_{L_{Max}}$

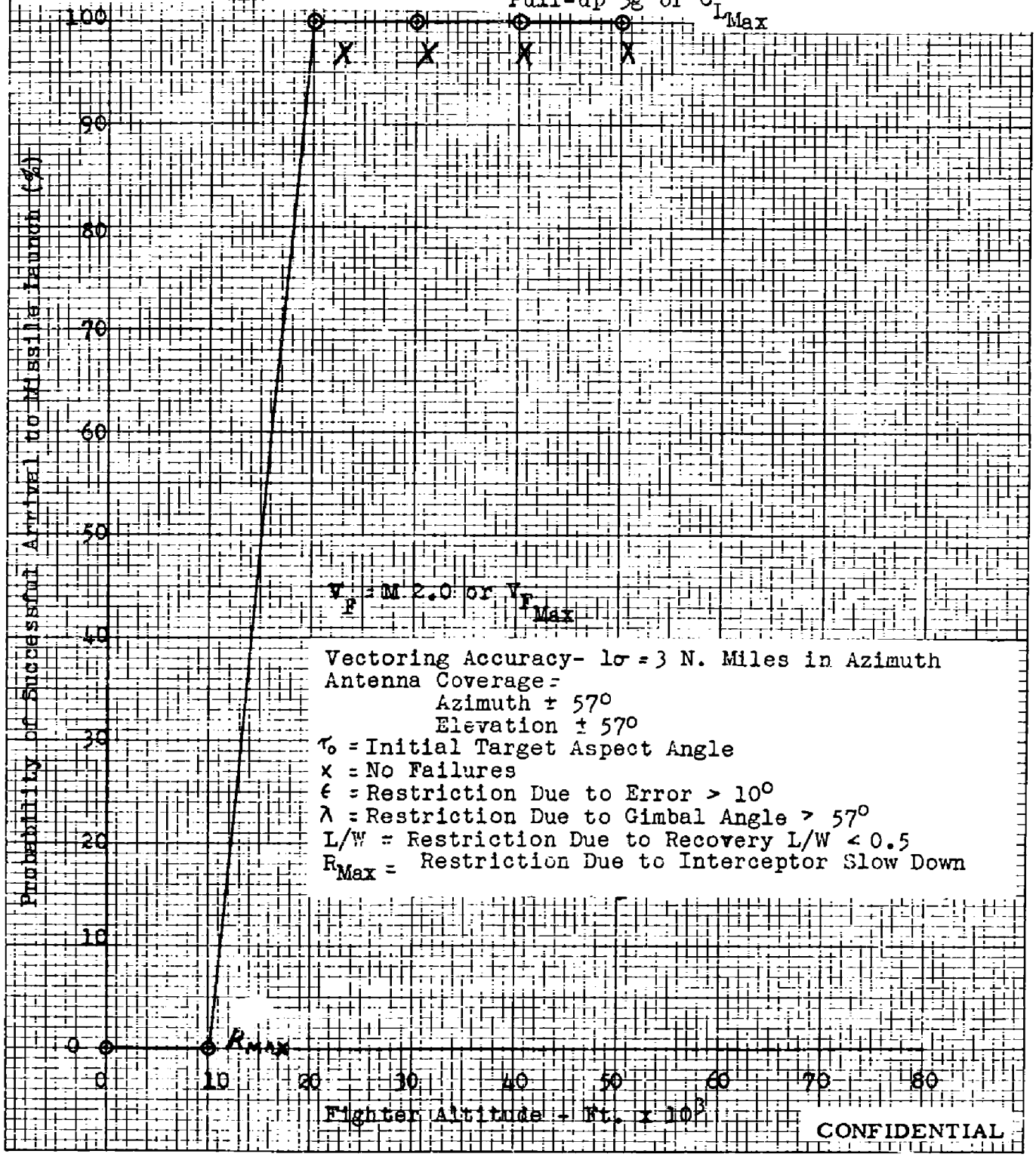

CONFIDENTIAL

Fig. 73- Probability of Successful Arrival to Missile Launch for Pull-up Attacks, $\tau_o = 15^o$ - AN/APQ-72 (XN-3) Radar
Mach 1.6 Target 50,000 Ft.
Pull-up 3g or $C_{L_{Max}}$

CONFIDENTIAL

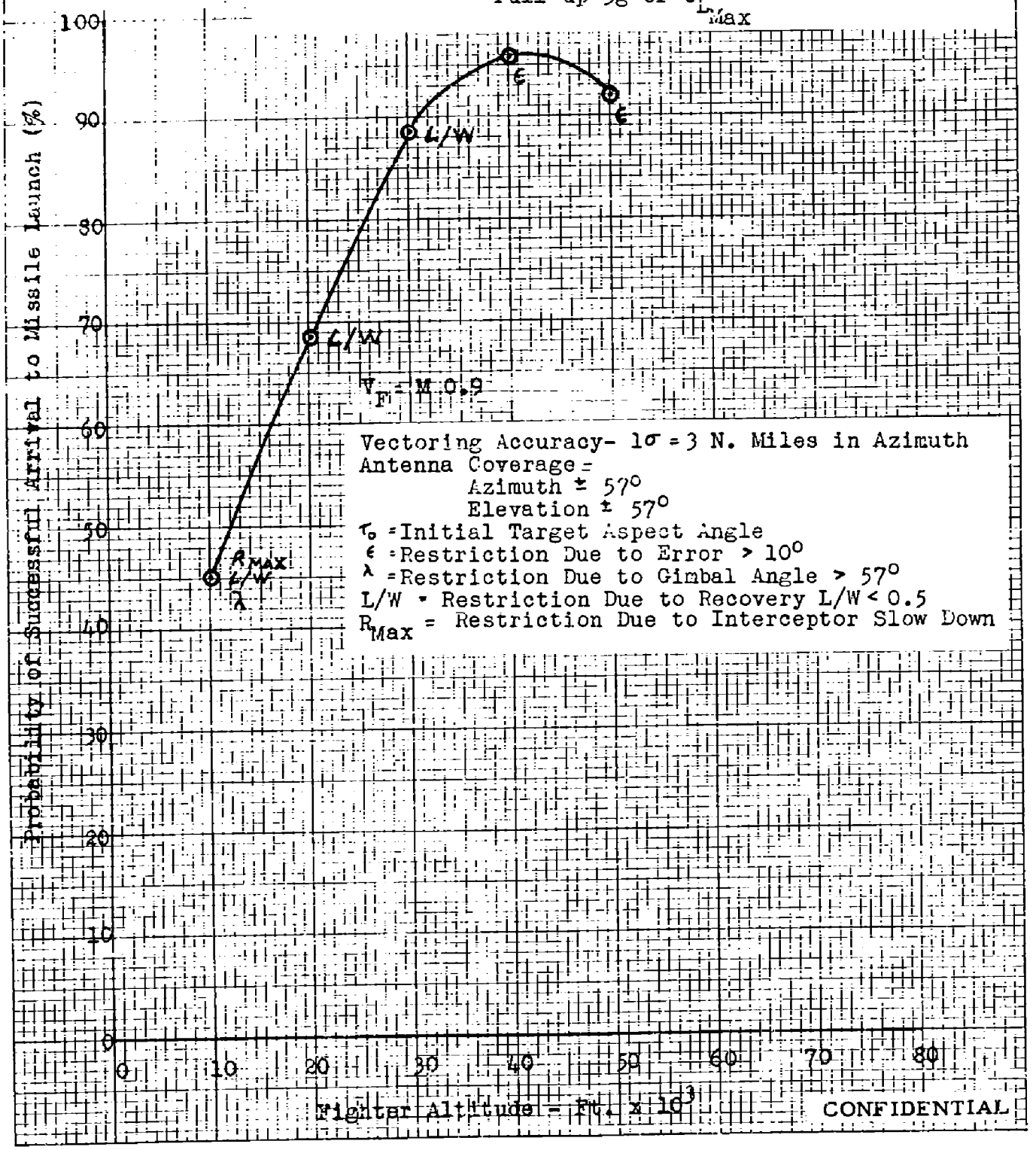

CONFIDENTIAL

CONFIDENTIAL

Fig. 74- Probability of Successful Arrival to Missile Launch for Pull-up Attacks, $\tau_o = 30^o$ - AN/APQ-72 (XN-3) Radar
Mach 1.6 Target 50,000 Ft.
Pull-up 3g or $C_{L_{Max}}$

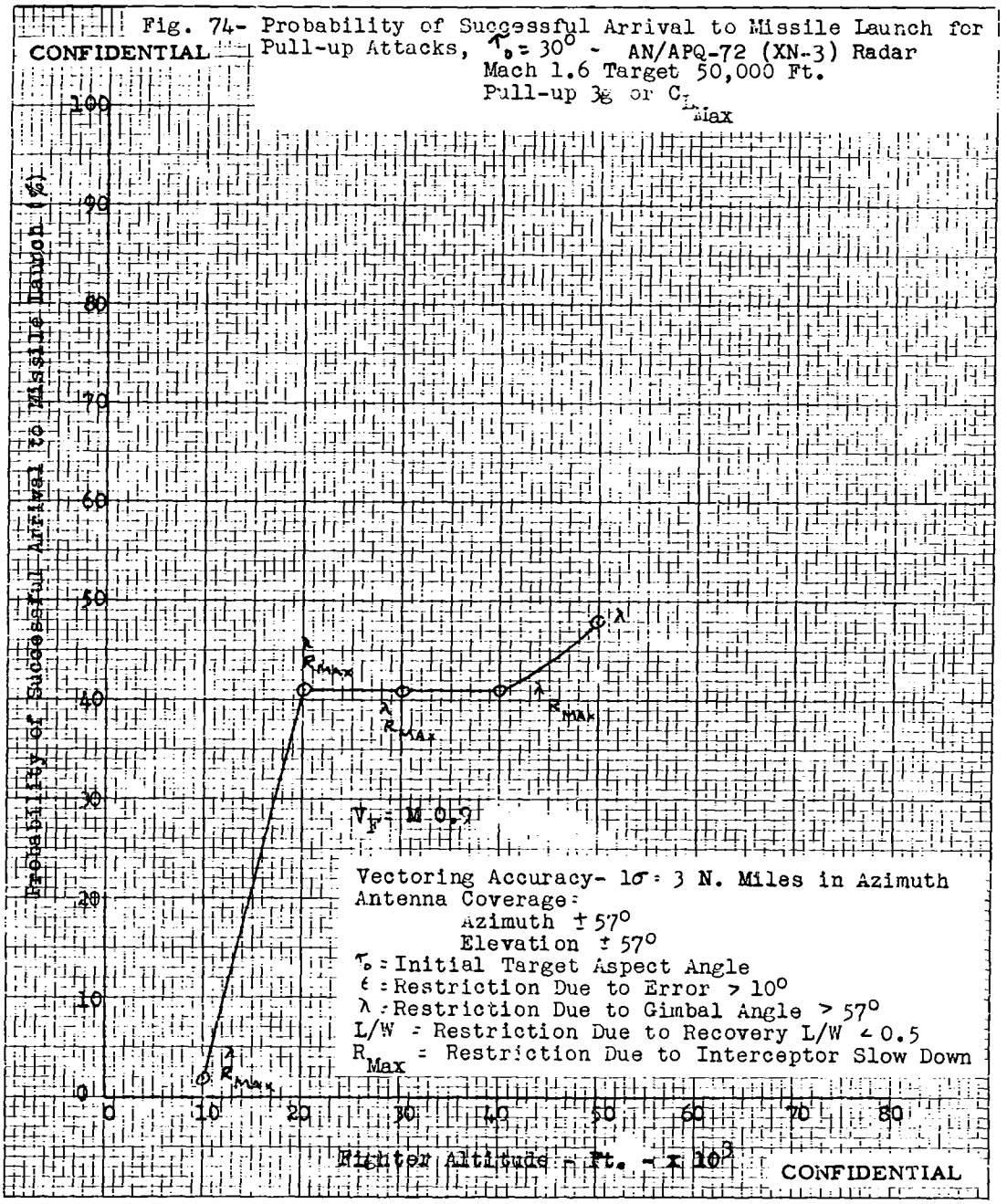

CONFIDENTIAL

Confidential

Fig. 75- Probability Grid from which Intercepts Originate

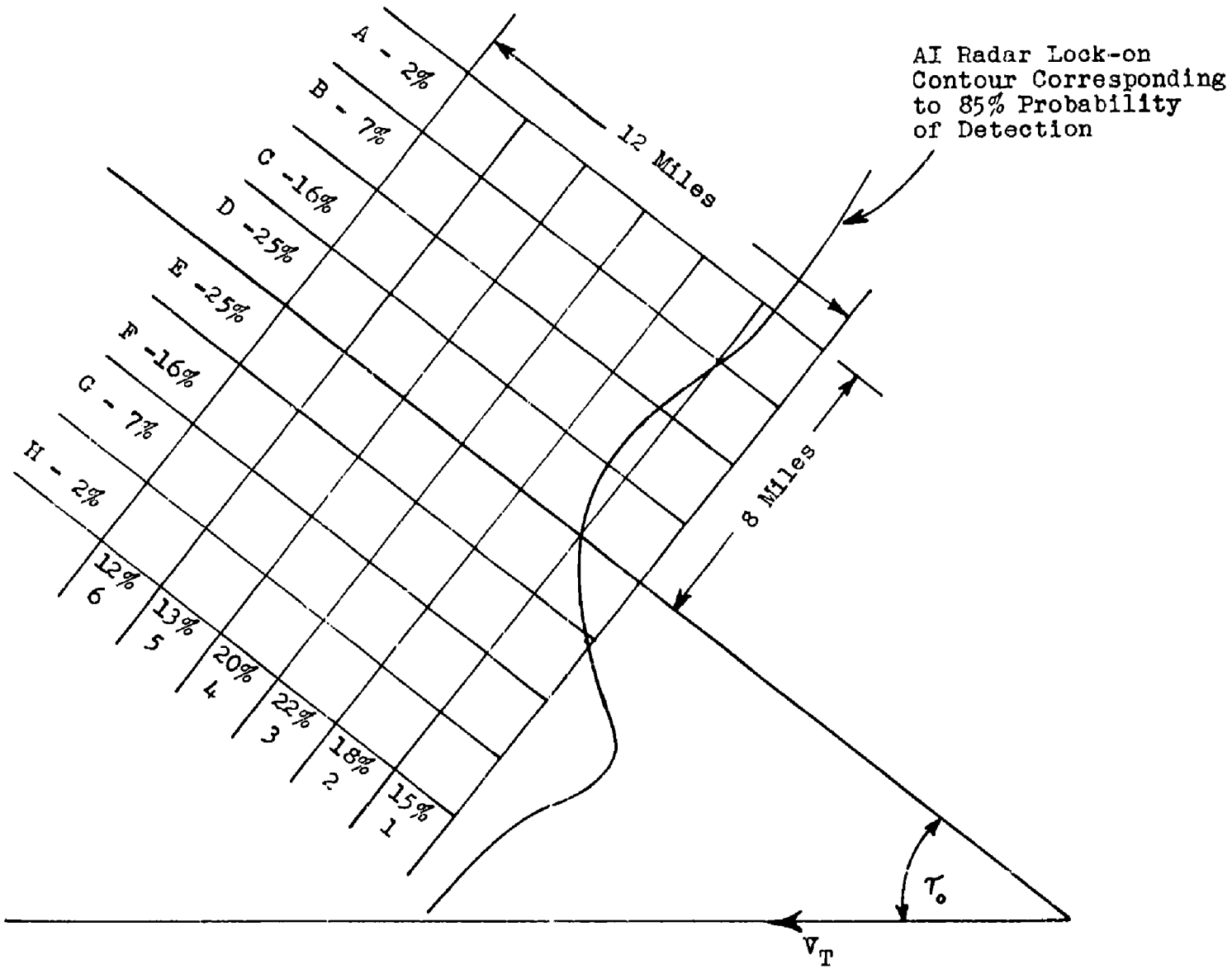

Confidential

CONFIDENTIAL

Fig. 76- Probability of Successful Arrival to Missile Launch for Pull-up Attacks - AN/APQ-72 (XN-3) Radar
Effect of Delayed Pull-ups
Mach 1.6 Target 65,000 Ft.
Pull-up 3g or $C_{L_{Max}}$

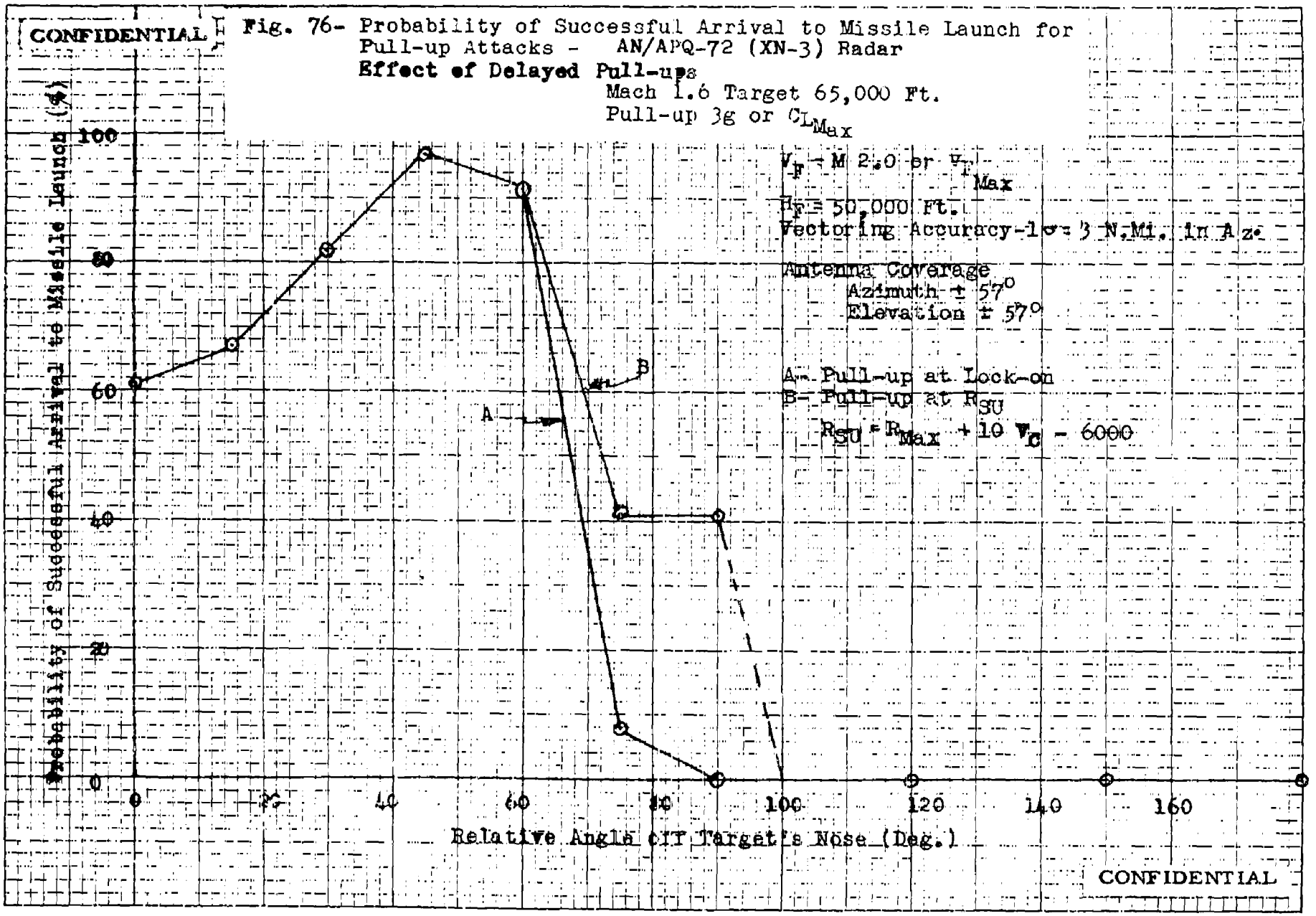

CONFIDENTIAL

CONFIDENTIAL

Fig. 77- Probability of Successful Arrival to Missile Launch for Pull-up Attacks - AN/APQ-72 (XN-3) Radar
Effect of Delayed Pull-ups
Mach 1.6 Target 65,000 Ft.
Pull-up 3g or $C_{L_{Max}}$

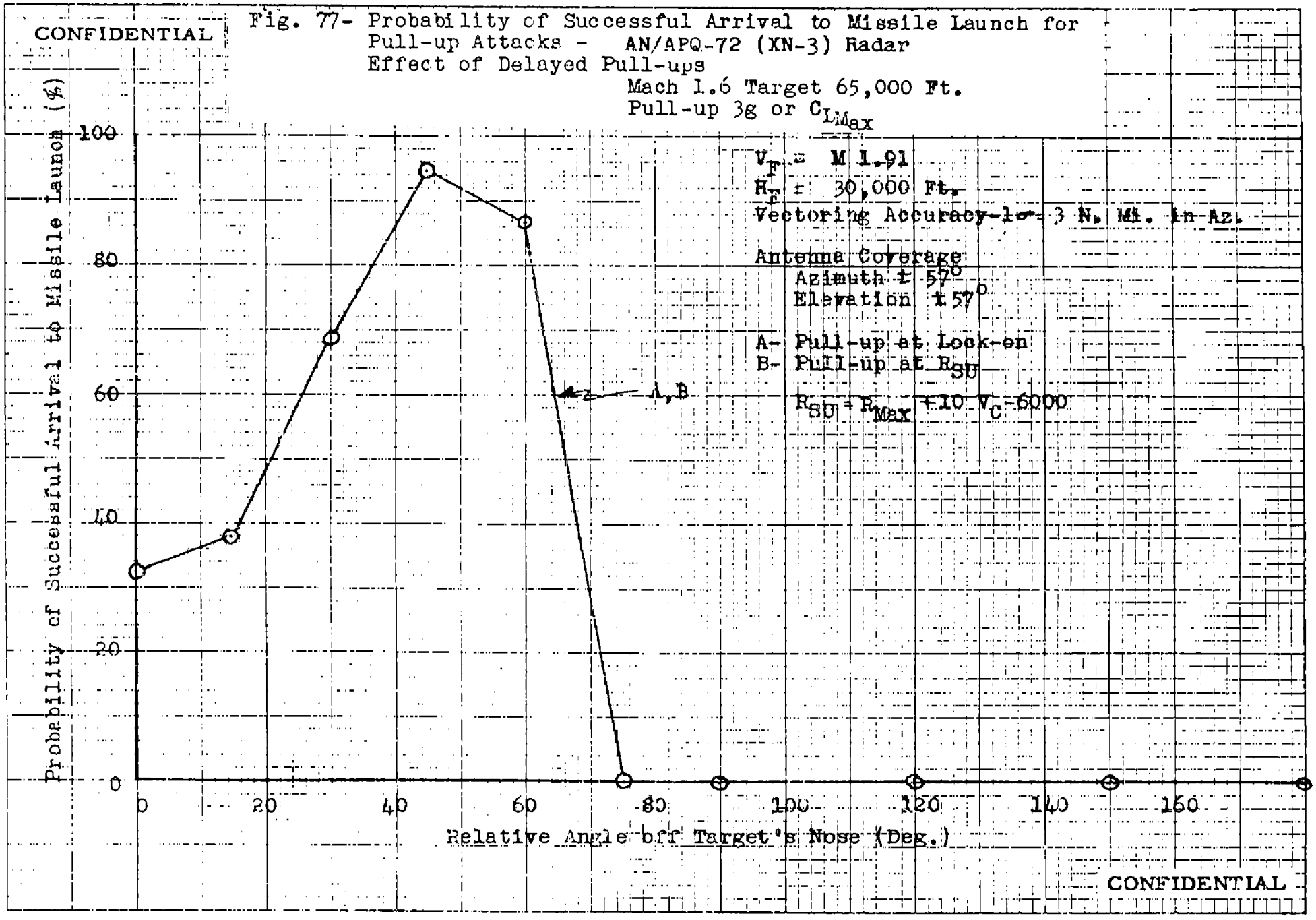

CONFIDENTIAL

1

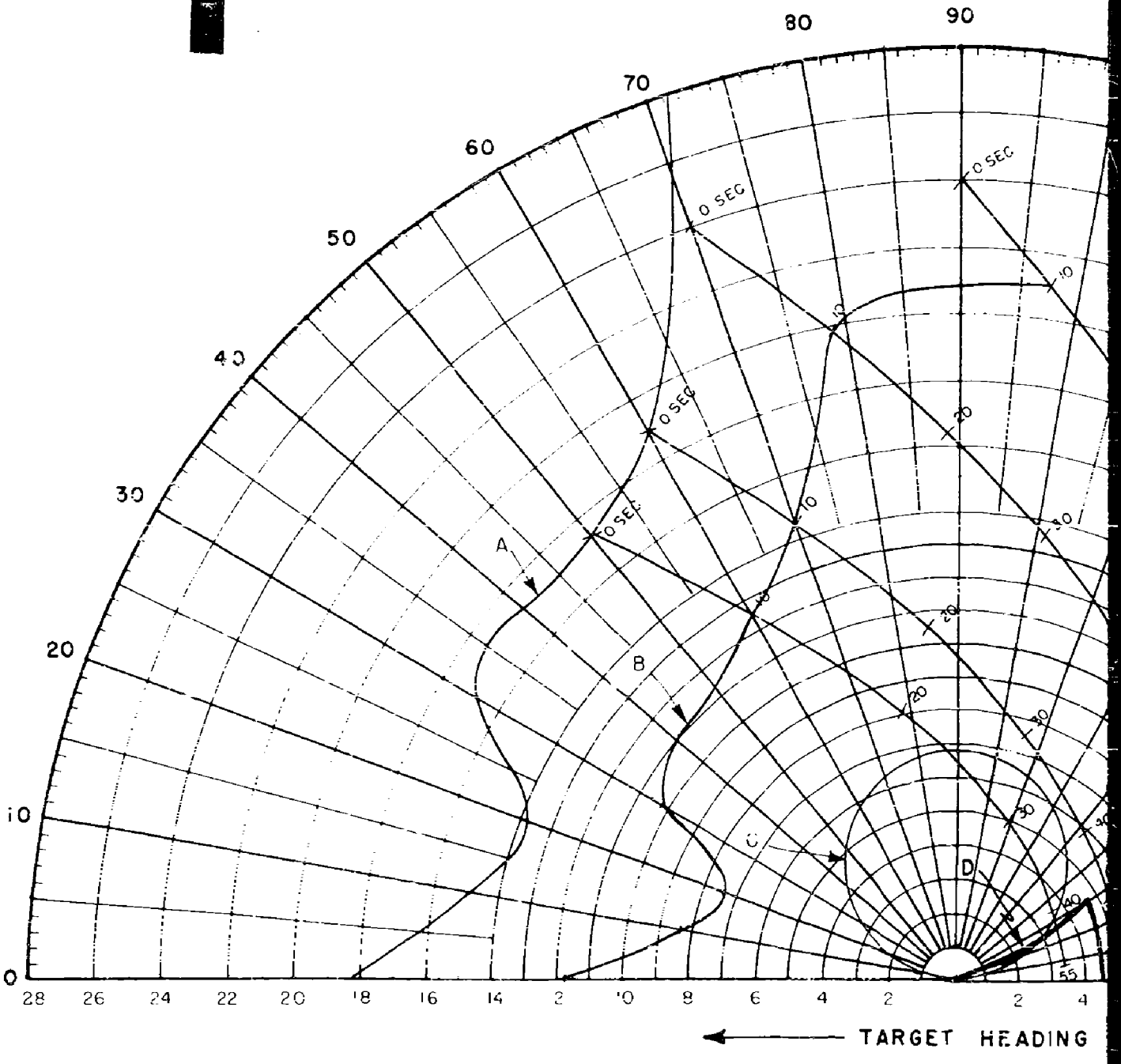

V_F = 1940 FT/SEC

V_T = 1940 FT/SEC

ALTITUDE = 50,000 FT.

A - 85 % DETECTION RANGE

B - LOCK-ON RANGE

C - CONSTANT LOAD FACTOR LOCUS (N_Z =

D - SIDEWINDER I-C LAUNCH ZONE

FIG. 78 - CO-ALTITUDE PURE PURSUIT ATTACK ZONE OVERLAYS.

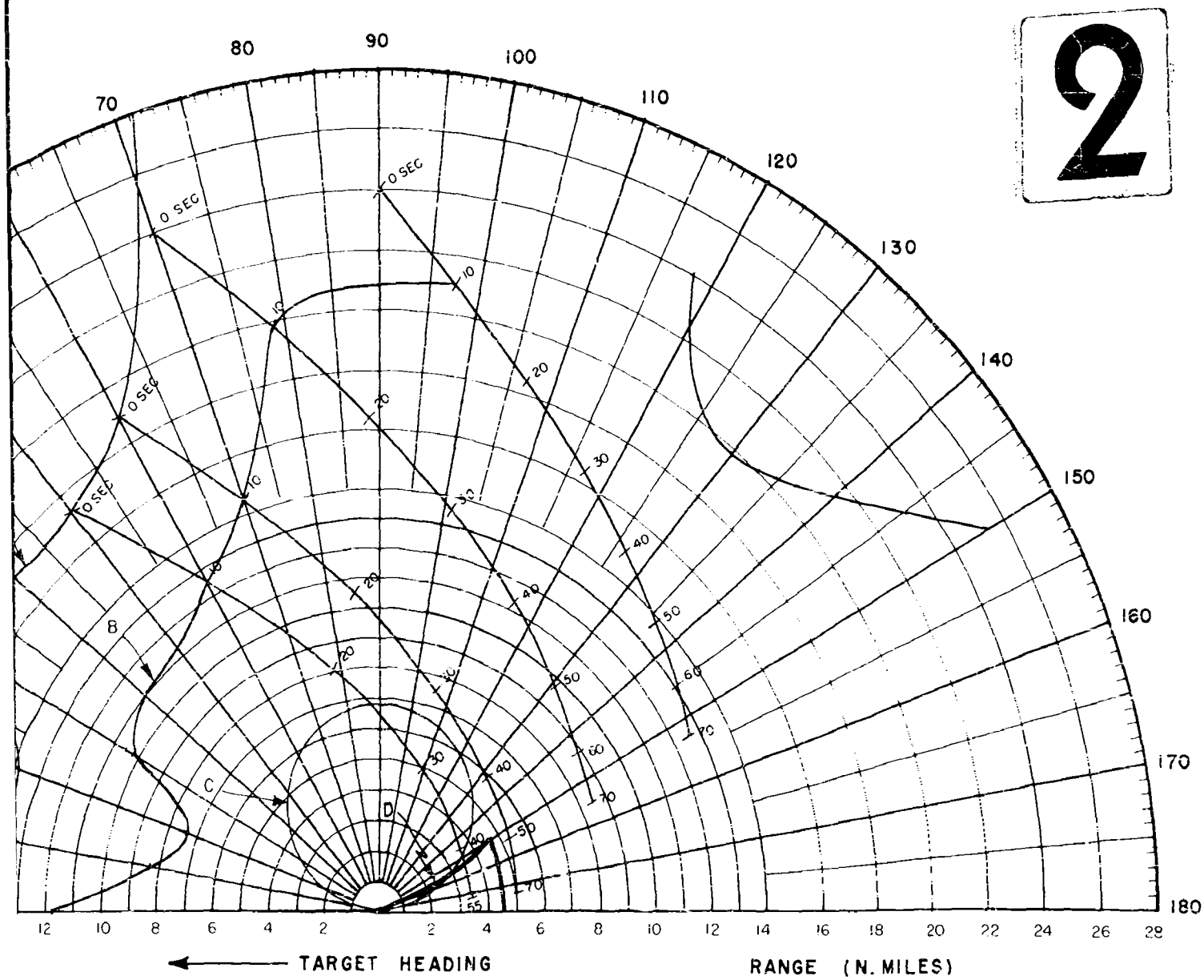

A - 85% DETECTION RANGE

B - LOCK-ON RANGE

C - CONSTANT LOAD FACTOR LOCUS (N_Z = 3)

D - SIDEWINDER I-C LAUNCH ZONE

CONFIDENTIAL

1

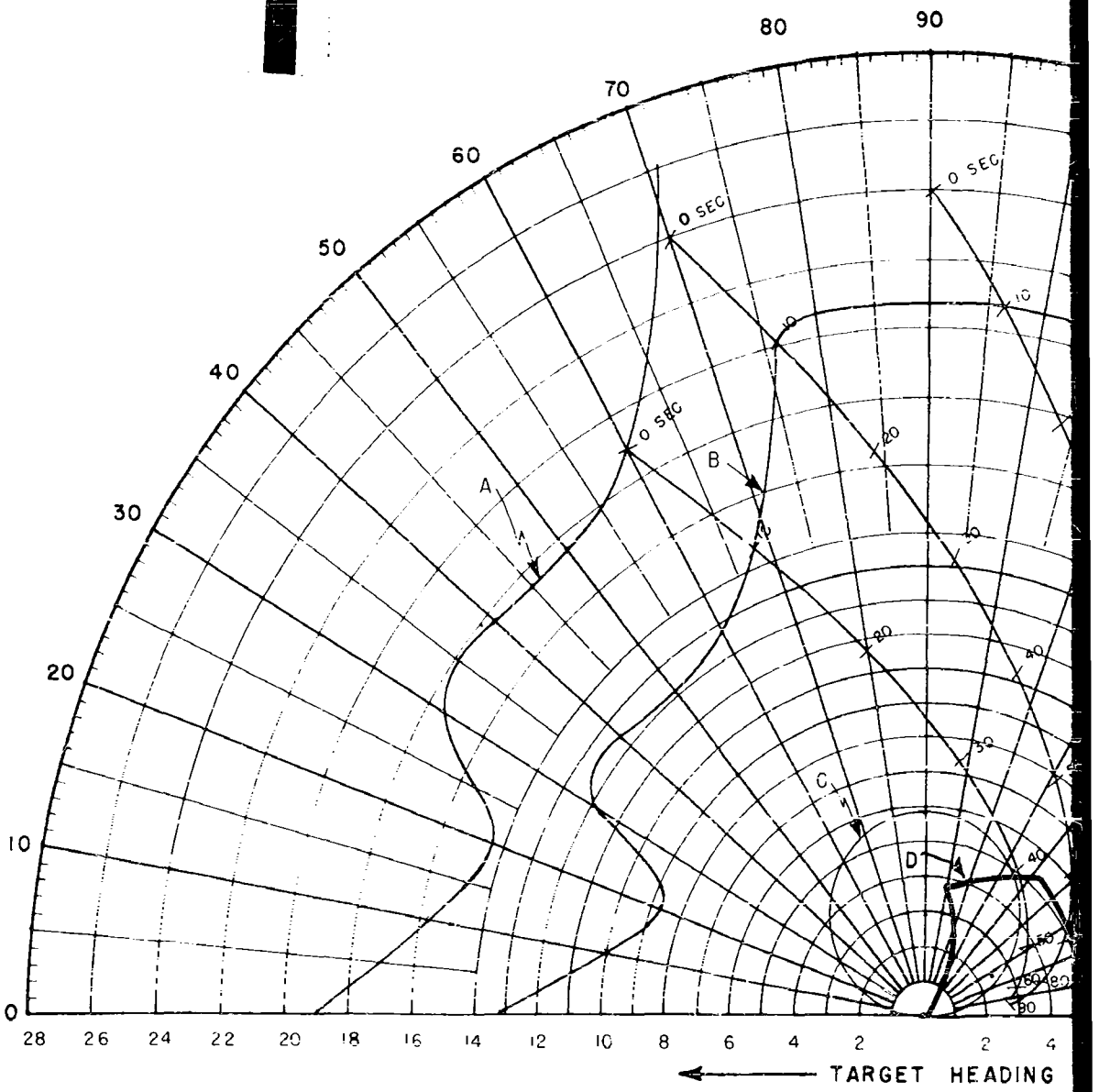

V_F = 1940 FT/SEC

V_T = 1552 FT/SEC

ALTITUDE = 50,000 FT.

A - 85 % DETECTION RANGE

B - LOCK-ON RANGE

C - CONSTANT LOAD FACTOR LOCUS (N_z =

D - SIDEWINDER I-C LAUNCH ZONE

FIG. 79 - CO-ALTITUDE PURE PURSUIT ATTACK ZONE OVERLAYS.

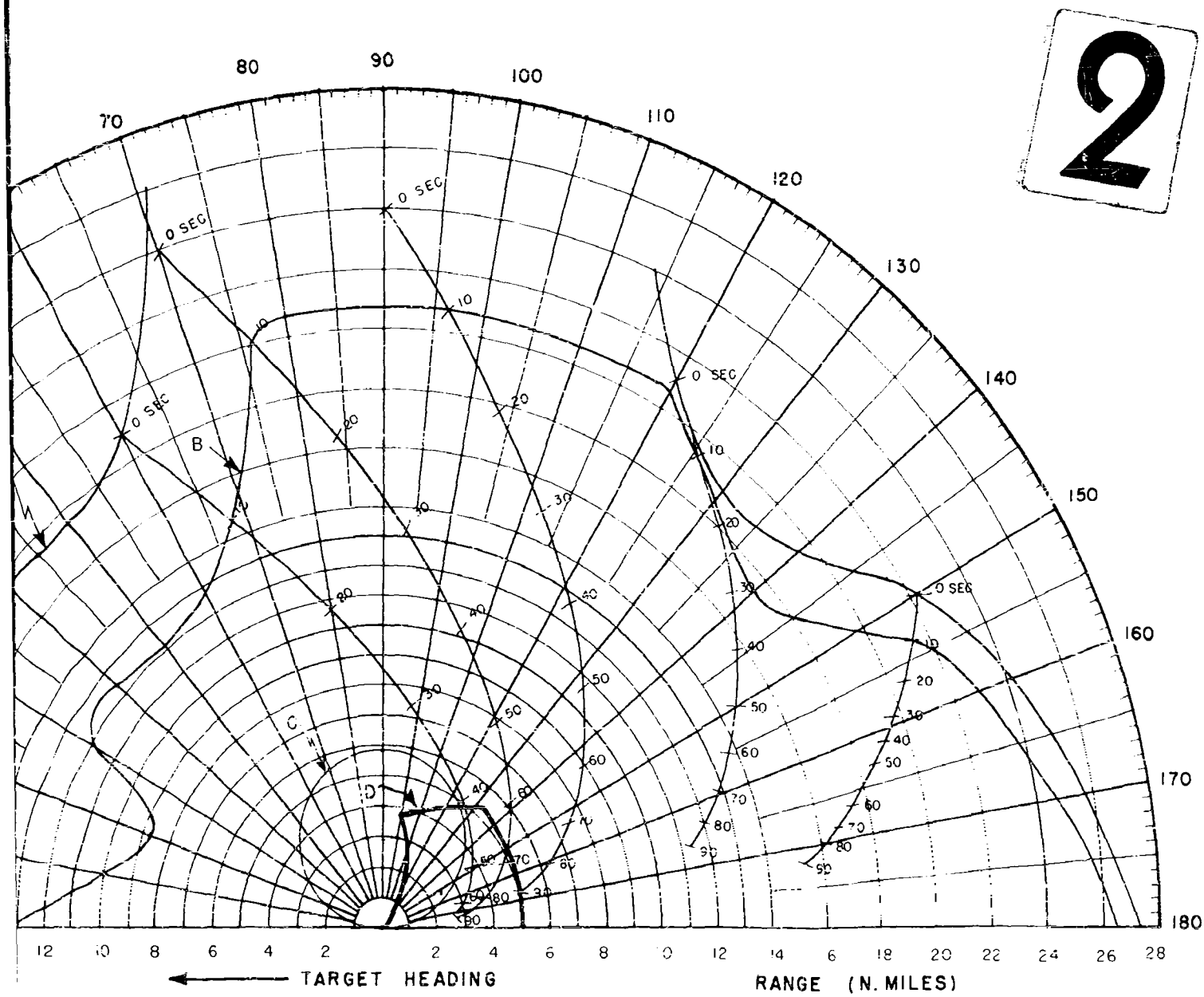

A - 85 % DETECTION RANGE

B - LOCK-ON RANGE

C - CONSTANT LOAD FACTOR LOCUS (N_z = 3)

D - SIDEWINDER 1-C LAUNCH ZONE

CONFIDENTIAL

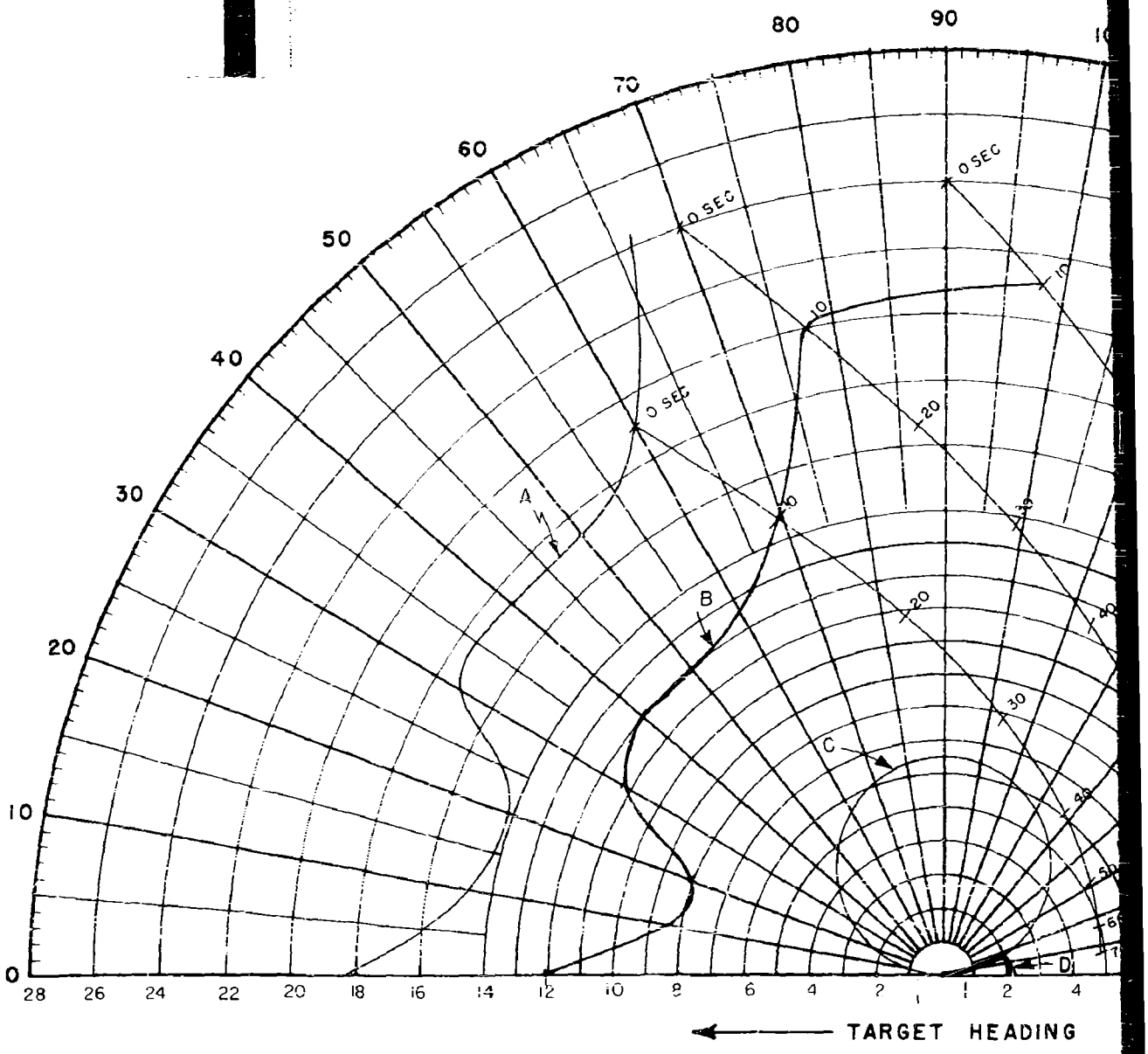

V_F = 1897 FT/SEC

V_T = 1897 FT/SEC

ALTITUDE = 30,000 FT

A - 85 % DETECTION RANGE

B - LOCK-ON RANGE

C - CONSTANT LOAD FACTOR LOCUS (N_Z = 3

D - SIDEWINDER HC LAUNCH ZONE

FIG. 80 - CO-ALTITUDE PURE PURSUIT ATTACK ZONE OVERLAYS.

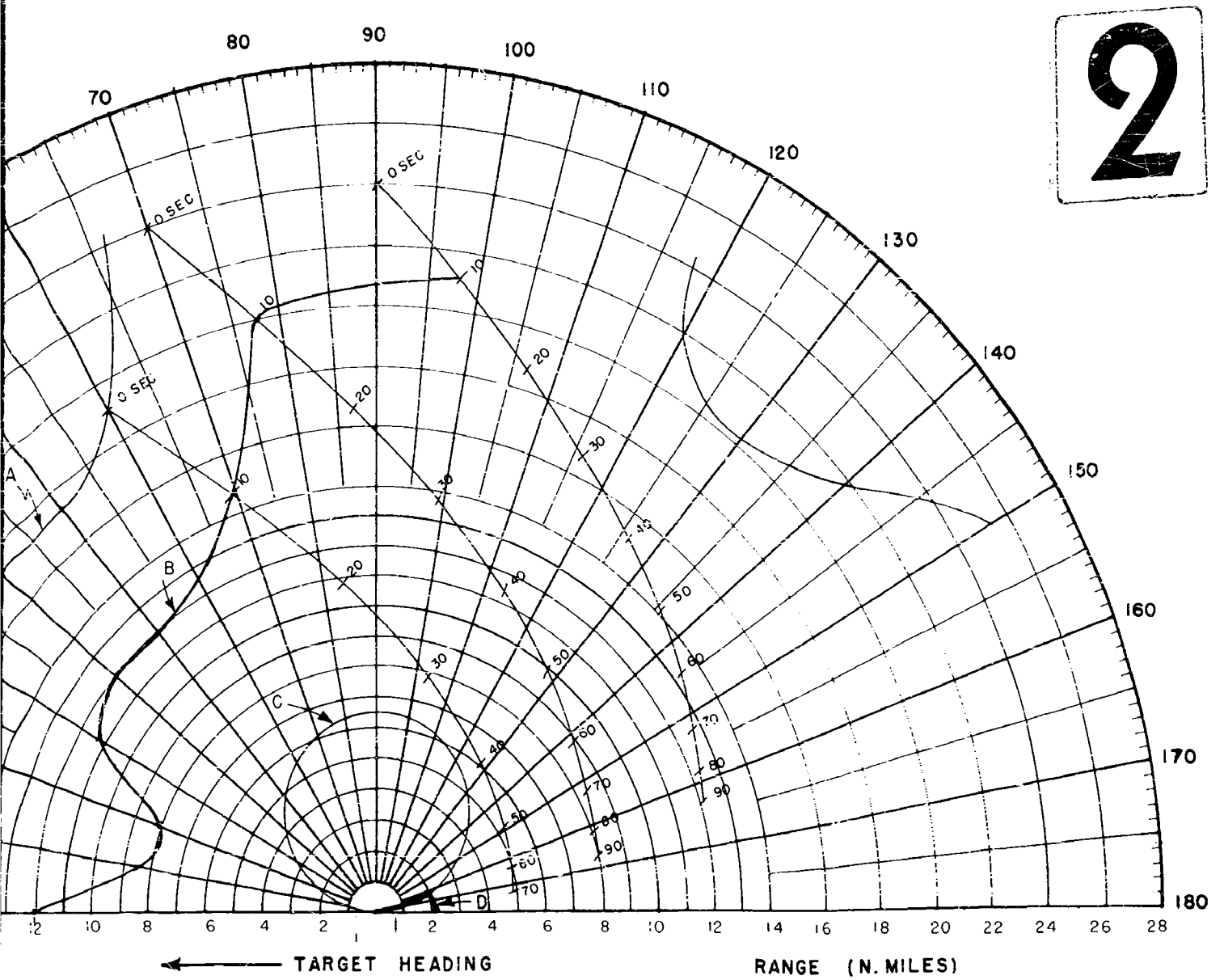

A - 85 % DETECTION RANGE

B - LOCK-ON RANGE

C - CONSTANT LOAD FACTOR LOCUS (N_z = 3)

D - SIDEWINDER 1-C LAUNCH ZONE

1

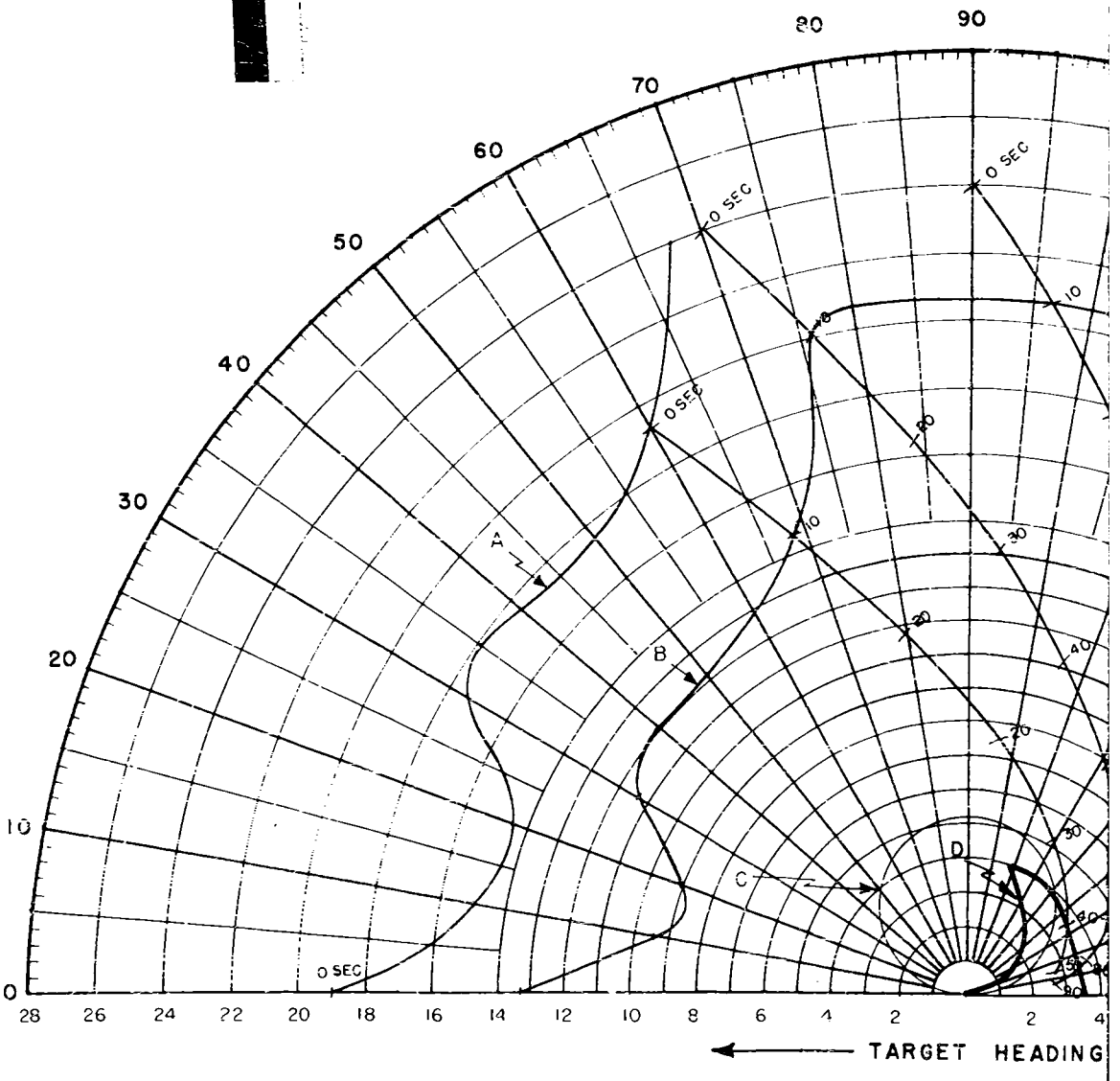

V_F = 1897 FT/SEC

V_T = 1518 FT/SEC

ALTITUDE = 30,000 FT.

A - 85 % DETECTION RANGE

B - LOCK-ON RANGE

C - CONSTANT LOAD FACTOR LOCUS (N_z =

D - SIDEWINDER IC LAUNCH ZONE

FIG. 81 - CO-ALTITUDE PURE PURSUIT ATTACK ZONE OVERLAYS.

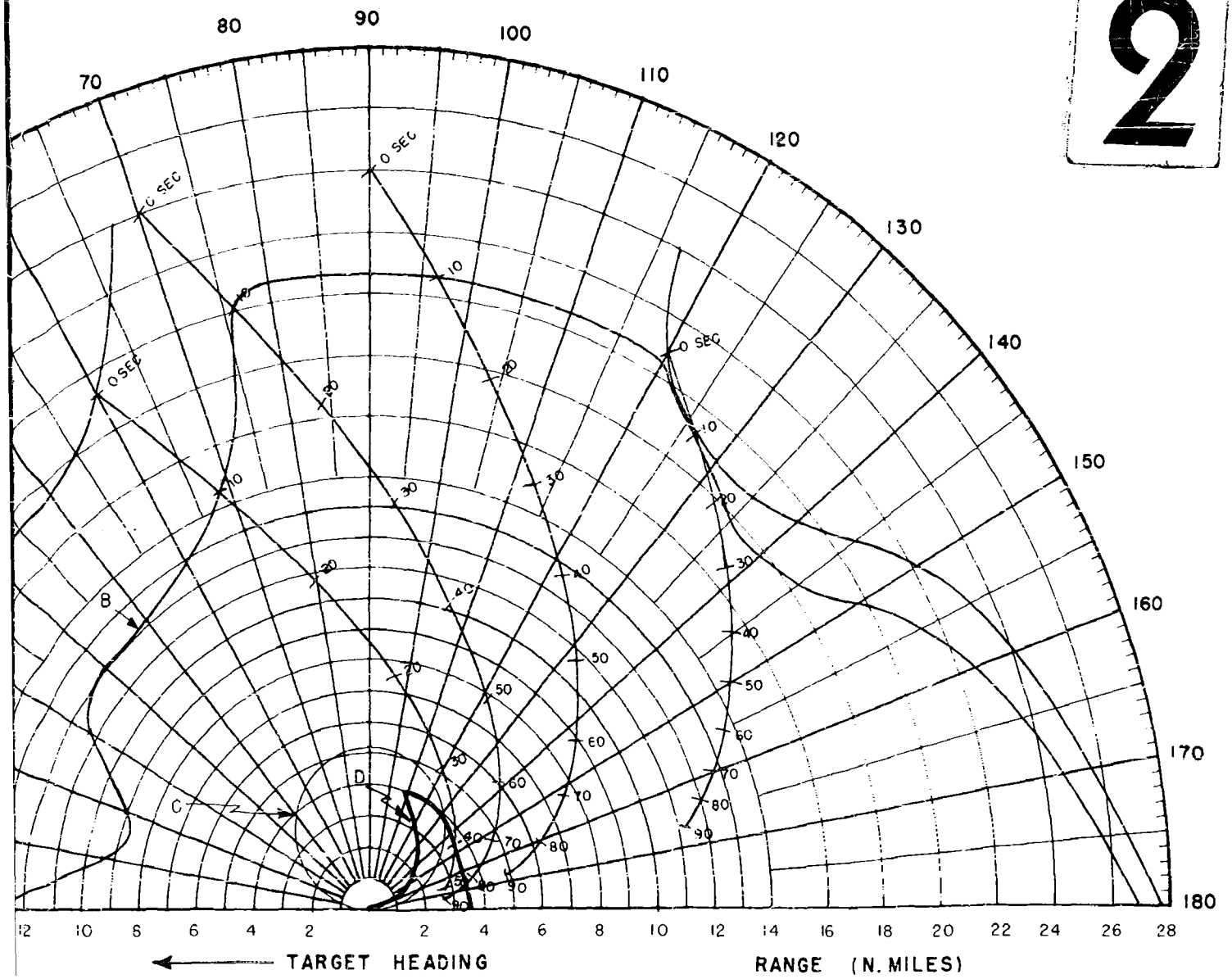

A - 85 % DETECTION RANGE

B - LOCK-ON RANGE

C - CONSTANT LOAD FACTOR LOCUS (N_z = 3)

D - SIDEWINDER IC LAUNCH ZONE

CONFIDENTIAL

Naval Research Laboratory
Technical Library
Research Reports Section

DATE: February 26, 2001

FROM: Mary Templeman, Code 5227

TO: **Code 5300 Paul Hughes**

CC: Tina Smallwood, Code 1221.1 ts 3/8/01

SUBJ: Review of NRL Reports

Dear Sir/Madam:

1. Please review NRL Report MR-754 Volumes I, II, III, IV, VII, VIII, IX, X, XI, XII, XIII, XIV, XV, MR-1372 and MR-1289 for:

   ☑ Possible Distribution Statement
   ☐ Possible Change in Classification

Thank you,

Mary Templeman

Mary Templeman
(202)767-3425
maryt@library.nrl.navy.mil

The subject report can be:

☒ Changed to Distribution A (Unlimited)
☐ Changed to Classification _____
☐ Other:

Ben H Cantrell 3-8-01

Signature Date

AN (1) AD- 345 945/XAG
FG (2) 160100
160300
160401
CI (3) (U)
CA (5) NAVAL RESEARCH LAB WASHINGTON D C
TI (6) SUMMARY OF NAVY STUDY PROGRAM FOR F4H-1 WEAPON SYSTEM. VOLUME IX
AU (10) Ryon ,J. C.
Bellavin ,I. N.
Loughmiller ,C. M.
Lister,R. L.
RD (11) Nov 1959
PG (12) 1 Page
RS (14) NRL-MR-754-Vol-9
RC (20) Unclassified report
DE (23) (*aircraft fire control systems, performance (engineering))
jet fighters, guided missiles (air to air), probability, navy, launching, search radar, radar tracking, tactical warfare, feasibility studies, tactical
DC (24) (U)
ID (25) an/apq-72, f-4 aircraft, sparrow
IC (25) (U)
AB (27) The Naval Research Laboratory is serving as technical directors of the Navy's Air to Air Missile Study. The results are presented in a series of volumes under NRL Memorandum Report 754. This volume is the ninth in the series. The study to date has been primarily concerned with the system employing the F4H-1 aircraft, the AN/APQ-72 radar and the Sparrow III6a missile. This volume represents a continuation of the study results presented in preceding volumes. (Author)
AC (28) (U)
DL (33) 02
CC (35) 251950